COMPARATIVE ACOUSTICAL AND PHYSIOLOGICAL STUDIES OF HEARING AND DIRECTIONALITY IN VERTEBRATES

by

ANNA GUPPY

A thesis submitted for the degree of

Doctor of Philosophy at the

Australian National University

Department of Behavioural Biology,

Research School of Biological Sciences,

Australian National University.

November 1985

DECLARATION

This thesis contains no material which has been accepted for the award of any other degree or diploma in any university. To the best of my knowledge and belief, this thesis contains no material previously published or written by another person, except where due reference is made in the text. Further, I declare that this thesis contains my own independent work except for collaboration in the following experiments only: 1/ acoustical measurements of directionality in the normal external ear of *Macropus eugenii* and 2/ electrophysiological recording of the cochlear microphonic potentials in *Tyto alba*. In these two series of experiments I participated equally, with one other person, in the planning, surgical procedures, collection of data and data analysis.

Signed

Anna Guppy

Anna Guppy

ACKNOWLEDGEMENTS

I would like to thank Dr. Roger Coles for his enthusiasm and patient supervision throughout the course of this work. I sincerely thank Dr. NH Fletcher (Institute of Physics, CSIRO Canberra) for many valuable discussions and expert advice on acoustics and for kindly writing the computer programs used to calculate the gain of acoustic horns.

I would also like to thank Dr. M. Littlejohn, Mr. P. Harrisson (Dept. of Zoology, University of Melbourne); Dr. PJ Fullagar, Sir SWG White (Division of Wildlife and Rangelands, CSIRO Canberra); Dr.K. Hews-Taylor (National Measurement Laboratories, CSIRO Sydney) and Dr. P. Rose (Dept. Linguistics, Australian National University, Canberra) for the use of sound analysis facilities.

I thank Dr. T. Lund (CCAE, Canberra) for the loan of the wave analyser and Dr. LM Aitkin(Dept.of Physiology, Monash University) for the loan of the Hewlett Packard oscillator.

In addition I gratefully acknowledge the assistance of Mr. CR Tidemann and Mr. MJ Grant (Dept. of Zoology, Australian National University, Canberra) with collection of *Nyctophilus gouldi*, and Prof. JD Pettigrew (Dept. of Physiology and Pharmacology, University of Queensland, Brisbane) for assistance with the collection of *Tyto alba*. I am also grateful to Mr B. Baker for the use of photographs of *Macroderma gigas* and *Nyctophilus gouldi*. Thanks are also due to the Dept. of Conservation and Agriculture in ACT and the Conservation Commission of Northern Territory for issuing animal permits and for much appreciated assistance.

I am extremely grateful to the staff of the services in the Research School of Biological Sciences of the Australian National University, in particular the RSBS computer and photography personnel for professional and personal support throughout this research.

Finally, sincere thanks must go to my mother whose moral and emotional support has kept me sane during the course of this thesis.

ABSTRACT

1. The acoustic pressure gain and directionality of the external ears of four mammalian species were studied by implanting small microphones in the ear canals either close to or replacing the tympanic membrane. The species studied were *Macroderma gigas*, *Nyctophilus gouldi*, *Macropus eugenii* and *Macropus giganteus*. In addition similar acoustical measurements using the same techniques were obtained in the barn owl *Tyto alba*, since this bird has a highly specialized external ear. Sound stimuli were delivered in the free field as pure tones or tone bursts in the range 0.2-150kHz.

2. The maximum pressure gain in the ear canals ranged from 20-30dB between 1.7-22kHz, depending on the species. In the mammals, two major factors which contribute to the overall gain curve of the external ear are meatus resonance (except for *N.gouldi)* and the pressure amplification by the pinna. For each species, pinna gain was determined by the difference curve between the intact and pinnaless conditions. Pinna gain increased rapidly in a low to mid frequency band between 5-30kHz, to reach 12-20dB depending on the species. Pinna gain curves were compared to the expected gain of a series of simple finite acoustic horns (paraboloidal, conical and exponential) based on the appropriate average dimensions of the pinna. In general, pinna gain most closely resembles the increasing efficiency of a finite conical horn as the stimulus wavelength decreases. There was a tendency for pinna gain to decrease at high frequencies presumably due to the irregular structure of each pinna. Pressure peaks on the rising slope of the pinna gain

curves (except for *M.eugenii)* were close to the predicted frequencies for horn resonance in each species.

3. In *Tyto alba*, the facial ruff forms an outer ear cavity and the gain curve for the ruff is close to that of a finite conical horn of equivalent size up to 8kHz (without horn resonance). Resonance of the internal head cavities of the barn owl was evident, probably involving the interaural and ear canals.

4. In each species, ear canal directionality was closely related, to a first approximation, to the sound diffraction properties of a circular aperture. The directivity of the main lobe was examined in terms of the -3dB acceptance angle and the angular separation between the acoustic axis and nulls (semi-angle). In each mammal species aperture size was based on the average radius of the open face of the pinna (mouth).

In *Tyto alba* the aperture size is determined by the average radius of the open face of the outer ear cavity formed by the facial ruff. Asymmetry between left and right ear canal directivity patterns is related to the structural asymmetry of the ear canal openings.

5. A frequency dependent movement of the acoustic axes was noted for azimuth and elevation in *M.gigas* and *N.gouldi* but in azimuth only in *T.alba*. Within limited bandwidths and depending on the species, the spatial location of the acoustic axis was predicted by a simple acoustical model based on the geometry of the obliquely truncated cone-like structure of the pinnae and the barn owl's outer ear cavity.

6. Neural recordings of auditory evoked potentials and single

neurones were studied in the inferior colliculus of *M.gigas* and *N.gouldi*. In *M.gigas*, the neural audiogram has two sensitivity peaks at 10-20kHz and 35-43kHz with extremely low thresholds of -16dBSPL (*re.* 20μPa) in the lower frequency region. Likewise, in *N.gouldi* the neural audiogram has sensitivity peaks at 8-14kHz (lowest thresholds 5dB SPL) and 22-45kHz. In both species the higher frequency sensitivity peak in the audiogram is correlated with the main energy band of the echolocation calls. The lower frequency hearing region in both species is used for social communication, in particular "audible calls" such as the chirp and squabble in *M.gigas* and the isolation or protest calls used by juvenile *N.gouldi*. The extremely high sensitivity to "low frequency" sound by the auditory system in *M.gigas* is discussed in relation to hunting by passive listening.

7. In *M.gigas* and *N. gouldi* contralateral pinna removal caused a frequency dependent increase in auditory evoked potential thresholds by up to 20dB in the inferior colliculus, supporting the idea of an amplifying role the pinna as observed from acoustical measurements in the ear canal.

8. The angular size (acceptance angle) of the response boundaries of "axial-type" spatial receptive fields (at 5dB above threshold) for a sample of auditory neurones from the inferior colliculus of *M.gigas* and *N.gouldi* were related to the diffraction limit produced by the open face of the pinna. In *M.gigas* it was possible to establish that the best position of axial-type receptive fields tended to move with frequency in a similar fashion to the acoustic axis of the pinna.

9. The directional sensitivity of the ear of *T.alba* was examined by recordings of the cochlear microphonic (CM) potentials. Below 5.5kHz the CM directionality was diffraction limited by the open face of the facial ruff and therefore comparable to ear canal directionality. The CM was non-directional above about 9kHz. Between 6-9kHz, which is the critical bandwidth for sound localization in *T.alba*, CM directivity patterns were distinct from ear canal directionality and characteristic of a mixed pressure and pressure gradient receiver. In this bandwidth the CM was directionally polarized, with the CM axial planes for each ear being symmetrical about the interaural midline. The interaural midline is inclined by 12° clockwise from the midline of the head, due to the asymmetry of the ear openings. The spatial location of the CM axis is closely related to the spatial position of maximum net pressure which would be expected to act on the tympanic membrane as a result of a pressure gradient. Likewise, along the CM directional plane, the -3dB acceptance angles and the position of nulls relative to the CM axis are determined by the pressure gradient at the tympanic membrane.

CONTENTS

CHAPTER 1: GENERAL INTRODUCTION

A principal difference between mammalian and non-mammalian hearing relates to the physical mechanisms at the periphery. Until recently it was commonly believed that all vertebrate ears were pressure receivers and acoustically isolated from each other. Some authors had reservations about this view (e.g. Schwartzkopff 1950, 1962) and evidence for pressure gradient reception has been found recently in non-mammalian vertebrate ears (Chung *et al.* 1978; Coles *et al.* 1980; Hill *et al.* 1980).

In mammals a single isolated ear which functions as a pressure receiver can be considered to have little inherent directionality. A physical mechanism has evolved in mammals to provide substantial directionality by embedding the ear in the head and connecting the tympanic membrane to an external wave-guide. The two ears can then experience differences in interaúral pressure (intensity) due to sound diffraction and differences in interaural time or phase due to their physical separation.

Rayleigh (1876, 1877, 1907) first suggested that the estimation of sound location in humans was largely dependent upon binaural audition. From many subsequent experiments (for reviews see Erulkar 1972; Gourevitch 1980; Lewis 1983) it has been concluded that interaural phase differences are an effective cue for localization at low frequencies, but become ambiguous at high frequencies because there is more than one position of the sound source which could give the same binaural phase difference. The differences in interaural intensity at the two ears which result from a sound shadow cast by the head are more effective cues at high frequencies. Indeed, Stevens and Newmann (1934) found that sound localization was degraded in an intermediate frequency region

where both phase and intensity were less effective in providing interaural cues. They found that human subjects localized tones with a similar degree of accuracy below 1kHz and above 7kHz but less accurately between 2-4kHz. Hence Steven and Newmann (1934) concluded that there was a dual mechanism (duplex theory) for the angular localization of tones in the horizontal plane i.e. phase differences at low frequencies and intensity differences at high frequencies, with intermediate frequencies that are poorly localized. These psychophysical observations were followed by neural studies which showed that the duplex theory for sound localization has a neural correlate in the response properties of binaural auditory neurones (Erulkar 1972). The low frequency properties of EE cells have been found to be sensitive to interaural time or phase by phase-locked discharges and EI cells presumably code for direction at higher frequencies because they are sensitive to differences in interaural intensity (Hind *et al.* 1963; Rose *et al.* 1966, 1967; Goldberg and Brown 1968, 1969). It is believed that the central auditory system processes the two physical cues of interaural intensity and phase as a meaningful neural code for sound direction and this forms the basis for the perception of sound locaton in space.

In mammals, the general design of the external ear, which includes the pinna, meatus and in some species a prominent tragus, is likely to contribute significantly to hearing and directionality by its horn-like appearance. Various aspects of the transformation of sound by the pinna, head and auditory meatus have been investigated in cats (Flynn and Elliott 1965; Wiener *et al.* 1966; Tonndorf and Khanna 1967; Gatehouse and Oesterreich 1972; Phillips *et al.* 1982; Calford and Pettigrew 1984), humans (Batteau 1967; Harrison and Downey 1970; Shaw

1974; Searle *et al.* 1975; Oldfield and Parker 1984a,b) rabbits (Fattu 1969) and monkeys, rats and bats (Harrison and Downey 1970).

Although the pinna is a mammalian invention, some owls have developed highly specialized external ears which may have a similar function to the mammalian pinna (Norberg 1978; Knudsen 1980). Some species of Notodontid moths possess a cup-like extension of their plural segments which have been likened to the mammalian pinna (Fullard 1984). The acoustic tracheae of several insect species have been studied for their role in hearing, particularly as horn-like sound guides (Lewis 1974; Michelsen and Nocke 1974; Nocke 1975; Seymour *et al.* 1978; Michelsen 1979, 1983; Larsen 1981; Hill and Oldfield 1981).

There is much diversity in the size and shape of the mammalian pinnae (Walker 1975). The greatest hypertrophy of the pinna, relative to the size of the head occurs in echolocating bats. Whereas, at the other extreme, the pinnae are relatively small compared to the size of the head in most primates and in a few mammals the pinnae are absent e.g. Notoryctidae (marsupial mole) and Talpidae (moles). However, the true moles are exceptional and probably use a pressure gradient for hearing (Coles *et al.* 1982).

Another feature of the mammalian pinna is the degree of articulation to the skull. Plains dwelling mammals such as Cervids and Macropods (see Fig. 4.12) have large erect and highly mobile pinnae, and the pinnae of volant mammals such as bats are also usually highly mobile. Examples of immobile pinnae occur mostly in the primates with the possible exception of some of the prosimians. Highly restricted pinna mobility may occur in some echolocating bats where the two pinnae are connected by a skin fold at the midline which may, in extreme cases, extensively fuse the medial edges of the pinnae as in Megadermatid bats

(Walker 1975; see Fig. 2.1). The mobility of the pinnae in many mammals may play an important role in hearing since denervation of the motor control of the pinnae affects the acoustic targeting reflex in cats (Santibanez 1976; Siegmund and Santibanez 1981). Normal pinna movements, as well as an intact pinna and tragus, are essential for accurate sound localization by echolocation in bats (Schneider and Mohres 1960; Flieger and Schnitzler 1973; Gorlinski 1976; Grinnell and Schnitzler 1977; Lawrence and Simmons 1982). Furthermore, pinna movements appear to be synchronized with the emission of sonar pulses (Griffin *et al.* 1962; Pye *et al.* 1962; Pye and Roberts 1970).

Traditionally the study of the mechanisms of directional hearing in non-echolocating mammals has been largely dominated by the use of dichotic stimulation which ignore the role of the pinna or pinna movement in spatial hearing (Erulkar 1972). However, studies in bats have consistently maintained an interest in the importance of the pinna in hearing by using free field stimuli (Grinnell and Griffin 1958; Grinnell 1963a,b; Grinnell and Grinnell 1965; Grinnell 1970, 1973; Neuweiler 1970; Grinnell and Hagiwara 1972a,b; Grinnell and Schnitzler 1977; review, Schnitzler and Henson 1980). More recently interest in the directional hearing of non-echolocating vertebrates has been rejuvenated by the use of free field sound sources (e.g. Knudsen *et al.* 1977; Chung *et al.* 1978; Pettigrew *et al.* 1978; Coles *et al.* 1980; Hill *et al.* 1980). The free field approach has been extended to studies of directional hearing in mammals such as the cat (Middlebrooks and Pettigrew 1981; Phillips *et al.* 1982; Semple *et al.* 1983; Aitkin *et al.* 1984; Calford and Pettigrew 1984; Middlebrooks and Knudsen 1984; Moore *et al.* 1984a,b) and guinea pig (Palmer and King 1982, 1983, 1985; King and Palmer 1983).

The current ideas on the mechanisms of sound localization in vertebrates are heavily influenced by the extensive data for the barn owl, *Tyto alba* (Konishi 1973a,b 1983; Knudsen *et al.* 1977; Knudsen and Konishi 1978a,b,c 1979, 1980; Knudsen *et al.* 1979; Knudsen 1980, 1981, 1982, 1983a,b,c 1984; Moiseff and Konishi 1981a,b 1983; Sullivan and Konishi 1984; Takahashi *et al.* 1984). It is important to know the extent to which the mechanisms for sound localization in the barn owl can be used as a model for vertebrates in general. Although the data available for the barn owl is impressive, potential problems arise in terms of the physical mechanisms involved in directional hearing. This is because in birds, as in insects and lower vertebrates, the ear can function as a pressure gradient receiver, whereas the ear of almost all mammals acts as a pressure receiver (Lewis 1983; Michelsen 1983). A further consideration is the "head-referenced" ear directionality in the barn owl, which contrasts with "pinna-referenced" ear directionality in mammals with mobile pinnae.

The use of the closed field or dichotic sound stimulation has been popular in neural studies of sound localization using mammalian species such as cats, monkeys and rabbits (see Erulkar 1972; Neff 1974; Gourevitch 1980; Gatehouse 1982). Many of these studies have addressed the problems of the neural coding of auditory space by manipulating interaural parameters such as intensity (pressure) and time (phase) with tones and bandwidth noise. In addition to the classical dichotic studies, single sound sources located in the free field have also been used to study the neural mechanisms of directional hearing (Gordon 1973; Dräger and Hubel 1975; Chalupa and Rhoades 1977; Harris *et al.* 1980). More recently there has been the convincing demonstration that localized areas of two dimensional space are represented at the neural level in

the vertebrate brain by auditory receptive fields (Knudsen and Konishi 1978a,b, 1980; Moiseff and Konishi 1981a, 1983; Middlebrooks and Pettigrew 1981; Knudsen 1982; 1983c, 1984; Palmer and King 1982, 1983, 1985; Phillips *et al.* 1982; Semple *et al.* 1983; King and Palmer 1983, 1985; King 1985; Fuzessery and Pollak 1984; Moore *et al.* 1984a,b; Jen *et al.* 1984; Poussin and Schlegel 1984; Middlebrooks and Knudsen 1984; Shimozawa *et al.* 1984; Takahashi *et al.* 1984).

The question of the topographic representation of auditory space in the vertebrate brain has been a major topic of debate. This is because the cochlea is regarded principally as a frequency analyser. The basilar membrane represents frequency topographically along its surface rather than auditory space *per se* and provides the basis for the tonotopic organization of the afferent auditory pathway (Webster and Aitkin 1978). This contrasts with the representation of visual space by the retina for example. Due to the apparent lack of a topographic representation of auditory space along the basilar membrane, it is considered necessary that such a map be generated in the nervous system by binaural integration of the directional information carried in each auditory nerve. There have been several successful (Pettigrew *et al.* 1978; Knudsen and Konishi 1978a,b, 1984; Palmer and King 1982, 1983, 1985; King and Palmer 1983; Middlebrooks and Knudsen 1984) and unsuccessful (Wise *et al.* 1982; Wise and Irvine 1983; Shimozawa *et al.*; 1984; Jen *et al.* 1984; Poussin and Schlegel 1984) attempts to find maps of auditory space in the vertebrate brain.

In the barn owl there are at least two separate neural maps of auditory space in the midbrain. Knudsen and Konishi (1978a,b) found a neural map of auditory space in a division of the MLD (inferior colliculus) and Knudsen (1982) also found an auditory space map in the

optic tectum of the barn owl which was in register with the visual map. By comparison, an equivalent space map has not been found in the inferior colliculus of mammals but has been described in the deeper layers of the superior colliculus (Palmer and King 1982, 1983, 1985; King and Palmer 1983; Middlebrooks and Knudsen 1984). However, there is evidence in the moustache bat (*Pteronotus parnellii*) that the location of axial-type auditory receptive fields in the inferior colliculus are frequency dependent (Fuzessery and Pollak 1984). This study on *P. parnellii* therefore raises the possibility that there may be a topographic representation of auditory space in the brain of certain vertebrates by virtue of the tonotopic organization. A similar suggestion has been made for the frog auditory midbrain (Pettigrew *et al.* 1978) but the physical mechanism for ear directionality in the frog is based on pressure gradients (Chung *et al.* 1978).

The neural data on the commonly described "axial-type" receptive fields in the cat and bat brain show that the positions of the receptive fields tend to be relocated with involuntary changes in pinna position (Middlebrooks and Pettigrew 1981; Semple *et al.* 1983; Jen and Sun 1984). Hence a single monaural auditory neuron could "map" auditory space by successive repositioning of the pinna during normal movements, but the influence of pinna position on the stability of the auditory space maps in the superior colliculus has not been tested. An important consideration is possible binaural or monaural basis of the auditory space map because a monaural (contralateral) map exists at threshold in unilaterally deafened guinea pigs but binaural (ipsilateral) input is necessary to maintain the map above threshold (Palmer and King 1983, 1985). Interestingly, the monaural space map in the guinea pig superior colliculus depends on the presence and presumably the directional

properties of the contralateral pinna (Palmer and King 1983, 1985) but similar effects have not been tested for neurones of the space mapped region of the superior colliculus in the cat (Middlebrooks and Knudsen 1984).

Aims of thesis

A principal aim of this thesis is to examine the nature of the external ear in several mammalian species and its relevence to the mechanisms of hearing and directionality. This approach is based on an increasing awareness in the role of the pinna in the directional hearing of many mammals. Several aspects of hearing are compared in the following mammalian species, the ghost bat *Macroderma gigas*, Gould's long-eared bat *Nyctophilus gouldi*, the tammar wallaby *Macropus eugenii* and the eastern grey kangaroo *Macropus giganteus*, in which there is natural variation in the design and mobility of the pinna. Detailed acoustical measurements of sound pressure are made in the ear canal of these species in order to determine the gain and directional characteristics of the external ear. An attempt is made to model, with particular reference to the pinna, the acoustical properties of these external ears in terms of an acoustic transformer and the physics of sound diffraction at an aperture. The biophysical measurements in *M. gigas* and *N. gouldi* are extended by examining the response properties of auditory neurones and evoked potentials in the inferior colliculus, with reference to directionality and frequency sensitivity. Several species-specific vocalizations are recorded and analyzed in *M. gigas*, *N. gouldi* and *M. giganteus* in order to identify the biologically important frequencies which are processed by each auditory system.

This thesis also includes experiments on the barn owl (*Tyto alba*) for which there is considerable data on directional hearing. Compared

to other birds, the barn owl has developed a highly specialized external ear, and the presence of the facial ruff suggests a similar acoustical function to the mammalian pinna. Therefore detailed acoustical measurements are made in the ear canal of *T. alba*, and compared to the pressure measurements obtained from the ear canal of mammals. In addition, the directional sensitivity of the cochlear microphonic (CM) is examined and compared to the ear canal directionality, in order to determine the contribution of pressure and/or pressure gradients to the physical mechanisms of directional hearing in the barn owl.

CHAPTER 2: ACOUSTICAL AND NEURAL PROPERTIES OF THE AUDITORY SYSTEM IN THE GHOST BAT *MACRODERMA GIGAS* [MICROCHIROPTERA: MEGADERMATIDAE] AND GOULD'S LONG-EARED BAT *NYCTOPHILUS GOULDI* [MICROCHIROPTERA: VESPERTILIONIDAE]

INTRODUCTION

It is generally recognised that the external ears of mammals provide binaural cues for sound localization such as interaural intensity and time (Erulkar 1972; Gourevitch 1980; Lewis 1983). The pinna plays an important role in the hearing of bats, and in particular influences directionality (Griffin 1958; Schneider and Mohres 1960; Grinnell 1963a,b,c; Suga 1964; Grinnell and Grinnell 1965 Neuweiler 1970; Flieger and Schnitzler 1973; Gorlinski, 1976; Grinnell and Schnitzler 1977; Lawrence and Simmons 1982; Fuzessary and Pollak 1984; Jen and Sun 1984; Jen *et al.* 1984). The acoustical properties of the external ear of bats have received relatively little attention despite considerable variation in structure and mobility. In this context measurements of directionality and acoustic pressure gain were made in *Macroderma gigas* and *Nyctophilus gouldi* by replacing the tympanic membrane with a small probe microphone. In conjunction with this biophysical approach, the response properties of auditory neurones and evoked potentials in the inferior colliculus were examined in relation to directionality and threshold sensitivity to sound (neural audiogram).

MATERIALS AND METHODS

Subjects

Nine adult ghost bats (*Macroderma gigas*) of both sexes (average weight 130gm) were obtained from a large colony in the Pine Creek area of the Northern Territory, Australia (see CHAPTER 3). Five adult female Gould's long-eared bats *Nyctophilus gouldi* (average weight 12gm) were obtained locally.

Apparatus and preparation

Experiments were conducted in an anechoic room (2.6m x 2.5m x 2.0m) with a primary echo level at least 39dB below the signal. The room contained a mobile speaker assembly comprising a vertically mounted aluminium track of 94cm radius, which could be rotated through about 330°. A trolley carrying an acoustic transducer was moved along the track. The combined motion of the trolley and track permitted sound to be delivered from various elevation and azimuth angles under remote control and with an accuracy of ± 0.5° in each dimension.

Acoustical measurements

A small calibrated 1/8" condenser microphone (Bruel and Kjaer Type 4148) was placed at the position normally occupied by the tympanic membrane. In the isolated head of a fresh cadaver of both species, microphone placement is possible by entry through the bulla using a ventral approach. In order to safely position the microphone, a very short piece of thin plastic tubing was placed at the end of the microphone which was then sealed in position with petroleum jelly. Using this replacement technique sound pressures at the tympanic membrane can be measured relative to the free field and as a function of stimulus direction.

Sound stimuli were continuous pure tones from 300Hz - 150kHz, produced by a function generator (Hewlett-Packard Model 3300A or Trio Model AG-202A). The electrical signals were amplified by a power booster (Pioneer BP-320) in the frequency range 300Hz-40kHz and by a custom built device for the frequency range 20kHz-150kHz. Amplified signals were connected to one of three acoustic tranducers via an attenuator (Hatfield Type 2125), depending on the frequency range required (300Hz-4kHz, Realistic Type 40-1909B; 2kHz-40kHz, Motorola piezohorn Type KSN 1025A; 20kHz-150kHz, custom made electrostatic transducer).

The output voltages from the implanted probe microphones were determined on a measuring amplifier (Bruel and Kjaer Type 2510, linear 2Hz-200kHz) using a high pass filter (Kohn-Hite Model 3550, high pass 100Hz).

For biophysical measurements of sound pressure in the ear canal, each preparation was placed in the anechoic room and mounted on an elevated platform at the centre of rotation of the semicircular track. The head was attached to a locking ball joint by a long screw glued to the dorsal surface of the skull. The intersection of the midline sagittal plane of the animal and the horizontal plane of the apparatus was used to define the longitudinal axis (0° azimuth, 0° elevation). The vertical orientation of the head was adjusted to suit data collection (see below) and was also referenced to a "sonar horizon" (see Figs. 2.1, 2.8, 2.10 and 2.16).

Calibration of the free sound field was determined by placing a calibrated microphone (1/4" Bruel and Kjaer Type 4135 or $\frac{1}{8}$" Bruel and Kjaer Type 4148) at the position normally occupied by the centre of the bats head, without the head, but all other apparatus present. Sound

pressure levels (dB SPL re. 20 uPa) were calibrated with the microphone directly facing the acoustic transducer along the longitudinal axis, at a distance of 94cm.

Neurophysiological recordings

The neural responses from the inferior colliculus of *Macroderma gigas* and *Nyctophilus gouldi* were studied by evoked potential and extracellular microelectrode recording techniques. Bats were initially anaesthetized with a mixture of Ketamine (20mg/kg) and Rompum (2.5mg/kg) and maintained under anaesthesia by periodic supplementary doses of these drugs. For neurophysiological recording experiments the head was held in a similar fashion to the biophysical experiments (see above).

Electrode placement in the inferior colliculus of both species was achieved under visual control by exposing the dorsal surface of the brain after surgical removal of part of the caudal skull overlying the forebrain and cerebellum close to the midline (see Fig. 2.18B). Auditory evoked potentials were recorded by placing a fine silver wire either on the dorsal surface of the inferior colliculus or up to 3mm below the surface. Recordings from auditory neurones were made using glass micropipettes filled with 3M NaCl. Both types of electrodes were positioned by attachment to the translator head stage of a Burleigh inch worm controller (Model PZ-550) and advanced into the neural tissue under remote control.

In the neurophysiological experiments auditory stimuli were generated as described for the biophysical experiments, with the addition of a custom built device which was used to produce repetitive trapezoidal sound pulses with variable rise and fall time (5-30msec) and plateau duration (25-200msec). The repetition rate was normally 2.5 pulses/sec. The same free field sound calibration procedures were used

as in the biophysical experiments.

Neural recordings from the inferior colliculus were amplified through a custom made preamplifier (x15) and a low level preamplifier (Tektronix Type FM 122: x1000). Auditory evoked potentials were averaged (Neurolog Model NL 750) from 32 stimulus repetitions and displayed on one channel of an oscilloscope. The oscilloscope beam and Neurolog signal averager were triggered by a timing pulse (Digitimer Model D130) which was also used to generate the tone bursts. A second channel of the oscilloscope was used to simultaneously display the electrical analog of the tone burst. Compound evoked potentials (averaged) or action potentials from single auditory neurons were displayed on the oscilloscope screen and response thresholds were discriminated visually or audio-visually by the experimenter.

Directionality data were plotted on a two dimensional zenithal projection of a hemisphere with 0° azimuth, 0° elevation at the centre of this projection (see Figs. 2.3, 2.12). The projection is similar to that originally used by Grinnell and Grinnell (1965) and Neuweiler (1970). It is equal area (distortion of solid angle < 5%) for angles greater than about 30° from the poles, and the poles are represented vertically.

RESULTS

Acoustical measurements

Acoustic axis

An acoustic axis is defined as the position in space where the sound pressure measured by the microphone in the ear canal is a maximum. This definition is consistent with that described by Middlebrooks and Pettigrew (1981) and Phillips *et al.* (1982) for the

cat's ear. Regions of equal pressure or sensitivity to sound are represented by a series of "iso-intensity" contours relative to the maximum value for a given directivity pattern.

(a) *Macroderma gigas*

Pressure gain

The maximum on-axis acoustic pressure in the ear canal relative to the free field was plotted as a function of frequency for five ears and the results are shown in Fig. 2.2A. The sound pressure developed at the position of the tympanic membrane is amplified for all frequencies between 1-55kHz. There is a rapid increase in amplification of pressure above 2.5kHz which peaks at 25-30dB between 5-8kHz. Above this frequency range positive gain progressively declines to values near 10dB at 40kHz. Above 40kHz there is a relatively sharp decrease in amplification to about 0dB at near 60kHz. Between 60-100kHz some amplification and attenuation of sound pressure occurs but remains within about 6dB of the free field. Pressure measurements were discontinued above 100kHz due to the difficulties in determining the acoustic axis (see below).

The contribution of various parts of the external ear to the pressure gain existing at the tympanic membrane in *M. gigas* were examined by removal of the tragus and pinna. In *M. gigas* the tragus has two lobes and is about 2.3cm in length, 1.4cm wide and bifurcated near the tip (see Fig. 2.1; Waite, 1900). Removal of the tragus had no measurable effect on the maximum pressure gain in the ear canal, but had a slight effect on directionality (see below, Fig. 2.9B).

The entire pinna extension can be surgically removed leaving only the entrance to the ear canal in the side of the head and this procedure involves separation of the two pinnae at the midline as they are fused

together (see Fig. 2.1). The concha of the pinna involves the side of the head also, although the pinna itself is much larger than the head as shown in Fig. 2.1. The pressure gain in the ear canal at the position of the tympanic membrane after pinna removal is shown in Fig. 2.2A, indicating that there is a general reduction in pressure gain by up to 15dB depending on frequency. The residual gain curve following pinna removal retains a peak in amplification of about 15dB at 7-8kHz. Above this frequency there is a progressive loss in gain and above 40kHz sound pressure in the ear canal is attenuated relative to the free field.

It seems likely that the peak in the pinna-removed gain curve may result from resonance of the remaining part of the external ear. The length of the meatus is approximately 1.1cm (see Table 2.1) which would show a closed tube resonance at a fundamental frequency of 7.8kHz as observed. The small peak in the pinna-removed gain curve near 20kHz may correspond to a higher harmonic mode of closed-tube resonance. If this suggestion is correct, then the peak in the normal gain curve for the intact ear (Fig. 2.2A) can be largely attributed to resonance in the meatus although there is a slight difference between the two curves in the frequencies at which the peaks occur. This difference may be due to the acoustic coupling between the pinna and the meatus, or resonance of the pinna itself (see DISCUSSION).

Difference curves between the pinna-removed and normal gain curves are shown in Fig. 2.2B for four ears and represent the effective gain of the pinna. These curves show that the pinna produces significant amplification of sound pressure above 2.5kHz which progressively increases to a maximum value of about 16dB at 5-6kHz. The gain of the pinna decreases to about 10dB between 8-15kHz and for higher frequencies amplification becomes more variable but maintains an average of around

8-10dB up to 100kHz (Fig. 2.2C). It was noted that a consistent loss in amplification produced a notch in the pinna gain curve near 30kHz. The gain of the pinna was compared with that of an acoustic transformer such as a simple horn by estimating the size of the mouth, throat and length of the pinna. Physical dimensions were measured from the actual pinna (see Fig. 2.1) and an endocast of the entire external ear. From Table 2.1 it can be seen that the average radius of the pinna mouth (a = 1.7cm) is based on the measured perimeter or circumference of the open face. The size of the throat of the pinna was estimated at the entrance to the meatus close to the base of the pinna after removal (a = 0.4cm). The shape of the pinna in *M. gigas* is extremely asymmetrical (Fig. 2.1) and therefore the length was estimated as the average of the distance from the tip of the pinna flange to the throat and the base of the tragus to the throat (2.4cm, see Table 2.1). For an ideal horn with these dimensions the maximum expected excess pressure at the throat at high frequencies (G_∞) would be about 13dB based on the ratio of the mouth to the throat cross-sectional areas (see Table 2.1 and APPENDIX 1).

Over the full frequency range the gain of a finite horn can be calculated from the equations given in APPENDIX 1. The pinna of *M. gigas* must be treated as finite in length since the frequency range of interest includes wavelengths which are comparable with and exceed both the length of the pinna and the circumference of the mouth (Olson 1947). The results of calculating expected gain curves for paraboloidal conical and exponential horns are expressed graphically in Fig. 2.2C and can be compared to the average gain curve of the pinna of *M. gigas*. The expected curves show horn resonance peaks of up to 15dB at fundamental frequencies between 4-5kHz and acoustic gain approaches an asymptotic

value of 13dB (G_∞) above about 50kHz. A comparison between the observed and expected curves suggests that the average gain curve of the pinna is probably closest to that of a conical horn (Fig. 2.2C). Both the conical and exponential horn expected gain curves rise similarly up to the first resonance peak which is somewhat broadened on average due to the variability of the peak in individual ears (Fig. 2.2B) but since the gain of the conical horn decreases more than the exponential horn above this peak, it suggests that the conical horn is probably a better approximation to the experimental data. In the case of the paraboloidal horn, the gain curve tends to increase slightly faster than the experimental data at low frequencies and produces a resonance peak a little lower in frequency than observed. In addition, for the paraboloidal horn gain decreases to lower levels than predicted by a conical horn particularly for frequencies immediately above the resonance peak, again suggesting that, of the three types of horns, the conical horn is probably the best fit to the experimental data.

Directionality

In *M. gigas* significant directionality occurred above 4kHz for the sound pressure measured at the position of the tympanic membrane. Directivity patterns were plotted in two dimensions as a series of iso-intensity (pressure) contours by using a hemispheric projection (see MATERIALS AND METHODS). A typical series of contour plots at various test frequencies is shown in Fig. 2.3. The acoustic axis is surrounded by a 1dB contour and iso-intensity contours depict the major and minor lobes as decreases in pressure at 5dB intervals relative to the axial pressure. The increase in directionality at higher frequencies is indicated by the closeness of the iso-intensity contours. The main lobe is characterised by oval-shaped contours at relatively high pressures

and above 20kHz localized regions of low pressure or minima occur within 45° of the axis. The progressive increase in directionality as a function of frequency can be summarized by measuring the maximum difference in sound pressure (dB_{max}) for any two positions in the directivity pattern. The results are shown in Fig. 2.4 and it can be seen that significant directionality (i.e. exceeding a 3dB limit) exists above 3-4kHz whereupon maximum directionality increases rapidly above 4kHz to reach a plateau of 30-35dB above 30kHz. Measurements of maximum directionality are limited by the dynamic range of the microphone (about 35dB for 1/8" Bruel and Kjaer) but the results in Fig. 2.4 demonstrate that there is a progressive increase in directionality with frequency, which results from the level of amplification of sound pressure on-axis and the development of regions of low pressure or minima in the response pattern.

A method of quantifying directionality is to examine the receiving or acceptance angle for a given decrease in sound pressure relative to the position of the acoustic axis. Although a criterion for directionality is arbitrary, a -3dB level relative to axial pressure is often used to compare directional devices (Beranek 1954). A -3dB acceptance angle is used to estimate the angular width of the main lobe as a function of frequency as shown for *M. gigas* in Fig. 2.5. Due to asymmetries in the directivity patterns (Fig. 2.3) the acceptance angles are computed as full width (2θ°) and estimated separately for azimuth and elevation. As shown in Fig. 2.5A, the -3dB acceptance angle in azimuth progressively decreases from 120° to 10° as frequency increases from 5kHz - 100kHz. Similarly in elevation (Fig. 2.5B) the -3dB acceptance angle decreases from 100° - 20° as frequency increases from 5kHz - 100kHz. Such a systematic increase in directionality as a

function of the stimulus wavelength (as shown in Fig. 2.5) strongly suggests that the external ear experiences sound diffraction phenomena. The experimental data in Fig. 2.5 are compared to sound diffraction generated by a single circular aperture whose size is taken as the average radius of the pinna opening which, in *M. gigas* is estimated to be 1.7cm based on measuring the perimeter of the pinna mouth (see Table 2.1; Fig. 2.1). The expected curves shown in Fig. 2.5 are derived from the directivity patterns for sound diffraction by a circular aperture in an infinite baffle (Beranek 1954) and the method of calculation is described in APPENDIX 2. Despite some scatter in the experimental data shown in Fig. 2.5, there is reasonable agreement with the expected values for diffraction. However, in elevation the acceptance angles below 8kHz are somewhat more directional than would be expected from a circular aperture of radius 1.7cm which may result from the elongated shape of the pinna face (see GENERAL DISCUSSION AND CONCLUSIONS, CHAPTER 6).

It was noted that an important feature of ear canal directionality was spatial regions of low pressure which formed minima or approximate nulls in the directivity patterns. Above certain frequencies, nulls are generated in the directivity pattern by sound diffraction at an aperture as a result of wave interference (see APPENDIX 2). The angle between minima or approximate nulls and the acoustic axis (semi-angle) was estimated from directivity patterns at various frequencies for *M. gigas* as shown in Fig. 2.6. Nulls were not evident in directivity patterns for frequencies below about 10kHz in the frontal hemisphere. As frequency increased above 10kHz null positions were observed to move progressively towards the acoustic axis up to 80kHz, with the semi-angle decreasing from a maximum of 110° to minimum values of 15°. There was

some difficulty in estimating the eccentricity of nulls due to the limited dynamic range of the probe microphone (Fig. 2.4) and irregularities in the directivity patterns especially at higher frequencies (Fig. 2.3). Nevertheless, the trend in the experimental data in Fig. 2.6 is very similar to the expected semi-angle of the main lobe based on sound diffraction at a circular aperture, with a radius equivalent to the average radius of the pinna face (a = 1.7cm; Table 2.1). The theoretical calculations for diffraction nulls are described in APPENDIX 2 and for a baffled opening with the average radius of the pinna mouth in *M. gigas* the most lateral null (i.e. 90° off-axis) should occur at 12kHz (ka = 3.83). This diffraction limit is consistent with the observed nulls being first detected in the frontal hemisphere in directivity patterns around 10kHz. The fact that nulls were detected for semi-angles greater than 90° suggests that the mouth of the pinna may be equivalent to an aperture at the end of a pipe, rather than necessarily in a plane wall (Beranek 1954; see also Fig. 4.9). At high frequencies, specifically above 40kHz, the experimental data suggests a slightly less directional response than would be expected from diffraction which may be due to the irregular structure of the pinna.

Movement of the acoustic axis with frequency

The ear canal directivity patterns in *M. gigas* tend to shift their relative position as a function of frequency and in particular the main lobe moves upwards and towards the midline as frequency increases (Fig. 2.3). An example of this effect is illustrated in Fig. 2.7 by plotting the movement of the acoustic axis in two dimensional space based on the left and right ear canal directivity patterns in the same animal. The average data for four ears is shown in Fig. 2.8 for both azimuth and elevation positions of the acoustic axis as a function of

frequency. The results in Figs. 2.7 and 2.8A show that in azimuth the acoustic axis moves progressively towards the midline starting from about 75° ipsilateral at 2kHz until both axes are within 20° of the midline above 20kHz. The closest position to the midline occurs at 40-60kHz where both acoustic axes are within 5° of the midline. Above 60kHz the acoustic axes tend to diverge from the midline. In elevation most of the upward movement of the acoustic axis occurs between 5-15kHz as shown in Fig. 2.8C and the axis remains stationary for frequencies above this range.

Anatomically the pinnae in *M. gigas* are essentially fixed in relation to the head because the medial edges are fused at the midline for half their length (Fig. 2.1). It is unusual for pinnae to be joined in mammals but a skin fold often occurs between the base of the pinnae in Microchiropteran bats (see *N. gouldi* Fig. 2.10), and reaches a maximum development in the Megadermatidae (see Walker, 1975). In the case of *M. gigas* gross pinna movements are impossible but small rocking movements can be observed in attentive individuals. Whereas the position of the acoustic axes in azimuth can be readily referenced to the midline, the definition of the horizontal plane is somewhat arbitary and needs to be referenced to natural head orientation during flight and sonar emission for example. Therefore, in Fig. 2.8C the position of the acoustic axis in elevation can be referenced to a horizontal plane for the head which would probably exist for the frequencies used during sonar pulse emission as shown in Fig. 2.8D (see also Fig. 2.18D and CHAPTER 3). In order to optimize data collection for the acoustical measurements in the ear canal, the head was tilted upwards by about 45° relative to this sonar horizon (Figs. 2.3, 2.7, 2.9) as indicated in Fig2.8C.

Although the pinna was treated as an ideal symmetrical horn in terms of acoustic gain and directionality it is obvious that the structure of the pinna in *M. gigas* is extremely asymmetrical in cross section resembling an obliquely truncated cone (Fig. 2.1). On this basis it is reasonable to expect that the acoustic axis may not be coincident with the geometric axis for all frequencies. By treating the pinna opening as an oblique truncation of a conical horn it is possible to develop a simple model to explain the movement of the acoustic axis which is based on the geometry of the cavity (see APPENDIX 3; Figs. 2.1, 2.8). The model is based on the assumption that a half wavelength sound path length difference can occur along the medial and dorsal surfaces of the pinna (Figs. 2.1) and may control the angle of the effective mouth and thus the relative position of the acoustic axis. This consideration is based on the geometry of the truncated opening of the pinna and the expected movement of the acoustic axis in azimuth and elevation is plotted in Fig. 2.8 and can be compared to the experimental data for acoustic axis movement. In azimuth (Fig. 2.8A) the lower frequency limit which can be used to calculate the expected position of the acoustic axis occurs 40° ipsilateral at 6kHz which is very close to the observed position at this frequency. As frequency increases the expected shift in the acoustic axis towards the midline is in close agreement to the observed movement, and crosses the midline near 40kHz. Curiously, for higher frequencies the expected movement of the acoustic axis continues into contralateral space and follows the observed movement of the acoustic axis of the opposite ear. In elevation the expected movement of the acoustic axis is in close agreement to the observed values in the frequency range 4-25kHz (Fig. 2.8C). Whereas the observed position of the acoustic axis remains on

the horizontal plane which defines the 'sonar' horizon above 25kHz, the expected values continue to move upwards by 20° at 100kHz.

Effect of pinna and tragus removal

The effect of pinna removal has been described previously and results in a significant decrease in pressure gain at the tympanic membrane due to its horn-like transformer properties (see Fig. 2.2). Since under normal circumstances directionality in the ear canal probably results from sound diffraction at the pinna opening (Figs. 2.5, 2.6) removal of the pinna is likely to produce a significant effect on directionality. As shown in Fig. 2.9A pinna removal results in a considerable loss of directionality which is indicated by the expansion of the iso-intensity contours. Typically null regions were eliminated and the location of new pressure maxima were more difficult to define than the original acoustic axis. Following pinna removal the position of new "acoustic axis" tended to be independent of frequency and aligned opposite the entrance to the meatus.

Removal of the tragus alone had only a slight effect on directionality as shown in Fig. 2.9B. The acoustic axis is marginally relocated following tragus removal and some null positions were slightly altered but the overall directionality pattern was not significantly disrupted.

(b) *Nyctophilus gouldi*

Pressure gain

Sound pressure was measured at the position of the tympanic membrane in *N. gouldi* using the same replacement technique and microphone (1/8" Bruel and Kjaer) as described for *M. gigas*. Sound pressure in the ear canal relative to the free field was plotted as a function of frequency for the intact external ear of *N. gouldi* (Fig.

2.11A). Significant amplification of sound pressure occurs above 4kHz and increases rapidly to values around 15-23dB in the range 7-22kHz. Above 22kHz amplification of pressure is progressively reduced and fluctuates from 5-11dB up to 100kHz.

The effect of pinna removal on sound pressure at the tympanic membrane was tested and an example is seen in Fig. 2.11A. Both the pinna and tragus were removed leaving only the base of the pinna (concha) which forms part of the side of the face as in *M. gigas* (Figs. 2.10, 2.1). The tragus is only 0.6cm long in *N. gouldi* (Table 2.1, Fig. 2.10) and was not removed separately from the pinna since the much larger tragus in *M. gigas* had no effect on the acoustic gain in the ear canal over the same range of test frequencies. Subsequent to pinna removal in *N. gouldi* pressure amplification was generally reduced to less than 10dB and the maximum residual gain occurred between 5-20kHz (Fig. 2.11A) although no clear peak was evident as seen in *M. gigas* (Fig. 2.2A). As frequency was increased above 22kHz in the pinnaless condition, amplification was reduced to less than 5dB and a maximum attenuation of sound pressure of 6dB was seen up to 100kHz. A small peak in gain was seen between 40-50kHz.

In *N. gouldi* the length of the external ear after pinna removal is very short and the meatus itself is only 0.2-0.3cm in length (Table 2.1). Therefore, it seems unlikely that the region of maximum pressure gain seen in Fig. 2.11A can be explained simply in terms of meatus resonance. However in this example the peak in gain for the pinna-removed curve which occurs at 40-45kHz (Fig. 2.11A) may be related to the resonance of the tube-like meatus.

The amplifying effect of the pinna on sound pressure is shown in Fig. 2.11B as the difference curve between the normal and pinnaless gain

curves as shown in Fig. 2.11A. From Fig. 2.11B the individual pinna gain curves generally start to rise rapidly above 4-5kHz to maximum values of about 12-17dB in the region 7-15kHz. A low frequency peak is suggested around 6-8kHz but gain averages around 10dB up to 20kHz (Fig. 2.11C). Pinna gain maintains a level of between 6-10dB as frequency is increased above 20kHz however there is increasing variability up to 100kHz. The gain curve for the pinna in *N. gouldi* can be compared to an acoustic transformer such as a horn in a similar fashion to *M. gigas*. The expected amplification curves for a finite paraboloidal, conical and exponential horn are shown in Fig. 2.11C and derived from calculations using the methods outlined in APPENDIX 1. The relevant physical dimensions of the pinna in *N. gouldi* are shown in Table 2.1 and the average radius of the mouth (pinna opening) is 0.85cm (see also Fig. 2.10) A throat of radius 0.2cm is formed at the base of the pinna which surrounds the invaginated opening to the ear canal in the side of the head. In treating the pinna as a horn, the length is estimated as the average path from the tip of the pinna to the throat compared with the path from the base of the pinna at the tragus to the throat. The average sound path is 1.3cm (Table 2.1, Fig. 2.10) and is an approximation due to the asymmetrical structure of the pinna. The maximum expected pressure gain (G_∞) for an ideal horn of these dimensions should approach 13dB at very high frequencies (see APPENDIX 1) but the observed gain of the pinna above 40kHz is about 5dB less than expected. Nevertheless, the average pinna gain of up to 20kHz is reasonably close to that of an finite conical horn (Fig. 2.11B,C) and loss of gain at higher frequencies is likely to result from the irregular shape of the pinna cavity. Horn resonance is to be expected since the pinna in *N. gouldi* is finite length in terms of the frequency

range of interest (Beranek 1954). The suggested peak in gain near 7kHz for the pinna (Fig. 2.11B,C) closely matches the fundamental resonance of a conical horn of equivalent dimensions. Similarly a paraboloidal horn would be expected to have a resonance peak but the gain curve tends to rise more steeply than the experimental data, peak at a slightly lower frequency and then loses more gain in the 10kHz region than observed. The expected gain curve for an exponential horn also starts to rise close to that of a conical horn, but the resonance peak is slightly higher in frequency and gain is maintained at a higher level than in the conical horn case. Overall the structure of the observed gain curve of the pinna suggests that a conical horn is probably the closest approximation.

Directionality

A typical series of directionality plots for *N. gouldi* is shown in Fig. 2.12 based on pressure measurements at the tympanic membrane. A localized region of maximum sound pressure for each ear canal could be found as low as 2kHz but the directionality was very poor since the -1dB iso-intensity contour often extended as far as ±90° in azimuth and elevation (Fig. 2.13). A clearly defined acoustic axis was evident above 5kHz. The main lobe of the directivity patterns were characterized by an acoustic axis surrounded by concentric oval or circular isointensity contours as indicated in Fig. 2.12 for a range of test frequencies between 10-40kHz. The closeness of iso-intensity contours which represent the main lobe indicates that directionality clearly increases as a function of frequency. Secondary lobes were formed by pressure minima or approximate nulls above about 15kHz. The development of directionality was compared for four ears by measuring the maximum difference in sound pressure (dB_{max}) for each directivity

pattern as a function of frequency and the results are shown in Fig. 2.13. The maximum directionality which can be measured by the present technique is limited by the dynamic range of the microphone (1/8" inch Bruel and Kjaer) but Fig. 2.13 shows that a relatively rapid increase in directionality occurs above 5kHz which approaches a limit of 30-35dB above 25kHz. The increase in directionality is produced by a combination of on-axis pressure amplification (Fig. 2.11A) and the development of nulls in the directivity patterns (Fig. 2.12). Ear canal directionality was further quantified by measuring the -3dB acceptance angle and the semi-angle of the main lobe of the directivity pattern in *N. gouldi* in a similar fashion as in *M. gigas* (Figs. 2.5, 2.6). The -3dB acceptance angles were measured for directivity patterns between 10-100kHz and expressed as the full angular width ($2\theta°$) as shown in Fig. 2.14. The results show that in azimuth (Fig. 2.14A) the -3dB acceptance angle decreases from values as high as 130° at 10-11kHz to a minimum of about 20° above 60kHz. In comparison, the -3dB acceptance angle in elevation (Fig. 2.14B) declines from 90° at 10kHz to about 25° at frequencies above 50kHz. The experimental data are compared to the -3dB acceptance angle based on sound diffraction by a circular opening in a plane wall as described in APPENDIX 2. In the case of *N. gouldi* the pinna opening has an average radius of 0.85cm (see Table 2.1 and Fig. 2.10). In Fig. 2.14A the expected curve for diffraction closely matches the experimentally observed increase in directionality in azimuth as a function of the wavelength but the observed acceptance angles are slightly less directional than expected above 60kHz. In elevation there is a reasonable correspondence between the expected and observed acceptance angles for most of the frequency range (Fig. 2.14B) however the observed values tend to be somewhat more directional than would be

expected below 15kHz reflecting the flattened appearance of the iso-intensity contours in the two dimensional representation of the main lobe (Fig. 2.12).

The occurrence of minima or nulls surrounding the main lobe particularly lateral and ventral to the acoustic axis (Fig. 2.12) were measured as a function of frequency. In Fig. 2.15 the angular separation between the acoustic axis and the null was seen to decrease systematically from about 110°-15° as frequency increased from 12-100kHz. Despite some variability, the separation of nulls from the acoustic axis follow a similar trend to that predicted for the semi-angle of the main lobe resulting from sound diffraction by a circular aperture with a radius equivalent to the average radius of the mouth of the pinna (a = 0.85cm; for diffraction theory see APPENDIX 2).

Movement of the acoustic axis with frequency

The spatial location of the acoustic axis in azimuth and elevation is plotted as a function of frequency for four ears as shown in Fig. 2.16. In azimuth (Fig. 2.16A) it is difficult to define the position of the acoustic axis below 5kHz. However, above 5kHz there is a tendency for the axis to move towards the midline starting at 50-60° ipsilateral. Between 5-25kHz the acoustic axis moves by about 50° towards the midline and remains within about 10° of the midline for higher frequencies. In contrast, the acoustic axis moves only 30° in elevation mainly between 10-35kHz (Fig. 2.16B).

Movement of the pinnae in *N. gouldi* is restricted, due to a skin fold joining the two ears at the base near the skull (Fig. 2.10). This is a similar restriction to that seen in *M. gigas* but does not involve an extensive fusion of the medial edges of the pinna. The only obvious pinna movements in *N. gouldi* occur during roosting where the tips of the

pinnae may be curled back into a "rams horn" configuration (see Strahan 1983). Consequently the acoustic axes in azimuth are head referenced to the midline in *N. gouldi* as shown in Fig. 2.16A,B. The orientation of the head in the vertical plane is arbitrary but the average elevation angle for the acoustic axes which occur above 35kHz, can be used to define a sonar horizon in a similar fashion to the definition used for *M. gigas* (Fig. 2.8B,D). Thus the sonar horizon in *N. gouldi* is based on the energy bandwidth used during sonar pulse emission and is likely to define the orientation of the head during horizontal flight (Fig. 2.16D). As in *M. gigas* (Figs. 2.7, 2.8), the frequency dependent movement of the acoustic axis over certain frequency bandwidths observed in *N. gouldi* suggests that the asymmetrical structure of the horn-like pinna may be responsible for this effect. Therefore, the same theoretical considerations which are outlined in APPENDIX 3 have been applied to the pinna of *N. gouldi* and are based on the potential half wavelength acoustic path length difference which exists along the extended edge of an obliquely truncated horn. The geometry of the cross section of the pinna in *N. gouldi* in azimuth and elevation (Figs. 2.10, 2.16) has been used to calculate the expected movement of the acoustic axis as a function of the wavelength (Fig. 2.16A,C). In azimuth the most lateral axis position which can be estimated is 65° from the midline at a frequency of 7kHz, which agrees closely with the observed position of the acoustic axis at this frequency. The acoustic axis is therefore approximately normal to the pinna face in azimuth at low frequencies. The expected movement of the acoustic axis in azimuth is similar to the observed shift up to about 80kHz (Fig. 2.16A). However, below 35kHz, there is a 10°-15° over estimation of axis position, which may be due to the difficulty in estimating the approximate dimensions of

the oblique truncation because of the irregular shape of the pinna. A limited movement of the acoustic axis in elevation can be predicted starting from a low frequency limit of 7kHz as shown in Fig. 2.16B and moving by 40° to a position corresponding to the sonar horizon at 40kHz. Thus although the observed and expected positions of the acoustic axis are similar over a limited bandwidth up to 50kHz, the observed axis remains stable in elevation for frequencies above 40kHz.

The effect of pinna removal

Pinna removal was found to decrease directionality as well as decreasing pressure gain at the tympanic membrane (Fig. 2.11A). Fig. 2.17 shows that pinna removal results in a considerable expansion of the iso-intensity contours signifying a marked loss in directionality of the main lobe and a relocation of the acoustic axis. In general, after pinna removal iso-intensity contours became irregular and difficult to define and null regions were either eliminated or relocated.

Neural responses from the inferior colliculus

(a) *Macroderma gigas*

Neural audiogram

The frequency sensitivity of the auditory system of *M. gigas* was determined by averaged evoked potential and single unit thresholds in the inferior colliculus (Fig. 2.18AC). In four animals auditory evoked potentials were recorded from the surface of the visually exposed inferior colliculus and in 2 further animals the silver wire electrode was inserted up to a depth of 3mm into the inferior colliculus (Fig. 2.18B). Evoked potential thresholds at each test frequency were determined visually from the average of 32 stimulus presentations displayed on an oscilloscope screen (see MATERIAL AND METHODS). Since neural thresholds were determined by the free field sound stimuli and

the acoustic axis is frequency dependent (Figs. 2.7, 2.8) the acoustic transducer was repositioned at each test frequency as required, to obtain the most sensitive thresholds for the evoked potential. The most sensitive thresholds were obtained for speaker positions contralateral to the recorded inferior colliculus and optimal directions closely corresponded to the frequency dependence exhibited by the acoustic axis. Complete neural audiograms determined by averaged auditory evoked potential thresholds are shown in Fig. 2.18A for three individual *M. gigas*, and the average neural audiogram from these results is shown in Fig. 2.18C. The lower and upper limits for hearing based on the neural audiogram occur at 2kHz and 100kHz respectively, where the threshold sensitivities exceed 70dBSPL. The neural audiogram from the inferior colliculus of *M. gigas* indicates two regions of peak sensitivity to sound which occur from 10-20kHz, where thresholds are as low as -16dBSPL, and from 35-43kHz where thresholds are as low as -3dBSPL. Between these two sensitivity peaks there is a conspicuous region of relative insensitivity which occurs from 27-32kHz where thresholds are as high as 30dBSPL. The low frequency sensitivity of the neural audiogram declines rapidly below 10kHz where thresholds are close to 0dBSPL, and decreases at a rate of 45dB/octave. Consequently, averaged evoked potential thresholds are 70-80dBSPL for frequencies below 3kHz. It was difficult to record evoked potentials below 3kHz and the lower limit for a reliable threshold was taken as 2kHz. At lower frequencies it was apparent that spurious sensitivity to sound may have been generated by the harmonic content of very intense tone bursts which were needed to generate an auditory response. Evoked potentials were detected as low as 300Hz, but real response thresholds are probably only valid to 2kHz despite the use of a low frequency transducer (see

MATERIALS AND METHODS).

The high frequency slope of the neural audiogram also declined very sharply at a threshold rate of 130dB/octave (Fig. 2.18A,C). Again, the actual upper limit of hearing using evoked potential thresholds is difficult to determine because of the difficulty in generating distortion-free high intensity ultrasound. It was found that the most insensitive thresholds approaching 90dBSPL occurred at 100kHz which probably represents the upper limit of hearing in *M. gigas*. Stimuli with frequencies above 100kHz appeared to produce more sensitive thresholds, but these are likely to have resulted from a spurious sensitivity to lower frequency distortion products or perhaps cochlear non-linearities.

In one animal, an attempt was made to compare auditory evoked potential thresholds from the inferior colliculus before and after removal of the contralateral pinna. The result of such a procedure is shown in Fig. 2.19 and the results, although limited, support the idea that the pinna contributes to neural sensitivity to sound as suggested by acoustical measurments in the ear canal (Fig. 2.2). In the region 10-25kHz the neural effect of the pinna contributes up to 15-20dB in sensitivity and up to 17dB in the region from 30-60kHz. The pinna starts to improve neural sensitivity to sound above 3kHz consistent with the increasing efficiency of the pinna as an acoustic horn as suggested by the pressure measurements in the ear canal (Fig. 2.2B,C). It was noted that there was only a small effect of pinna removal on neural thresholds in the narrow frequency zone near 30kHz which corresponds to a distinctive region of relative insensitivity to sound in the normal audiogram (Fig. 2.18AC) and poor amplification of sound by the external ear and pinna (Fig. 2.2).

In Fig. 2.18C the distribution of best frequency thresholds for a sample of 90 auditory neurons recorded from the inferior colliculus of four animals is shown in comparison to the average neural audiogram. The distribution of the most sensitive unit thresholds across frequency corresponds very closely to the neural audiogram based on evoked potentials. In general, unit thresholds varied over 60dB for a given frequency range. Unit data were collected from a total of 24 separate dorso-ventral penetrations through the inferior colliculi of the experimental animals. It cannot be claimed that auditory neurons were sampled randomly from every region of the inferior colliculus, but the sample size was large enough to suggest that best frequencies tended to cluster between 30-45kHz in the high frequency band, which is used for sonar and possibly in a lower frequency band below 12kHz which is used for social communication (Fig. 2.18D and CHAPTER 3). Both the single unit and evoked potential data indicate that *M. gigas* has highly sensitive hearing in a low frequency "audio" region between 10-20kHz. In addition both types of neural data suggest a discrete ultrasonic region of high sensitivity to sound at 40kHz.

Directional sensitivity of inferior colliculus neurons

The directional sensitivities of 44 auditory neurons from the inferior colliculus of *M. gigas* were studied by locating the most sensitive spatial region (best position) at best frequency and plotting receptive field boundaries at various sound pressures above the most sensitive threshold. The majority of these neurons (95%) displayed circular or oval shaped threshold boundaries based on excitatory thresholds (Fig. 2.20A) closely resembling "axial" or "circumscribed" receptive field types commonly described for auditory neurons at the level of the inferior colliculus in other mammals (Semple *et al.* 1983;

Fuzessery and Pollak 1984; Jen and Sun 1984; Moore *et al.* 1984a,b). In *M. gigas* spatial receptive fields of auditory neurones typically had their best response areas located contralateral to the recorded inferior colliculus and characteristically increased in size with increases in stimulus intensity above threshold (Fig. 2.20).

The size of the receptive field boundaries were compared in azimuth and elevation for auditory stimuli at 5dB above threshold at the best frequency of each neuron as indicated in Fig. 2.20A. The results are shown in Fig. 2.21 for 38 neurons with best frequencies ranging between 6-62kHz. Across this frequency range the 5dB threshold boundary of receptive fields in azimuth (Fig. 2.21A) decrease from a maximum of 150° at 6.5kHz to minimum values of 20° above 30kHz. In elevation (Fig. 2.21B) the 5dB threshold boundaries decrease from a maximum of 130° at 9kHz to a minimum of about 15° for best frequencies above 30kHz. The response boundaries of receptive fields can be compared with the -5dB acceptance angles which would result from sound diffraction by a circular aperture of radius 1.7cm which is equivalent to the average radius of the mouth of the pinna in *M. gigas* (see APPENDIX 2) as shown in Fig. 2.21. The results suggest that in general the size of spatial receptive fields in the inferior colliculus may be diffraction limited by the pinna, although the azimuth boundary size is less directional than would be expected (Fig. 2.21A). Estimates of receptive field size in elevation are closer to an expected diffraction limit, and together with field size in azimuth, emphasize the oval shape or flattened appearance of the receptive fields when plotted in two dimensional space (Fig. 2.20A). Nevertheless, these results indicate that inferior colliculus neurons with higher best frequencies are substantially more directional than neurons with lower best frequencies as seen in Fig.

2.21 and that the receptive fields can be referred to as "axial-type". It was also noted that the spatial location of receptive fields tended to shift upwards and towards the midline with increasing frequency (Fig. 2.20A). This effect was difficult to demonstrate in a single auditory neuron because of the generally narrow tuning limits. Therefore, the spatial location or best position of auditory receptive fields were compared for different neurons at their best frequencies in each preparation. In Fig. 2.20A receptive fields (at 5dB above threshold) of 4 neurons with different best frequencies, tend to move from a position 45° contralateral and 30° below the horizontal plane at 8.6kHz, to a position very close to the midline and near the horizontal plane at a frequency of 62kHz. Note that vertical head orientation in these neural experiments is such that the high frequency axial-type receptive fields are aligned to the sonar horizon (see above and Fig. 2.8). A summary of the movement of axial-type receptive field centres is shown in Fig. 2.21B for neurons with a range of best frequencies in three separate preparations. The frequency dependent locations of receptive field centres are similar to the trend shown by the acoustic axis and further suggests that the acoustical properties of the pinna are encoded neurally.

(b) *Nyctophilus gouldi*

Neural audiogram

A neural audiogram was obtained by measuring the threshold sensitivity of averaged evoked potentials from the inferior colliculus of *N. gouldi* for frequencies between 2-100kHz (see MATERIALS AND METHODS). Complete neural audiograms based on the evoked potential thresholds is shown in Fig. 2.22A for three animals. The most sensitive thresholds were 5dBSPL and occurred in a region between 8-14kHz. A

second slightly less sensitive region of peak sensitivity occurred between 22-45kHz where thresholds reached a minimum of 10dBSPL. These two regions are separated by a region of relative insensitivity between 18-20kHz but much less distinct than in *M. gigas* (Fig. 2.18). Below the most sensitive region for the neural audiogram, thresholds decreased at a rate of approximately 32dB/octave. The lowest frequency for which a reliable evoked potential could be recorded was 2kHz where threshold sensitivites normally exceeded 70dBSPL. As in *M. gigas*, it was very difficult to generate an evoked potential for frequencies below 2kHz in *N. gouldi* without the risk of spurious sensitivities due to harmonics etc. Above 40kHz evoked potential threshold sensitivities declined rapidly by an average rate of 66dB/octave. The upper limit for reliable evoked potentials occurred at 90kHz where thresholds exceeded 75dBSPL. Threshold sensitivities above 90kHz were considered artifactual due to the probable distortion generated by the high sound pressure levels required to produce an evoked potential at these frequencies.

The effect of pinna removal on neural threshold sensitivity in the inferior colliculus was also studied, following removal of the contralateral pinna as shown in Fig. 2.23 for one individual. There was a general decrease in threshold sensitivity after pinna removal and above 4kHz a loss of about 16dB occurred between 6-9kHz. A general loss of around 10dB was found up to 45kHz and for higher frequencies the effect of pinna removal decreased to less than 5dB. The "neural" gain of the pinna is shown in Fig. 2.23B together with the average acoustic gain of the pinna as determined by ear canal measurements (Fig. 2.11) and both curves have a similar structure. In particular, both gain curves start to rise above 4kHz and range between 8-14dB over a frequency bandwidth between 10-45kHz. The peak in gain between 6-9kHz

resulting from a neural change in threshold after pinna removal coincides with the suggested acoustical resonance of the pinna (Fig. 2.11B,C).

The response properties of a small sample of 29 auditory neurons in the inferior colliculus were studied, and despite a limited sample size, the frequency distribution of unit thresholds at best frequency seen in Fig. 2.22B supports the average threshold sensitivities determined by evoked potentials. The most sensitive unit thresholds were about 10dBSPL and less sensitive thresholds occurred below 9kHz and above 35kHz.

The average evoked potential audiogram can be compared to the energy bandwidth for the sonar signal of *N. gouldi* and several social communication sounds used by juveniles, which are summarized in Fig. 2.22D (see below). The FFT spectral analysis of the echolocation call is also shown in Fig. 2.22C.

Directional sensitivity of inferior colliculus neurons

The directional properties of 15 inferior colliculus neurons were studied by plotting spatial receptive field boundaries at various sound pressure levels above threshold and the response boundaries of all neurons expanded with intensity at their best frequency. Several examples of receptive fields are shown in Fig. 2.24 for best frequencies between 8-30kHz and appear as oval or circular shaped fields, reminiscent of axial-type fields seen in other mammals (Semple *et al.* 1983; Fuzessery and Pollak 1984; Jen and Sun 1984; Moore *et al.* 1984a,b). At a constant stimulus level above threshold (+ 5dB) receptive fields were seen to decrease in size with increasing frequency (Fig. 2.24) and the changes in directionality were analysed in terms of the angular size of the receptive field boundary in azimuth and

elevation at best frequency (Fig. 2.25A,B). Although the sample size is limited there is a strong suggestion that the field size is determined by a diffraction limit, which is consistent with the observations at the ear canal (Fig. 2.14). In the case of axial-type receptive fields in the inferior colliculus of *N. gouldi*, an expected -5dB acceptance angle curve is indicated, based on the average radius (0.85cm) of pinna mouth (see APPENDIX 2). There was a tendency for the best position of axial-type receptive fields to move upwards towards the sonar horizon, and towards the midline with increasing best frequency (Fig. 2.24) but the sample of inferior colliculus neurons was too small to identify a clear trend as in *M.gigas* (Fig. 2.20).

Echolocation and Social calls of *Nyctophilus gouldi*

Sonar recordings were obtained from captive adult *N. gouldi* and individuals were released into an anechoic chamber (see MATERIALS AND METHODS this Chapter) to record echolocation pulses during flight. The social calls of juvenile *N. gouldi* were obtained from hand held individuals in the anechoic chamber. Sound recording and analysis techniques were the same as outlined in CHAPTER 3. Echolocating pulses during flight ranged between 3.5-11msec in duration depending on the task and typical pulses are shown in Fig. 2.26C. Sonographic analysis indicates that the frequency content of the sonar pulses contain a dominant fundamental frequency range which is modulated from 70-35kHz with a weak second harmonic. In addition the energy band for sonar emission can be determined by FFT analysis (Fig. 2.22C) and is shown in comparison to the neural audiogram (Fig. 2.22A).

Several social sounds used by *N. gouldi* were recorded and analysed as shown in Fig. 2.26. In Fig. 2.26A, the isolation calls of two-day old individuals have a duration of 13-32msec, with descending frequency

modulation of the fundamental from 26-12kHz. A higher energy band, possibly harmonically related to the fundamental also occurs from 50-28kHz in the isolation call. In Fig. 2.22B, a protest call elicited from a 29 day old individual is illustrated and is similar in structure to the isolation call of the young neonate, but the fundamental energy band ranges in frequency from 45-25kHz. A summary of the energy in the social sonar calls is indicated in Fig. 2.22D and suggests that the higher peak of hearing sensitivity in the neural audiogram above 25kHz (Fig. 2.26B) corresponds to the energy band of the sonar signal, and also the protest call. In contrast the isolation call of the young neonate corresponds to the lower region of maximum auditory sensitivity below 20kHz.

DISCUSSION

Acoustic gain of the pinna

In the two Microchiropteran bats studied here, about 25dB of pressure amplification occurs at the position of the tympanic membrane as a result of a transformation by the external ear (Figs. 2.2,2.11). In both *M. gigas* and *N. gouldi* the acoustic gain of the pinna is similar in a mid-frequency band where the pinnae become reasonably efficient horns. In *M. gigas* there is meatus resonance which, together with the gain of the pinna, creates a distinct peak in amplification of sound pressure in the ear canal between 5-9kHz. There is some suggestion that pinna resonance may also occur, which can be understood from a comparison with the expected gain curves for a series of finite horns with equivalent dimensions (Fig. 2.2B,C). The normal gain curve for the external ear in *N. gouldi* also reveals a possible resonance of the pinna but in the absence of any clear meatus resonance (Fig. 2.11). The

smaller size of the external ear in *N. gouldi* compared to *M. gigas* results in an extremely short meatus (Table 2.1) which fails to demonstrate any clear resonance.

The method of comparing the acoustic pressure gain at the tympanic membrane before and after pinna removal is only an approximate procedure for identifying the effective gain of the pinna since the pinna and meatus are normally acoustically coupled. Nevertheless, this approach is useful in identifying the pinna as a horn-like pressure transformer. In both *M. gigas* and *N. gouldi* the frequency development of pinna gain resembles, to a first approximation, the increasing efficiency of a simple conical horn although in reality the pinnae of both species have substantial asymmetries and lose efficiency at high frequencies. The rising slope of the gain curve for the pinna of *M. gigas* is shifted by about an octave compared to *N. gouldi* suggesting a greater efficiency at lower frequencies in *M. gigas* because of the larger pinna size (Table 2.1). In order to model the acoustical gain of the pinnae in *M. gigas* and *N. gouldi* it was necessary to consider the pinnae as finite horns (see APPENDIX 1; Olson 1947, Beranek 1954). Consequently horn resonance is expected and probably corresponds to the low frequency peaks on the rising slope of the gain curve for each species (Figs. 2.2, 2.11). In each case horn resonance lies between a half and quarter wave series which depends on the flare of the pinna (cone angle) when treated as a finite horn (see APPENDIX 1 and also Table 2.1; Beranek 1954).

The effect of the pinna on the neural sensitivity of the auditory system to sound was examined by measuring threshold changes for evoked potentials recorded from the inferior colliculus of *M. gigas* and *N. gouldi* (Figs. 2.19, 2.23). The results are tentative in both species

but suggest that there is a significant contribution of the pinna to neural threshold sensitivity which is similar to the acoustic gain of the pinna over a similar frequency range. There are, of course, limitations in measuring the effect of the pinna on neural responses at the level of the inferior colliculus because there are many other influences on auditory sensitivity which are not obvious from measurements of acoustic pressure in the ear canal. In *M. gigas* the contribution of the pinna to neural sensitivity appears greatest in the two regions of peak sensitivity which lie between 10-20kHz and 30-50kHz but there is a slight mismatch between the bandwidth of maximum pressure amplification by the external ear as a whole and the lower region of maximum neural sensitivity to sound (Figs. 2.2, 2.19). Thus, although the pinna makes a significant contribution to neural sensitivity, there may well be unrecognized specializations, in the cochlea or basilar membrane for example, which relate to low frequency hearing in Megadermatids (Fiedler *et al.* 1982). In the case of *N. gouldi*, the effect of the pinna on neural sensitivity is more consistent with the acoustical data on pressure gain.

Frequency sensitivity of the auditory system

The neural audiogram obtained in *M. gigas* under normal conditions shows remarkably high sensitivity in the "audio" bandwidth between 10-20kHz where both averaged evoked potentials and unit thresholds approach -16dBSPL. Similar thresholds in this frequency range have been reported for another Megadermatid bat, *Megaderma lyra* using a similar evoked potential recording technique from the midbrain (Neuweiler *et al.* 1984). In *M. lyra* neural thresholds are very close to those obtained by measuring the behavioural audiogram, at least for frequencies below 20kHz (Schmidt *et al.* 1984). Megadermatid bats appear to have the most

sensitive hearing thresholds yet reported for Microchiropteran bats (see Dalland 1965; Long and Schnitzler 1975; Neuweiler 1984) and which rival threshold sensitivities reported for other nocturnal predators such as owls (Konishi 1973a; Van Dijk 1973) and the cat (Neff and Hind 1955; Flynn and Elliott 1965).

Double sensitivity peaks for hearing have been observed for a number of Microchiropteran bats and often can be related to the energy bands used for sonar and social communication (Dalland 1965; Long and Schnitzler 1975; Schuller 1980; Suthers and Summers 1980; Neuweiler 1984; Neuweiler *et al.* 1984). Such a relationship exists between hearing and vocalizations in *M. gigas* (Fig. 2.18 and CHAPTER 3). For example, the high frequency sensitivity peak in the audiogram of *M. gigas* between 35-43kHz is clearly related to sonar processing since the fundamental frequencies used in the echolocation pulse are suppressed relative to the dominant higher harmonics (Figs. 2.18, 3.1). In contrast, commonly used social communication sounds such as the chirp and squabble contain energy bands which are matched to the low frequency sensitivity peak below 20kHz (Figs. 2.18, 3.3, 3.4, 3.6). In addition the sound energy in the chirp and squabble contains frequencies which would be highly amplified by the external ear (Fig. 2.2A). High amplification by the external ear, coupled with very sensitive hearing below 20kHz may be particularly important for the chirp call since it is used for long distance communication in the foraging areas at night (see CHAPTER 3).

The high frequency sensitivity peak between 22-45kHz in the neural audiogram of *N. gouldi* is correlated with sonar frequencies (Figs. 2.22. 2.26) and although social vocalizations were not studied in detail, it seems likely that the low frequency sensitive region between 8-14kHz is

used extensively for social communication as suggested by the neonatal vocalizations (Figs. 2.22,2.26). A similar relationship between hearing sensitivity and vocal energy has been demonstrated for *Antrozous pallidus* (Brown and Grinnell 1980) which is a neotropical species occupying a similar ecological niche to *N. gouldi*.

Low frequency hearing in bats

The existence of sensitive "low frequency" hearing in several bat species may be linked to acoustic orientation by passive listening in contrast to the active process of echolocation. There is evidence that captive *Megaderma lyra* can catch live prey in total darkness without the use of sonar (Fiedler 1979). The ability of some bats to hunt passively by listening is analogous to the techniques of nocturnal predators such as the barn owl (Payne 1971; Konishi 1973a,b). Clearly the threshold sensitivities for hearing seen in the present study for *Macroderma gigas* and those reported in *Megaderma lyra* (Neuweiler *et al.* 1984; Schmidt *et al.* 1984) may represent specific adaptations to foraging by listening. However, there is evidence that other gleaner bats probably hunt by passive listening such as *Antrozous pallidus* (Bell, 1982) and *Nyctophilus gouldi* (Grant, personal communication). In comparison to Megadermatid bats, *A. pallidus* and *N. gouldi* do not appear to have developed such extreme threshold sensitivities to sound (Brown *et al.* 1984 and Fig. 2.22). Highly sensitive hearing thresholds are obviously an advantage for the detection of prey noises by listening but the evidence presented here for *M. gigas* also supports the idea of a specific low frequency communication channel which is used for social interactions (see CHAPTER 3).

There is clear evidence supporting the role of passive listening for hunting in *Trachops cirrhosus* and this species discriminates between

poisonous and palatable species of frogs on the basis of species specific advertisement calls (Tuttle and Ryan 1981; Ryan and Tuttle 1983). *T. cirrhosus* is likely to rely on frequencies below 5kHz based on the energy bands contained in the advertisement calls of potential prey species (Rand and Ryan 1981; Ryan and Tuttle 1983). The detection and recognition of such prey is supported by unusually sensitive low frequency hearing below 5kHz as demonstrated by behavioural thresholds to sound (Ryan *et al.*, 1983). Similarly, *Eptesicus fuscus* has an unusual sensitivity to frequencies near 1kHz (Poussin and Simmons 1982) and this species is known to orientate towards distant frog and cricket choruses (Buchler and Childs 1981). Clearly prey detection by listening to low frequencies is useful in terms of long range orientation, but the definition of "low frequency" is relative and more data is necessary on the bandwidths used for prey capture by listening.

The Megadermatidae probably rely heavily if not exclusively on passive listening for prey capture rather than sonar and the data on auditory sensitivity presented here for *Macroderma gigas* (Fig. 2.18) and also reported for *Megaderma lyra* (Neuweiler 1984; Neuweiler *et al.* 1984; Schmidt *et al.* 1984) suggest that the "low frequency" bandwidth between 10-20kHz may be particularly useful for passive prey detection. The development of relatively large pinnae in bats, as seen in the Megadermatidae (Fig. 2.1 and Walker 1975) may serve to enhance auditory sensitivity particularly at lower frequencies which are not used for sonar. However, there are examples in which large ears are obviously linked with the use of low frequency sonar signals e.g. *Euderma maculatum* (Woodsworth *et al.* 1981; Leonard and Fenton 1983).

Function of the tragus

The tragus is a cartilaginous protuberance which is positioned at the entrance to the pinna. It only occurs in Microchiropteran bats and is absent in some species. A tragal notch can be identified in most mammalian pinnae but is considered vestigial. The tragus, as an accessory structure of the external ear, has been associated with hearing in bats although its function has remained somewhat obscure. *M. gigas* has a particularly well developed tragus (Fig. 2.1) but an acoustical function could not be clearly identified in the present experiments. Removal of the tragus had no measurable effect on pressure gain at the tympanic membrane and only a very small effect on directionality (Fig. 2.9). The lack of effect on pressure gain in *M. gigas* is consistent with the neural data of Grinnell and Grinnell (1965) following tragus removal in *Myotis* and *Plecotus*. These authors also reported a small effect on neural directionality since minima in the directivity patterns and the acoustic axis were relocated in space, but precise details were not given. Similar effects of tragus removal were also apparent in the present study on *M. gigas* based on acoustical measurements in the ear canal but the possible function of the tragus in this species remains to be determined.

Lawrence and Simmons (1982) found that the spatial acuity for vertical localization in *Eptesicus fuscus* was degraded by manipulation of the tragus. Although *M. gigas* has a prominant tragus, a role in vertical localization cannot be concluded from the present acoustical measurements.

Directionality of hearing in bats

In *M. gigas* and *N. gouldi* it was clear that the pinna plays a major role in controlling the directionality of sound pressure at the tympanic

membrane by sound diffraction at the open face or mouth. The characteristics of the main lobe of the ear canal directivity patterns are close to that expected from sound diffraction at a single circular aperture (Figs. 2.5, 2.6, 2.14, 2.15 and see APPENDIX 2). The importance of the pinna in producing directionality is also supported by the effect of pinna removal (Figs. 2.9A, 2.17) which decreases directionality and severely disrupts the normal directivity patterns, including the position of the acoustic axis. Previous experiments on *Myotis l. lucifugus* and *Plecotus townsendi* have shown that folding back the pinna severely disrupts directionality (Grinnell and Grinnell 1965). In bats with mobile ears, experimental manipulation of the orientation of the pinna on the head affects the directional sensitivity of the auditory system, notably by relocation of the main lobe (Neuweiler 1970; Grinnell and Schnitzler 1977; Jen and Sun 1984).

The absolute size of the pinna influences the degree of directionality due to diffraction by a specific relationship between the size of the opening and the wavelength of the incident sound (APPENDIX 2). Consequently the pinna in *M. gigas* which has an open face about four times larger in area than that of *N. gouldi*, becomes directional at significantly lower frequencies. In acoustical terms the development of maximum directionality in *M. gigas* precedes *N. gouldi* by about an octave (Figs. 2.4, 2.13). The key parameter which determines directionality is the ratio between the circumference (and hence radius) of the opening and the wavelength, which can be conveniently expressed as the ka value (Olson, 1947; Beranek 1954; see also GENERAL DISCUSSION AND CONCLUSION and APPENDIX 2). In both species the development of maximum directionality (Figs. 2.4, 2.13), the -3dB acceptance angle (Figs. 2.5, 2.14) and the semi-angle of the main lobe (Figs. 2.6, 2.15) can be

favourably compared in terms of ka values (see also GENERAL DISCUSSION AND CONCLUSIONS, Figs. 6.1, 6.2). Thus directionality becomes significant when the average radius of the pinna face starts to exceed about one fifth of the wavelength ($ka > 1.25$) and becomes highly directional when the average radius exceeds half of the wavelength ($ka > 3.14$; Beranek 1954; Fletcher and Thwaites 1979).

From a limited sample, the directional properties of midbrain auditory neurons examined in *M. oigas* and *N. gouldi* typically displayed "axial-type" spatial receptive fields as originally defined in the cat auditory cortex (Middlebrooks and Pettigrew 1981). A test for "axiality" by passive reorientation of the pinnae on the head is not feasible in *M. gigas* and *N. gouldi* because the pinnae cannot be moved without considerable distortion. Nevertheless, measurement of the "neural" acceptance angle derived from spatial receptive field boundaries (Figs. 2.21, 2.25) strongly suggest that directionality is also diffraction-limited and therefore linked to the acoustical properties of the pinna. Of course, neural directionality is also influenced by binaural processing which is likely to sharpen directionality (Grinnell 1963b; Neuweiler 1970).

Neural data from other Microchiropteran bats show that the sharpness of directionality increases with frequency and depends on the species (Suga 1964; Grinnell and Grinnell 1965). In *Plecotus townsendii*, Grinnell and Grinnell (1965) found the sensitivity range of N_4 (collicular) potentials within the frontal hemisphere reached 36dB between 27-32kHz. Whereas in *Myotis l. lucifugus* the average directional sensitivity increased to 37dB from 60kHz. These differences in neural sensitivity ranges can be understood in terms of the wavelength effect on the different sized pinnae in these two species

(see Table 2.1), as is evident for *M. gigas* and *N. gouldi*.

Since sound diffraction by the pinna mouth generates nulls in the directivity pattern they play an important role in determining the angular gradient (dB/degree) for directionality at the ear. The null regions seen in the ear canal directivity patterns of *M. gigas* and *N. gouldi* can be explained by diffraction (Figs. 2.6, 2.15) although the pinna mouth is not part of an ideal symmetrical horn-like waveguide. In comparison to the directivity of a baffled circular opening, the presence of nulls in the frontal hemisphere have a lower limit near $ka = 3.83$ (see APPENDIX 2) for both *M. gigas* and *N. gouldi*, which means of course that a greater angular resolution of the main lobe is possible at lower frequencies in *M. gigas* because of the larger pinna (Table 2.1; Figs. 2.6, 2.15). This fact may have an important bearing on the accuracy of sound localization at low frequencies in *M. gigas* in view of the extreme good sensitivity to sound below 20kHz (Fig. 2.18). However, experimental data on passive sound localization, comparable to that available for the barn owl (Knudsen and Konishi 1979; Knudsen *et al.* 1979), has yet to be obtained in gleaning bats such as *M. gigas*.

Relationship between auditory space and frequency

The data presented in this chapter support the idea that the directionality of hearing in *M. gigas* and *N. gouldi* increases with frequency as a result of sound diffraction by the pinna. In both *M. gigas* and *N. gouldi* it was found that the spatial location of the main lobe, as estimated by the position of the acoustic axis, was frequency dependent for certain bandwidths (Figs. 2.7, 2.8, 2.16). This phenomenon appears to be related to the asymmetry of the pinna which resembles an obliquely truncated conical horn (Figs. 2.1, 2.8, 2.10, 2.16; APPENDIX 3). The significance of the frequency dependent location

of the acoustic axis is unclear at present but appears to determine the position of spatial receptive fields of neurons in the inferior colliculus of *M. gigas* for example (Fig. 2.20). A similar relationship has been reported in *Pteronotus parnellii* for cochlear microphonic directionality and inferior colliculus neuronal spatial receptive fields (Fuzessery and Pollak 1984). In the case of *P. parnellii*, the relationship between auditory space and frequency is demonstrated for the energy bands used during echolocation. In contrast, the present findings for *M. gigas* and *N. gouldi* show that auditory space and frequency at the ear are covariant for frequencies below the echolocation bandwidth (Figs. 2.7, 2.8, 2.16) and may be related to aspects of spatial orientation during social communication (see CHAPTER 3) or passive prey capture where pinna movements are not possible.

TABLE 2.1: DIMENSIONS AND PARAMETERS FOR VARIOUS EXTERNAL EARS IN VERTEBRATES

SPECIES	PINNA/OUTER EAR CAVITY (MOUTH)				DIRECTIONALITY		PINNA/OUTER EAR CAVITY (THROAT)		HORN LENGTH			MEATUS	TYMPANIC MEMBRANE	HORN PARAMETERS		
	circum-ference $2\pi a$ (cm)	av. radius a (cm)	height (cm)	width (cm)	onset ka=1.25 (kHz)	high ka = 3 (kHz)	circum-ference $2\pi a$ (cm)	av. radius a (cm)	Long (cm)	Short (cm)	Average (ℓ) (cm)	length (cm)	av. radius (cm)	G_∞ (dB)	cone angle	$\frac{2a}{\ell}$ (mouth)
Macroderma gigas[a]	10.7	1.7	5.6	2.2	4.0	9.6	4.0	0.4	4.3	0.6	2.4	1.1	0.14	13	29°	1.4
Nyctophilus gouldi[a]	5.3	0.85	2.8	1.2	8.1	18	1.1	0.2	2.2	0.4	1.3	0.25	0.14	13	27°	1.3
Macropus eugenii[a]	16	2.5	7.0	3.5	2.7	6.4	2.5	0.4	7.5	1.5	4.5	1.6	0.25	16	25°	1.1
Macropus giganteus[a]	24.5	3.9	8.2	3.0	1.76	4.2	6.9	1.1	9	2	5.5	3.2	0.27	11	27°	1.4
Tyto alba[a]	19	3.0	7.0	4.5	2.3	5.4	2.2	0.4	7.0	1.8	4.4	0.8	0.46	18	30°	1.4
Myotis l. lucifugus[b]	3.8	0.6	1.4	0.7	11.0	27										
Plecotus townsendii[b]	8.4	1.3	3.7	1.2	5.0	12										
Felis catus[c]	14.5	2.3	5.5	3.0	2.9	7.1	2.5	0.4	6.0	2.5	4.3	2				
Trichosurus vulpecula[c]	14.2	2.3	5.8	3.3	3.0	7.3			5.5	1.1	3.3					

a = present study, b = Grinnell & Grinnell 1965, c = personal observations

Fig. 2.1. General appearance of the head of the ghost bat (*Macroderma gigas*). Dimensions are in millimeters, see also summary in Table 2.1, 6.1.

A. Sagittal view of head. Vertical orientation is relative to the sonar horizon as indicated by the horizontal line (see text, also Fig. 2.8). Note the prominent noseleaf and bi-lobed tragus.

Below: Schematic diagram of a vertical cross section through the asymmetrical pinna indicating the geometry used to predict movement of the acoustic axis in elevation as a function of frequency (see APPENDIX 3 and text for details). Dashed line = open face of pinna; dotted line (a_o) = mouth of pinna at the approximate truncation point (as in C).

B. Frontal view. Note fusion of pinnae at their medial edge over the midline of the head (arrow) and prominent tragi. Inter-naral separation is indicated (see CHAPTER 3).

C. Horizontal view, indicating the mutual inclination of the pinnae to the midline of the head and their junction at the rostral end of the dorsal skull.

Below: Inclination of the pinna to the midline and schematic geometry of pinna based on a horizontal cross section as used to predict the movement of the acoustic axis in azimuth as a function of frequency, as in A. For details see APPENDIX 3 and text.

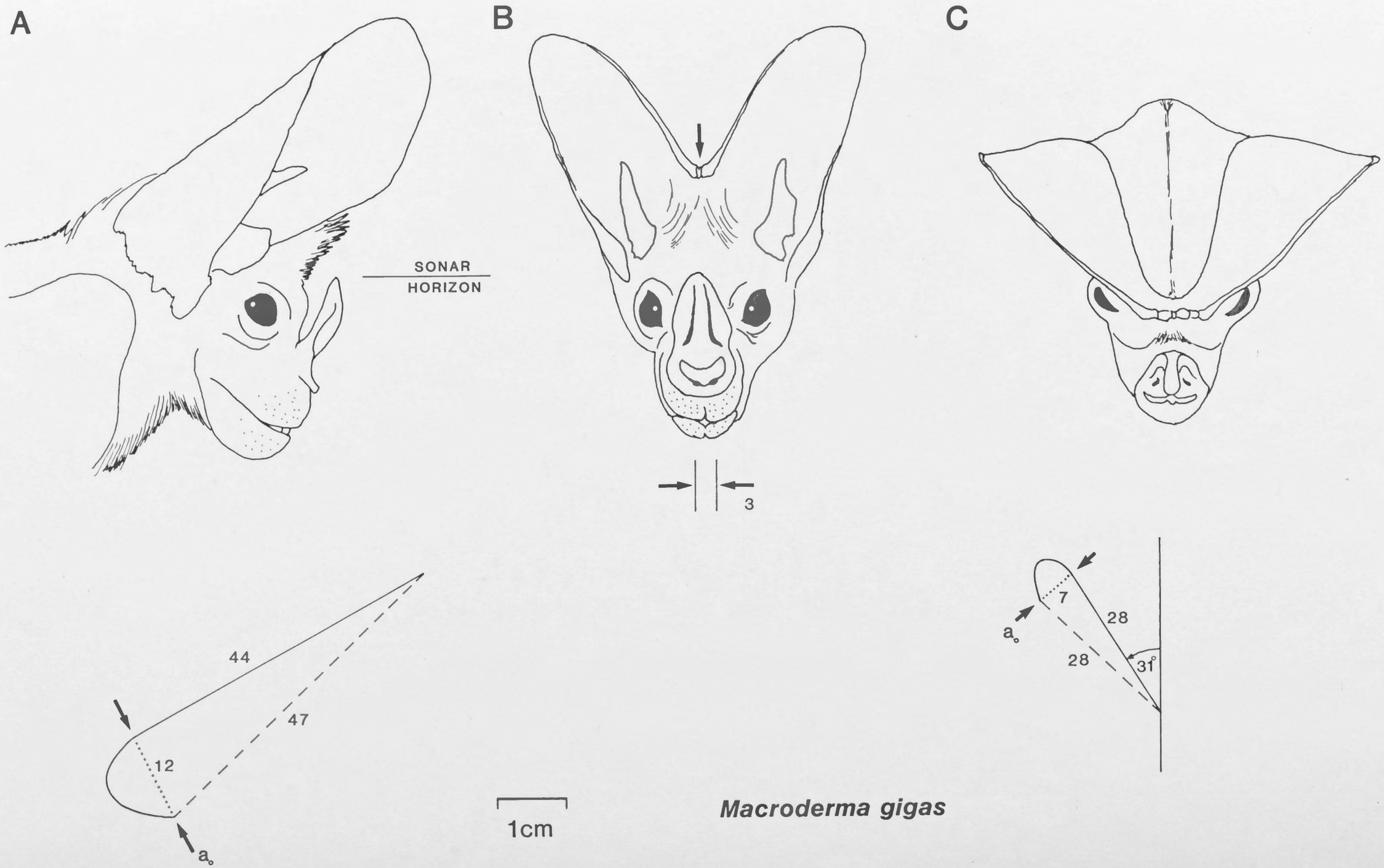

Macroderma gigas

Fig. 2.2: Measurements of acoustic pressure gain obtained from a replacement microphone ($\frac{1}{8}$ " Bruel and Kjaer Type 4148) in the ear canal of *Macroderma gigas* at the position of the tympanic membrane.

A. Gain curves for five ears under normal (intact) conditions (solid lines). Dotted curve is a typical example of a gain curve from one ear after removal of the ipsilateral pinna.

B. The effective gain of the pinna (four ears) calculated as difference curves between normal and pinna-removed gain curves as shown in A. The ratio of the circumference of the open face of the pinna (mouth) relative to the wavelength (ka) is represented as a scale (see Table 2.1, and text for details). Dotted line is expected gain for an equivalent finite conical horn based on the dimensions of the pinna (see APPENDIX 1, Table 2.1 and text).

C. Average gain curve (solid line) for the pinna of *M. gigas* based on the curves in B. Dotted lines are expected gain curves for a finite paraboloidal, conical and exponential horn based on the dimensions of the pinna as given in Table 2.1 (see also Fig. 2.1 for morphology of pinna). For details of calculations see APPENDIX 1.

A

Macroderma gigas

ACOUSTIC PRESSURE GAIN OF THE EXTERNAL EAR (dB)

FREQUENCY(kHz)

B

ka

GAIN OF THE PINNA (dB)

FREQUENCY (kHz)

C

ka

GAIN OF THE PINNA (dB)

EXP

CON

PARA

FREQUENCY (kHz)

Fig. 2.3: Examples of ear canal directionality at various test frequencies (as indicated in kHz) for the left ear in *Macroderma gigas*. Directivity patterns are represented as a series of iso-intensity (pressure) contours plotted onto a two dimensional projection of the frontal hemisphere (see MATERIALS AND METHODS). The position of the acoustic axis is located within the 1dB contour which is plotted relative to the axial sound pressure (solid line, open circles). Likewise a series of "iso-intensity" contours are plotted at 5dB intervals down to -25dB relative to the on-axis pressure.

Macroderma gigas Acoustic axis iso-intensity contours (left ear)

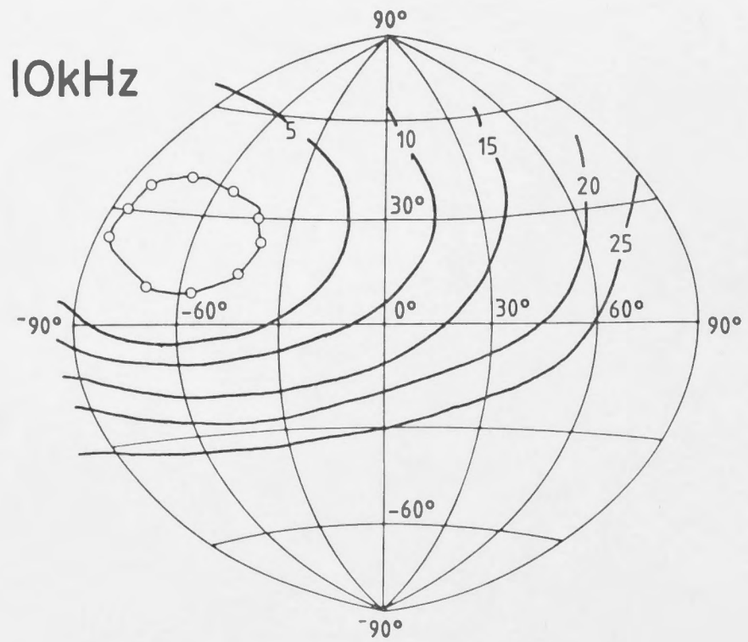

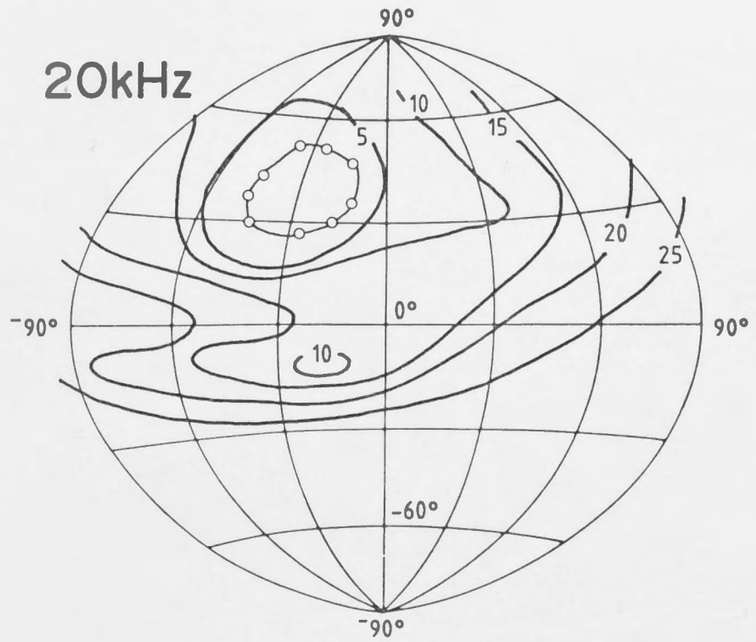

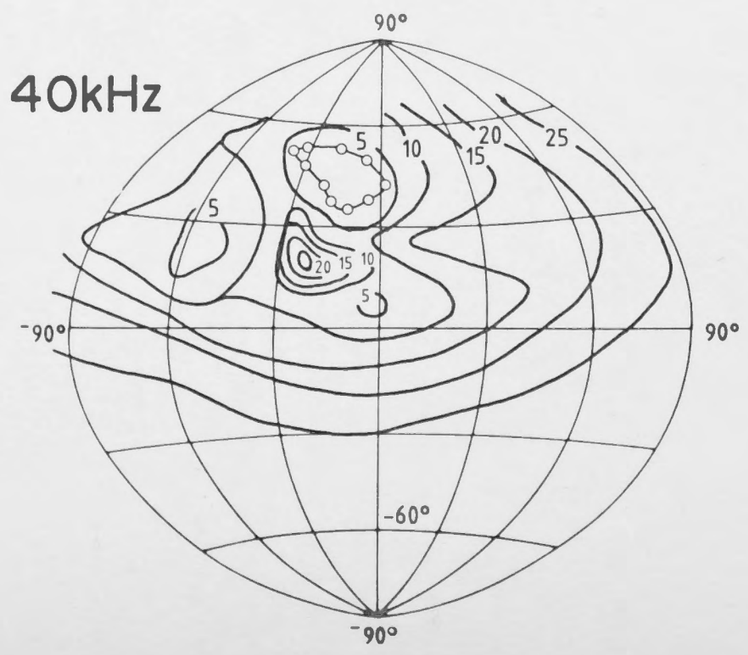

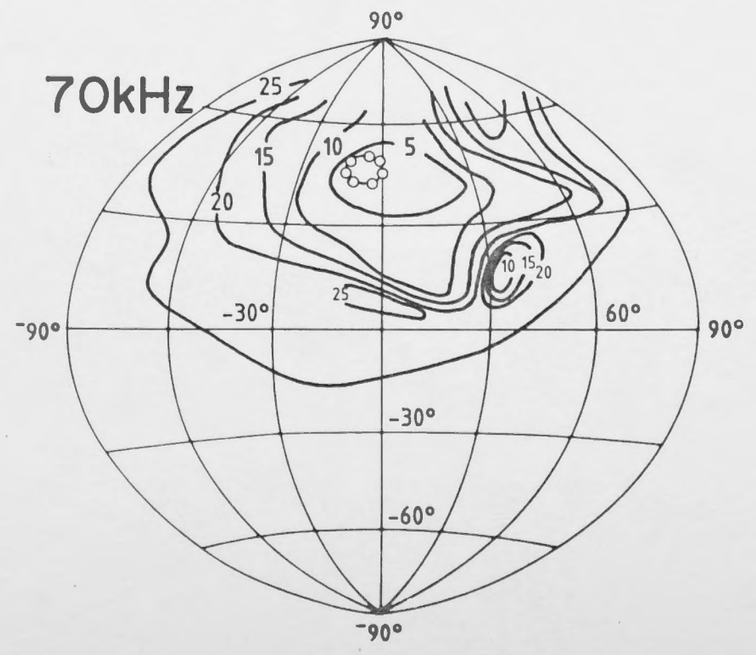

Fig. 2.4: Summary of the maximum difference in sound pressure (dB_{max}) for ear canal directivity patterns in *Macroderma gigas* (as in Fig. 2.3) as a function of frequency (4 ears). The ratio between the circumference of the pinna face (mouth) to the wavelength is represented as a *ka* scale (a = 1.7cm see Table 2.1) as for a circular aperture in a physical system (see Beranek 1954).

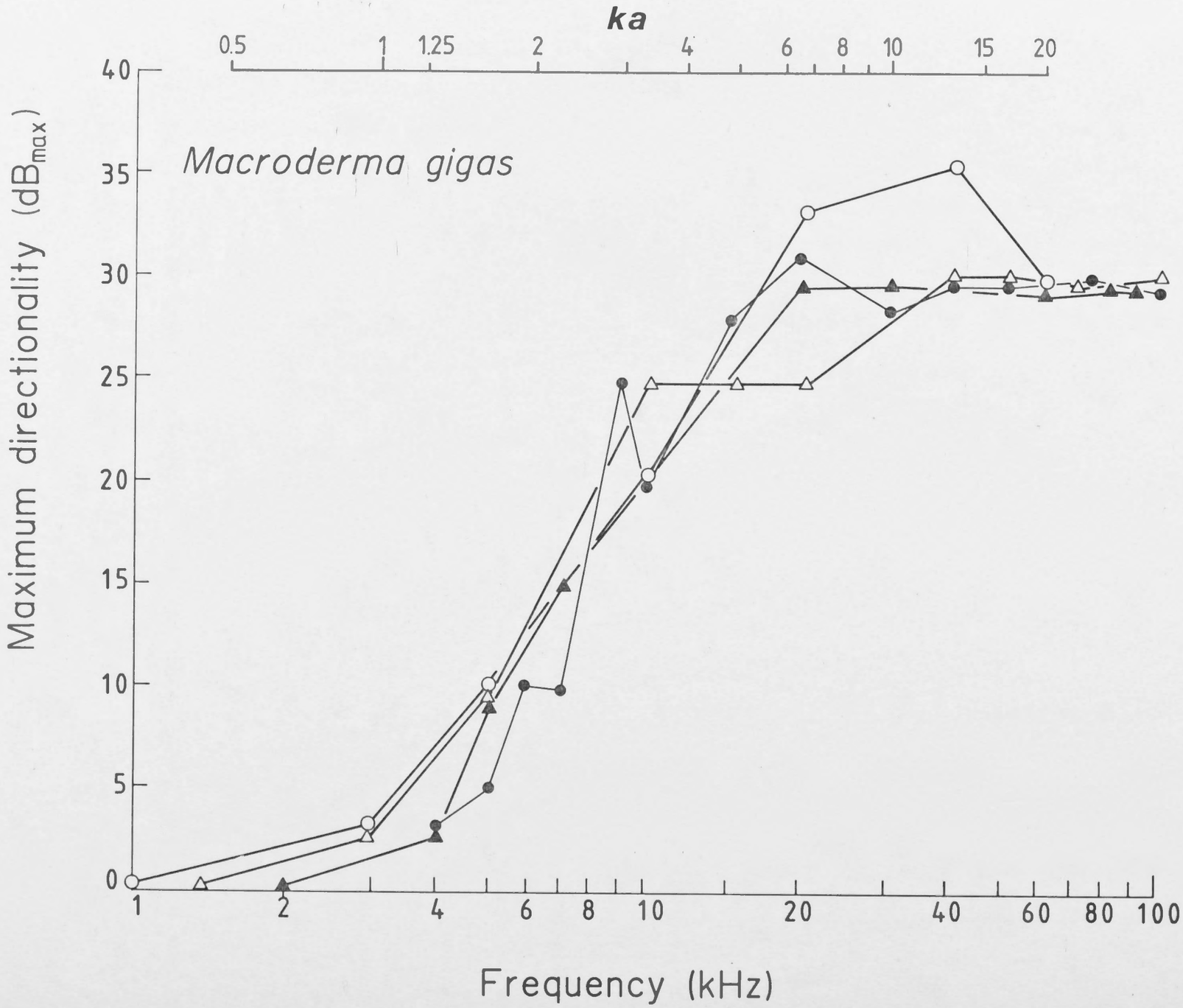
ka
0.5
1
1.25
2
4
6
8
10
15
20
Macroderma gigas
Maximum directionality (dB$_{max}$)
40
35
30
25
20
15
10
5
0
1
2
4
6
8
10
20
40
60
80
100
Frequency (kHz)

Fig. 2.5: Measurement of the acceptance angle (-3dB relative to the on-axis sound pressure) for ear canal directionality in *Macroderma gigas* (four ears) as shown in Fig. 2.3 and expressed as the full angular width ($2\theta°$). A = azimuth; B = elevation. Solid curves are expected -3dB acceptance angles for sound diffraction by a circular aperture with an average radius equal to that of the open face of the pinna in *M. gigas* (a = 1.7cm; Table 2.1). For details of calculations see APPENDIX 2 and text.

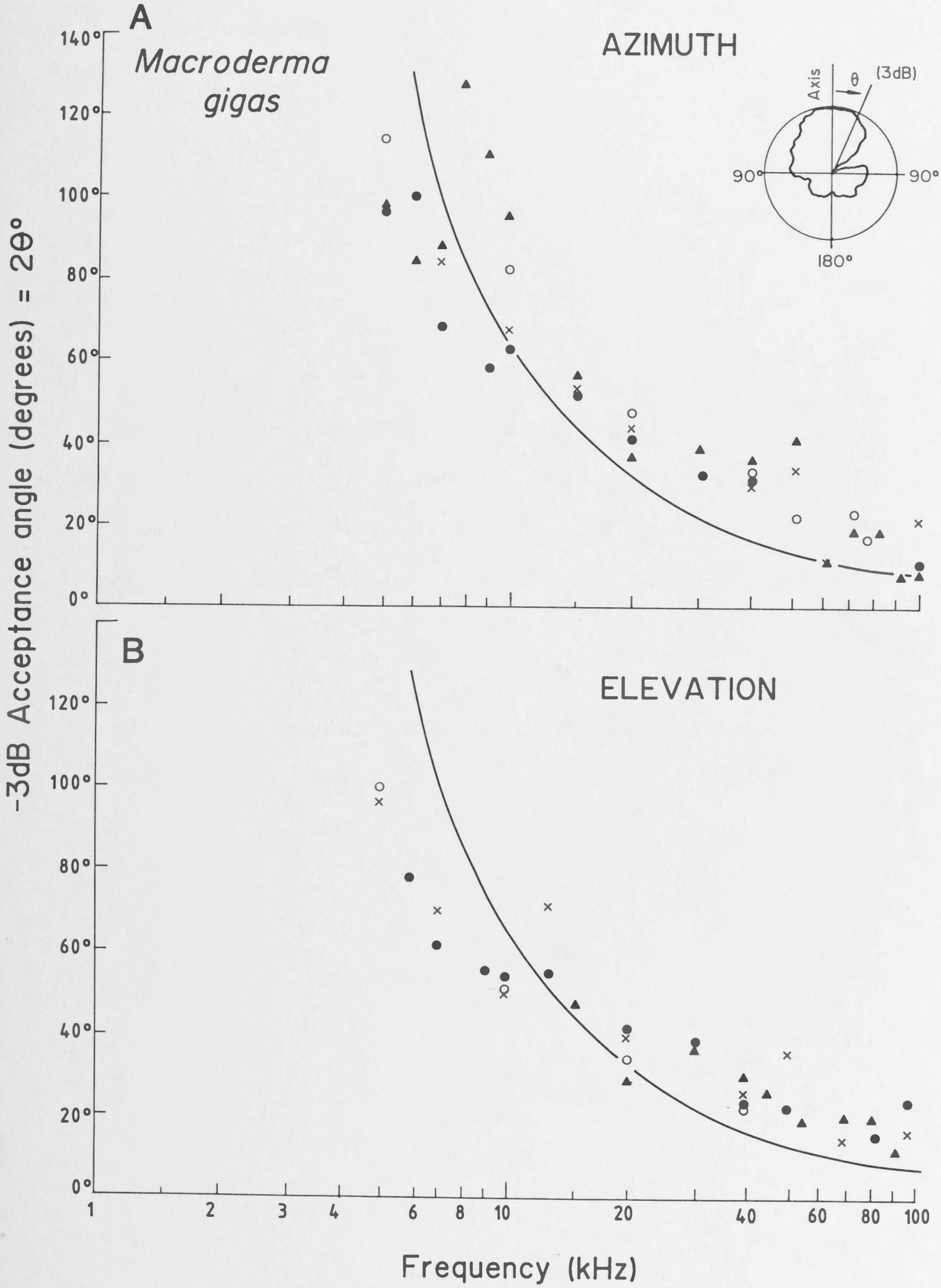
A
Macroderma gigas
AZIMUTH
Axis
θ
(3dB)
90°
90°
180°
140°
120°
100°
80°
60°
40°
20°
0°
B
ELEVATION
120°
100°
80°
60°
40°
20°
0°
-3dB Acceptance angle (degrees) = 2θ°
1
2
3
4
6
8
10
20
40
60
80
100
Frequency (kHz)

Fig. 2.6: Positions of nulls from ear canal directivity patterns in *Macroderma gigas* relative to the position of the acoustic axis (θ°) as a function of stimulus frequency (four ears). Solid curve represents the expected semi-angles which would result from sound diffraction by a circular aperture in a plane wall with a radius equivalent to the average radius of the pinna mouth (a = 1.7cm; Table 2.1). For details of calculations see APPENDIX 2 and text. The lower frequency limit for a diffraction null in frontal space generated by a circular aperture in a plane wall occurs at 90° off axis and is indicated at ka = 3.83, (see Beranek 1954 and APPENDIX 2).

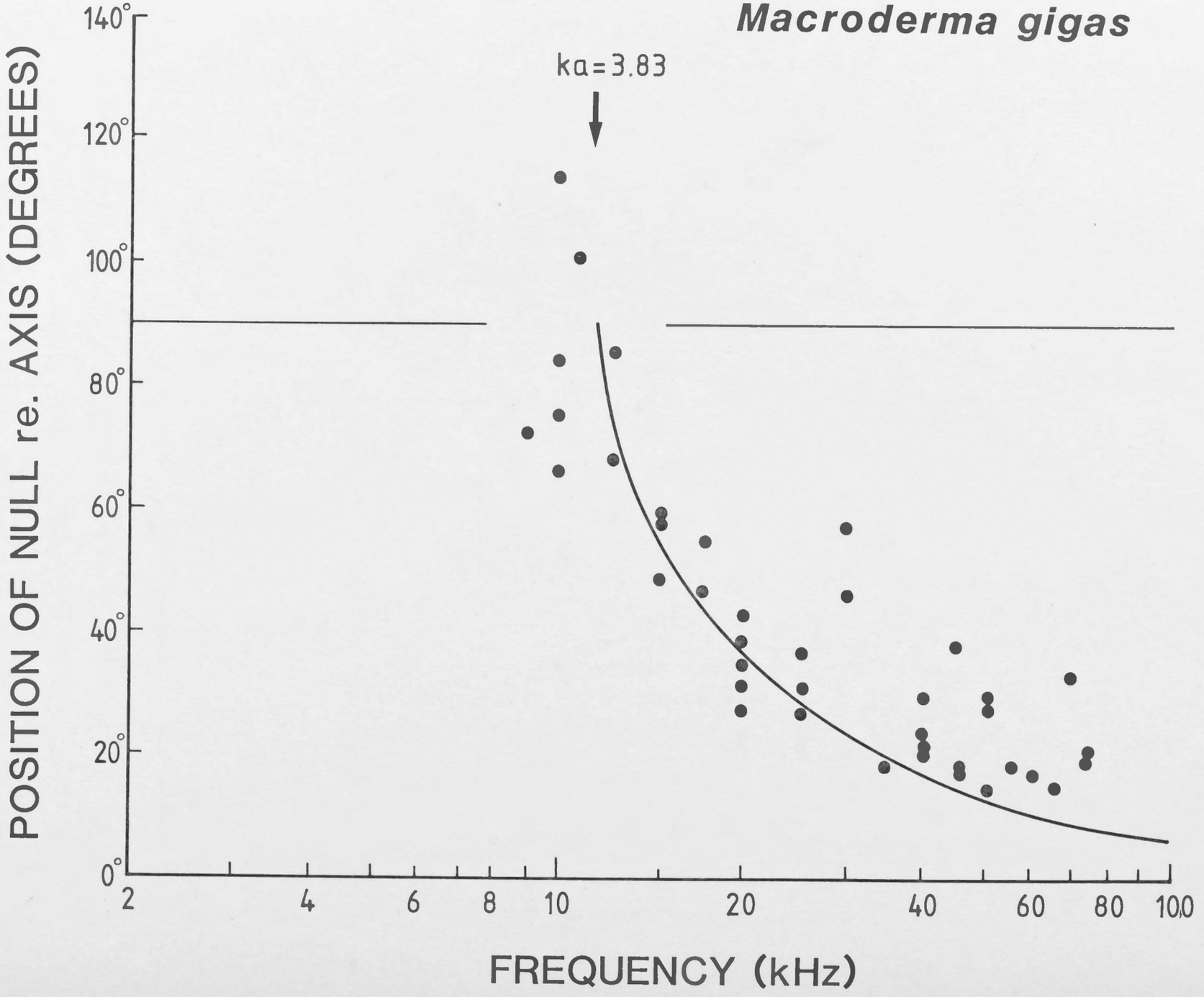
Macroderma gigas
ka=3.83
POSITION OF NULL re. AXIS (DEGREES)
140°
120°
100°
80°
60°
40°
20°
0°
2
4
6
8
10
20
40
60
80
100
FREQUENCY (kHz)

Fig. 2.7: Movement of the acoustic axis in two dimensional space for the left and right ear of an individual *Macroderma gigas*. Numbers connected by lines are acoustic axes for each test frequency (kHz). The midline of the head was aligned in the 0° azimuthal (vertical) plane and thus the acoustic axes are approximately symmetrical about this plane. In elevation the position of the horizontal plane is arbitrary but acoustic axis positions above 20kHz may constitute a "sonar" horizon (see Fig. 2.8 and text).

Macroderma gigas
Acoustic axis versus
Frequency (kHz)

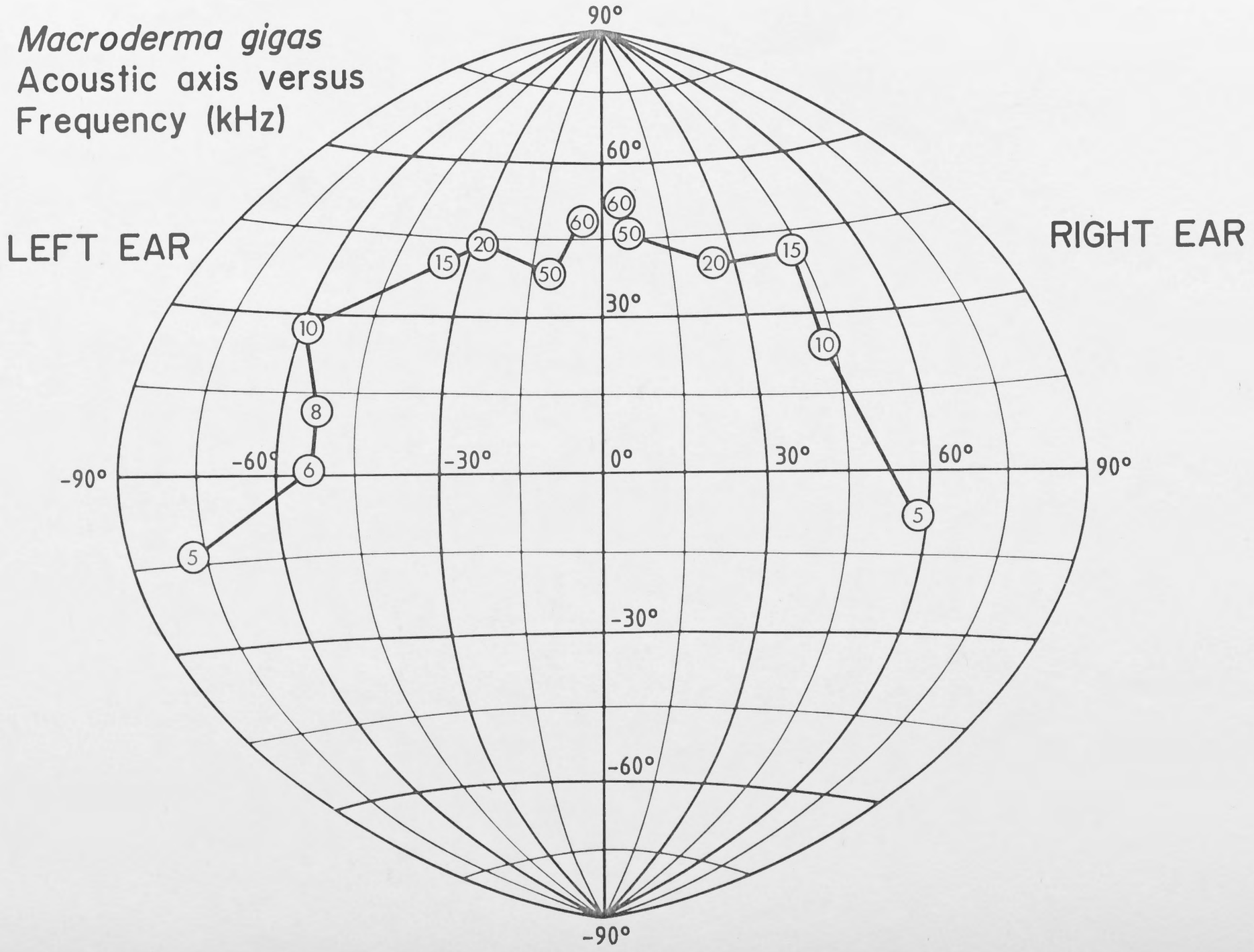

Fig. 2.8: A. Average movement of the acoustic axis in azimuth (solid curve) in *Macroderma gigas* (four ears). Vertical bars are standard errors.

B. Horizontal view of the head and pinnae of *M. gigas* for reference to A (see also Fig. 2.1C).

C. Average movement of the acoustic axis in elevation (solid curve) as in A. For data collection head orientation in the vertical plane can be referenced to an arbitrary horizontal plane (0°) as used in Figs. 2.3, 2.7, 2.9 (left ordinate axis in C), or referenced to a "sonar" horizon used in Fig. 2.20 (right ordinate axis in C) which is based on the elevation positions of acoustic axes for frequencies above 20kHz (sonar bandwidth indicated by bars in C and A, for details see CHAPTER 3, Fig. 3.1 also Table 3.1; see also CHAPTER 2, Fig. 2.18).

D. Sagittal view of the head of *M. gigas* as in Fig. 2.1 showing orientation of head with respect to a "sonar" horizon which is probably used during horizontal flight.

In A. and C. dotted curve = expected movement of acoustic axis based on geometry of the oblique truncation of the pinna in *M. gigas*, as shown schematically in Fig. 2.1A,C. Calculations for theoretical movement of the acoustic axis as a function of wavelength are given in APPENDIX 3. For further details see text.

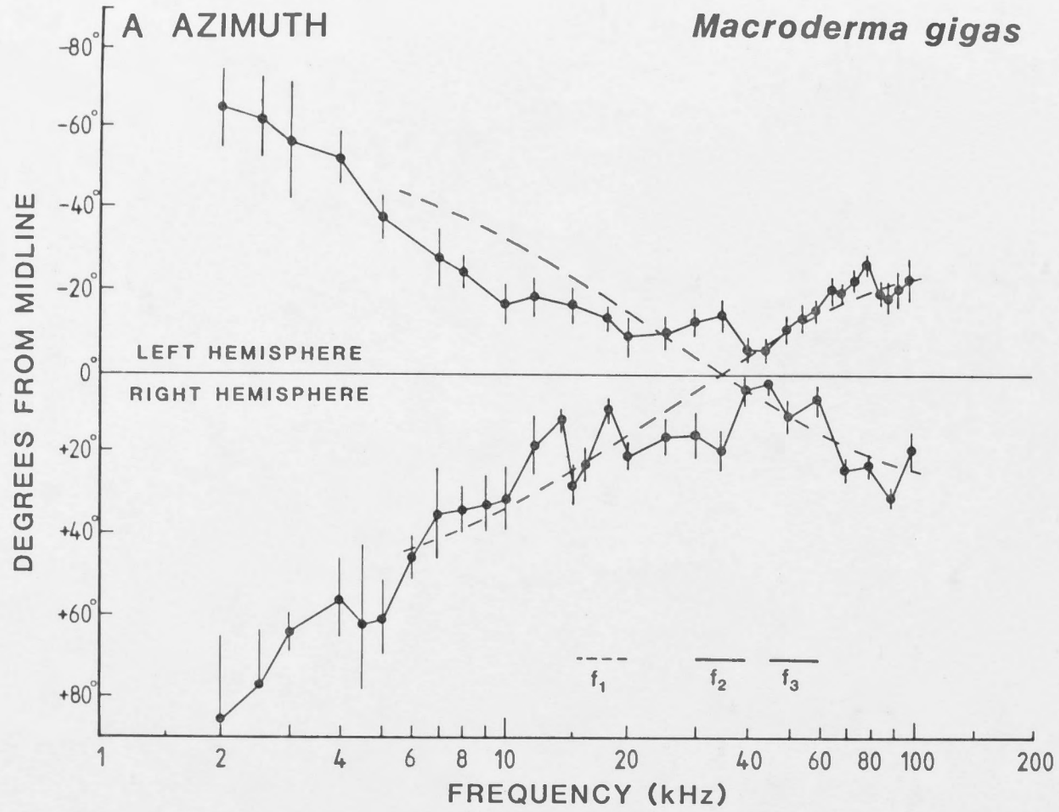
A AZIMUTH
Macroderma gigas
DEGREES FROM MIDLINE
-80°
-60°
-40°
-20°
0°
+20°
+40°
+60°
+80°
LEFT HEMISPHERE
RIGHT HEMISPHERE
f1
f2
f3
1
2
4
6
8
10
20
40
60
80
100
200
FREQUENCY (kHz)

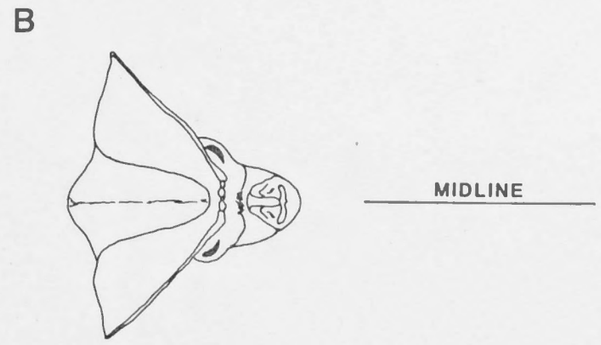
B
MIDLINE

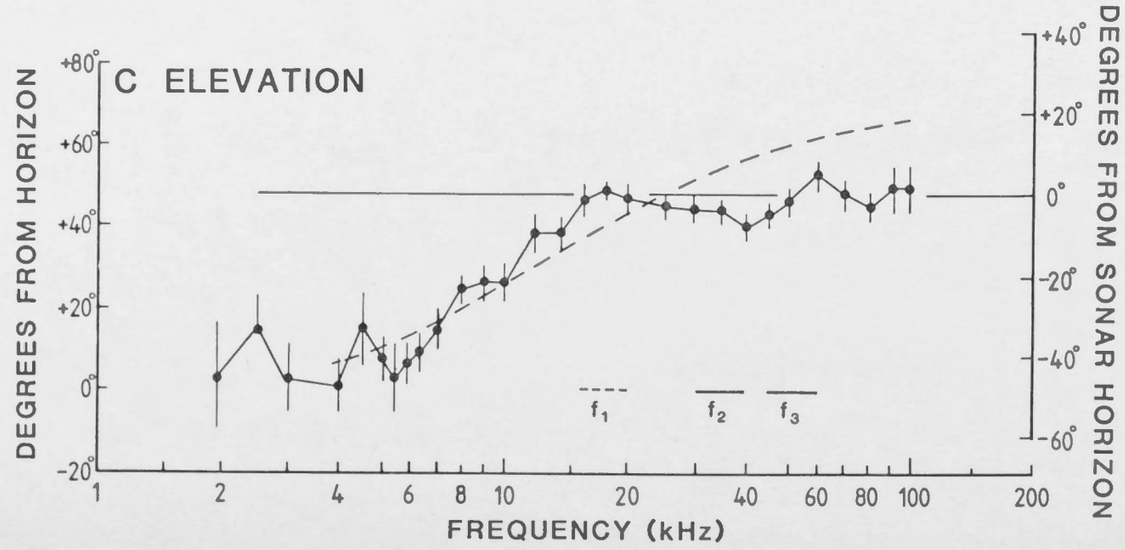
C ELEVATION
DEGREES FROM HORIZON
+80°
+60°
+40°
+20°
0°
-20°
DEGREES FROM SONAR HORIZON
+40°
+20°
0°
-20°
-40°
-60°
f1
f2
f3
1
2
4
6
8
10
20
40
60
80
100
200
FREQUENCY (kHz)

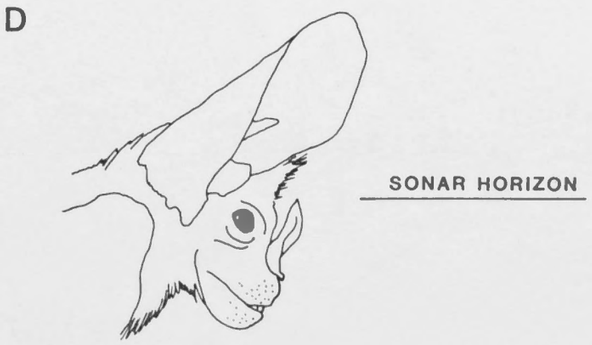
D
SONAR HORIZON

Fig. 2.9: A. Comparison between ear canal directivity patterns for normal (pinna-on) and pinna removed (pinna-off) in *Macroderma gigas* (right ear, 20kHz and 50kHz). Details of plots as for Fig. 2.3.

B. Comparison between ear canal directivity patterns in *M. gigas* for normal conditions and tragus (only) removed at 40kHz. Vertical orientation of head referenced to the sonar horizon (see Fig 2.8C).

Macroderma gigas

A

20kHz
PINNA ON

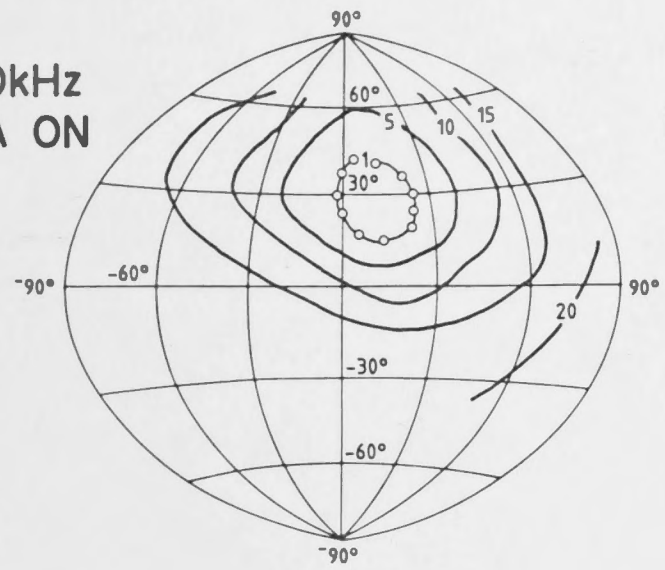

50kHz
PINNA ON

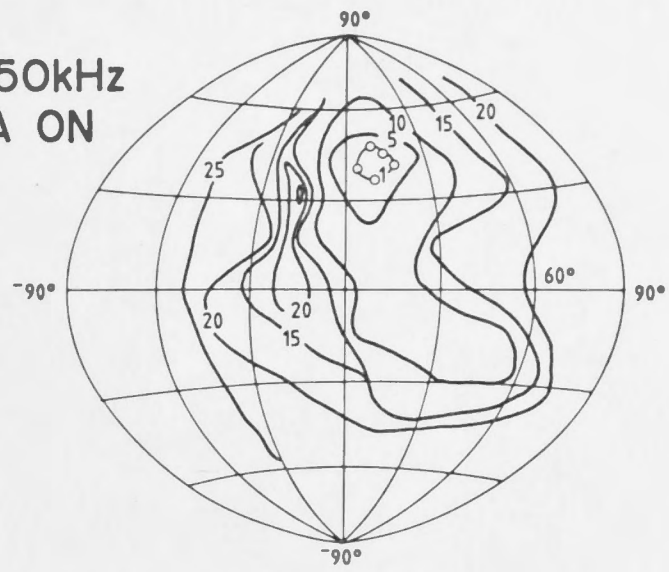

20kHz
PINNA OFF

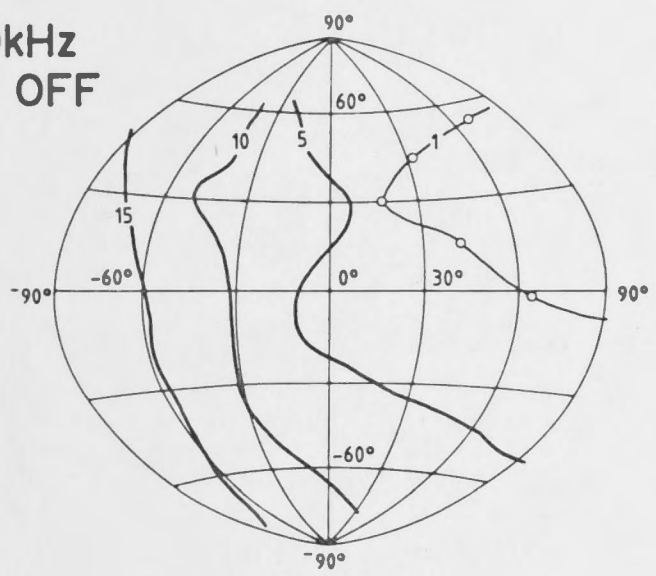

50kHz
PINNA OFF

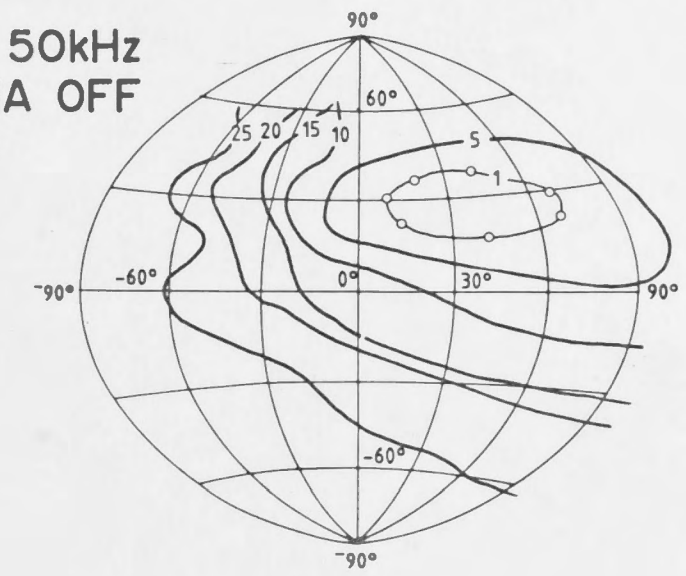

B

40kHz
TRAGUS ON

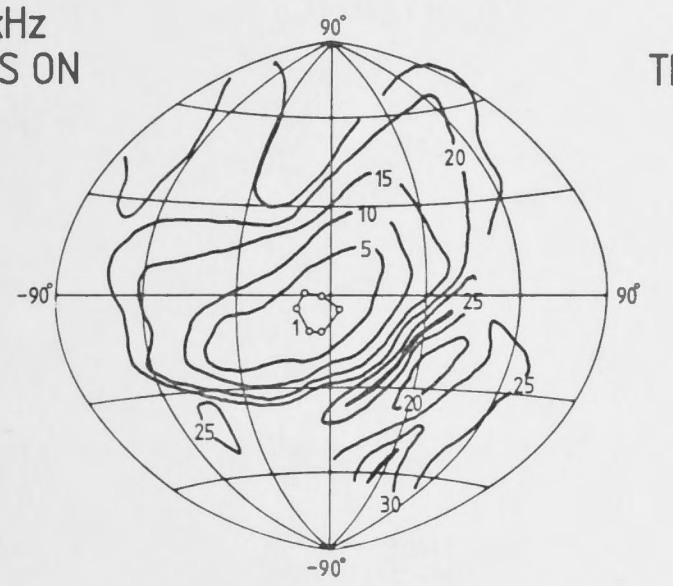

40kHz
TRAGUS OFF

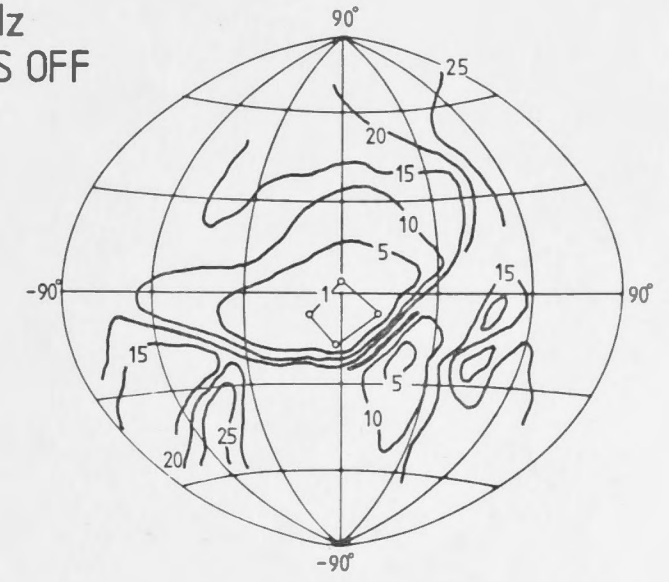

Fig. 2.10: General appearance of the head of Gould's long-eared bat (*Nyctophilus gouldi*). Dimensions are in millimeters, see also Table 2.1.

A. Sagittal view of head and pinnae. Vertical orientation of the head is relative to the sonar horizon as indicated (see text, also Fig. 2.16).

Below: Schematic vertical cross-section through the asymmetrical pinna. The geometry is used to predict movement of the acoustic axis in elevation as a function of frequency (see APPENDIX 3 and text for details). Dashed line = open face of pinna; a_o = mouth of the pinna at the approximate truncation point (as for C).

B. Frontal view. Note partial fusion of pinnae at the base of their medial edges above the midline.

C. Horizontal view of head and pinnae.

Below: Schematic view of horizontal cross-section through the asymmetrical pinnae indicating the geometry and dimensions of the oblique truncation of the pinna. Dimensions and angles are used for calculation of the predicted movement of the acoustic axis as a function of wavelength (see APPENDIX 3 and text). Details as for A.

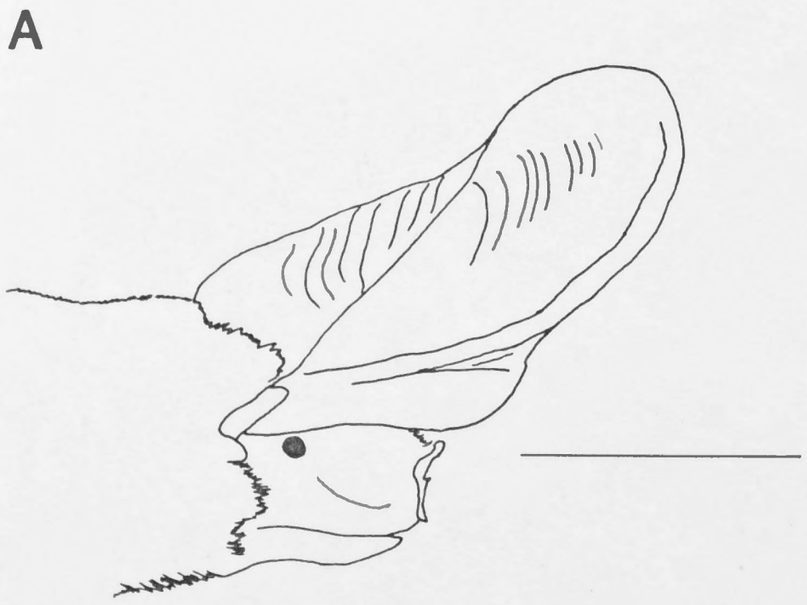

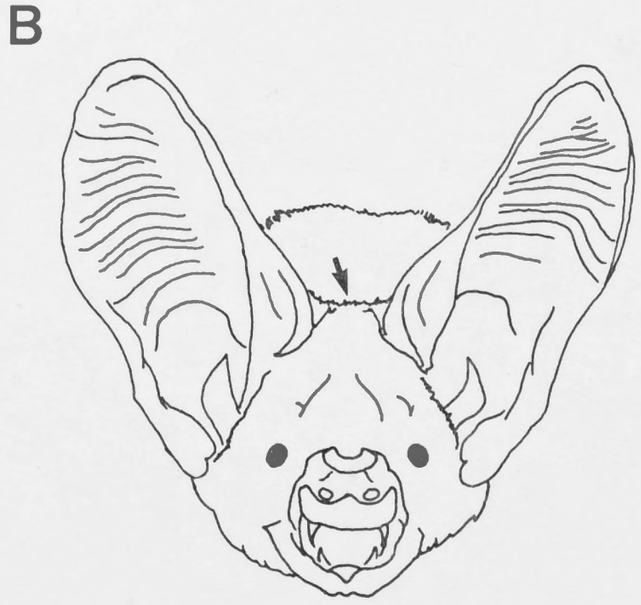

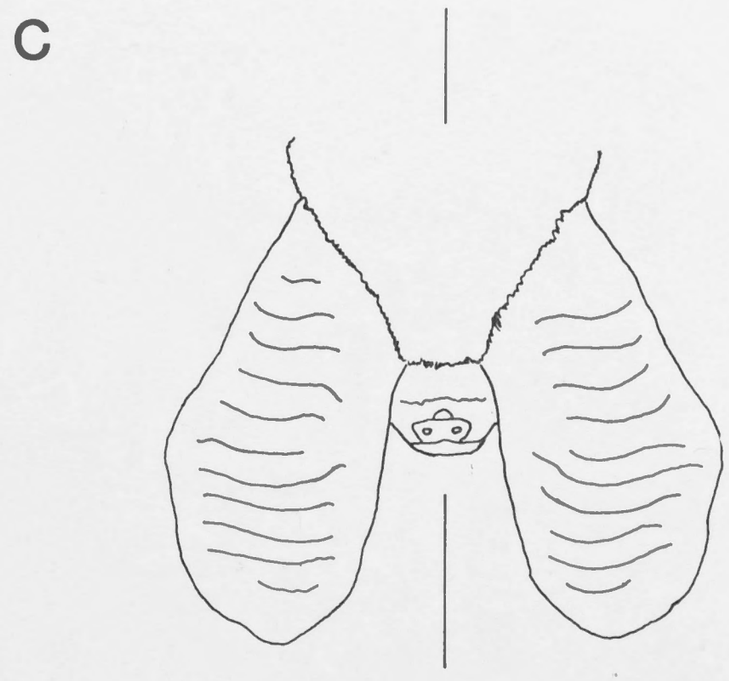

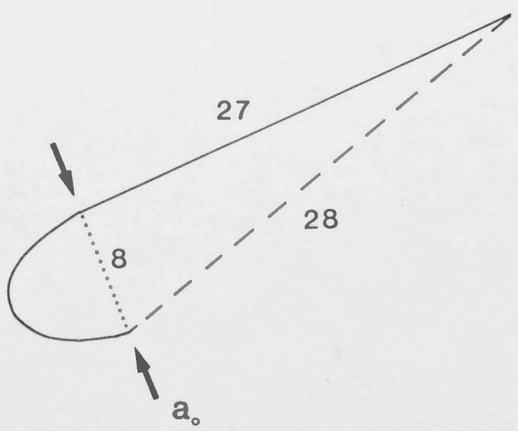

1cm

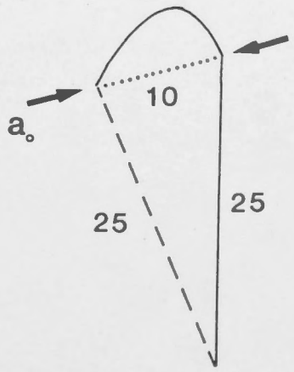

Nyctophilus gouldi

Fig. 2.10: General appearance of the head of Gould's long-eared bat (*Nyctophilus gouldi*). Dimensions are in millimeters, see also Table 2.1.

A. Sagittal view of head and pinnae. Vertical orientation of the head is relative to the sonar horizon as indicated (see text, also Fig. 2.16).

Below: Schematic vertical cross-section through the asymmetrical pinna. The geometry is used to predict movement of the acoustic axis in elevation as a function of frequency (see APPENDIX 3 and text for details). Dashed line = open face of pinna; a_o = mouth of the pinna at the approximate truncation point (as for C).

B. Frontal view. Note partial fusion of pinnae at the base of their medial edges above the midline.

C. Horizontal view of head and pinnae.

Below: Schematic view of horizontal cross-section through the asymmetrical pinnae indicating the geometry and dimensions of the oblique truncation of the pinna. Dimensions and angles are used for calculation of the predicted movement of the acoustic axis as a function of wavelength (see APPENDIX 3 and text). Details as for A.

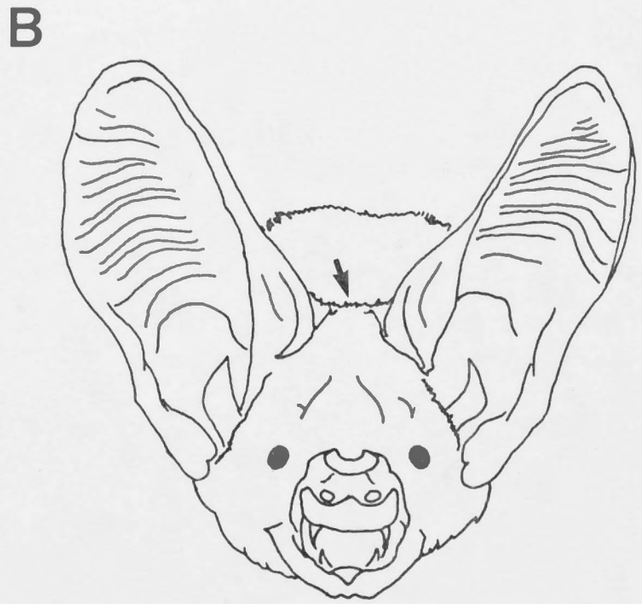

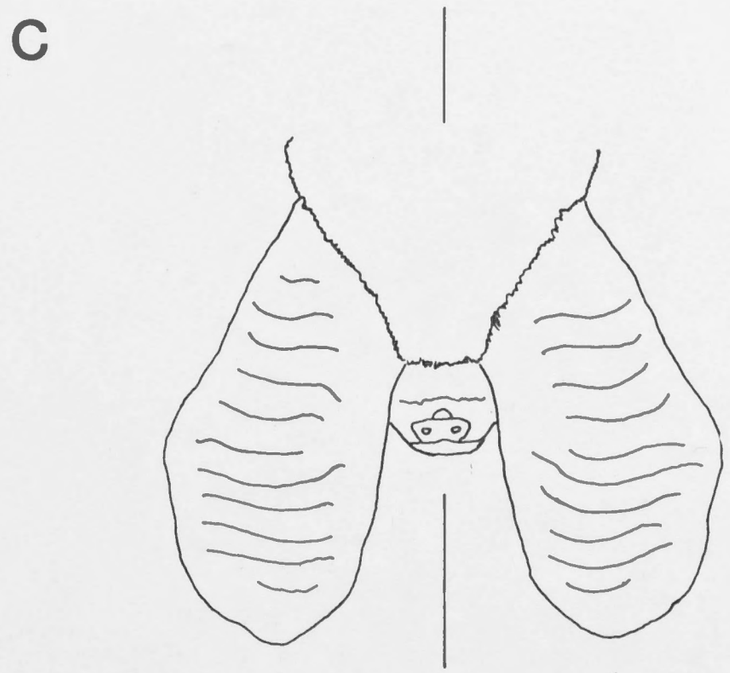

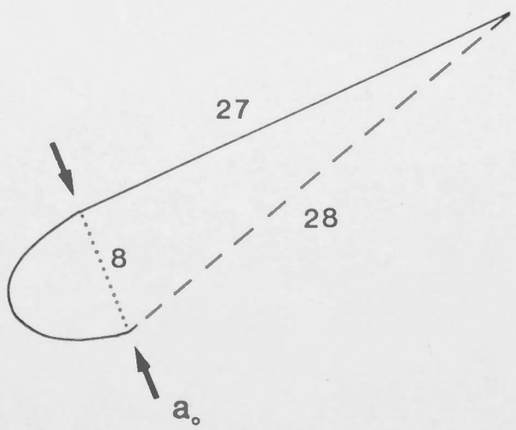

1cm

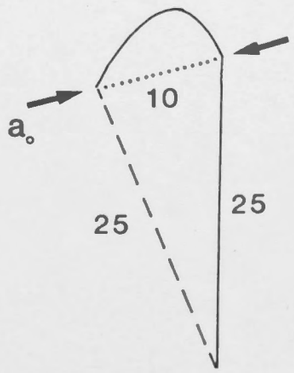

Nyctophilus gouldi

Fig. 2.11. Measurements of acoustic pressure gain obtained from a microphone ($\frac{1}{8}$" Bruel and Kjaer Type 4148) replacing the tympanic membrane at the end of the ear canal in *Nyctophilus gouldi*.

A. Gain curves (solid lines) for three ears under normal (intact) conditions. Dotted curve is a typical example of gain from one ear after removal of the ipsilateral pinna.

B. The effective gain of the pinna (3 ears) calculated from difference curves between normal and pinna-removed gain curves as shown in A. At top of graph, the ratio of the circumference of the open face of the pinna (mouth) relative to the wavelength (ka) is represented as a scale, (see text and Beranek 1954). Dotted curve is expected gain for finite conical horn based on the physical dimensions of the pinna (see APPENDIX 1; Table 2.1 and text).

C. Average gain curve (solid curve) for the pinna *N. gouldi* based on the curves in B. Dotted curves are expected gain curves for a finite paraboloidal, conical and exponential horn and based on the dimensions of the pinna as given in Table 2.1 (see also Fig. 2.10 for morphology of pinna). For details of calculation see APPENDIX 1.

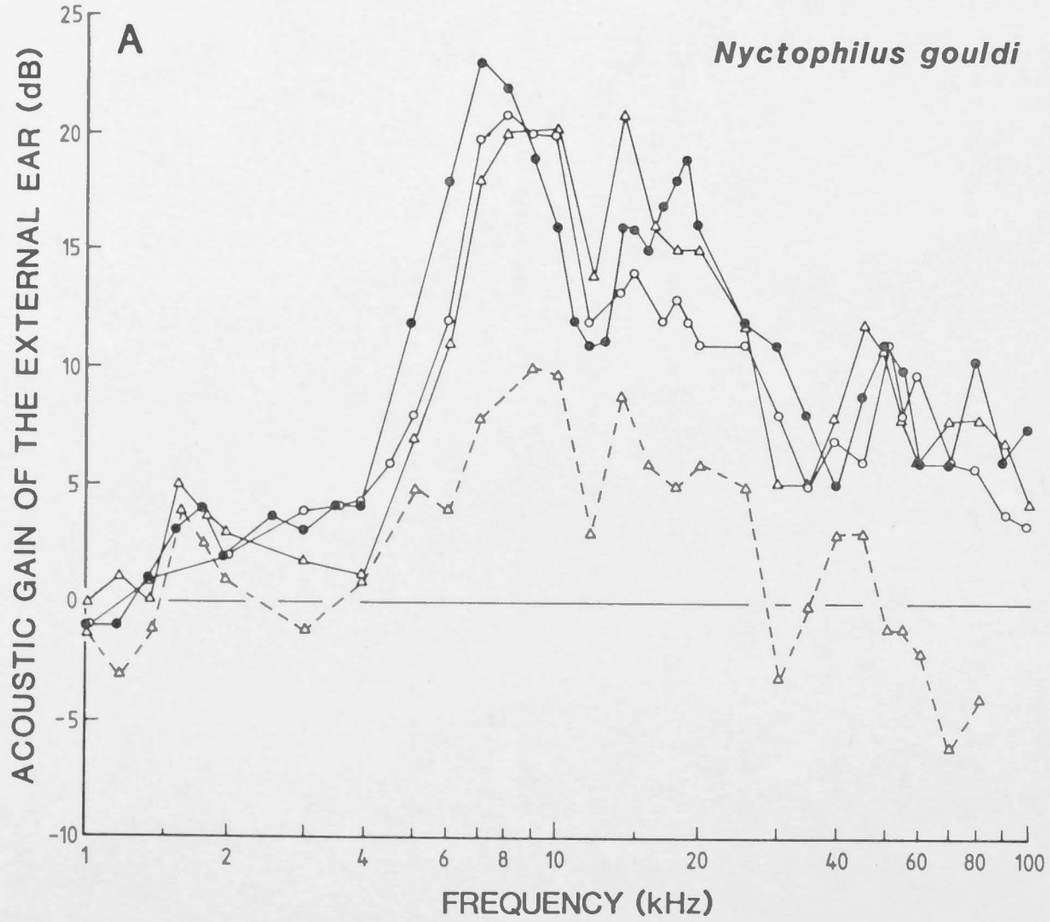
A
Nyctophilus gouldi
ACOUSTIC GAIN OF THE EXTERNAL EAR (dB)
25
20
15
10
5
0
-5
-10
1
2
4
6
8
10
20
40
60
80
100
FREQUENCY (kHz)

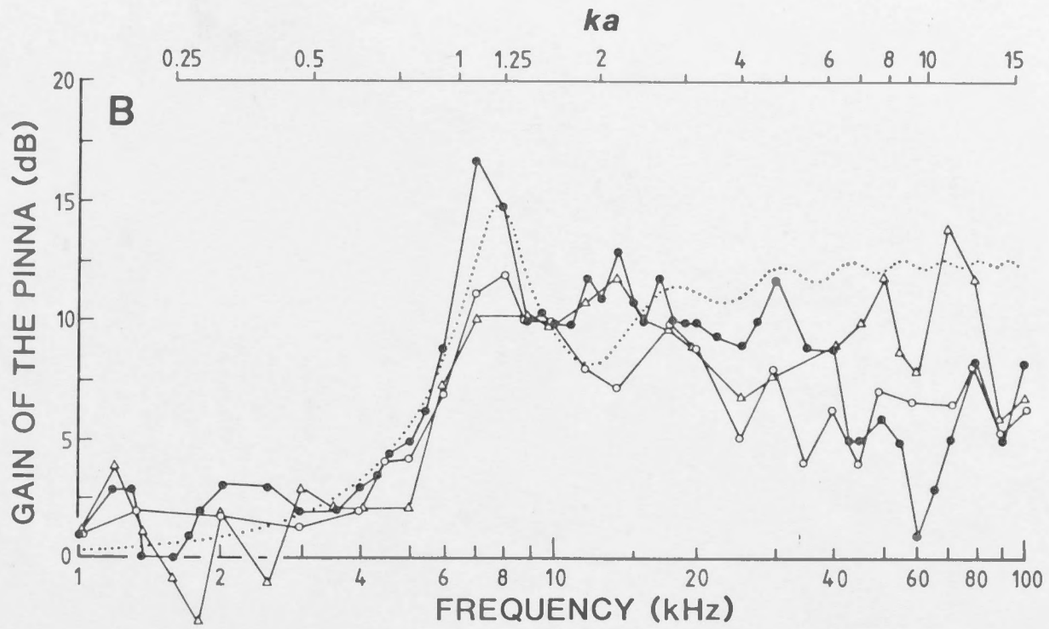
ka
0.25
0.5
1
1.25
2
4
6
8
10
15
B
GAIN OF THE PINNA (dB)
20
15
10
5
0
1
2
4
6
8
10
20
40
60
80
100
FREQUENCY (kHz)

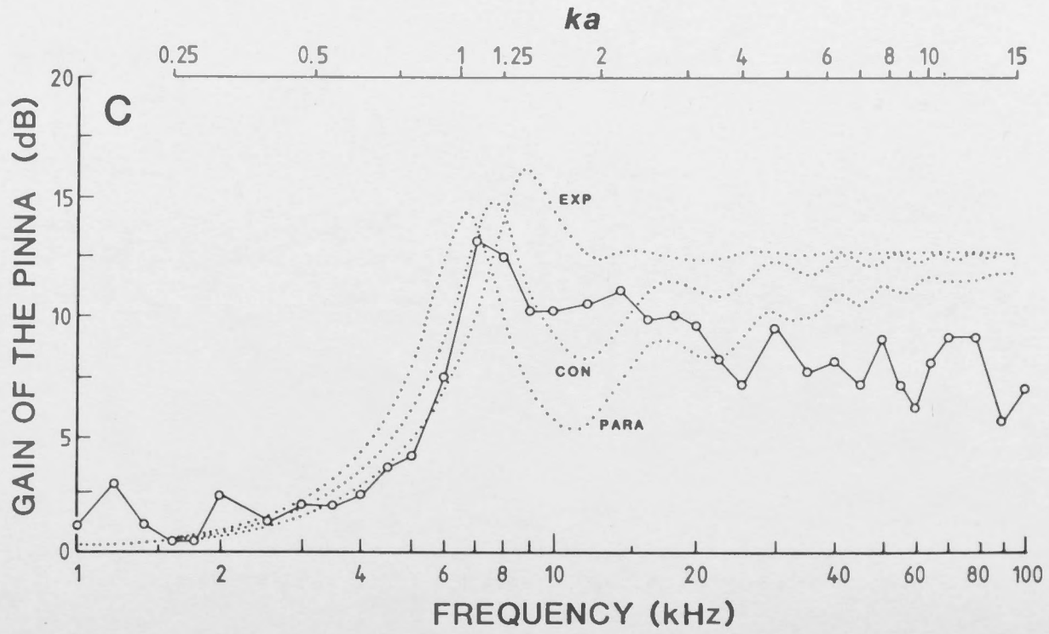
ka
0.25
0.5
1
1.25
2
4
6
8
10
15
C
GAIN OF THE PINNA (dB)
20
15
10
5
0
EXP
CON
PARA
1
2
4
6
8
10
20
40
60
80
100
FREQUENCY (kHz)

Fig. 2.12: Examples of ear canal directionality at various test frequencies (kHz) for the right ear in *Nyctophilus gouldi*. Directivity patterns are represented as a series of iso-intensity (pressure) contours plotted onto a two-dimensional projection of the frontal hemisphere (see MATERIALS AND METHODS). The position of the acoustic axis is located within the 1dB contour which is plotted relative to the axial sound pressure (solid line, open circles). Likewise a series of contours are plotted at 5dB intervals down to -25dB below the on-axis pressure.

Nyctophilus gouldi RIGHT EAR CANAL

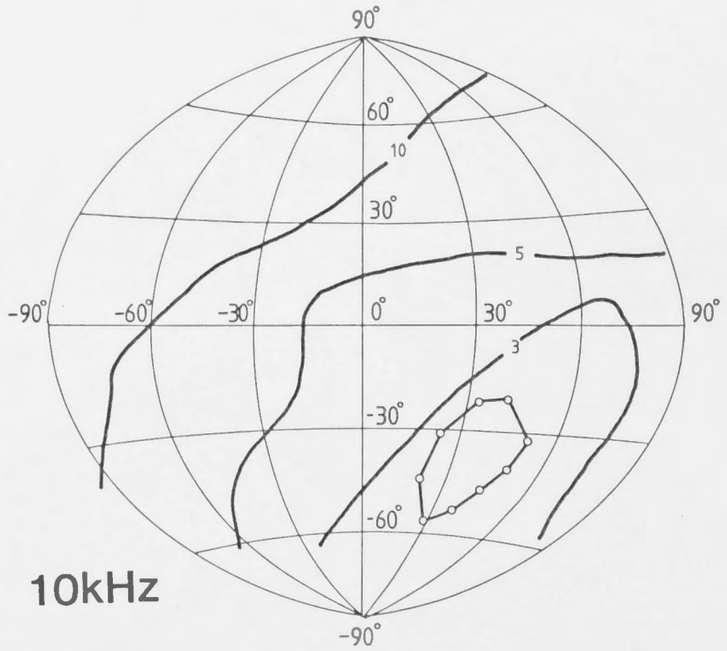

10kHz

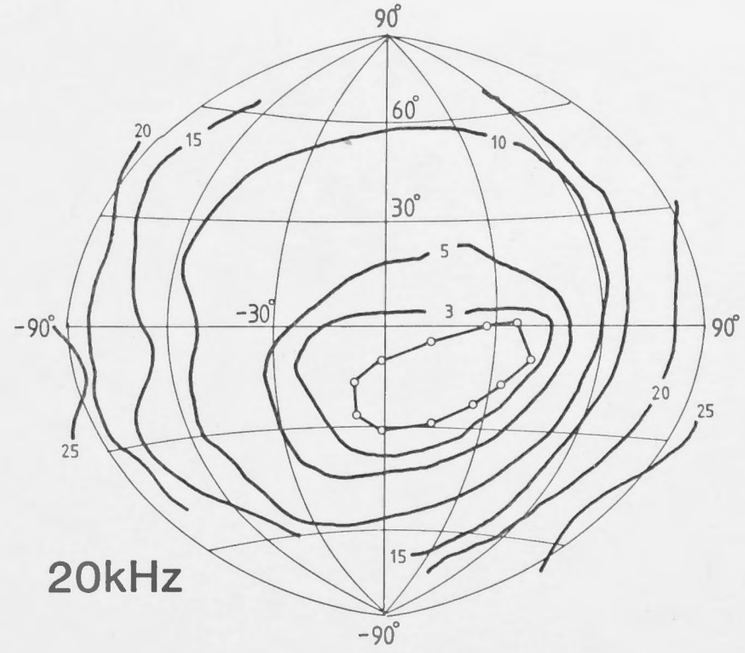

20kHz

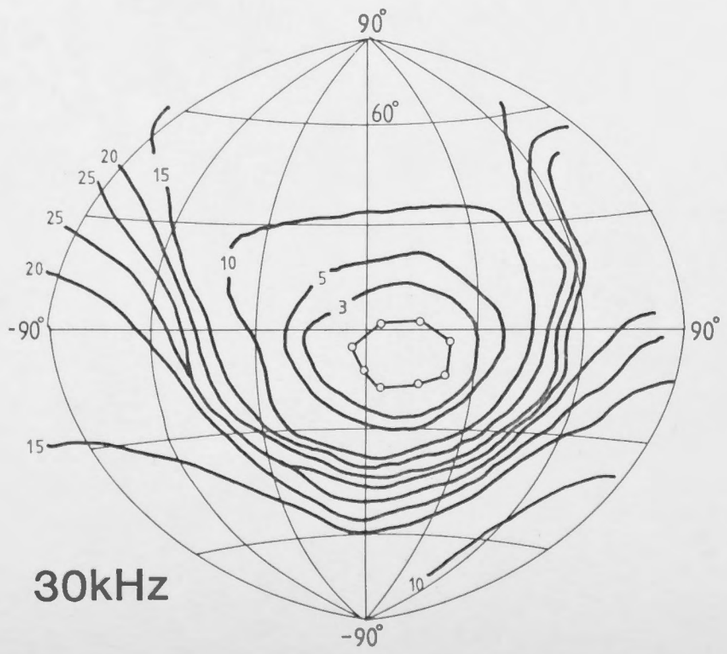

30kHz

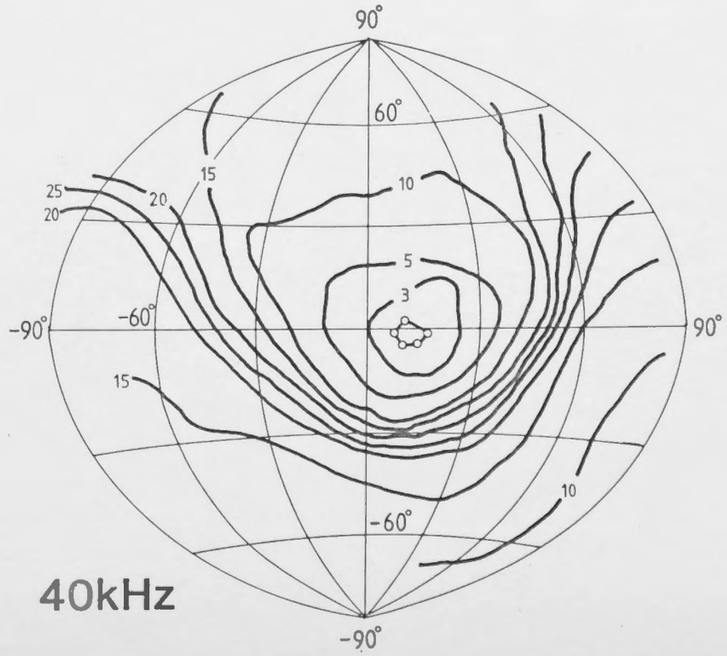

40kHz

Fig. 2.13: Summary of the maximum difference in sound pressure (dB_{max}) for ear canal directivity patterns in *Nyctophilus gouldi* as a function of frequency (four ears). The ratio between the circumference of the pinna face (mouth) to the wavelength is represented as a *ka* scale (a = 0.85cm see Table 2.1) as for the circular aperture in a physical system (see Beranek 1954).

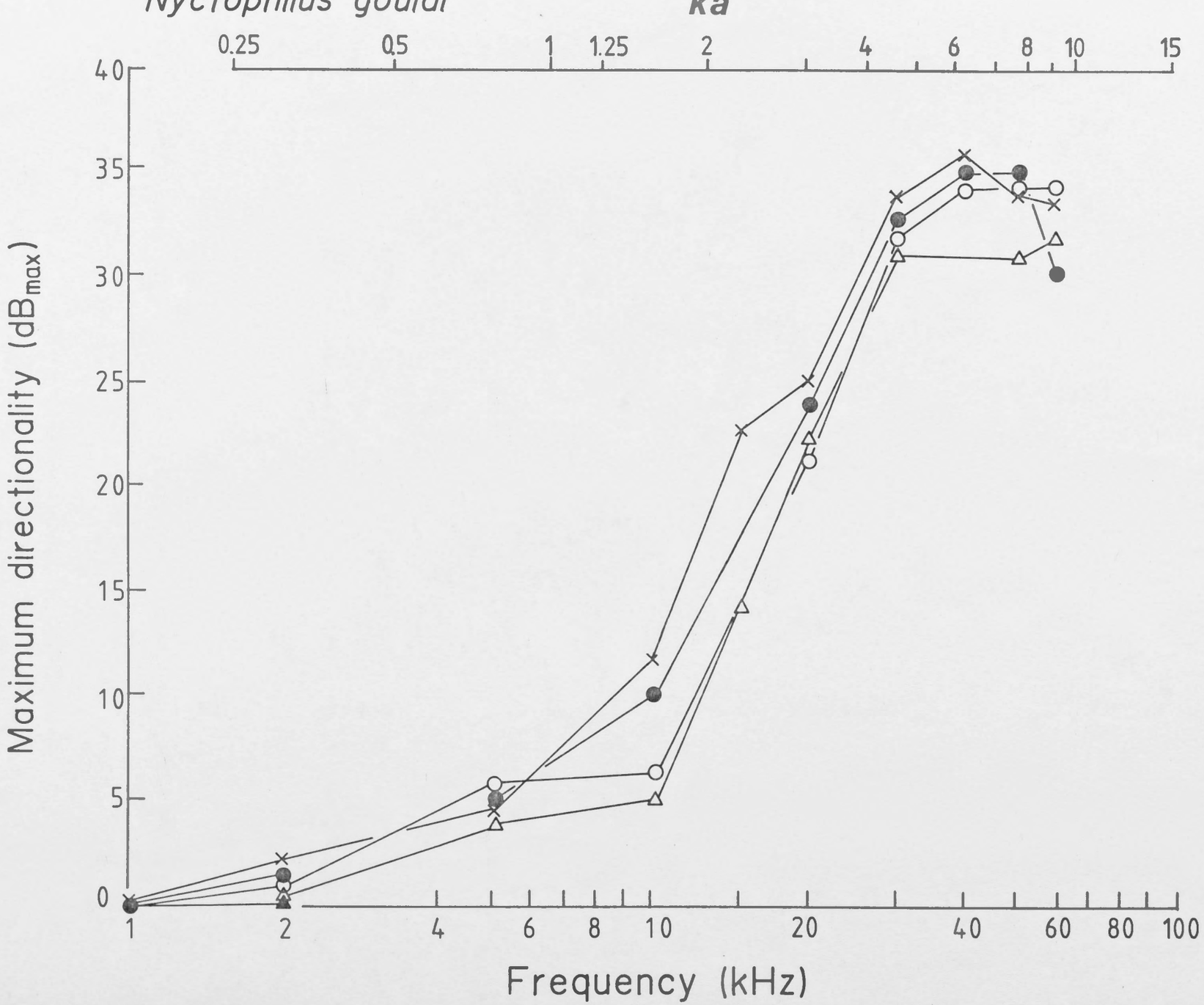
Nyctophilus gouldi
ka
0.25
0.5
1
1.25
2
4
6
8
10
15
40
35
30
25
20
15
10
5
0
Maximum directionality (dB$_{max}$)
1
2
4
6
8
10
20
40
60
80
100
Frequency (kHz)

Fig. 2.14: Measurement of the acceptance angle (-3dB relative to the on-axis sound pressure) for ear canal directionality in *Nyctophilus gouldi* (four ears) as shown in Fig. 2.12, and expressed as the full angular width ($2\theta°$). A = azimuth; B = elevation. Solid curves are the expected -3dB acceptance angles for sound diffraction by a circular aperture in a plane wall based on a radius equal to the average radius of the open face of the pinna in *N. gouldi* (a = 0.85cm; Table 2.1). For details of calculations see APPENDIX 2 and text.

Nyctophilus gouldi

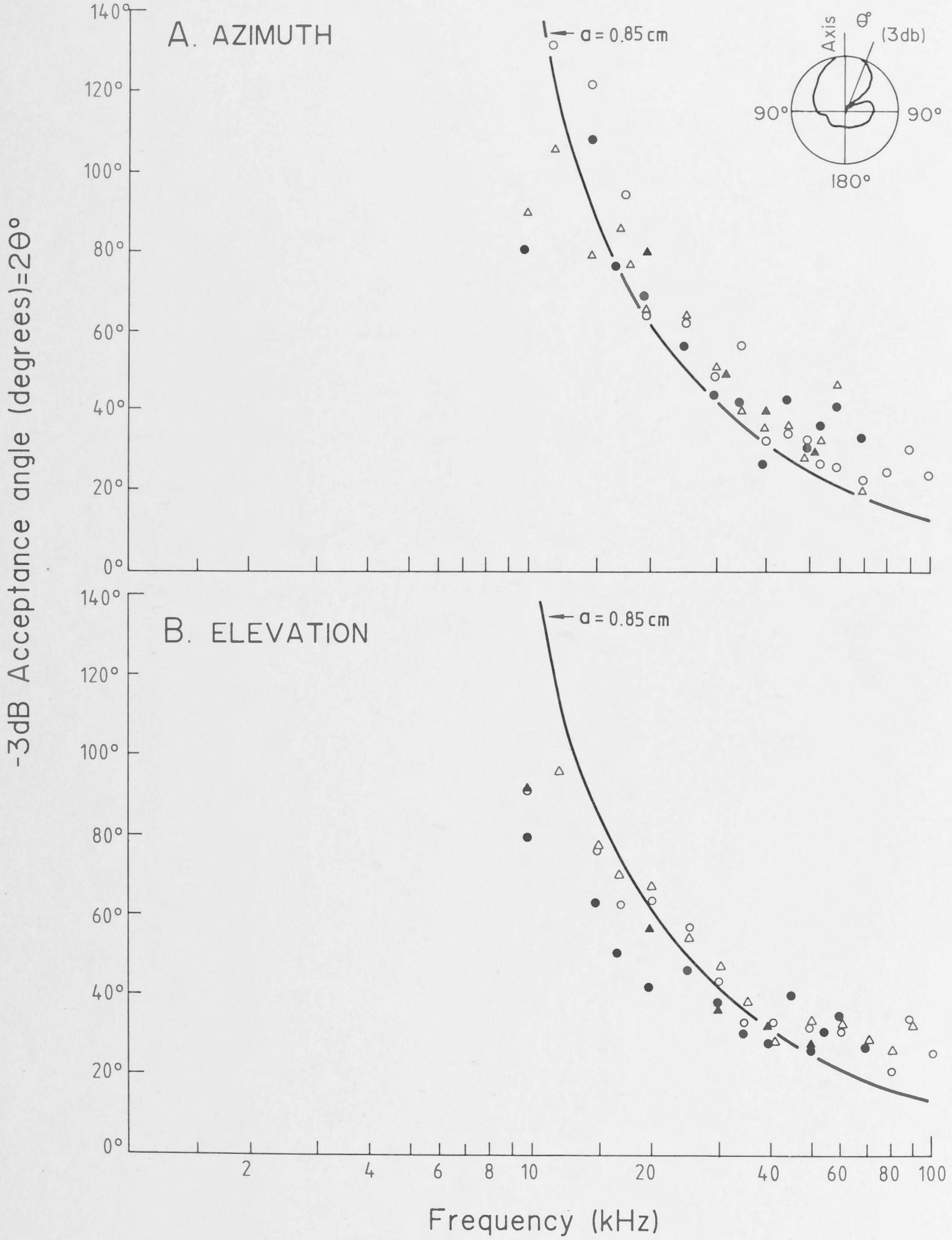

Fig. 2.15: Positions of nulls in ear canal directivity patterns in *Nyctophilus gouldi* relative to the position of the acoustic axis ($\theta°$) as a function of stimulus frequency (four ears). Solid curve represents the expected semi-angles which would result from sound diffraction of a circular aperture in a plane wall, with a radius equivalent to the average radius of the pinna mouth (a = 0.85cm). For details of calculations see APPENDIX 2 and text. The lower frequency limit for diffraction nulls in frontal space for a circular aperture in a plane wall occurs for nulls 90° off-axis and is indicated at ka = 3.83 (see APPENDIX 2, also text and Beranek 1954).

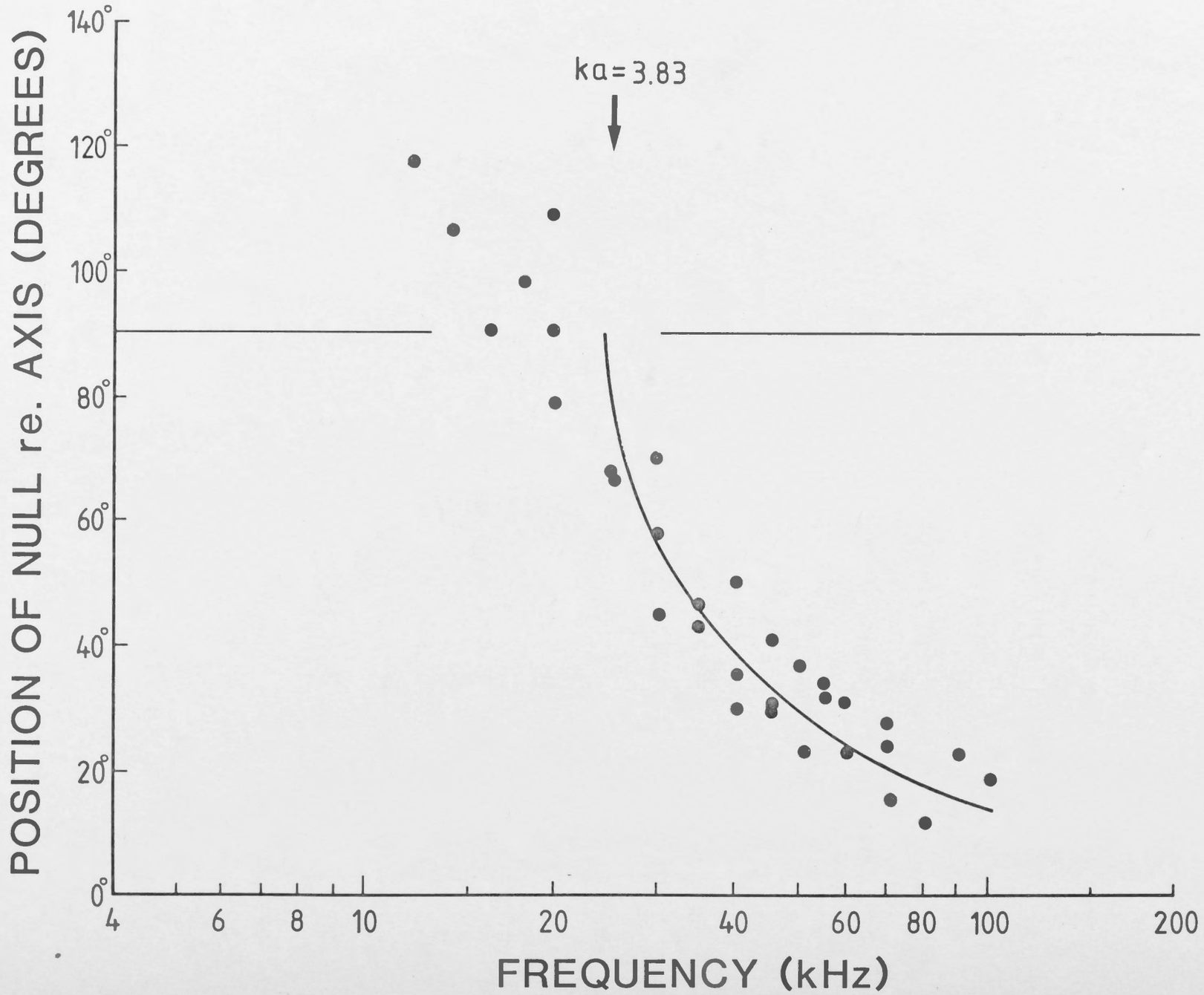
Nyctophilus gouldi
ka = 3.83
POSITION OF NULL re. AXIS (DEGREES)
140°
120°
100°
80°
60°
40°
20°
0°
4
6
8
10
20
40
60
80
100
200
FREQUENCY (kHz)

Fig. 2.16: A. Average movement of the acoustic axis in azimuth in *Nyctophilus gouldi* (three ears). Vertical bars are standard errors.

B. Horizontal view of head and pinnae of *N. gouldi* for reference to A (see also Fig. 2.10).

C. Average movement of the acoustic axis in elevation, as in A. The head orientation of *N. gouldi* was referenced to a "sonar" horizon which is based on the elevated positions of acoustic axes for frequencies above 35kHz (sonar bandwidth indicated by bar in C and A, for detail see Figs. 2.22, 2.26).

D. Sagittal view of the head of *N. gouldi* as in Fig. 2.10 showing orientation of head with respect to a "sonar" horizon which may be used during horizontal flight for reference to C.

In A and C dotted curves = predicted movement of acoustic axis based on geometry of the oblique truncation of the pinnae in *N. gouldi* as shown schematically in Fig. 2.10A,C. Calculations for theoretical movement of the acoustic axis as a function of wavelength are given in APPENDIX 3 and for further details see text.

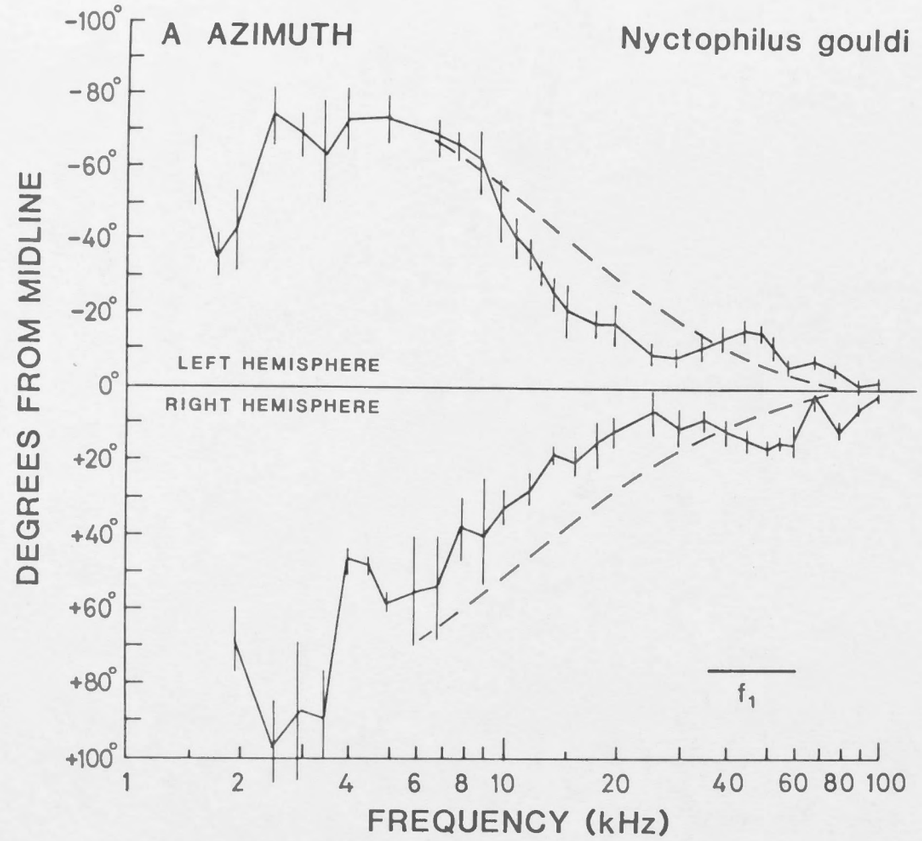
A AZIMUTH
Nyctophilus gouldi
DEGREES FROM MIDLINE
-100°
-80°
-60°
-40°
-20°
0°
+20°
+40°
+60°
+80°
+100°
LEFT HEMISPHERE
RIGHT HEMISPHERE
f1
1
2
4
6
8
10
20
40
60
80
100
FREQUENCY (kHz)

B

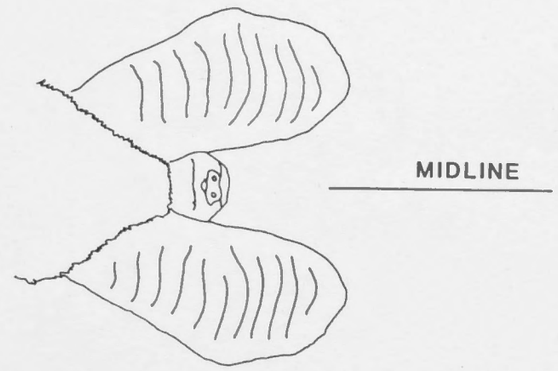
MIDLINE

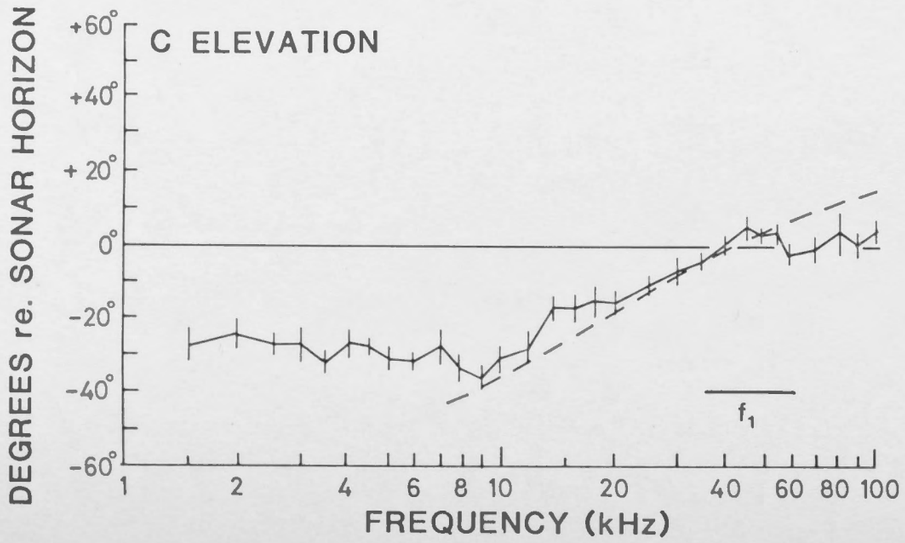
C ELEVATION
DEGREES re. SONAR HORIZON
+60°
+40°
+ 20°
0°
-20°
-40°
-60°
f1
1
2
4
6
8
10
20
40
60
80
100
FREQUENCY (kHz)

D

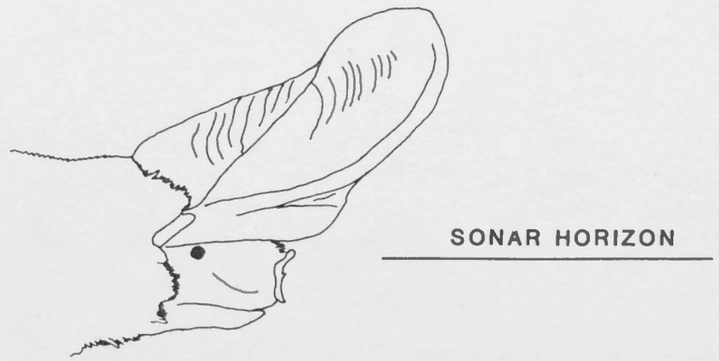
SONAR HORIZON

Fig. 2.17: Comparison between ear canal directivity patterns for normal (intact A and C) and pinna removed (pinna-off B and D) in *Nyctophilus gouldi* (right ear, 20kHz and 50kHz). Details of plots as for Fig. 2.12.

Nyctophilus gouldi

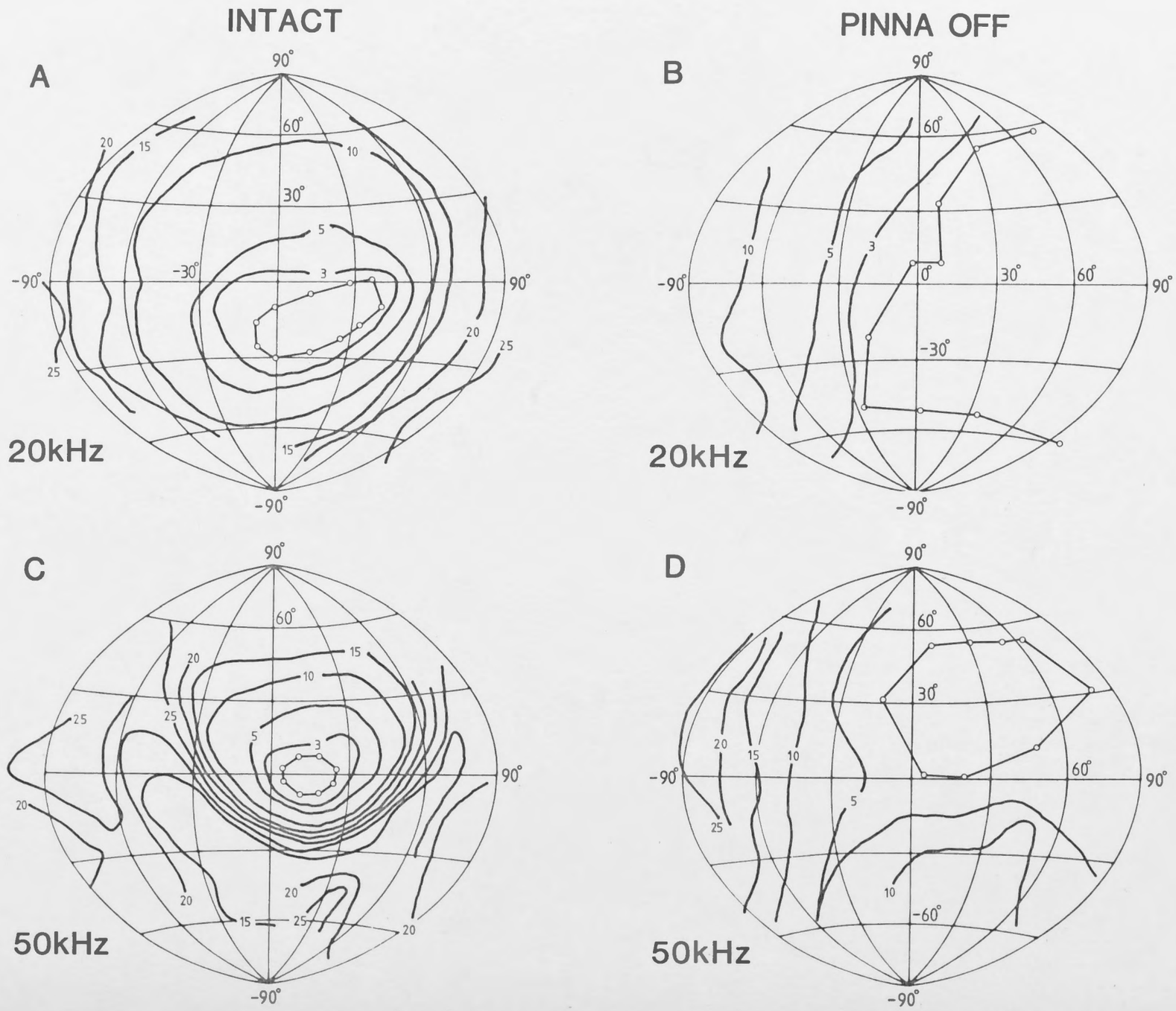

Fig. 2.18: A. Averaged auditory evoked potential thresholds (neural audiogram) recorded from the inferior colliculus of *Macroderma gigas* (N = 3). Dotted lines indicate data points for thresholds below 2kHz and above 100kHz which are tentative, and possibly affected by acoustical distortions of the stimulus or even cochlea distortions for high intensities at these frequencies.

B. Sagittal and horizontal views of the brain of *M. gigas* indicating the location of the inferior colliculus for recordings of the auditory evoked potentials and single auditory neurons.

C. The average evoked potential audiogram from the inferior colliculus taken from the curves in A (solid line). Filled circles represent the distribution of excitatory unit response thresholds for a sample of 90 auditory neurons sampled from the inferior colliculus in four *M. gigas*.

D. Summary of the main energy bandwidths of a range of social vocalizations and sonar signals used by *M. gigas* as described in CHAPTER 3.

A

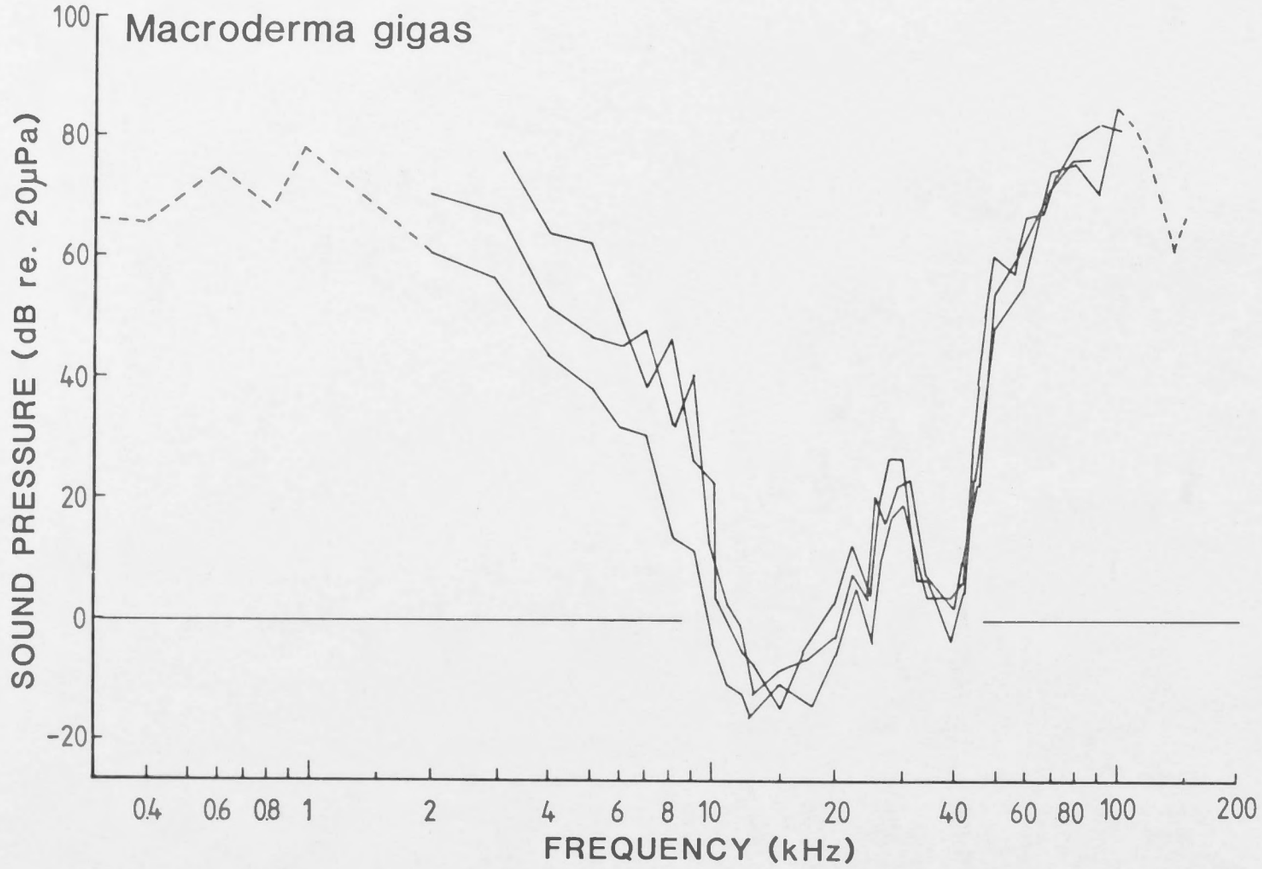
Macroderma gigas
SOUND PRESSURE (dB re. 20µPa)
100
80
60
40
20
0
-20
0.4
0.6
0.8
1
2
4
6
8
10
20
40
60
80
100
200
FREQUENCY (kHz)

B


IC
IC
5mm

C

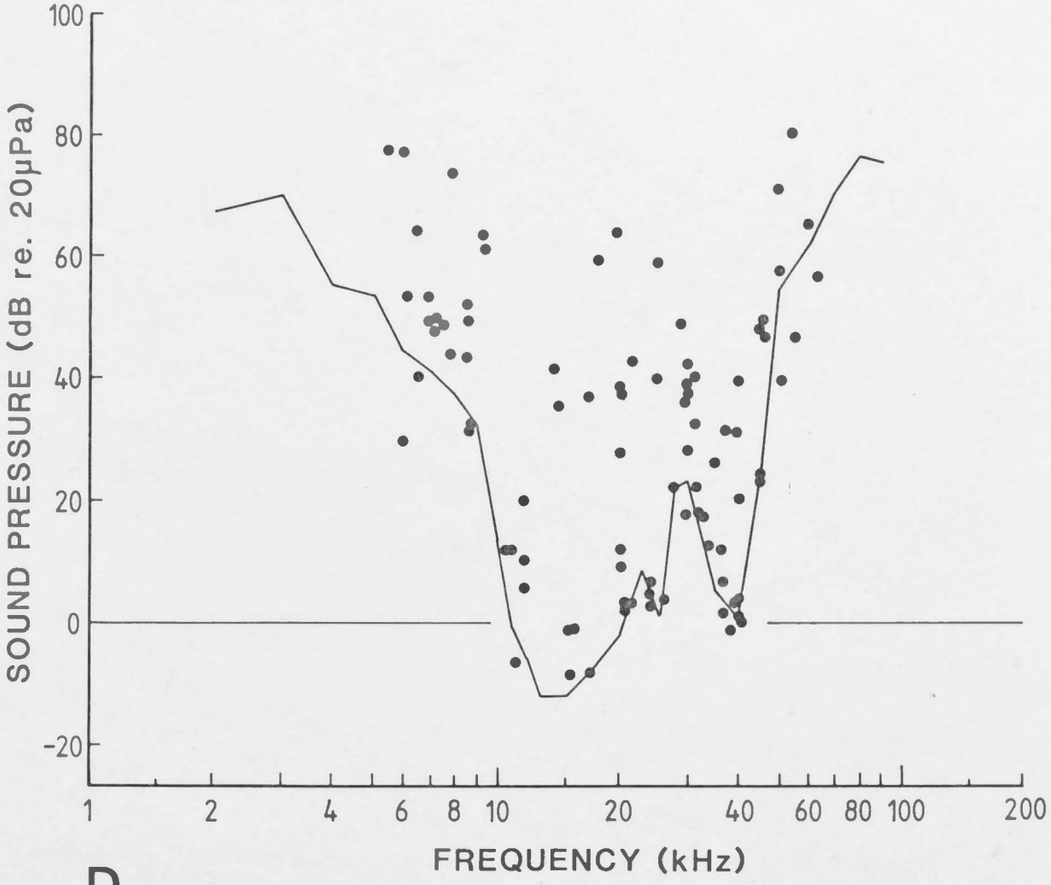
SOUND PRESSURE (dB re. 20µPa)
100
80
60
40
20
0
-20
1
2
4
6
8
10
20
40
60
80
100
200
FREQUENCY (kHz)

D

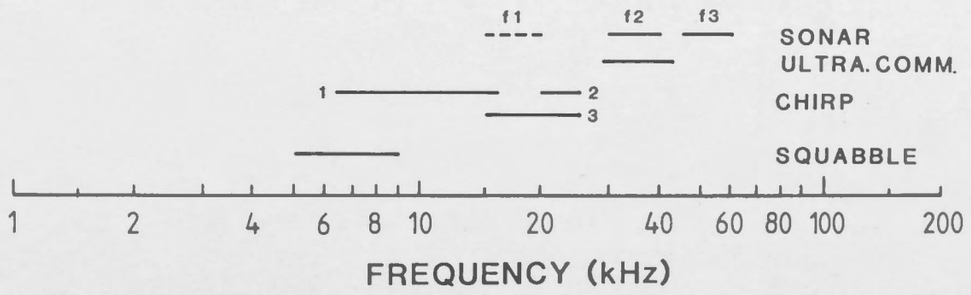
f1
f2
f3
SONAR
ULTRA.COMM.
1
2
3
CHIRP
SQUABBLE
1
2
4
6
8
10
20
40
60
80
100
200
FREQUENCY (kHz)

Fig. 2.19: A. Comparison between averaged auditory evoked potential thresholds from a single *Macroderma gigas*, under normal conditions (filled circles, solid line) and after removal of the pinna contralateral to the recorded inferior colliculus (open circles, dotted line).

B. Effect of contralateral pinna on neural thresholds calculated by the difference curve in A, (filled circles, solid line). Dotted line is the average acoustic gain of the pinna (in dB) as taken from the data in Fig. 2.2B,C.

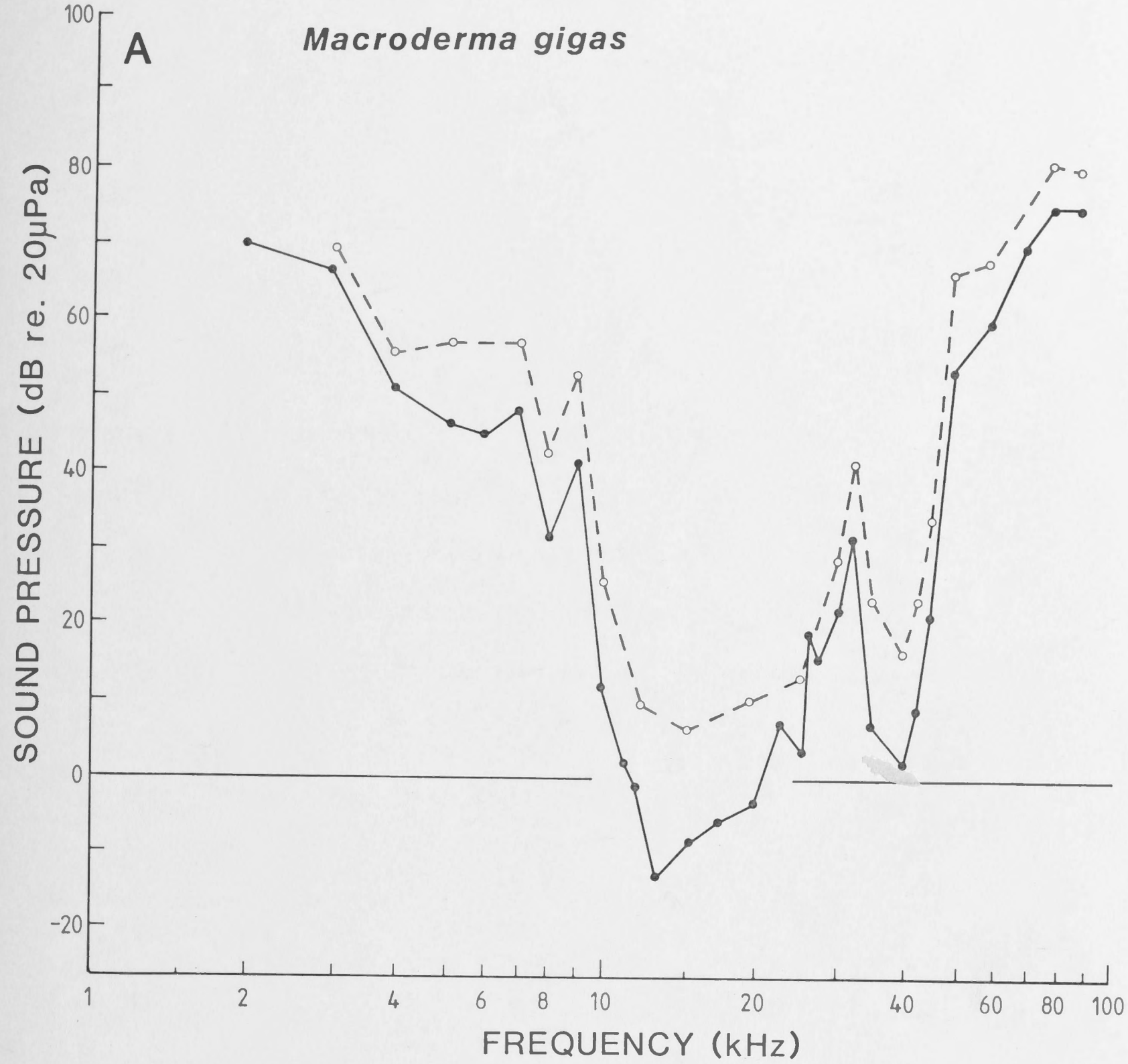
A
Macroderma gigas
SOUND PRESSURE (dB re. 20μPa)
100
80
60
40
20
0
-20
1
2
4
6
8
10
20
40
60
80
100
FREQUENCY (kHz)

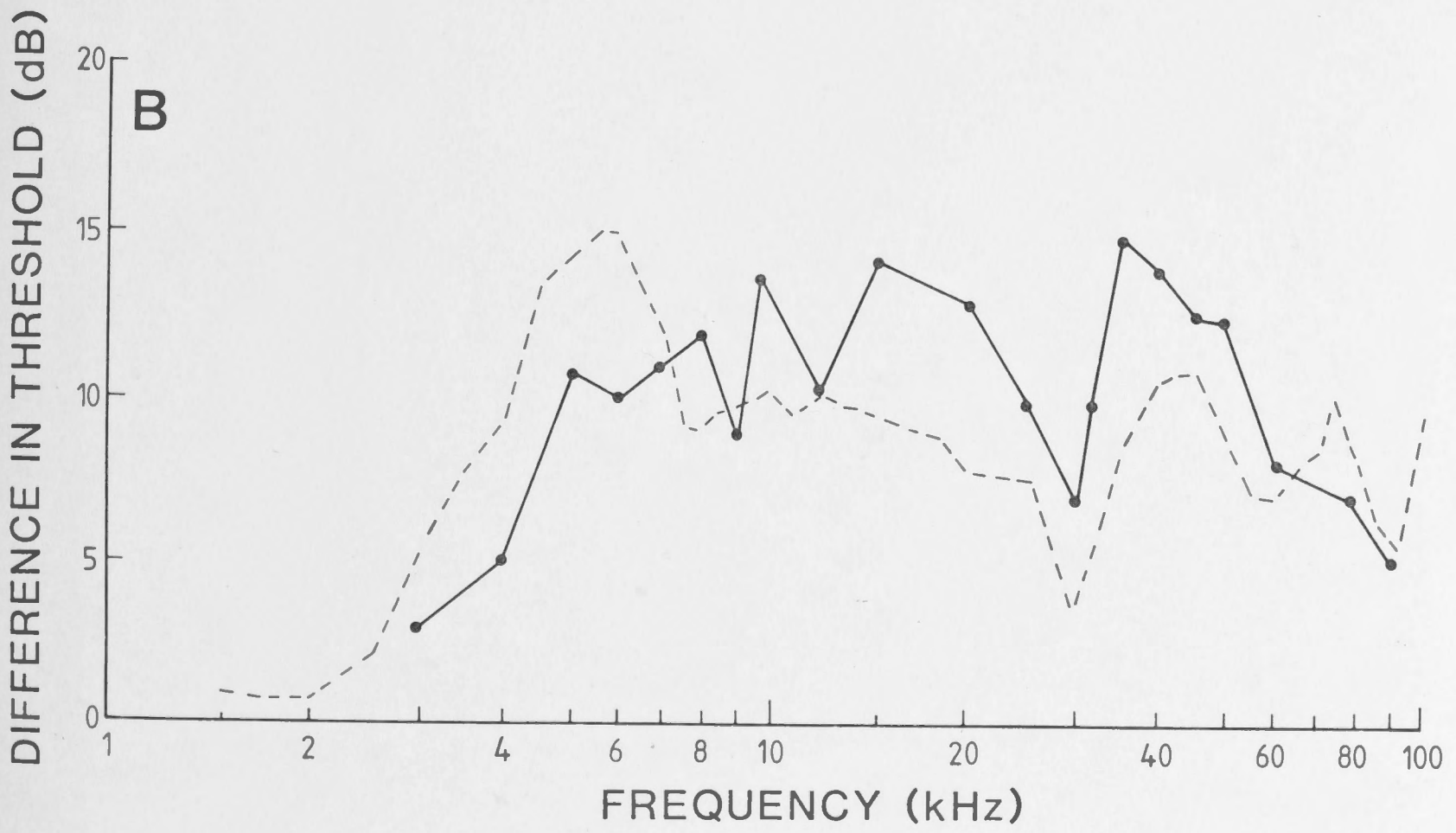
B
DIFFERENCE IN THRESHOLD (dB)
20
15
10
5
0
1
2
4
6
8
10
20
40
60
80
100
FREQUENCY (kHz)

Fig. 2.20: A. Examples of "axial-type" spatial receptive fields for four auditory neurons in *Macroderma gigas*, recorded from the left inferior colliculus in the same individual. Response boundaries are indicated by solid lines at 5dB above threshold at the (excitatory) best frequency for each neuron (as indicated). Best position is indicated by cross.

B. Summary of the best positions of auditory receptive fields at best frequency (circled number = kHz) for typical sequences of units recorded from the left and right inferior colliculus in three individuals.

In A and B the neural data for auditory spatial receptive fields were collected with the head vertically orientated with respect to the "sonar" horizon (as defined in Fig. 2.8).

A ***Macroderma gigas***

LEFT INFERIOR COLLICULUS
AXIAL TYPE RECEPTIVE FIELDS
(5dB ABOVE THRESHOLD)

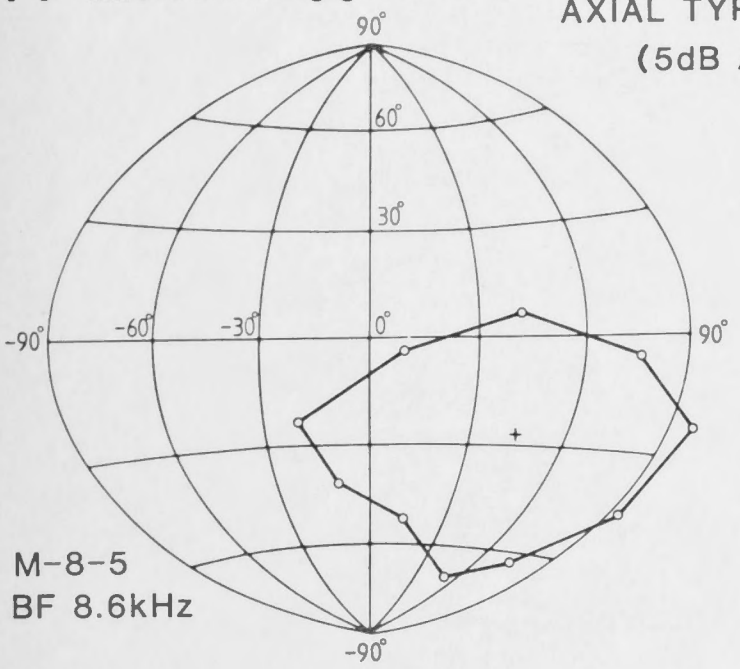

M-8-5
BF 8.6kHz

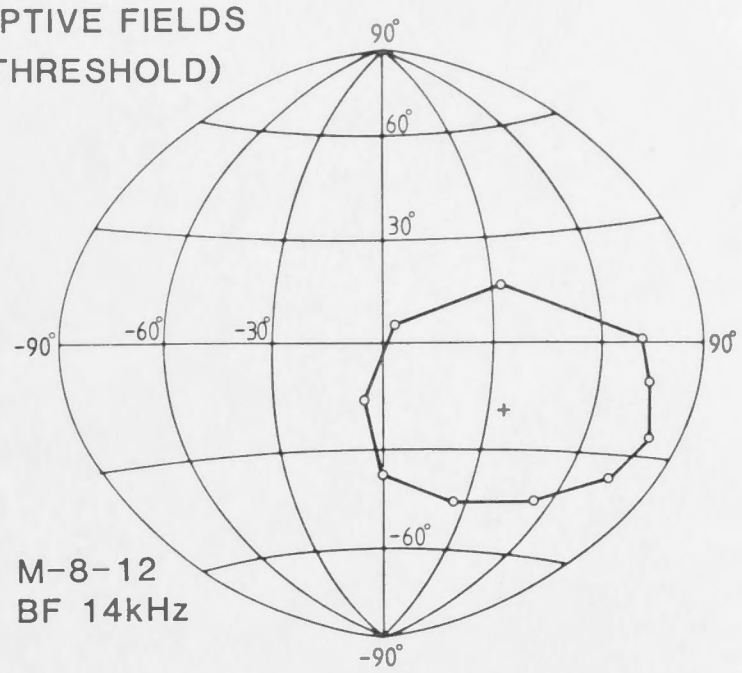

M-8-12
BF 14kHz

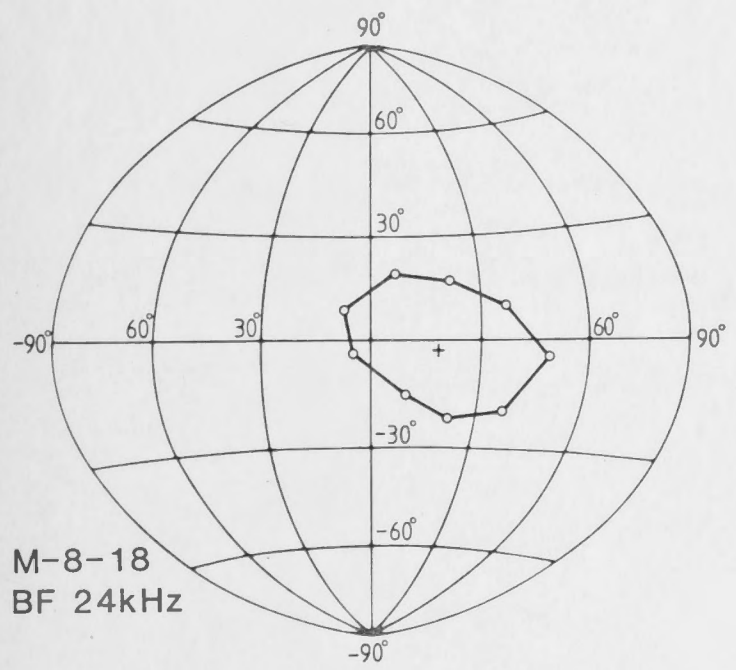

M-8-18
BF 24kHz

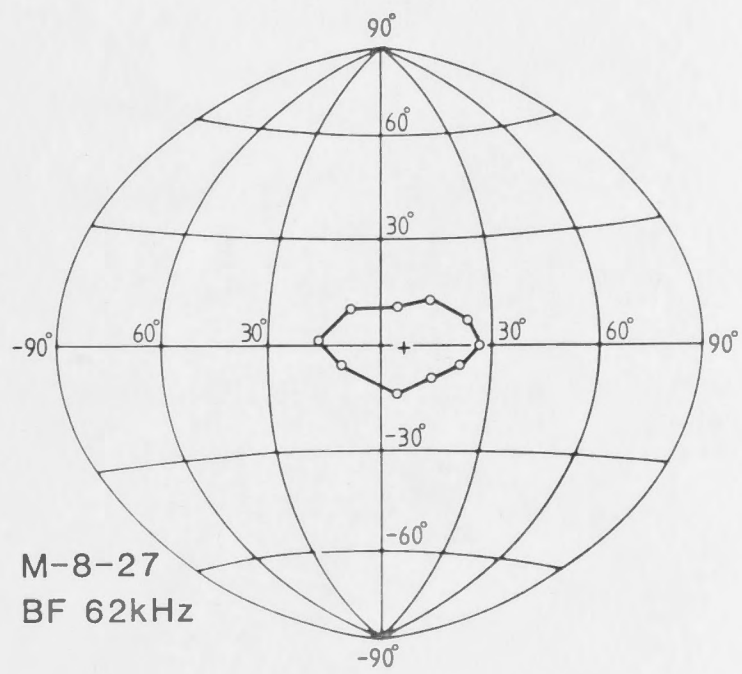

M-8-27
BF 62kHz

B AXIAL TYPE RECEPTIVE FIELDS

BEST POSITION AT BEST FREQUENCY (kHz)

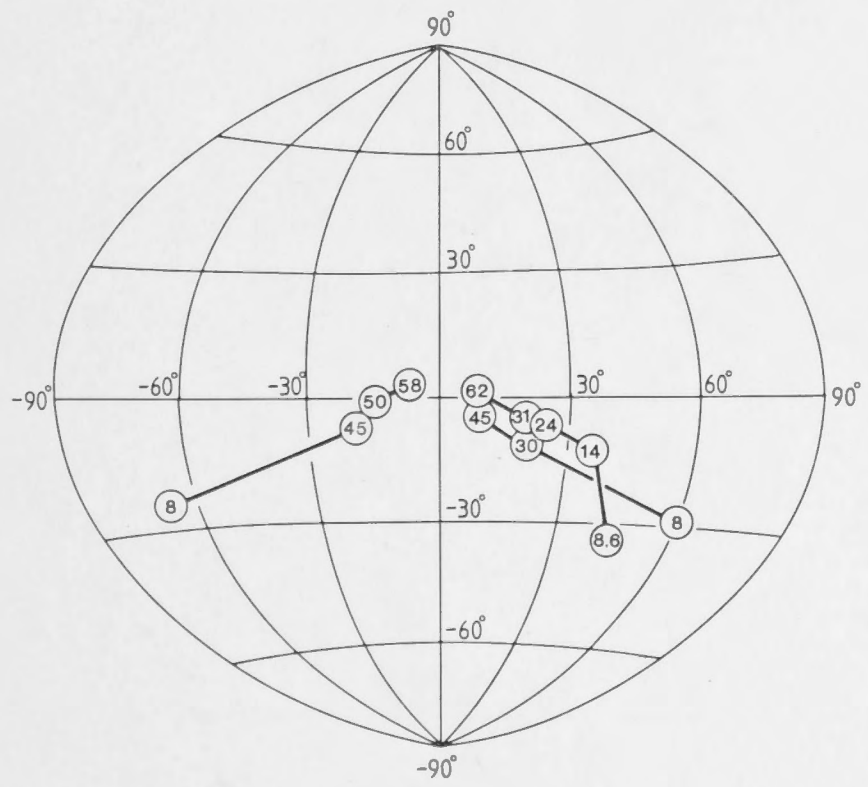

Fig. 2.21: Summary of the angular size of axial-type spatial receptive fields recorded from inferior colliculus neurons in *Macroderma gigas* (as shown in Fig. 2.20A). Data points are based on the full angular width (2θ°) of the threshold response boundaries obtained at 5dB above best position threshold sensitivity as a function of best frequency, for a sample of 38 neurons. Solid lines in A (azimuth) and B (elevation) represent the expected -5dB acceptance angle (2θ°) which would result from sound diffraction by a circular aperture with a radius equivalent to the average radius of the open face of the pinna in *M. gigas* (a = 1.8cm, see Table 2.1 and Fig. 2.1). For details of calculations of expected -5dB acceptance angle see APPENDIX 2.

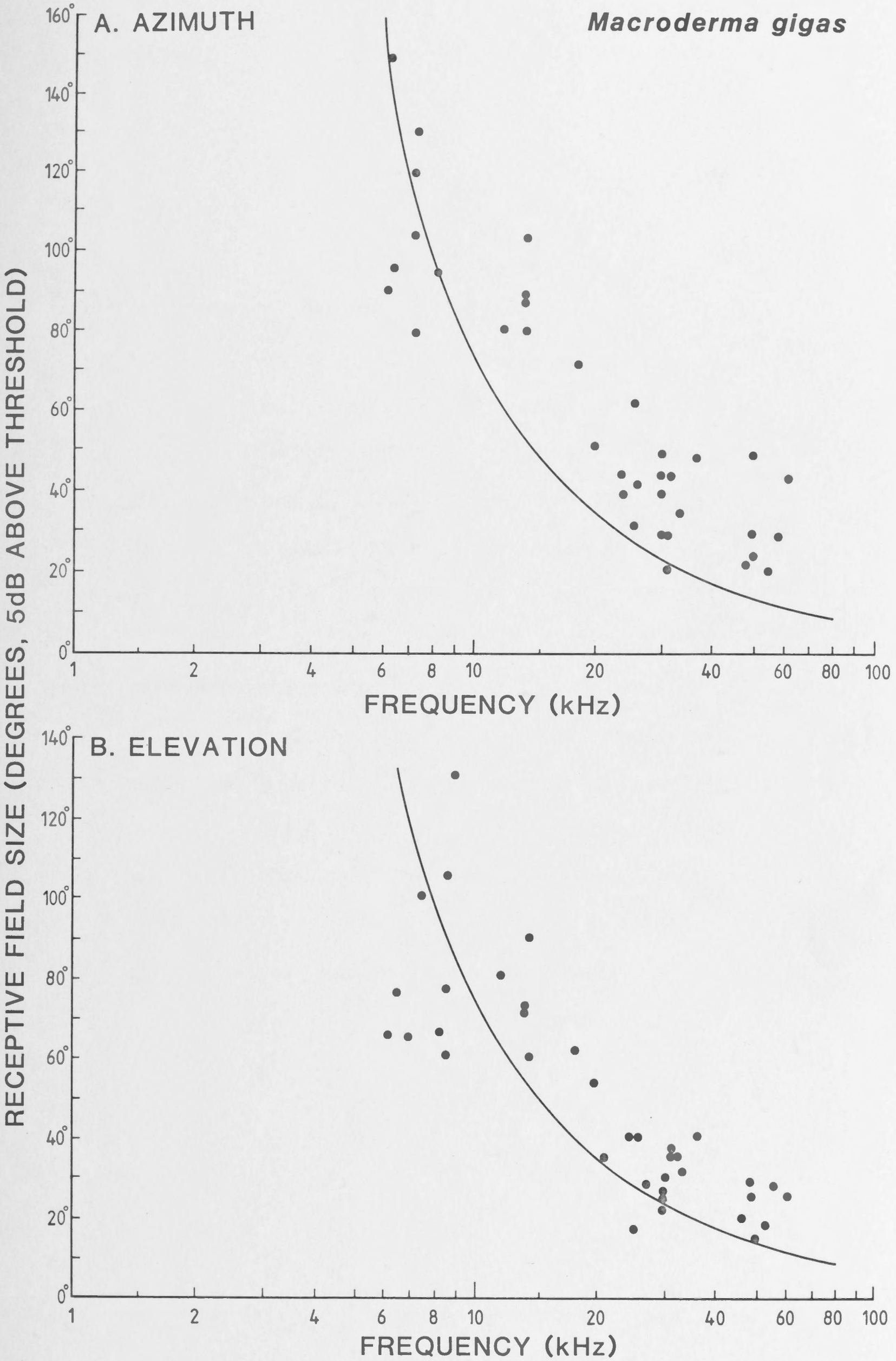
A. AZIMUTH
Macroderma gigas
RECEPTIVE FIELD SIZE (DEGREES, 5dB ABOVE THRESHOLD)
160°
140°
120°
100°
80°
60°
40°
20°
0°
1
2
4
6
8
10
20
40
60
80
100
FREQUENCY (kHz)
B. ELEVATION
140°
120°
100°
80°
60°
40°
20°
0°
1
2
4
6
8
10
20
40
60
80
100
FREQUENCY (kHz)

Fig. 2.22: A. Averaged auditory evoked potential thresholds (neural audiogram) recorded from the inferior colliculus of three individual *Nyctophilus gouldi*.

B. Average neural audiogram based on the threshold curves in A (solid line). The distribution of excitatory response thresholds (filled circles), at best frequency, for a sample of 29 neurons recorded from the inferior colliculus of *N. gouldi* is also shown for comparison.

C. Frequency distribution of energy peaks in the sonar pulse of an adult *N. gouldi*, computed at 2msec intervals through the pulse by FFT analysis. The energy bandwidth can be compared to the frequency sensitivity of the neural audiogram in A.

D. Summary of main energy bandwidths for adult sonar signals (as in C. and Fig. 2.26) and the energy bandwidths of isolation and protest calls used by juvenile *N. gouldi* (Fig. 2.26).

A *Nyctophilus gouldi*

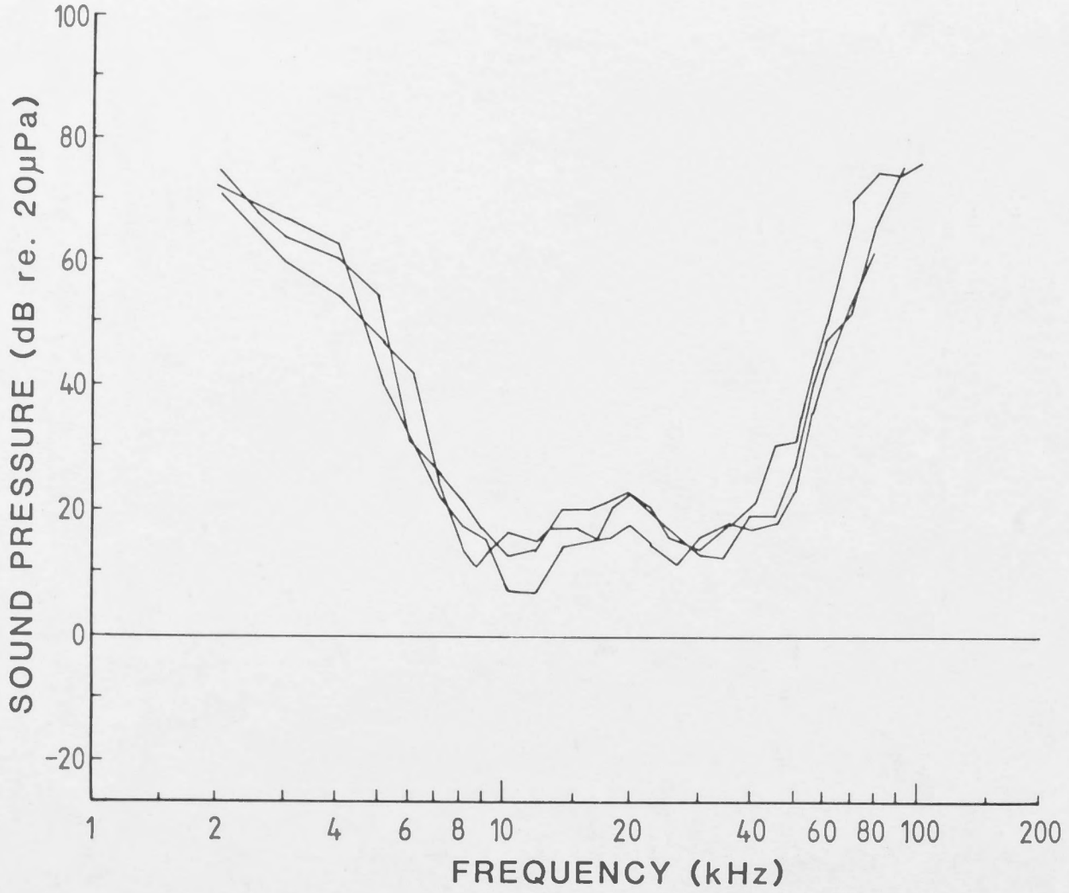

B

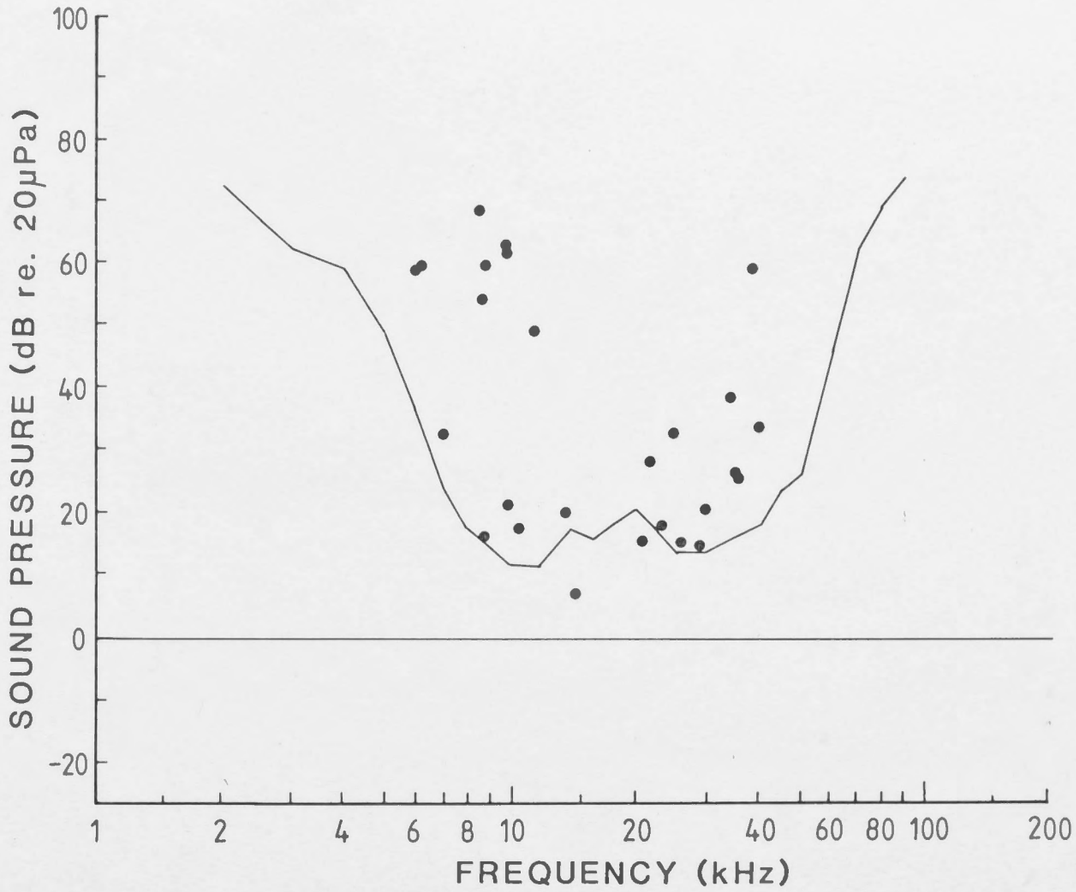

C

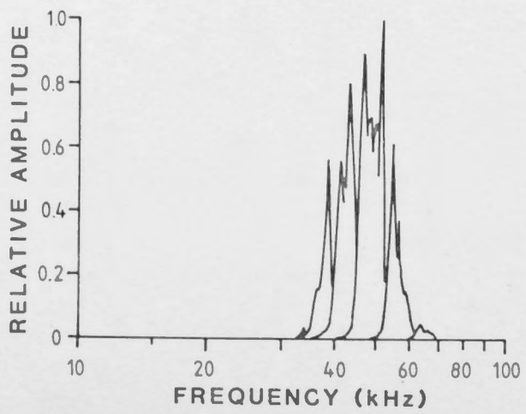

D

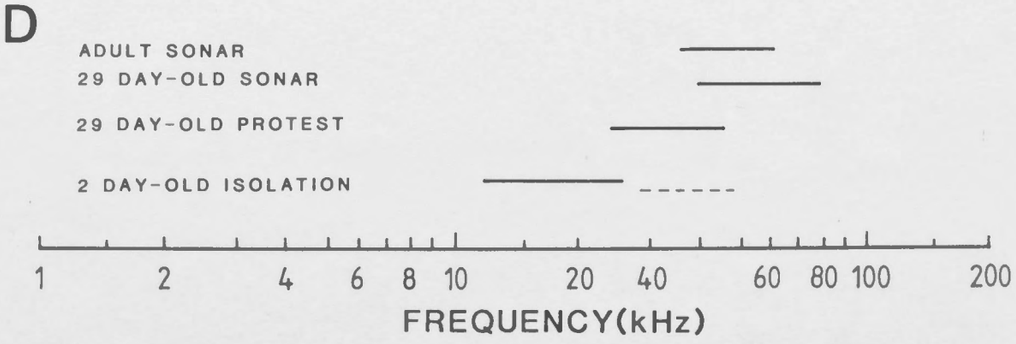

Fig. 2.23: A. Comparison between averaged auditory evoked potentials from a single *Nyctophilus gouldi*, under normal conditions (filled circles, solid line) and after removal of the pinna contralateral to the recorded inferior colliculus (open circles, dotted line).

B. Effect of contralateral pinna removal on neural thresholds calculated as the difference curve from A (filled circles, solid line). Dotted line is the average acoustic gain (in dB) of the pinna as estimated in Fig. 2.11B,C.

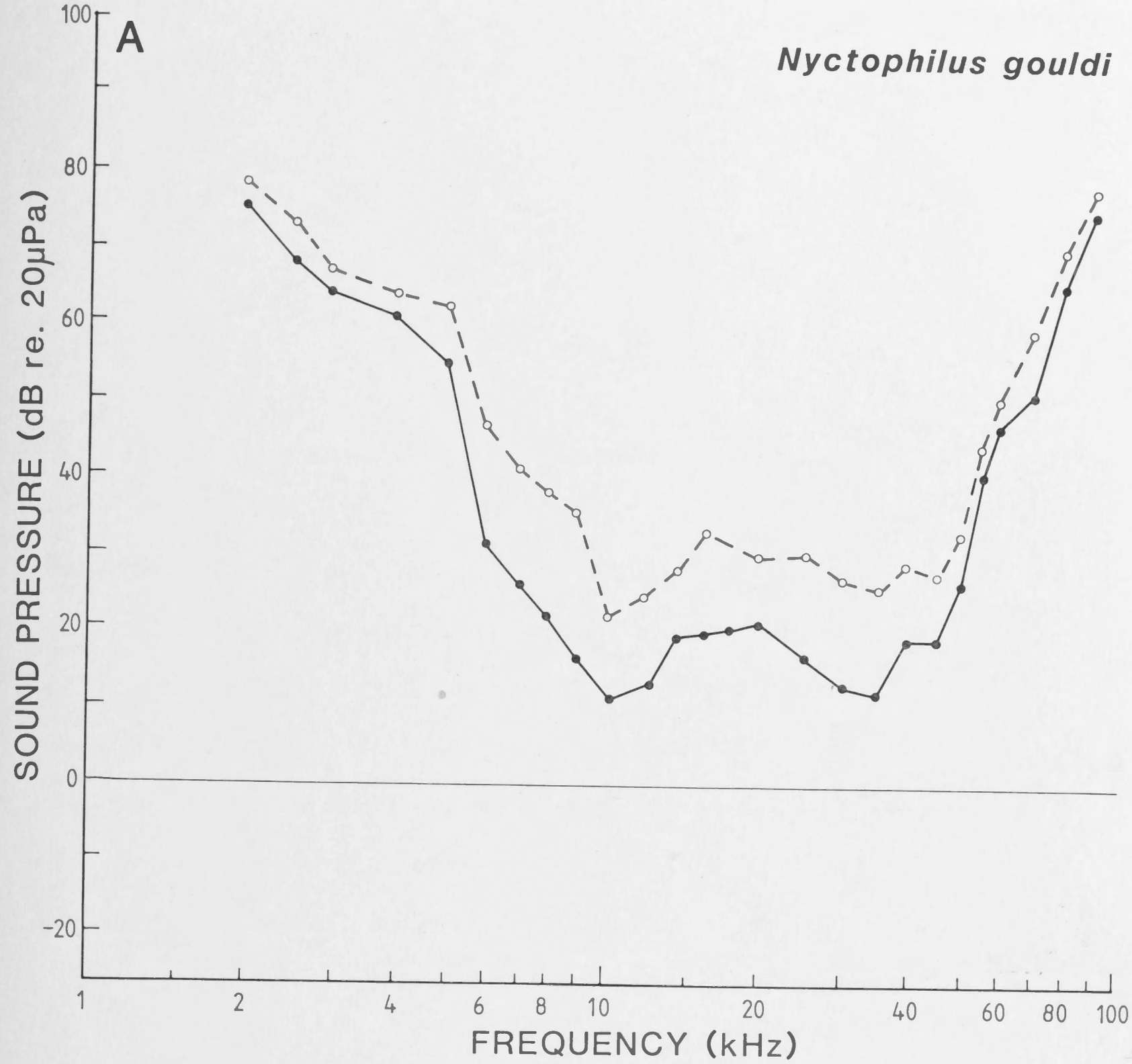
A
Nyctophilus gouldi
SOUND PRESSURE (dB re. 20µPa)
100
80
60
40
20
0
-20
1
2
4
6
8
10
20
40
60
80
100
FREQUENCY (kHz)

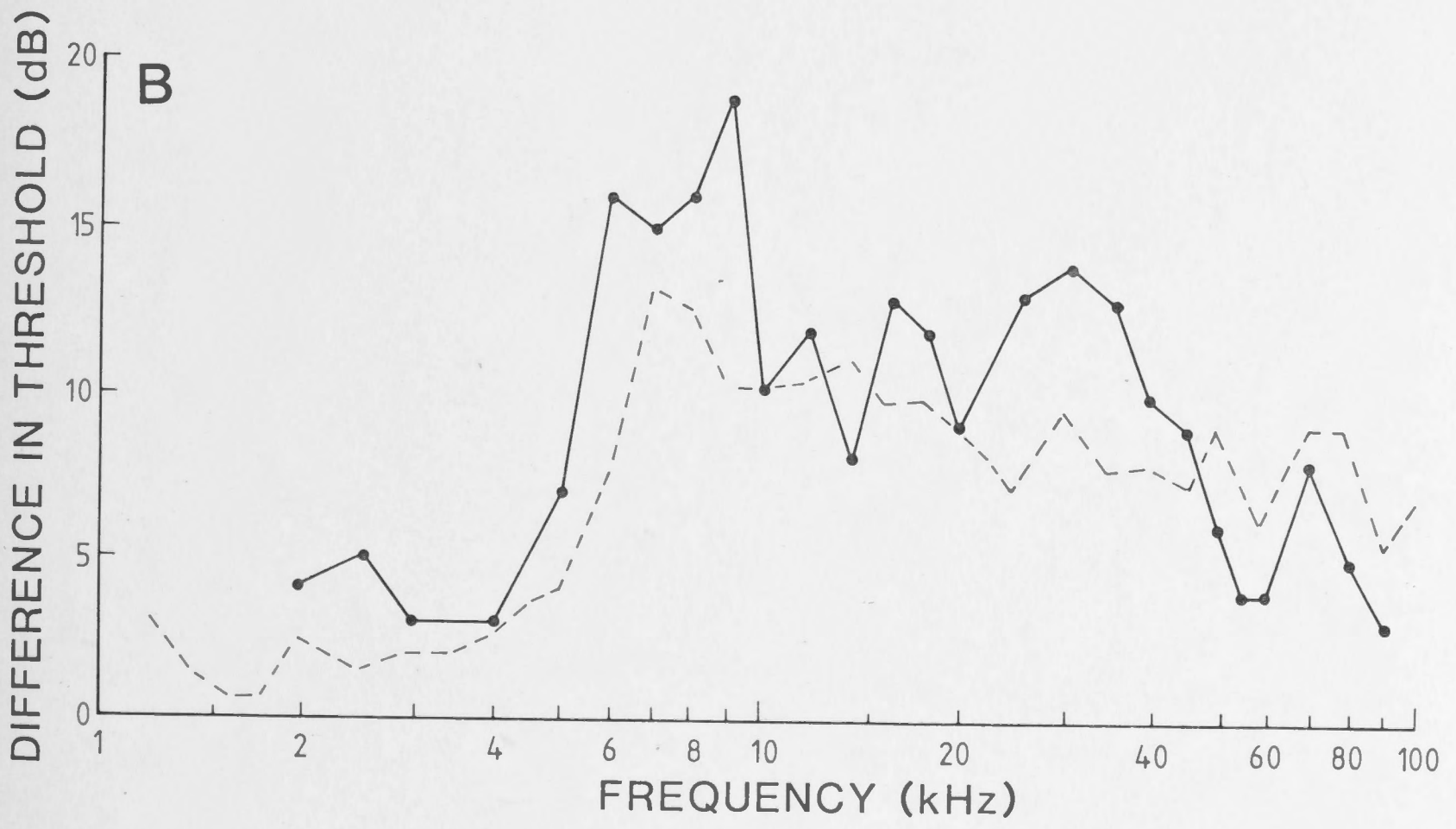
B
DIFFERENCE IN THRESHOLD (dB)
20
15
10
5
0
1
2
4
6
8
10
20
40
60
80
100
FREQUENCY (kHz)

Fig. 2.24: Examples of "axial-type" spatial receptive fields for four auditory neurons in *Nyctophilus gouldi*, recorded from the left inferior colliculus in one individual. Response boundaries are indicated by solid lines, and based on excitatory thresholds at various levels above best position at the best frequency threshold (open circles = 5dB above thresholds; closed circles = 10dB above threshold). Best position is indicated by a cross. Head alignment in the vertical plane is based on the sonar horizon and taken from acoustical measurements (Fig. 2.16).

AXIAL TYPE RECEPTIVE FIELDS
LEFT INFERIOR COLLICULUS

Nyctophilus gouldi

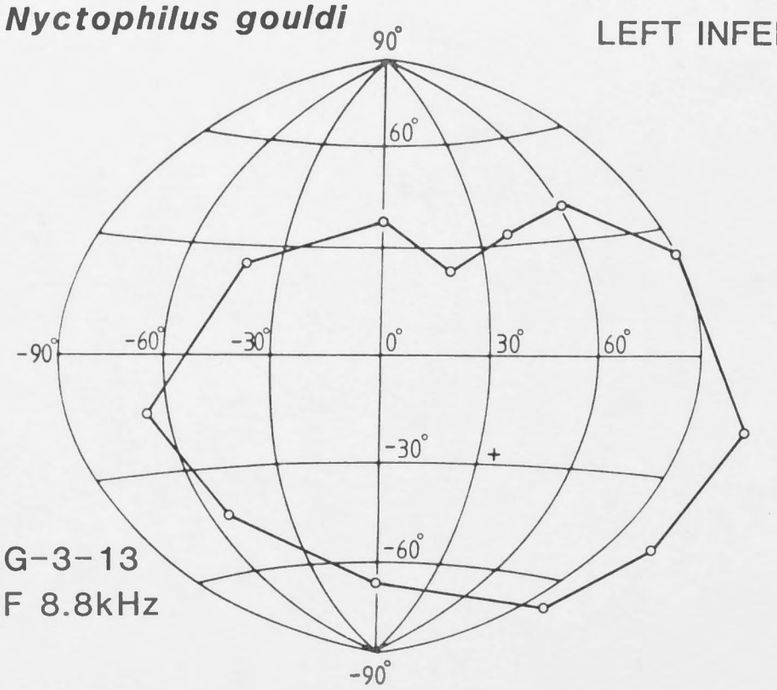

NG-3-13
BF 8.8kHz

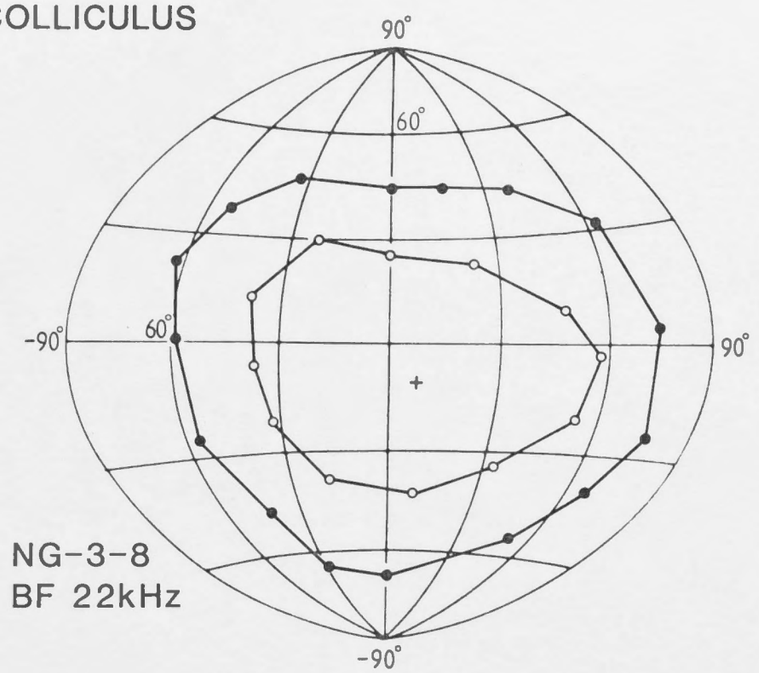

NG-3-8
BF 22kHz

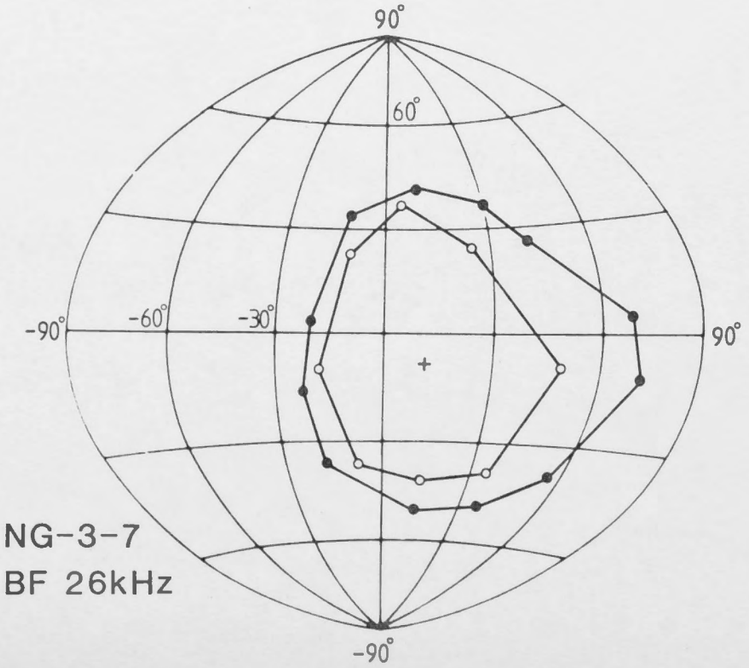

NG-3-7
BF 26kHz

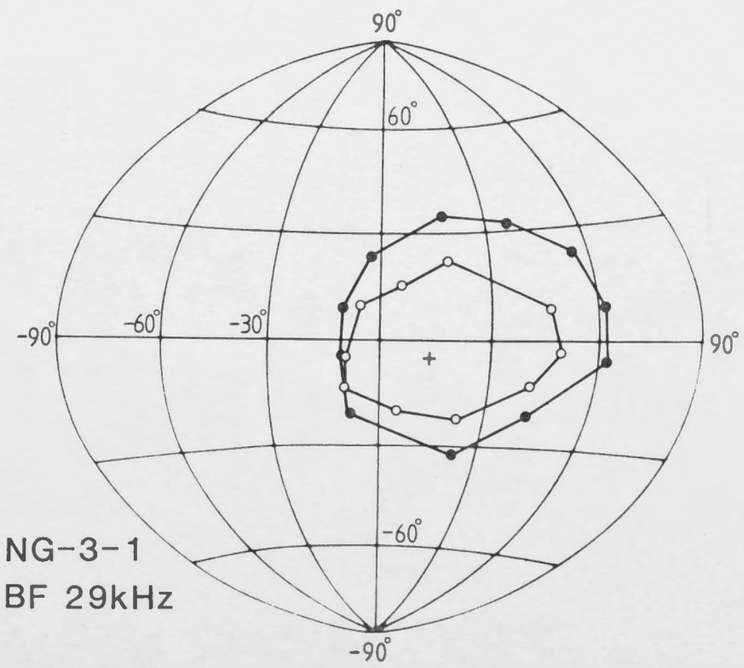

NG-3-1
BF 29kHz

Fig. 2.25: Summary of the angular size of axial-type spatial receptive fields for a sample of 15 inferior colliculus neurons in *Nyctophilus gouldi* (as shown in Fig. 2.24). Data points are based on the full angular width (2θ°) in azimuth (A) and elevation (B) for receptive field boundaries at 5dB above best position threshold sensitivity and at best frequency. Solid curves in A and B represent the expected -5dB acceptance angle (2θ°) which would result from sound diffraction by a circular aperture with a radius equivalent to the average radius of the open face of the pinna in *N. gouldi* (a = 0.85cm, see Table 2.1 and Fig. 2.10). For details of calculations of expected -5dB acceptance angle see APPENDIX 2.

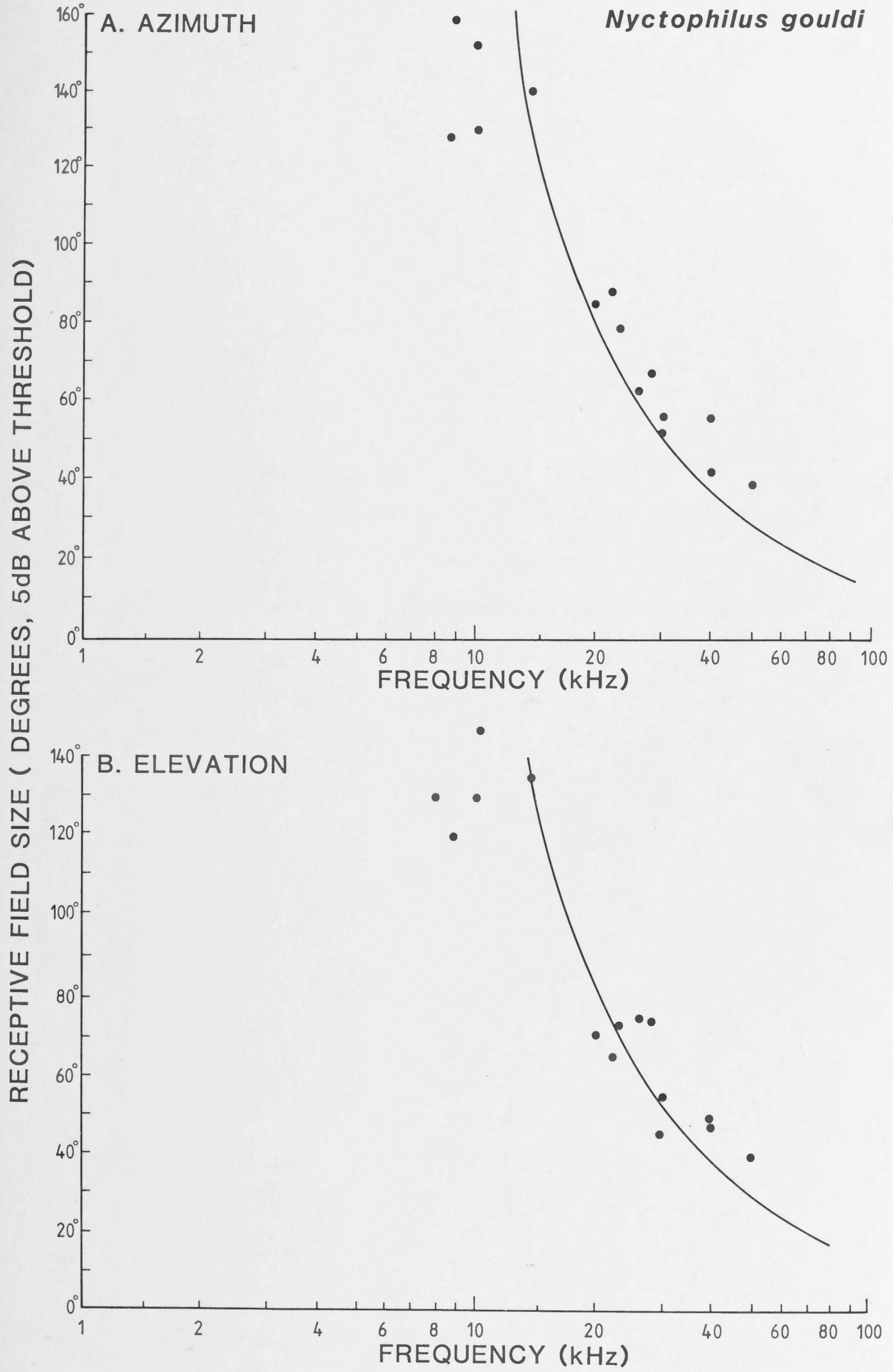
A. AZIMUTH
Nyctophilus gouldi
160°
140°
120°
100°
80°
60°
40°
20°
0°
1
2
4
6
8
10
20
40
60
80
100
FREQUENCY (kHz)
B. ELEVATION
RECEPTIVE FIELD SIZE (DEGREES, 5dB ABOVE THRESHOLD)
140°
120°
100°
80°
60°
40°
20°
0°
1
2
4
6
8
10
20
40
60
80
100
FREQUENCY (kHz)

Fig. 2.26: Sonograms of social calls and sonar pulses used by juvenile and adult *Nyctophilus gouldi*.

A. Isolation calls from two day old *N. gouldi*.

B. Protest calls from 29 day old *N. gouldi*.

C. Sonar signals from 29 day old and adult *N. gouldi*. See also Fig. 2.22 for FFT analysis of echolocation pulse.

Nyctophilus gouldi

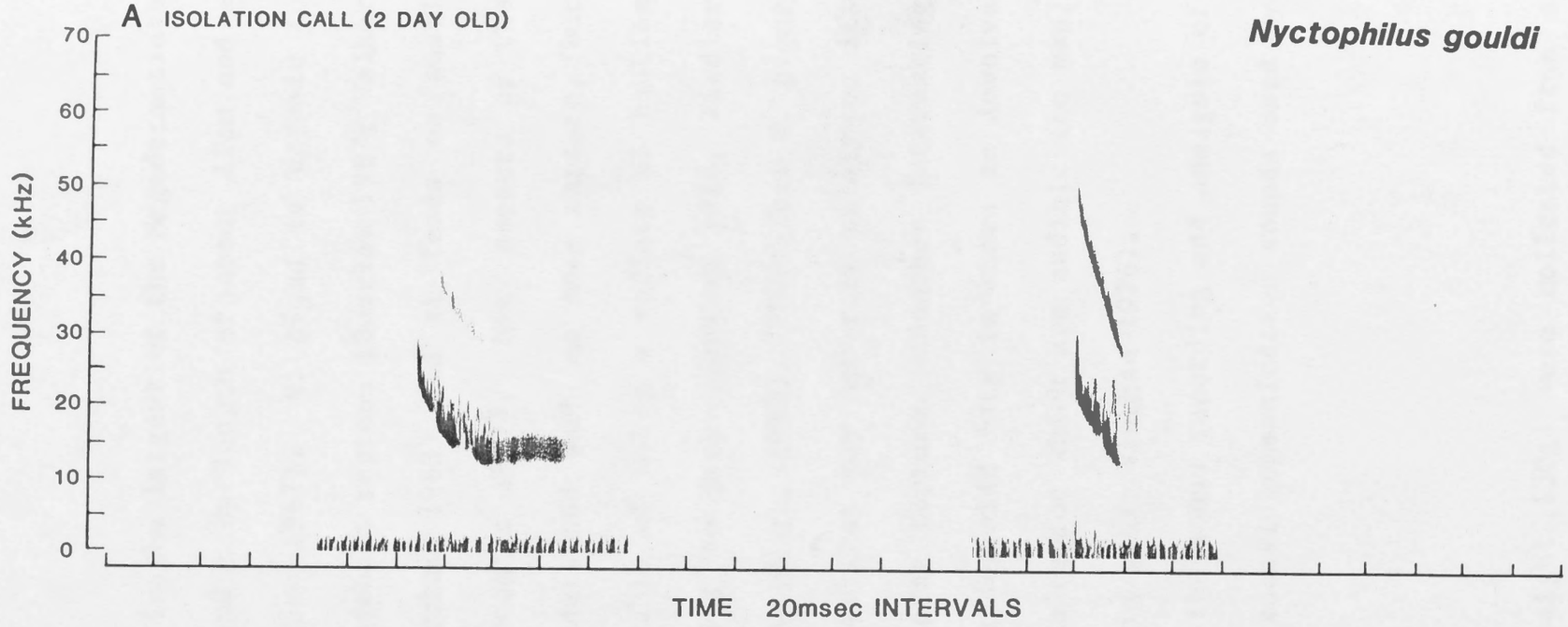

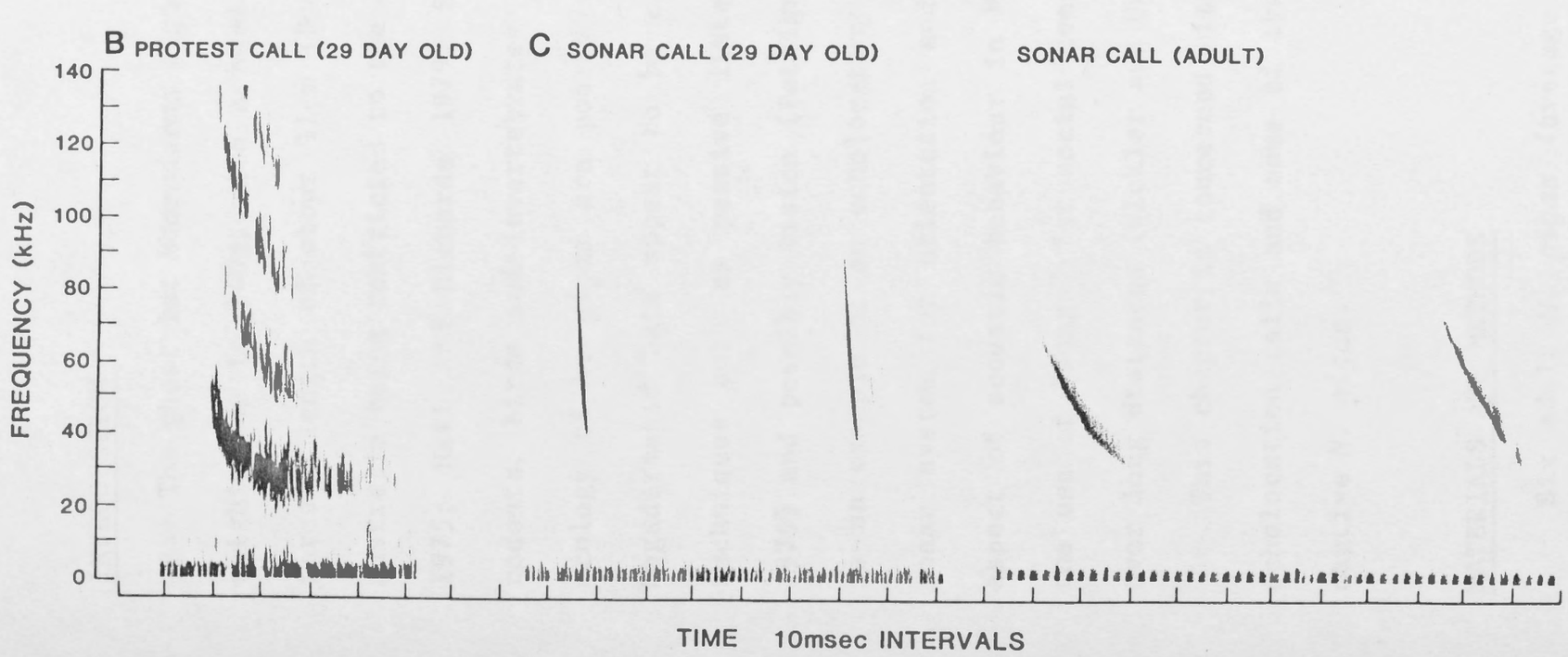

CHAPTER 3: ECHOLOCATION AND ACOUSTIC COMMUNICATION SOUNDS IN THE GHOST BAT, *MACRODERMA GIGAS* [MICROCHIROPTERA: MEGADERMATIDAE]

INTRODUCTION

The ghost bat *Macroderma gigas* is the largest of the Megadermatidae weighing up to 140g, with a head and body length of about 11cm and a forearm length of about 11cm (Douglas 1967). *M. gigas* is endemic to Australia being restricted to the northern regions (Douglas 1967; Walker 1975; Hall and Richards 1979; Strahan 1983) and it feeds on small rodents, birds and invertebrates (Douglas 1967). Many aspects of the ecology of *M. gigas* are poorly understood such as prey capture, but Megadermatid bats appear to be capable of using a variety of hunting techniques such as passive listening to prey (Vaughan 1976; Fiedler 1979) and possibly vision (Pettigrew *et al.* 1983). Therefore *M. gigas* is an example of an echolocating bat that may not rely solely on its sonar system for orientation and prey capture. Another interesting aspect of acoustic behaviour in Megadermatid bats is known to involve the use of "songs" for social communication which are audible (to man) over long distances (Wickler and Uhrig 1969; Vaughan 1976).

This chapter is concerned with the sound recording and analysis of echolocation calls and some of the social communication sounds used by captive *M. gigas*.

MATERIALS AND METHODS

Six adult *M. gigas* (average weight 130g) were collected from a colony at Pine Creek in the Northern Territory, Australia. They were kept in a spacious indoor enclosure with controlled temperature and humidity in Canberra, ACT and fed on a diet of mice (Guppy and Coles

1983). Sound recordings were obtained over a period of time from individuals in flight or roosting on the walls of an anechoic chamber as described in CHAPTER 2. Echolocation signals were recorded from bats flying in the anechoic chamber and whilst avoiding obstacles. Social calls were recorded from isolated or paired individuals in the chamber under lighted and darkened conditions.

The sound recording system comprised a QMC bat detector Model S100 (microphone response: 10-180kHz ± 5dB) or a ¼" Bruel and Kjaer microphone (Type 4135) with preamplifier (Type 2633) (response bandwidth : 4Hz - 100kHz ± 2dB). Microphone output was recorded on a Racal Store 4D instrumentation recorder at 152 cm/sec (response bandwidth: 50Hz-300 kHz ± 3dB)

Sound analyses were performed on a Kay Sonograph (Model 6061-B), Kay Digital Sonagraph (Model 7800) or a Voiceprint (Model 700). Pulse repetition rate was determined by replaying slowed recordings through an oscilloscope (Tektronix Type R561B) and filming the screen at a high speed with a 35mm camera (Kymograph Model C4R). For additional analysis a transient recorder was used to digitize signals and a sequential FFT analysis, was produced using a Hewlett-Packard (Model 8205A) real-time spectrum analyser.

RESULTS

Echolocation signals

Pulse structure

The sonar orientation pulses of *M. gigas* were always very short in duration, ranging from a minimum of 0.6msec during obstacle avoidance up to a maximum of 2.3msec at rest (N=90). The average pulse duration when the bat was in flight was about 1.2msec (range 0.8 - 2.3msec N=60). The

orientation pulses of *M. gigas* are frequency modulated and contain multiple harmonics (Fig. 3.1). Each pulse contains three to four harmonics with most of the energy in the second or third harmonic and the fundamental frequency is modulated by 5kHz from 20-15kHz. However during landing or obstacle avoidance, frequency modulation is steeper (up to 11kHz, ranging from 23-12kHz) with four harmonics present. In all cases most of the energy in the sonar pulses of *M. gigas* is concentrated in the second and third harmonic and the fundamental remained suppressed.

Pulse patterning

During echolocation the pulse repetition rate of *M. gigas* ranged from 2 pulses per second (pps) at rest up to 110pps during flight (Fig. 3.2). From 8 flight trials the temporal pattern of pulse emission was found to be grouped into three (36%), four (26%) or occasionally five pulses. Within a group of pulses the first two were always closer together, having an average interval of 30msec (see Fig. 3.2). The average pulse repetition rate during flight was found to be 32pps however as the bats approached an obstacle such as the recording microphone, pulse repetition rate increased to 85pps and the pulses became paired. When bats were about to land the average pulse rate was 50pps and no pulse grouping was apparent (Fig. 3.2).

Social communication signals

Chirp.

In captivity a frequent vocalization used by *M. gigas*, excluding sonar signals, is a 'chirp' which is audible to the human ear and previously noted by Douglas (1967). It is often elicited at dusk and throughout the night by roosting bats and is characterised by a sequence

of up to 5-9 very intense stereotyped syllables. Two complete syllables from a typical chirp sequence are shown in Fig. 3.3 and the temporal structure reveals three elements to each chirp syllable. The first high amplitude element is about 70msec long with 6-10 amplitude modulations. Sonagraphic analysis of the frequency-time structure of the chirp call reveals that the first element has an initial high amplitude descending frequency modulated section with energy from 15-12kHz (Fig. 3.4). The subsequent amplitude and frequency modulated sections of the first element have a less clear structure but resemble pulsed bandwidth noise between 6-10kHz. The interval between the beginning of the first and second elements of the chirp is about 110msec and the interval between the second and third elements is about 20-30msec. The second and third elements are often paired and spectral analysis (Fig. 3.5) reveals that the first pulse in the pair has a duration of about 5msec and is frequency modulated from 25-20kHz (Fig. 3.5). In the second element the initial frequency modulated section is followed by a constant frequency of 20kHz. The third element of the chirp (Fig. 3.5) is shorter in duration than the second element, about 3msec, and has a descending frequency (fundamental) sweep from 25-15kHz. The paired pulses in the chirp syllable both contain harmonics and in each case the fundamental frequencies are prominent.

Squabble.

A second type of social signal used by *M. gigas* was called a squabble and often occurred when bats were fighting over food, or when one bat landed on another roosting individual. As shown in Fig. 3.6, the squabble call is poorly modulated in amplitude and frequency and is a 'noisy' signal with a highly restricted energy band between 5-9kHz. Bouts of squabbling were variable in duration, depending on the severity

of the food struggle for example but continued up to 3sec or so.

Ultrasonic communication signals

There were several ultrasonic vocalizations used by *M. gigas* which were but not associated with sonar emission nor part of the chirp. Ultrasonic social communication pulses were often emitted by stationary bats, particularly in the presence of, or being approached by a second flying individual. A pair of captive bats when resting at some distance from each other were frequently found to use this type of communication. Fig. 3.7 shows one type of ultrasonic communication signal which is similar in duration to the normal sonar signal (see Fig. 3.1) This social call is frequency modulated but only the second harmonic is expressed in contrast to the harmonic structure of normal sonar pulses (Fig. 3.1) or even the high frequency chirp elements (Fig. 3.5). Unlike sonar pulses, ultrasonic communication signals were emitted singly or in an irregular sequence.

DISCUSSION

The sonar pulses reported here for *M. gigas* have a similar frequency content to other Megadermatid bats (Novick 1958; Mohres 1967; Mohres and Neuweiler 1966; Table 3.1) but in the present study, detailed spectral analyses show that the pulses are in fact rapidly frequency modulated with multiple harmonics. This conclusion is supported by Pye (1980). Megadermatid bats are known to emit extremely short sonar pulses in comparison to other echolocating bats (Schnitzler and Henson 1980) and short pulses reduce problems of pulse-echo overlap associated with close targets. The duration of the sonar pulse of *M. gigas* is similar to that found in *Megaderma lyra* and *M. spasma*, although shorter than the pulses observed in *Cardioderma cor* (Table 3.1; Mohres and

Kulzer 1957; Mohres and Neuweiler 1966; Mohres 1967). The frequency modulation range of the sonar pulse in *Macroderma gigas* is relatively shallow however the presence of multiple harmonics produce a broad spectral bandwidth. Short pulses with relatively wide bandwidths provide good range resolution and localization characteristics (Buchler and Mitz 1980).

In view of the highly developed noseleaf in *M. gigas* (Fig. 2.1) the echolocation signals are likely to be emitted exclusively through the nostrils, and the noseleaf may act as a horn or reflector (Pye 1961). The external nares are separated by about 0.3cm (Fig. 2.1B) which is approximately half of the wavelength of the third harmonic (58kHz) of the sonar pulse. Such a relationship is known to cause lateral interference for sound emission through the nares, resulting in forward amplification and improved directional beaming of the signal (Schnitzler and Grinnell 1977). In contrast, social vocalizations may well be emitted through the mouth particularly calls with substantial low frequency energy such as the chirp and squabble. However a combination of mouth and nostril emission seems likely, since *M. gigas* can alter the relative energy between the harmonic frequencies used for sonar and social communication (Figs. 3.1, 3.5, 3.7).

The pulse repetition rate of *M. gigas* is similar to that described for *Megaderma lyra* (Mohres and Neuweiler 1966; Mohres 1967) although more pulses per group were observed in the present study. Mohres and Neuweiler (1966) also reported pairing of pulses when *M. lyra* approached objects, similar to the present findings in *Macroderma gigas*. Paired pulses have been observed in several other species of echolocating bats (Schnitzler and Henson 1980) and occurs during echolocation in the shrew *Sorex vagrans* (Buchler and Mitz 1980), cave-dwelling swiflets *Collocalia*

spodiopygia (Coles *et al.* 1982) and Megachiropteran fruit bats of the genus *Rousettus* (Sales and Pye 1974). The significance of pulse pairing is unclear at present but may be an energetically efficient strategy for certain echolocators with low intensity pulses, such as the Megadermatidae, in order to increase the signal to noise ratio while retaining short broadband pulses (Buchler and Mitz 1980). Pulse grouping is facultative in *M. gigas* since, for example, it does not necessarily occur during landing. Sonar pulse grouping has been observed in other Microchiropteran bats (Grinnell and Griffin 1958; Schnitzler and Henson 1980) and may be related to wing beat frequency (Schnitzler and Henson 1980).

The use of echolocation calls in a social context has been described in *Rhinolophus ferrumequinum* (Mohres 1967) and has also been shown in *Eptesicus serotinus, Nyctalus noctula, Pipistrellus pipistrellus* (Miller and Degn 1981). These bats also emit ultrasonic calls that differ from their echolocation calls and in *Noctilio albiventris* social contact is maintained by using modified sonar signals (Brown *et al.* 1983). In the present study, high frequency or ultrasonic 'social' calls in *M. gigas* were found to be similar to the echolocation calls but differed in the expression of harmonics and duration. A degree of similarity between ultrasonic calls and sonar pulses may be expected in *M. gigas*, since in evolutionary terms Megadermatids have been considered "primitive" echolocators (Simmons and Stein 1980).

M. gigas was found to use certain calls with the maximum energy concentrated below 15kHz, suggesting a relatively low frequency communication channel in addition to the use of social and sonar signals confined to the ultrasonic range. Audible calls similar to the chirp in *M. gigas* have been described in other Megadermatid bats such as

Cardioderma cor (Vaughan 1976) and *Lavia frons* (Wickler and Uhrig 1969). In *C. cor*, Vaughan (1976) has described a song which is used in foraging areas to establish territories and also a flight call which he considered a long range call for communicating location and direction of flight. From Vaughan's description, both of these 'audible' calls resemble the 'chirp' used by *M. gigas* in that they have repeated high intensity pulses containing energy up to 12kHz. Wickler and Uhrig (1969) have described a sharp "schrei" associated with territorial behaviour in *L. frons* perhaps bearing some resemblance to the 'chirp' of *M. gigas*. Relatively low frequency calls have been associated with mating behaviour in *Myotis lucifugus* (Barclay and Thomas 1979) and *Carollia perspicillata* (Porter 1979). Irritation calls similar to the squabble call of *M. gigas* have been described for *Antrozous pallidus* (Brown 1976), *M. lucifugus* (Barclay and Thomas 1979) and *C. perspicillata* (Porter 1979). The energy in these calls occur in the frequency range 5-30kHz but, as in the 'squabble' call of *M. gigas*, they are poorly modulated and noisy signals.

Finally, there has been some interest in the foraging strategies of Megadermatid bats since under laboratory conditions, *Megaderma lyra* can passively locate prey without the use of echolocation and in complete darkness (Fiedler 1979; see CHAPTER 2 and also GENERAL DISCUSSION AND CONCLUSION). Some aspects of the foraging strategy of *Macroderma gigas* have been studied (Tidemann *et al.* 1985) but the use or not of sonar during prey capture in the wild has not been established. In general, Megadermatid bats may rely on passive listening (or vision) for prey capture rather than sonar due to the limited echo range provided by low intensity sonar pulses (Mohres and Neuweiler 1966). In this context both *M. gigas* and *Megaderma lyra* have their most sensitive hearing below 20khz and therefore well below the sonar range (see CHAPTER 2; Neuweiler

et al. 1984). The audible chirp call reported here for *Macroderma gigas* in captivity is used extensively both in the day roost and in the foraging area at night (personal observations). The main energy of the chirp call matches the extremely sensitive low frequency hearing region in *M. gigas* (see CHAPTER 2; Fig. 2.18) and suggests a highly specific acoustic communication channel in this species which could be used for hunting as well.

TABLE 3.1: Characteristics of Megadermatid sonar signals.

	Macroderma gigas[1]	Megaderma lyra[2,3,4]	Megaderma spasma[4]	Cardioderma cor[5,6]	Lavia frons[7]
Pulse duration and range (msec)	1.0 (0.6 - 2.25)	1.3 (0.42 - 1.76)	1.0 (0.8 - 1.4)	3	
Fundamental frequency (kHz)	20 - 16	19.6	20	20	
No. harmonics	3 or 4	3 or 4	4	3 or 4	
Dominant harmonic	2, 3 or 4	3 or 4		1 or 3	
Frequency range (kHz)	20 - 90	15 - 80	17 - 88	18 - 100†	
Pulse intensity (dB)		80 - 85			
Repetition rate (pps)	2 - 110	10 - 300		35	
Pulses per group	2, 3 or 4	2			
Body weight (gm)	100 - 140	20 -50	20 - 50	20 - 50	
Forearm length (mm)	105 - 115	50 - 70	50 - 70	50 - 70	53 - 63
Body length (mm)	115 - 140	65 - 85	65 - 85	65 - 85	65 - 85
Diet	insects, small vertebrates	insects, small vertebrates	insects, small vertebrates	insects small vertebrates	insects

[1]Present Study [2]Mohres, 1967 [3]Mohres and Neuweiler, 1966 [4]Novick, 1958 [5]Mohres and Kulzer, 1957
[6]Vaughan, 1976 [7]Walker, 1975.

Fig. 3.1. Digitized waveform (top) and time-frequency structure (bottom) of an echolocation pulse used by a flying *Macroderma gigas*, and recorded in an anechoic chamber. The FFT analysis of the sonar pulse (bottom) was based on sequential spectra taken at 200 μsec intervals through the pulse (top).

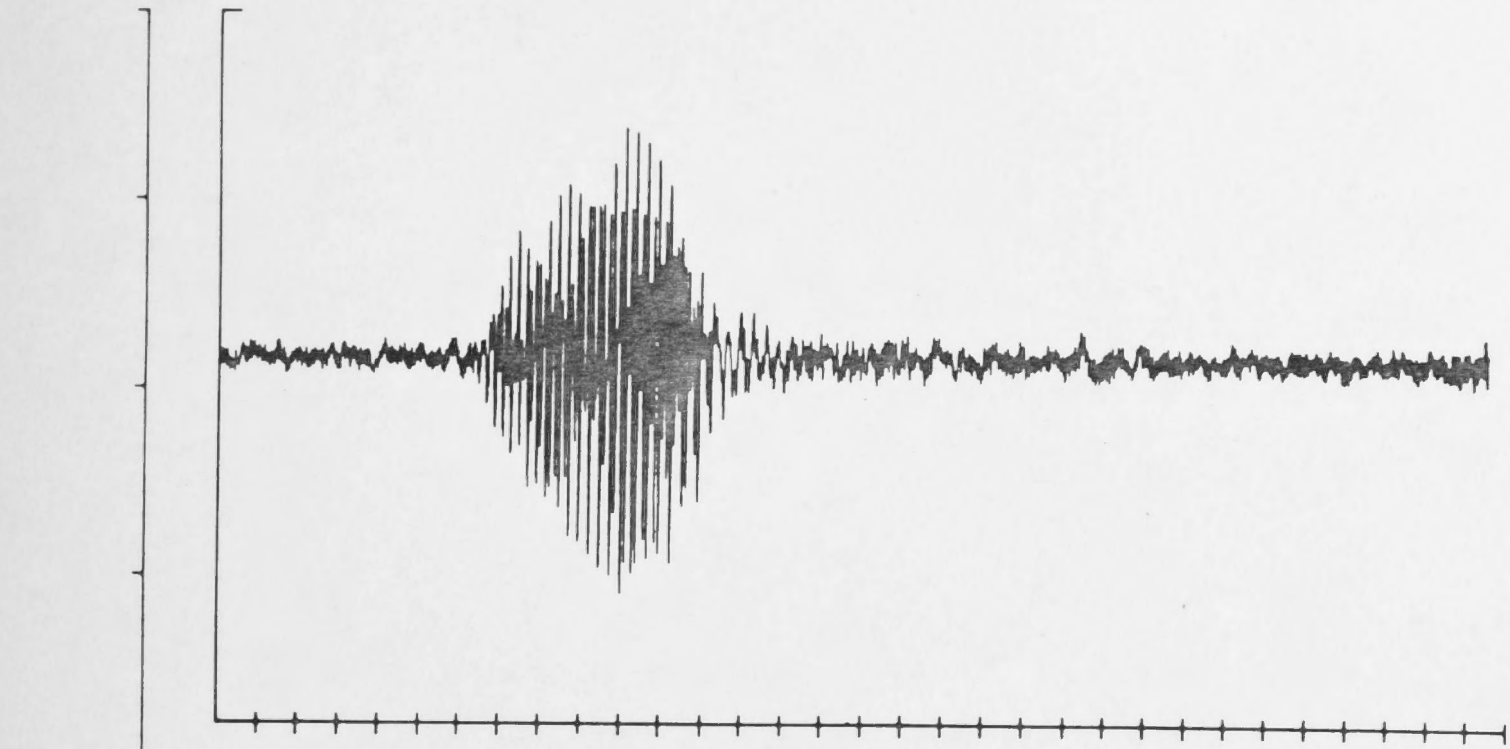
Time (200μsec/div)

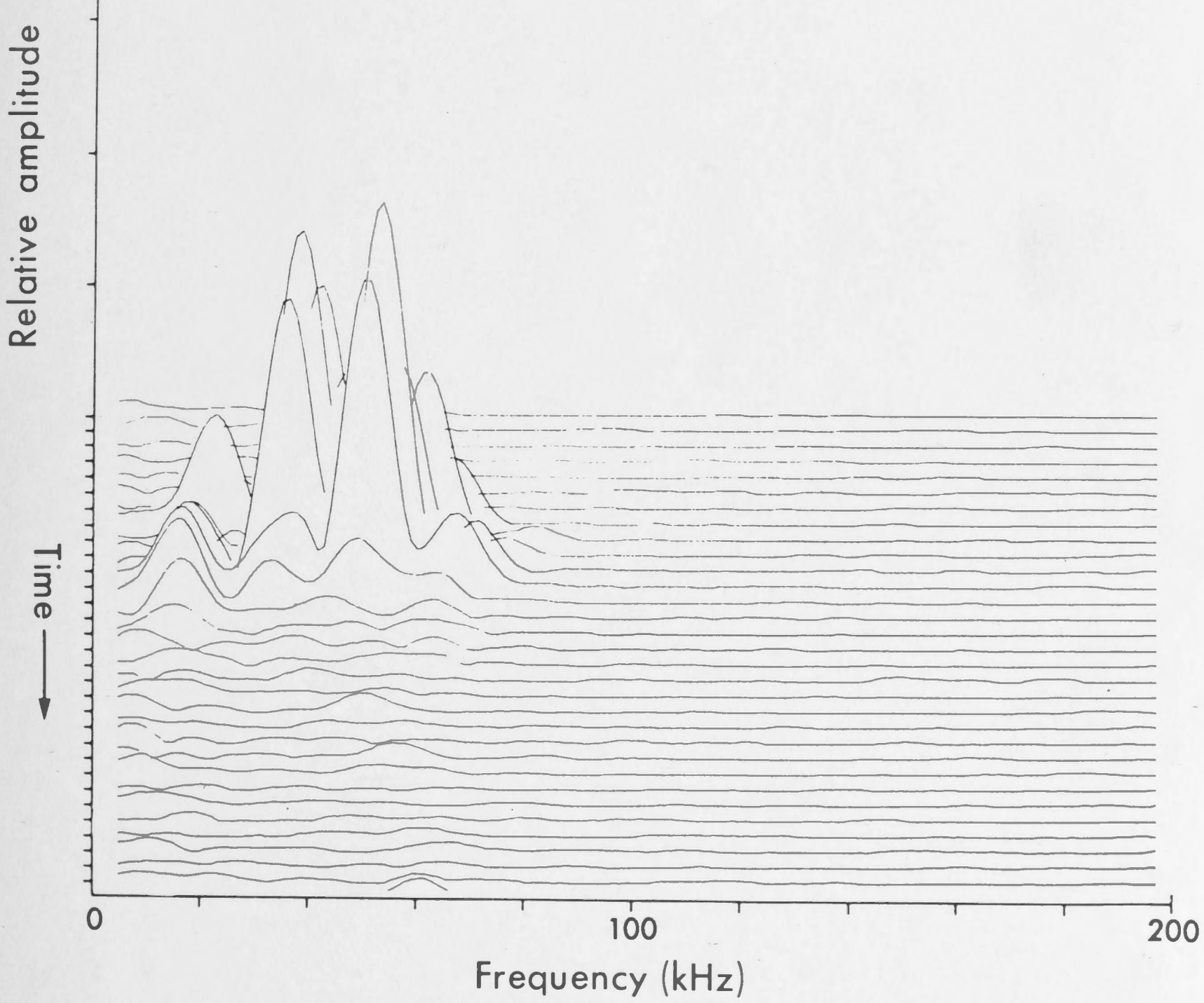
Relative amplitude
Time
0
100
200
Frequency (kHz)

Fig. 3.2 Sonar pulse repetition rate recorded from *Macroderma gigas* while flying undisturbed, avoiding an obstacle (recording microphone) and finally landing on the wall of an anechoic chamber. Temporal pulse pattern is shown schematically above.

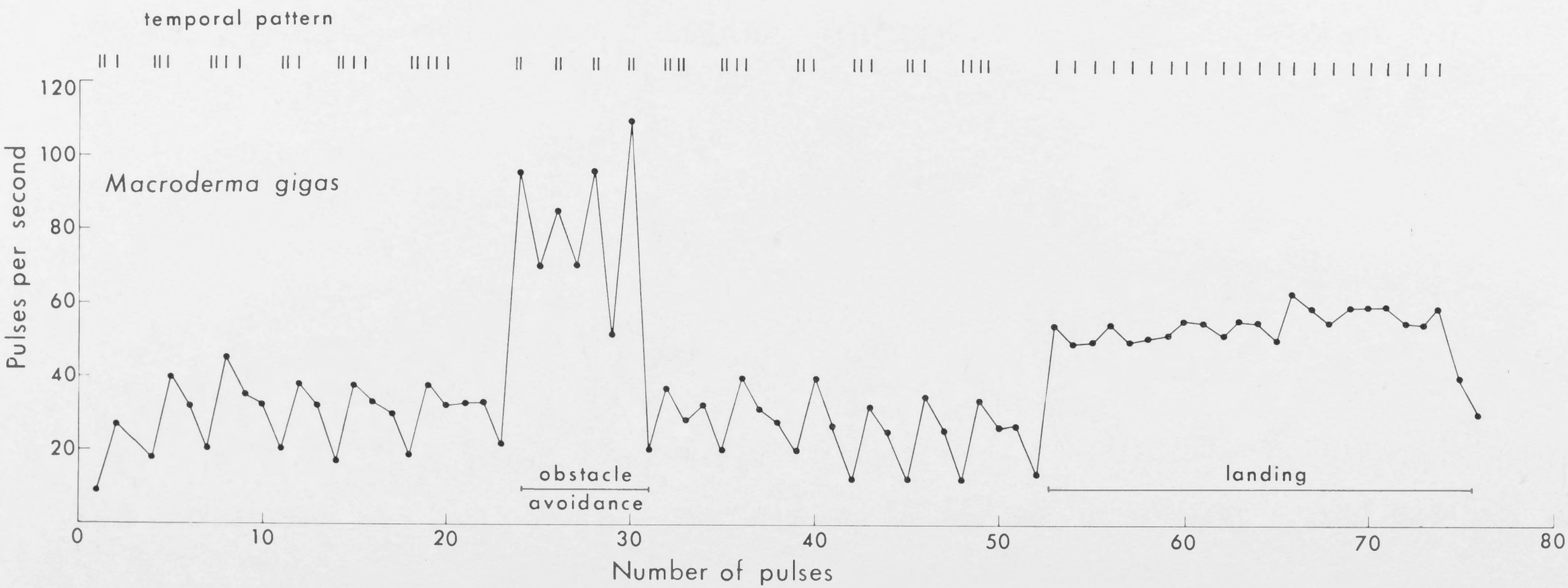
temporal pattern
Macroderma gigas
Pulses per second
120
100
80
60
40
20
0
10
20
30
40
50
60
70
80
obstacle
avoidance
landing
Number of pulses

Fig. 3.3. Oscillogram of a section of the 'chirp' social communication signal used by *Macroderma gigas*, showing the timing of the three elements in each syllable (elements indicated by numbers).

Chirp vocalization. M. gigas

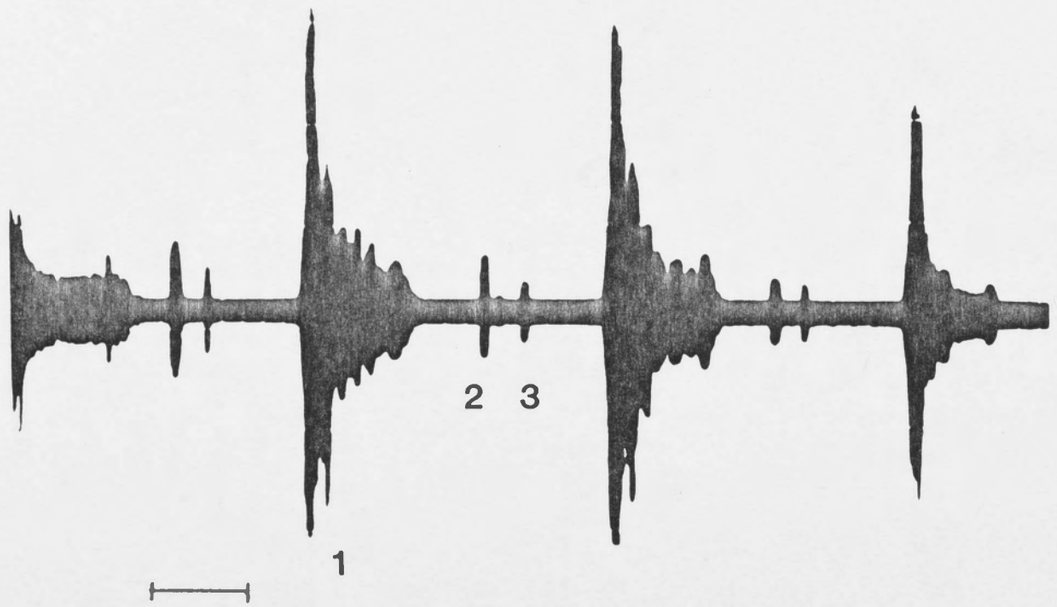

60msec

Fig. 3.4. Sonograph of a chirp sequence for *Macroderma gigas* similar to that shown in Fig. 3.3. The longest duration audible component (1, as in Fig. 3.3) is followed by the two lower amplitude high frequency pulses (2, 3 as in Fig. 3.3).

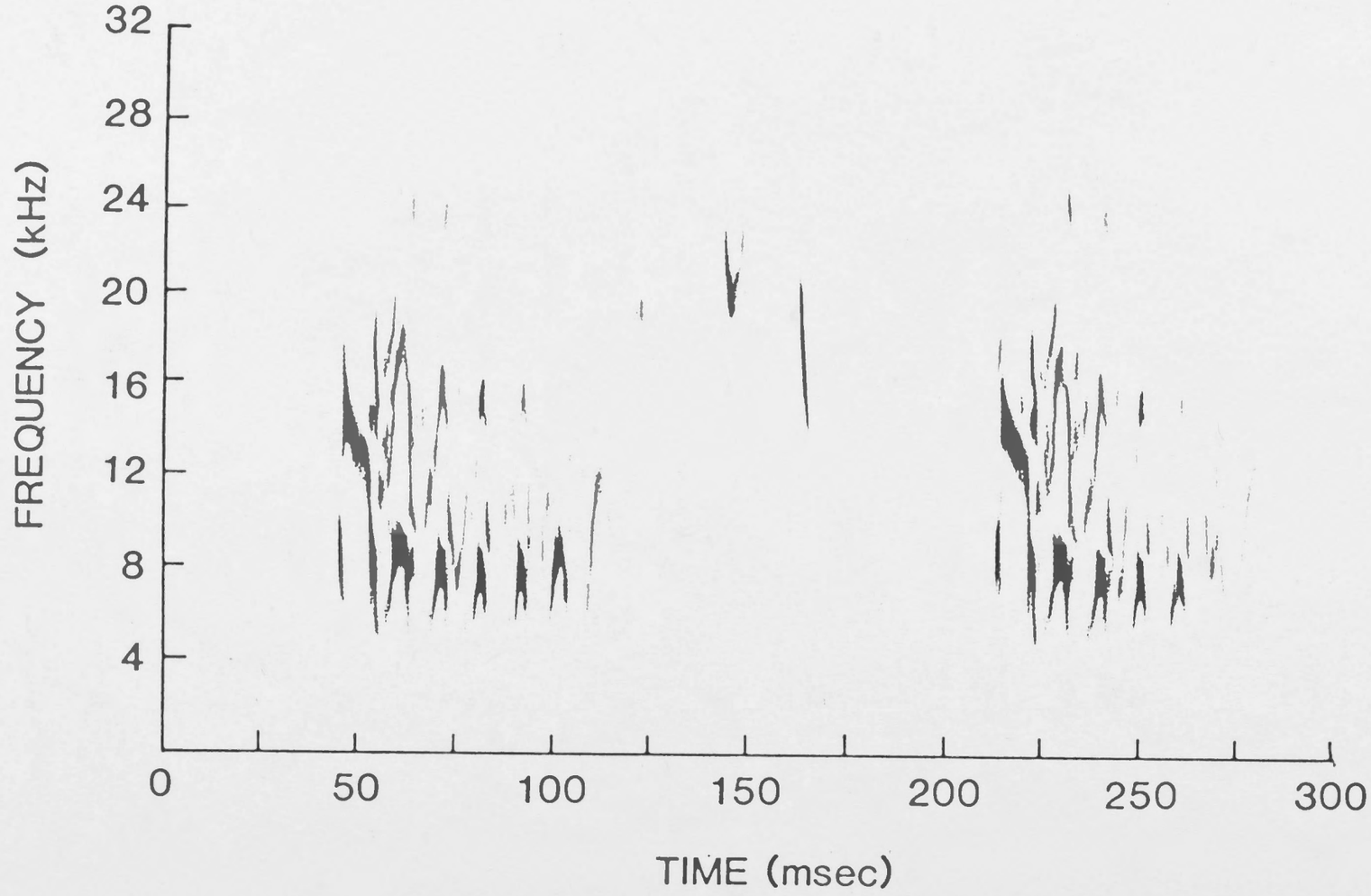
FREQUENCY (kHz)
32
28
24
20
16
12
8
4
0
50
100
150
200
250
300
TIME (msec)

Fig. 3.5. Digitized waveforms (top) and time-frequency structures (bottom) of the two high frequency pulses of the "chirp" vocalization for *Macroderma gigas* (as shown in Figs. 3.3 and 3.4). Left = second element; Right = third element. Sequential FFT analysis (bottom) computed at 200 μsec intervals through the pulses (at top).

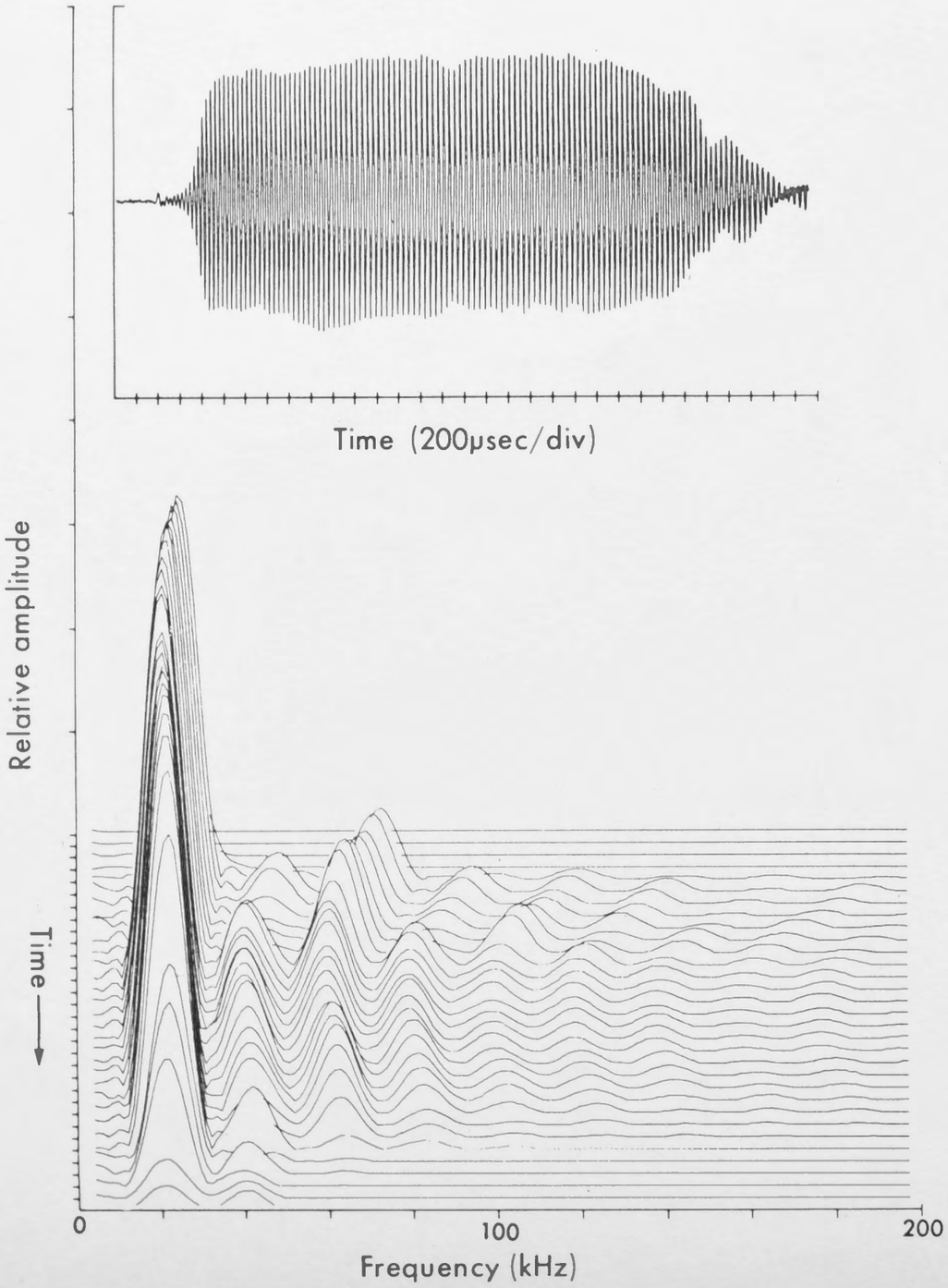
Time (200μsec/div)
Relative amplitude
Time
0
100
200
Frequency (kHz)

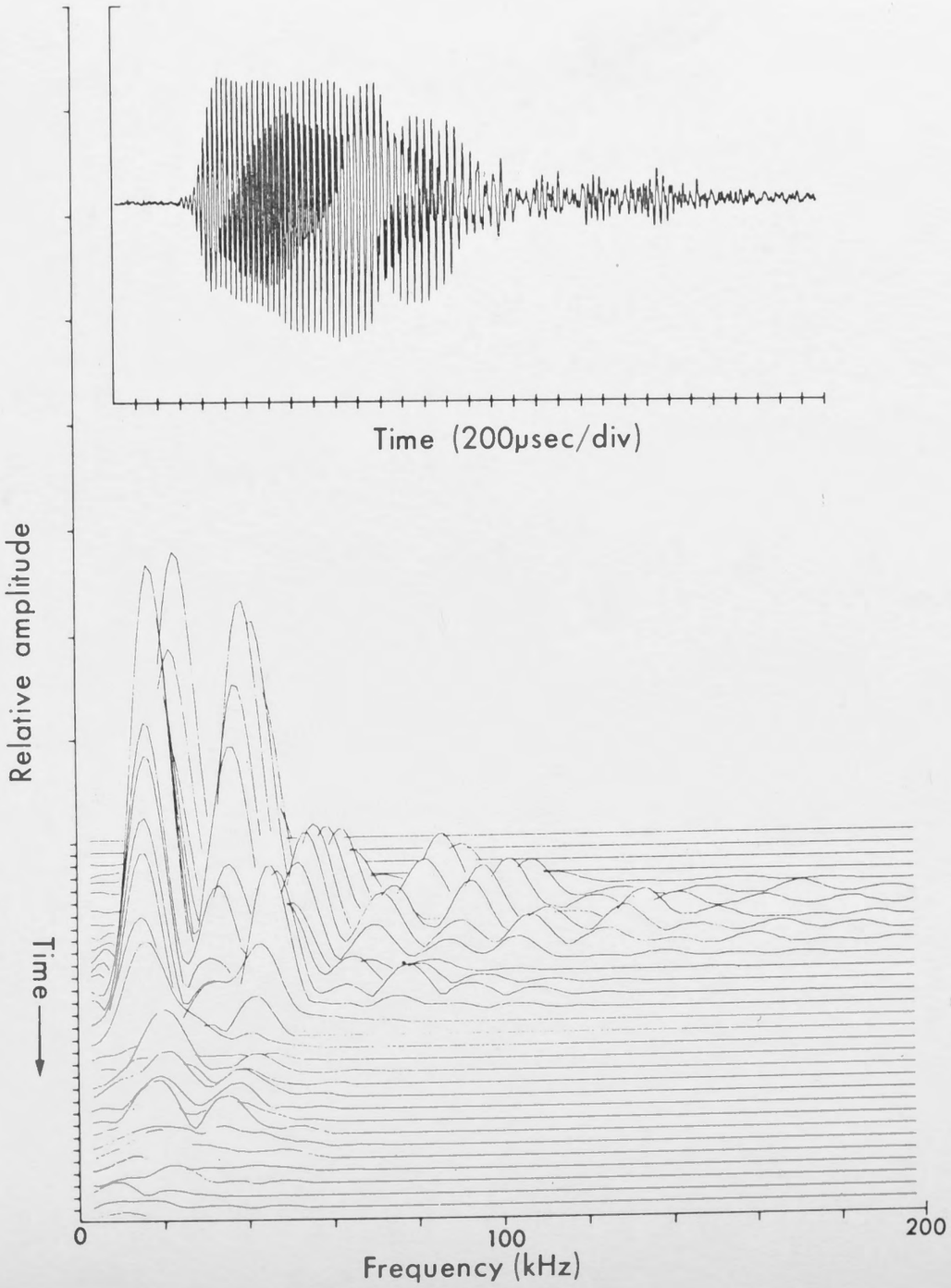
Time (200μsec/div)
Relative amplitude
Time
0
100
200
Frequency (kHz)

Fig. 3.6. Digitized waveform (top) and time-frequency structure (bottom) of a mid-section of a "squabble" call used by *Macroderma gigas* during a fight over food. For analysis details see Fig. 3.1. and text.

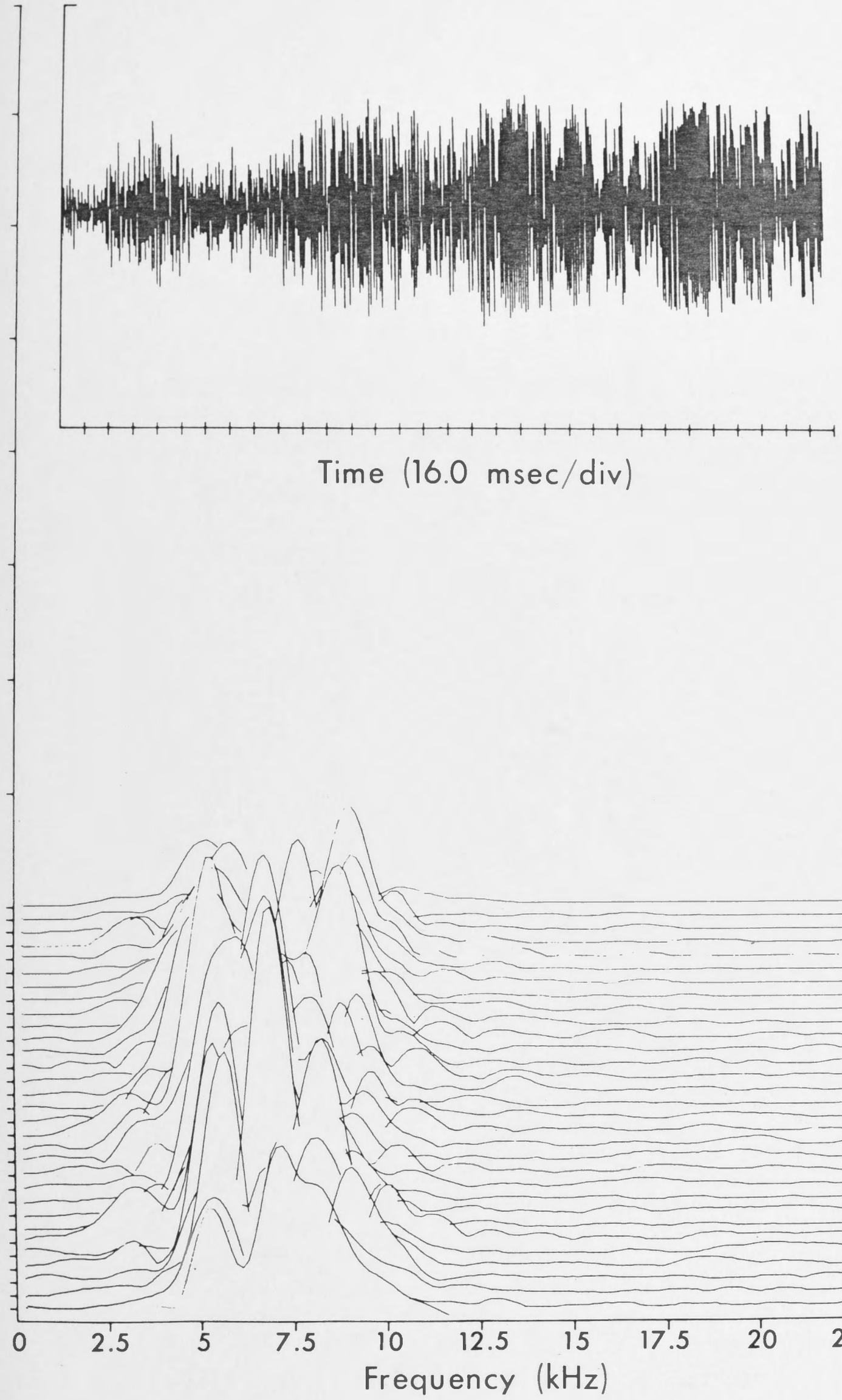
Time (16.0 msec/div)
Relative amplitude
Time
0
2.5
5
7.5
10
12.5
15
17.5
20
22.5
25
Frequency (kHz)

Fig. 3.7. Digitized waveform (top) and time-frequency structure (bottom) of an ultrasonic communication signal recorded from one individual of a pair of *Macroderma gigas* roosting on the wall of an anechoic chamber. For analysis see Fig. 3.1. and text.

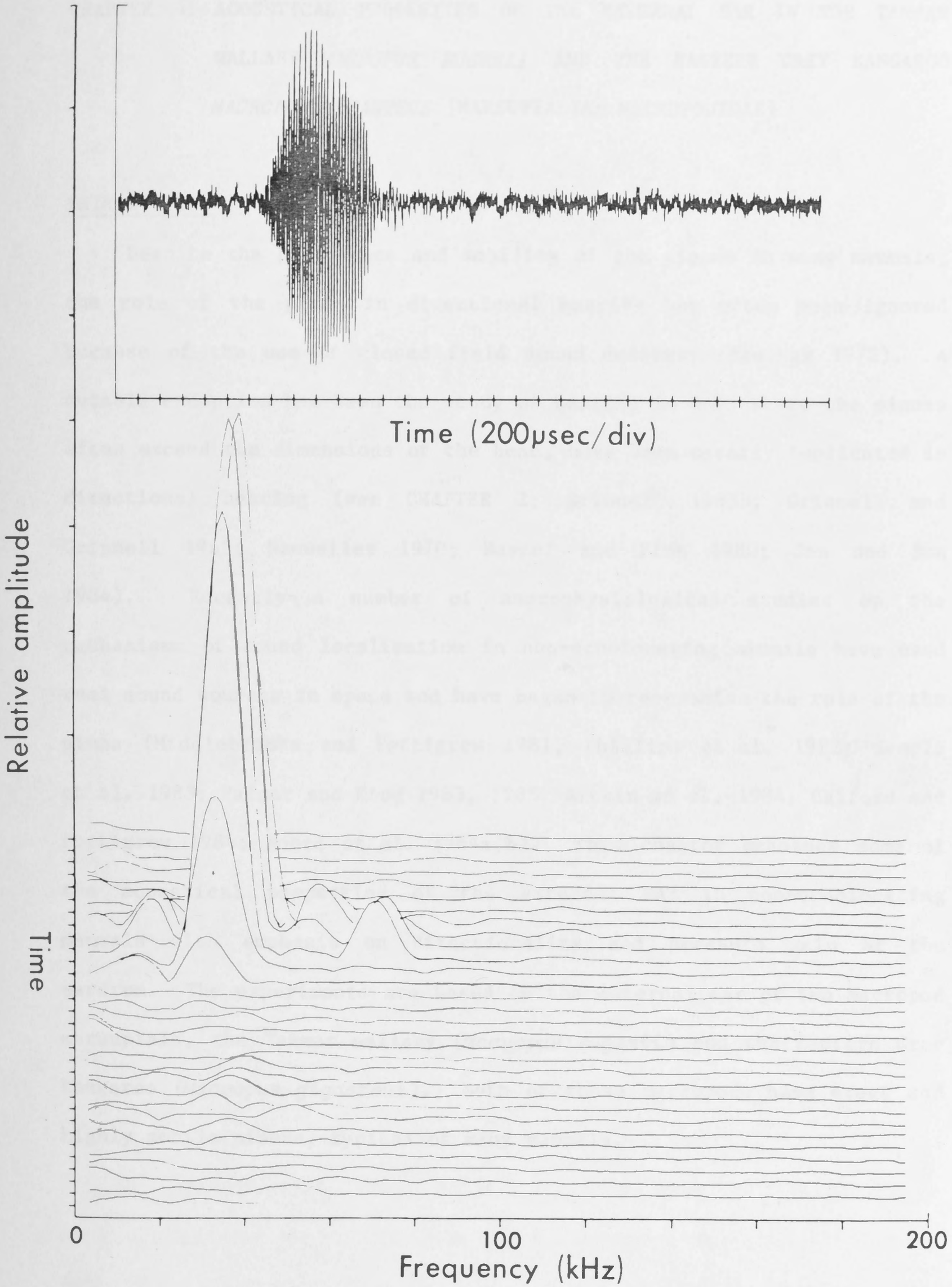
Time (200μsec/div)
Relative amplitude
Time
0
100
200
Frequency (kHz)

CHAPTER 4: ACOUSTICAL PROPERTIES OF THE EXTERNAL EAR IN THE TAMMAR WALLABY *MACROPUS EUGENII* AND THE EASTERN GREY KANGAROO *MACROPUS GIGANTEUS* [MARSUPIALIA: MACROPODIDAE]

INTRODUCTION

Despite the prominence and mobility of the pinnae in many mammals, the role of the pinna in directional hearing has often been ignored because of the use of closed field sound delivery (Erulkar 1972). A notable exception has been the study of hearing in bats where the pinnae often exceed the dimensions of the head, have been clearly implicated in directional hearing (see CHAPTER 2; Grinnell 1963b; Grinnell and Grinnell 1965; Neuweiler 1970; Busnel and Fish 1980; Jen and Sun 1984). Recently a number of neurophysiological studies on the mechanisms of sound localization in non-echolocating mammals have used real sound sources in space and have begun to re-examine the role of the pinna (Middlebrooks and Pettigrew 1981, Phillips et al. 1982; Semple et al. 1983; Palmer and King 1983, 1985; Aitkin *et al*. 1984; Calford and Pettigrew 1984; Moore et al. 1984a,b). This chapter examines some of the acoustical properties of the external ear in non-echolocating mammals with emphasis on directionality and pressure gain at the eardrum. The experiments are based on the external ear of two Macropod marsupials, the Tammar wallaby (*Macropus eugenii*) and the Eastern Grey kangaroo (*Macropus giganteus*). Both of these Macropods have erect and highly mobile pinnae, typical of many mammals.

MATERIALS AND METHODS

Subjects

The left and right ears of nine Tammar wallabies (*Macropus eugenii*) and four eastern grey kangaroos (*Macropus giganteus*) were used in this study. The animals were obtained from resident colonies maintained by the Research School of Biological Sciences at the Australian National University. The wallabies were adult or sub-adult females weighing 3.5 - 4.5 kg and the kangaroos were adults weighing 30-60kg.

Apparatus

Biophysical measurements were made in the same anechoic room as described in CHAPTER 2. Briefly, the room contained a mobile speaker assembly comprising a vertically mounted aluminium track of 94cm radius, which could be rotated through about 330°. A trolley on the track was able to move along its length, carrying a loudspeaker. Both the movement of the track and trolley were remotely controlled for changing azimuth and elevation angles, with an accuracy for speaker position of ± 0.5°.

Preparation

In both Macropod species small calibrated microphones (¼" Brüel and Kjaer Type 4135) were implanted into the left and right ear canals through a hole in the wall of the bony meatus close to the tympanic membrane. The protection grid was left in place in order to protect the delicate microphone diaphragm. A very short piece of heat-shrink plastic was also fitted to the end of the microphone and extended about 1mm from the top of the protection grid. Any effect of the protection grid and plastic tubing on sound pressure measurement was calibrated. With microphones in position, the head of a fresh cadaver was mounted on a small platform at the centre of rotation of the mobile speaker

assembly in the anechoic room. The orientation of the head and pinnae (Figs. 4.1, 4.2, 4.3 and 4.12) were adjusted to natural positions taken from photographs and single frame analysis of ear and head movements in *M. eugenii* (see also Fig. 4.12).

Stimuli and recordings

Continuous pure tones (0.2 - 40kHz) were generated from a Hewlett-Packard function generator (Model 3300A) amplified (Pioneer BP-320) and connected to a loudspeaker (Motorola piezohorn KSN 1025A: frequency range 1.5 - 40kHz or Realistic 40-1909B: frequency range 0.2 - 3kHz) via a Hatfield attenuator (Type 2125). A calibrated microphone (¼" Bruel and Kjaer Type 4135) was used to determine the free field sound pressure at the position of the wallaby head and maintained between 68 - 70dB SPL re. 20 μPa. Free field measurements were taken with the microphone facing the speaker without the head present, but at a position on the midline in line with the open faces of the pinnae. The output voltage from the microphones implanted into each ear canal was determined either on a measuring amplifier (Bruel and Kjaer Type 2510) in conjunction with a third octave filter set (Bruel and Kjaer Type 1618), or a portable sound level meter (Bruel and Kjaer Type 2203) using an octave filter set (Bruel and Kjaer Type 1613).

Definitions

For each species the longitudinal axis was defined as the point 0° azimuth and 0° elevation (see Figs. 2.2, 2.5, 2.14) which projects from the centre of the head (where the free field was calibrated) to the surface of the imaginary sphere (radius 94cm) which is described by the speaker movements in two dimensions. The vertical plane at azimuth 0° contained the animal's midline. Data points representing sound pressure level were determined by speaker position and plotted on a zenithal

projection of a hemisphere. This projection is based on a 0° azimuth and 0° elevation centre point and extends 90° in all directions (see Grinnell and Grinnell 1965; Neuweiler 1970 and also Fig. 4.5), with the poles represented vertically. Using this projection, distortion of area and thus of solid angle, is within 5% except for positions closer than 30° to the poles. Polar plots were also collected for the horizontal plane and some elevational planes at various azimuths.

Sound recording and analysis

Sound recordings were made from populations of *M. giganteus* to identify the energy bandwidth of some of the species-specific vocalizations. A wild population was studied on the shores of Blowering Dam (NSW) and vocalizations were also recorded from captive *M. giganteus* maintained at the Research School of Biological Science, Australian National University (ACT).

Vocalizations were recorded by a Sennheiser T-U microphone (Model MKH 416 with wind shield) and a Sony portable tape recorder (Model 510) at tape speed of 19cm/sec. Sound analysis of selected vocalizations was performed on a Kay Sonograph (Model 6161-B) using the wideband filter setting (300Hz), flat shaping and the 8 or 16kHz frequency analysis range.

RESULTS

Acoustic axis

For test frequencies above 1kHz in *M. giganteus* and 2kHz in *M. eugenii* there was a region in space where the sound pressure measured by the implanted microphone in the ear canal was a maximum (see Figs. 4.2, 4.14). This area was defined as the acoustic axis (± 0.5dB) and can be represented as a single point in space accompanied by a 1dB confidence

limit in the form of an iso-intensity (pressure) contour when plotted in two-dimensions (Fig. 4.5), consistent with the definition of Middlebrooks and Pettigrew (1981) and Phillips et al. (1982) in the cat.

(a) *Macropus eugenii*

Acoustic pressure gain

The pressure gain of the external ear was plotted as a function of frequency by referencing the maximum sound pressure in the ear canal (i.e. at the position of the acoustic axis) to the free field. For each test frequency the speaker was repositioned as necessary and the results shown in Fig. 4.3 are gain curves for four ears based on the maximum on-axis pressure at each test frequency. For the most part, the sound pressure level at the tympanic membrane has positive gain i.e. the sound pressure is amplified relative to the free field, for frequencies between 1-30kHz. From Fig. 4.3 it can be seen that there is a rapid increase in pressure gain above about 1.5kHz, rising to a peak of 25-30dB between 4-5kHz. Above 6kHz the pressure amplification declines progressively to values below 10dB between 16-20kHz. Additional decreases in pressure gain occur above 20kHz resulting in attenuation of sound pressure relative to the free field between 30-40kHz. Local sound diffraction inside the pinna and meatus may have contributed to the attenuation of sound at these high frequencies particularly in view of the irregular shape of the external ear (Fig. 4.1). Since gain values became erratic and inconsistent above 40kHz detailed measurements were discontinued. There were no differences in acoustic pressure gain between left and right ears.

The effect of pinna removal on acoustic pressure gain is shown in Fig. 4.4A. The pinna was surgically removed until flush with the contour of the skin of the head. In *M. eugenii* almost the entire pinna

flange can be removed (see Fig. 4.1C) but it is partially recessed into the muscles of the head and pinna itself. The most complete pinna removal that can be achieved leaves a small opening with an average radius of about 0.4cm (see Table 4.1, Fig. 4.1C) and which is very close to the entrance of the cartilaginous meatus. Fig. 4.4A shows the effect of pinna removal on pressure gain and the difference between the two curves suggests that the pinna has an amplifying effect which increases progressively from about 5-20dB in the frequency range 1.5-30kHz (Fig. 4.4B). In the pinnaless condition (Fig. 4.4A), measurements at the tympanic membrane show a residual pressure gain curve which retains a distinct peak of about 15dB in the 4-8kHz region. Since the length of the meatus is about 1.6cm (Table 4.1, Fig. 4.1), the residual peak in pressure gain can be attributed to a closed-tube resonance where the sound wavelength is four times the length of the meatus (see DISCUSSION and GENERAL DISCUSSION AND CONCLUSION). By removing the pinna as part of the external ear, it is thereby possible to identify the contribution of the resonating meatus to the entire pressure gain, although normally the pinna and meatus are acoustically coupled.

The effective gain of the pinna was estimated for three ears and the results are shown in Fig. 4.4B, in comparison with the expected amplification values for a finite conical horn. In Fig. 4.4C the expected excess pressure at the throat of a finite paraboloidal, conical and exponential horn has been plotted as a function of frequency, based on the relevant physical dimensions of the pinna (see APPENDIX 1; Table 4.1, Fig. 4.1). The calculations for the gain of a horn are based on the equations given in APPENDIX 1. The pinna of *M. eugenii* must be treated as a finite length horn because the range of test frequencies involves wavelengths which are comparable to and exceed the length of

the pinna (see Olson 1947; Beranek 1954 and GENERAL DISCUSSION AND CONCLUSION). Theoretically in *M. eugenii* the high frequency gain of the pinna (G_∞) should approach an asymptotic value of 16dB based on the ratio of the mouth to throat cross-sectional areas (see Table 4.1 and APPENDIX 1, Eqn 11). The mouth of the pinna has an average radius of 2.5 cm estimated from the circumference of the opening which is 16 cm. The throat of the pinna is formed by a rapid change in cross-section along the external ear where the entrance to the meatus occurs (Fig. 4.1, Table 4.1) and the throat has an average radius of 0.4 cm. Since the pinna of *M. eugenii* is asymmetrical in cross section, the sound path length was taken as the average distance from the tip of the pinna to the throat and the tragal notch (base of pinna) to the throat which was about 4.5cm (Fig. 4.1; Table 4.1). The results in Fig. 4.4B,C show that the pressure gain produced by the pinna is reasonably close to that predicted by a finite conical horn of equivalent dimensions. In comparison the gain of a finite exponential horn tends to overestimate the pressure gain above 3kHz, and a finite paraboloidal horn tends to underestimate the pressure gain above this frequency (Fig. 4.4C).

There is no clear evidence of a horn resonance for the pinna of *M. eugenii* which would be expected near 2.5kHz for an equivalent finite conical horn (see APPENDIX 1; Fig. 4.4B,C). The possibility that the peak in the normal pressure gain curve (Fig. 4.4A) was due to horn (pinna) resonance rather than meatus resonance was tested by making an artificially enlarged pinna. An enlarged pinna was made from cardboard with the same shape as normal but approximately double the linear dimensions. The enlarged pinna was then placed over the normal pinna and generally increased the pressure by about 4-5dB (Fig. 4.4A) as a result of increasing the surface area of the mouth. However, the peak

in the gain curve is maintained around 5kHz which does not support the idea of a horn resonance producing the prominent peak in gain at this frequency, which would otherwise have shifted to a lower frequency as a result of the increased path length of the pinna. Thus the normal peak in the amplification of sound pressure by the external ear results mainly from meatus resonance.

Directionality

A typical series of directionality plots *M. eugenii* is shown in Figs. 4.5 and 4.6 as a function of frequency. The position of the acoustic axis in space can be determined from the maximum sound pressure measured at the tympanic membrane and the main lobe can be depicted as a series of iso-intensity contours (Fig. 4.5) or as a polar curve for speaker movements in the horizontal plane (Fig. 4.6). In *M. eugenii* the position of the acoustic axis depends on the orientation of the pinna on the head. Under natural conditions each pinna can be rotated without distortion, through angles of up to 100° in the horizontal plane in both *M. eugenii* and *M. giganteus* (see Fig. 4.12) and the pinnae were set to the "resting position" for data collection in *M. eugenii* (see Figs. 4.2; 4.11A). A physical re-positioning of the pinna independent of head position, was found to move the acoustic axis and the main lobe of directionality plot accordingly with the forward or rearwards limits normally determined by the muscular control of the pinna. It is useful to note that the acoustic axis is located approximately perpendicular to the open face of the pinna in the horizontal plane (for frequency effects see below). In the vertical plane the face of the pinna (in the living animal) is normally held in an inclined position, about 40° to the horizontal plane (see Figs. 4.1, 4.2).

From the two dimensional plots shown in Fig. 4.5, the 1dB contour

surrounding the acoustic axis is almost circular for low frequencies up to about 6kHz. As stimulus frequency increases to 20kHz, the central high pressure region of the directionality plot becomes elliptical and tilted towards the midline (Fig. 4.5, at 10kHz). For frequencies above 20kHz there was a tendency for the axial region to become somewhat flattened in the vertical plane (Fig. 4.5 at 20kHz). Above 30kHz, directionality became very difficult to determine reliably, most likely due to irregularities in the shape of the pinna. The presence of the head also produces increasingly complex sound paths at very high frequencies.

It was clear that as frequency increased the ear became more directional, which is indicated both by the closeness of the iso-intensity contours near the acoustic axis (Fig. 4.5) and the sharpness of the main lobe (Figs. 4.2 and 4.6). Changes in directionality were quantified by measuring the greatest difference in pressure (dB_{max}) between any two positions on the directionality plot for each test frequency. The results are shown in Fig. 4.7 for 4 ears and indicate that below 1.5kHz no appreciable directionality exists in the external ear. Directionality starts to rise steeply above 4kHz, ranging from up to about 50dB for frequencies above 6kHz. High directionality is largely determined by the presence of nulls in the directivity patterns (Figs. 4.2, 4.5 and 4.6, see below) as well as by a combination of high pressure amplification in the mid frequency range (Fig. 4.3).

Another method of assessing directionality is to examine the angle covered by a given decrease in pressure from the acoustic axis. In physical systems a -3dB point (relative to the maximum response) is often used to compare directional devices (Beranek 1954). Fig. 4.8 shows the estimated full angular width or acceptance angle in degrees

(2θ°) as a function of frequency, using the -3dB point either side of the acoustic axis. Both the azimuth (Fig. 4.8A) and the elevation (Fig. 4.8B) acceptance angles have been calculated separately because of some asymmetry of the main lobe at high frequencies (see Fig. 4.5). From Fig. 4.8 it can be seen that the angular width of the main lobe of the directivity patterns is inversely related to frequency in a systematic fashion. Non-directional patterns have acceptance angles exceeding 180° and acceptance angles ranging from 180°-120° characterize weakly directional patterns up to 2kHz, where the position of the acoustic axis is difficult to define. As directionality starts to increase rapidly above 3.5kHz (Fig. 4.7) the acceptance angle in azimuth decreases from 120° to about 20° for frequencies above 15kHz. A similar effect is also seen in the vertical plane (Fig. 4.8B).

The systematic decrease in the acceptance angle for the external ear of *M. eugenii* as a function of frequency strongly resembles the sound diffraction properties of a single aperture. The experimental data can be compared to the directionality generated by a circular aperture for example, based on the average radius of the pinna opening. The aperture of the pinna in *M. eugenii* has been calculated from the circumference of the face and gives an average radius of 2.5cm (see above for gain of pinna, and Table 4.1, Fig. 4.1). The expected curves are shown in Fig. 4.8 and are derived from the directivity function for a rigid circular piston in a plane baffle, which by reciprocity is equivalent to the directivity patterns for sound diffraction by a circular aperture (see APPENDIX 2; Morse 1948; Beranek 1954).

From APPENDIX 2 the expected acceptance angle at 3dB below the axial pressure, has been calculated as a function of wavelength for

diffraction by a circular aperture of given radius, as shown in Fig. 4.8. There is generally an excellent correspondence between the experimental data and theoretical curve for diffraction with the best fit between 3-30kHz. At low frequencies below 3kHz the pinna of *M. eugenii* is somewhat more directional than would be predicted (Fig. 4.8A). On the other hand at higher frequencies above about 16kHz the pinna tends to become less directional in azimuth than would be predicted. This effect is seen as an oval-shape of the main lobe when plotted as two dimensional contours (Fig. 4.5) and probably results from the elliptical shape of the pinna face (see DISCUSSION).

A significant feature of the directivity patterns generated by the external ear of *M. eugenii* were regions of low pressure forming extreme minima. The formation of these approximate nulls became obvious as stimulus frequencies exceeded 4kHz. In the lower frequency range up to about 7.5kHz nulls were generated behind the pinna face up to 150° from the acoustic axis (Figs. 4.2 and 4.5).

The contour plotting method was unsuitable for examining the features of both the acoustic axis and rearward nulls due to their large angular separation and the use of a hemispheric projection. Polar plots were therefore best suited to showing the development of nulls particularly at lower frequencies providing the centre of the null was contained in the horizontal plane (see Figs. 4.2 and 4.6). As frequency increased above 7.5kHz a second null was seen to develop at the side of the main lobe containing the acoustic axis i.e. within 90°. This null normally occurred on the medial or leading side of the plane of the pinna face relative to the midline, i.e. towards the front of the head as shown in Figs 4.2, 4.5 and 4.6 and was particularly prominent near 10kHz. At higher frequencies multiple nulls were seen and the

directivity patterns became very complex, including double sensitivity peaks above 20kHz (see Fig. 4.5).

The relationship between major null regions in the directivity patterns were quantified as a function of frequency by measuring the angular separation between the null and the acoustic axis (see Figs. 4.2, 4.5 and 4.6). The results are summarized in Fig. 4.9 for 35 nulls determined at various test frequencies in 7 ears. The most lateral nulls are grouped between 160° and 90° from the axis in the frequency range 4-8kHz, whilst the medial leading nulls occur between 65°-30° off-axis in the frequency range 8-20kHz. Nulls on the leading side of the pinna tend to move progressively towards the acoustic axis as frequency increases thus increasing directionality in frontal space. The results shown in Fig. 4.9 represent a somewhat simplified view of null behaviour since obviously several nulls can exist in a single directivity pattern and in different planes, particularly at high frequencies (see Figs. 4.5, 4.6). Nevertheless, it is useful to compare the present data with the expected position of nulls based on diffraction by a circular aperture, in a similar fashion to that shown for the acceptance angle of the main lobe (Fig. 4.8).

From Eqn (14) in APPENDIX 2 the semi-angle of the major lobe of the directivity pattern is plotted as a function of stimulus wavelength (Fig. 4.9). These calculations are based on a circular aperture of radius a = 2.5cm, taken from measurements of the circumference of the pinna face (see Table 4.1). The calculated curve in Fig. 4.9 is based on a circular aperture in an infinite baffle or plane wall and consequently the first diffraction null is generated at 90° off-axis, in the direction of the plane of the opening. For the pinna of *M. eugenii* this will occur at a frequency of approximately 8.2kHz (see

APPENDIX 2). The results in Fig. 4.9 show that the position of nulls relative to the acoustic axis in the frequency range 7-20kHz bear a close relationship to the expected values from sound diffraction. It was also possible to plot null positions behind the plane of the pinna opening, reflecting progressively weaker directionality at lower frequencies. Under these conditions it is more appropriate to consider the location of nulls behind the plane of opening of the pinna in terms of an aperture at the end of or in the side of a long tube (see Beranek, 1954). However, this arrangement is much more complicated mathematically compared to an aperture in an infinite baffle since sound can be received from all directions and will also be diffracted around the edge of the tube before reaching the front of the opening. A single value for a predicted null position from the directivity pattern of a circular aperture in the end of a long pipe has been indicated in Fig. 4.9 at 6.4kHz (ka = 3) taken from Beranek (1954) and compares favourably with experimental values.

Pinna removal

Pinna removal, as described previously (see Fig. 4.4), not only caused a decrease in pressure gain in the ear canal but also resulted in a marked loss of directionality. In Fig. 4.10A, for a directivity pattern at 6kHz, removal of the pinna results in a considerable expansion of the iso-intensity contours emphasizing the decrease in directionality. In addition, the polar plot in Fig. 4.10B shows the loss in directionality and elimination of the null region. The presence of the pinna is therefore essential for the normal directivity patterns measured in the ear canal. However the head will have an increased effect on sound diffraction at very high frequencies.

Movement of the acoustic axis with frequency

There was a tendency for the position of the acoustic axis to vary with frequency. From Fig. 4.11A, for azimuth angles above 1.6kHz the acoustic axis tends to move away from the midline by about 25° up to 30kHz. However the effect is not regular and variation occurs between individual ears. In elevation (Fig. 4.11B) the acoustic axis moves gradually towards the horizontal plane. At low frequencies (below 3kHz) the acoustic axis is at about 15° below the horizontal plane, while above 7kHz the acoustic axis is maintained close to the horizonal plane. The results for absolute azimuth position of the acoustic axis are dependent on the physical orientation of the pinna on the head, which in Fig. 4.11A relate to the resting position (see Fig. 4.2). In the vertical plane the pinna face has a natural angle of inclination (see Fig. 4.1C) which results in the elevation position for the acoustic axis being close to the horizontal plane for most frequencies. Overall, there was only a very weak relationship, if any, between the spatial location of the acoustic axis and stimulus frequency for the external ear of *M. eugenii*.

(b) *Macropus giganteus*

Acoustic pressure gain

The on-axis sound pressure measured by the microphone implanted at the base of the ear canal in *M. giganteus* was compared to the free field for a similar range of frequencies as used in *M. eugenii*. The resulting gain curve for the intact ear of *M. giganteus* is shown in Fig. 4.13A for 3 ears. Significant amplification of sound pressure occurred above 900Hz and rapidly increased to a peak of about 30dB between 1.7-3.5kHz. Above this peak the pressure amplification declined gradually to values of around 10dB at 16kHz. A local peak in gain occured near 20kHz

however the gain in the meatus decreased rapidly to values of -7dB near 30kHz. Pressure measurements were discontinued above 40kHz due to variability caused by complex directivity patterns. The effect of the pinna on pressure gain in the ear canal was studied by the same removal procedure as for *M. eugenii*. Both *M. giganteus* and *M. eugenii* have a very similar external ear, the major difference being the larger absolute size in *M. giganteus* (Table 4.1; Figs. 4.1, 4.12). After pinna removal the pressure gain in the meatus was reduced compared to normal as shown by the example in Fig. 4.13A. In the pinna-less condition a residual peak in pressure amplification of about 20dB remains near 2.5-3kHz. A smaller peak in gain near 9kHz may be harmonically related to the main peak at 3kHz suggesting a quarter wave resonance of the meatus, as for *M. eugenii*, but at a lower fundamental frequency in *M. giganteus* based on a longer meatus (Table 4.1). The effective gain curve of the pinna is shown in Fig. 4.13B as the difference curve between the intact and pinnaless condition as shown in Fig. 4.13A. Significant acoustic gain is produced by the pinna above 1kHz and increases to peak values of 10-14dB up to 14kHz (Fig. 4.13B). At higher frequencies the gain curves display some oscillation but generally maintain pressure around 11dB up to about 40kHz. There is a sharp peak in pinna gain at 14kHz which may be an artifact of the recording technique. However such a peak was not apparent in pinna gain curves of *M. eugenii* (Fig. 4.4B) using an identical procedure. By treating the pinna of *M. giganteus* as an acoustic transformer in the same fashion as for *M. eugenii*, the gain curves of a series of simple acoustic horns can be calculated from the relevent physical dimensions (Table 4.1 and APPENDIX 1). The expected gain curves for finite paraboloidal, conical and exponential horns of equivalent dimensions to the pinna of *M.*

giganteus are shown in Fig. 4.13C. All three expected gain curves have a similar structure particularly up to about 1.8kHz but above this frequency the finite conical horn is probably the closest fit to the average pinna gain curve (Fig. 4.4C) despite fluctuations in the experimental data at high frequencies. The finite exponential horn curve tends to overestimate the observed gain above 2kHz, but both the expected conical and exponential horn curves are similar. The expected gain curve for a finite paraboloidal horn tends to underestimate the observed pinna gain above 2kHz.

Horn resonance can be expected by the pinna of *M. giganteus* due to its finite length (see APPENDIX 1 and GENERAL DISCUSSION AND CONCLUSIONS and there is some suggestion of a resonance peak in the pinna gain curve near 2kHz (Fig. 4.13B,C). The high frequency gain (G_∞) observed experimentally for pinna of *M. giganteus* is about 11dB based on the ratio of the mouth and throat sectional areas and is reasonably close to the gain that would be expected by an ideal acoustic horn (see Table 4.1; Fig. 4.13C and APPENDIX 1).

Directionality

Directivity patterns for the external ear of *M. giganteus* were studied for a range of test frequencies between 0.2-40kHz and a typical series of two-dimensional directionality plots are shown in Fig. 4.14. Directivity patterns for *M. giganteus* were similar to that seen in *M. eugenii* (Fig. 4.5) and the main lobe was characterized by a series of circular or oval shaped iso-intensity contours concentric to the acoustic axis. A main lobe was clearly apparent at about 1.0kHz and as frequency increased pressure patterns became increasingly directional as judged by the closeness of the iso-frequency contours which represent steeper spatial gradients (Fig. 4.14).

The maximum directionality was determined by the difference between the maximum and minimum pressures (dB_{max}) for any spatial positions in the directivity patterns (Fig. 4.15). As a function of frequency, the maximum directionality (Fig. 4.15) was seen to increase rapidly above 1.5kHz. Peak values for maximum directionality exceeded 40dB above 4.5kHz, and are limited by the dynamic range of the microphone (noise level) and the level of pressure amplification by the external ear.

The frequency dependence of directionality in *M. giganteus* was quantified by measuring the -3dB acceptance angle for the main lobe (see APPENDIX 2) in a similar fashion to the ear canal measurements in *M. eugenii*. The results in Fig. 4.16 show that there is a systematic decrease in the -3dB acceptance angle as a function of increasing frequency. In both azimuth and elevation, acceptance angles start to decrease from around 100°-120° at 1.5kHz to reach minimum values of 15° at 30-40kHz. The experimental data in Fig. 4.16 can be compared to the expected values for diffraction by a circular aperture (see APPENDIX 2). In *M. giganteus* the average radius of the pinna face is 3.9cm which is estimated from the measurement of the perimeter of the pinna face (see Fig. 4.12 and Table 4.1). In Fig. 4.16 it can be seen that there is a reasonably close correspondence between the expected -3dB acceptance angles due to sound diffraction and the experimentally observed values particularly above 4kHz. However, in azimuth the acceptance angles are somewhat less directional than expected, which may be due to the elliptical shape of the pinna face (Fig. 4.12). In the case of an elliptical opening the directionality will be poorest in the plane of the minor axis, which would be in azimuth for the pinna of *M. giganteus* (Fig. 4.12; Table 4.1).

Nulls in directivity patterns can be expected as a result of sound

diffraction by a circular aperture (see APPENDIX 2) and discrete regions of low pressure or approximate nulls were found in *M. giganteus* for directivity patterns above 2.5kHz (Fig. 4.17). The angular position of these nulls relative to the acoustic axis was plotted as a function of frequency (Fig. 4.17) and the increasing directionality of the main lobe is reflected by the progressive decrease in the semi-angle as stimulus frequency increases. The maximum separation between the null and the acoustic axis (90°) occurred at about 6kHz and nulls moved to positions within 20° of the acoustic axis for frequencies above about 20kHz. The experimentally observed trend in null position as a function of wavelength corresponds reasonably closely to the predicted values for diffraction nulls (see APPENDIX 2). Theoretically the lower limit for diffraction nulls in the frontal hemisphere will occur at 5.4kHz for an aperture of radius 3.9cm in a plane wall (Table 4.1, APPENDIX 2). This limit is close to the observed frequencies for which nulls appear in the frontal hemisphere in *M. giganteus*. Rearward nulls also occur experimentally and a diffraction model may also predict their position but involves more complicated mathematical computation as suggested in *M. eugenii* (see above, Fig. 4.9).

Movement of the acoustic axis with frequency

The position of the acoustic axis was measured in azimuth and elevation in ear canal pressure measurements in *M. giganteus*. The pinnae were placed into an approximate "resting" position as estimated from natural pinna positions taken from photographic analysis of ear movements as in *M. eugenii* (Fig. 4.12). No systematic relationship could be found between acoustic axis position and frequency (Fig. 4.18). The position of the acoustic axis in azimuth (Fig. 4.18A) remains about 30° from the midline between 2-40kHz and is simply

determined by the physical orientation of the pinna on the head (in this case the resting position). Likewise, the acoustic axis in elevation is maintained within about 10° of the horizontal plane between 2-40kHz.

Vocalizations

Vocalizations were recorded from adult and juvenile grey kangaroos and four commonly used sounds are shown in Fig. 4.19. Fig. 4.19A is a sonogram of a "clucking call" from an adult female. This call is elicited when the female is separated from her young and is characterized by a series of repeated pulses of about 90msec in duration. The clucking call has a relatively wide energy band containing harmonics but the main energy band occurs between 3-5kHz. The "hur call" which is commonly elicited from adult males during fighting bouts is relatively low in amplitude with poor modulation (Fig. 4.19B). The duration of this call is about 200msec and the main energy band occurs between 2.5-4.5kHz. Juvenile kangaroos, particularly pouch young, use a "distress call" when separated from their mothers (Fig. 4.19C). Juvenile "distress calls" in the grey kangaroo consist of three syllables repeated at irregular intervals with a maximum duration of 100 msec for each syllable. The energy in the "distress call" is broadband up to about 8kHz with a harmonic structure (Fig. 4.19C). Juvenile grey kangaroos also use an "aggressive call" which consists of a single note of about 400msec duration (Fig. 4.19D). The "aggressive call" has a strong harmonic structure but most of the energy occurs between 3-4kHz and relatively little energy occurs above 7kHz.

DISCUSSION

The present study demonstrates that the external ears of both *M. eugenii* and *M. giganteus* provide frequency dependent amplification

and directionality for sound pressure reaching the eardrum. Moreover, an acoustic axis for the ear can be identified as a property of the pinna, which is consistent with observations in bats (see CHAPTER 2; Grinnell and Grinnell 1965; Neuweiler 1970) and the cat (Middlebrooks and Pettigrew 1981; Phillips et al. 1982; Calford and Pettigrew 1984). *M. eugenii* and *M. giganteus* are therefore typical of many mammals which rely on the pinna and its relative position on the head for directionality and some pressure gain. This is clearly distinct from primates which generally have immobile pinnae combined with the highly significant influence of head shadow (Harrison and Downey 1970; Shaw 1974).

Acoustic pressure gain

In both Macropod species studied in this chapter, on-axis pressure measurements show that sound reaching the eardrum is amplified to a varying degree across the frequency range 1-30kHz. The physical basis for the pressure gain of the external ear (Figs. 4.3, 4.13) can be explained by two major components.

Firstly, the removal of the pinna causes an overall decrease in amplification eventually resulting in attenuation of high frequency sound above 10-12kHz in both Macropod species. The pinna gain curve in *M. eugenii* (Fig. 4.4B,C) shows a gradual increase with frequency exceeding 10dB above about 4kHz. In comparison the gain curve for the pinna of *M. giganteus* reaches average values of 10-12dB slightly below 2kHz. If the pinna is considered to act as an acoustic transformer or horn then it is possible to calculate an expected amplification of sound pressure at the throat as in APPENDIX 1. Calculations based on a comparison of the area of the face of the pinna to the aperture (throat) at the junction of the pinna and meatus (the point at which the pinna

was removed) result in a maximum high frequency gain (G_∞) of 16dB for *M. eugenii* and 11dB for *M. giganteus* (Table 4.1, and APPENDIX 1, Eqn. 11) for an efficient horn. Such an expected value is close to the experimentally observed values for both Macropod species (Figs. 4.4B,C, 4.13B,C). However, the efficiency of an acoustic horn will depend on the size of the mouth and the length of the horn, relative to the wavelengths involved (Beranek 1954). For finite horns such as the Macropod pinnae studied here the pinna of *M. giganteus* is more efficient about an octave lower than *M. eugenii* because, although both pinnae (if considered conical horns) have similar cone angles (Table 4.1), *M. giganteus* has a proportionately larger pinna. The pressure gain curves for both Macropod pinnae are reasonably close to the predicted curves for a finite conical horn and are useful first approximations considering the asymmetrical shape of the pinnae (Figs. 4.4, 4.13).

It should be noted that the expected gain curves shown in Figs. 4.4B,C, 4.13B,C are exact solutions for finite length horns and involve resonance. A possible horn resonance peak was seen near 2kHz in *M. giganteus* as expected (Fig. 4.13B,C) but none was apparent for the pinna of *M. eugenii* (Fig. 4.4). In both species horn resonance may be expected to occur at frequencies between a half and quarter wave series, depending on the flare and length of the pinna. The lack of clear horn resonance for both Macropod pinnae is probably due to the oblique conical shape, which would tend to reduce the reflection coefficient of the mouth (Fletcher pers. comm.) and the fact that as horns, the pinnae are rather short in length compared to the mouth diameter (Table 4.1; Beranek 1954).

A second contributing factor to the acoustic gain in the external

ears of *M. eugenii* and *M. giganteus* was revealed by removal of the pinna. As indicated in Figs. 4.4A and 4.13A the remaining meati of the external ear produces a distinct peak in gain which strongly suggests tube resonance. The meatus in the wallaby has a length of about 1.6 cm from the base of the pinna to the tympanic membrane with relatively little change in cross-sectional area and the meatus in *M. giganteus* has a similar morphology but is about 3.2cm in length (Table 4.1). If sound is reflected back into the tube-like meatus from the open end it is reasonable to expect closed-tube resonance at a frequency where the wavelength is four times the length of the meatus, since the tympanic membrane represents a relatively rigid termination or closed end (Shaw 1974; Moller 1983). On this basis the fundamental frequency for meatus resonance in *M. eugenii* should occur at 5.4kHz which corresponds closely with the measured peak in pressure gain in the external ear near 5-6kHz, (Fig. 4.4A). In *M. giganteus*, quarter wave resonance should occur at a fundamental frequency of 2.7kHz based on a meatus length of 3.2cm and is supported by the experimental data (Fig. 4.13A). An additional resonance peak may occur near 9kHz as seen in Fig. 4.13A.

The pressure measurements in this chapter for both Macropod species compare favourably with the measurements of sound transformation in the cat (Wiener *et al.* 1966) who found a maximum pressure gain of 14dB between the entrance to the meatus and the eardrum. The peak in gain, which occurred at 4-6kHz was also predicted by modelling the meatus as a small rigid tube. Wiener *et al.* (1966) were able to establish a maximum pressure gain from (on-axis) free field measurements of 21dB in the same frequency region, suggesting a 7dB increase in pressure gain due to the pinna. A recent study of the cat external ear (Phillips *et al.* 1982) has claimed a 28dB amplification due to the pinna determined from

cochlear microphonic measurements. In view of the similarity in size and shape between the cat and the pinna of *M. eugenii* in particular (Table4.1), it would seem that this value has been over-estimated. In *M. eugenii* the pinna produces up to 16dB of pressure amplification based on direct acoustical pressure measurements in the intact and pinnaless condition.

The discrepancy between the two studies probably results from the extent to which the pinna and part of the meatus were removed in order to assess the contribution to pressure gain. In the study of Phillips et al. (1982) less than 0.5-0.8cm of the meatus was left intact after pinna removal, compared to the normal meatus length of about 2.0cm (Wiener *et al.* 1966). Consequently the amplifying effect of meatus resonance on the sound pressure developed near the tympanic membrane would not be retained in the cochlear microphonic sensitivity functions studied by Phillips et al. (1982). By removing the pinna and most of the meatus, their results (Phillips et al. 1982, Fig. 6) are much closer to the sound pressure transformation by the entire external ear (free-field to eardrum) as previously described in the cat by Weiner *et al.*, (1966). Thus the apparently large "amplification by the pinna" of about 25-30dB around 3.5kHz reported by Phillips et al. (1982) is more likely to result from a meatus resonance peak of about 14dB (Weiner *et al.*, 1966) rather than pinna (horn) resonance as suggested by Calford and Pettigrew (1984). Similarly, the present study has also identified the important contribution of meatus resonance to the pressure gain of the external ear. The horn-like properties of the pinna also contribute to the pressure gain in the ear canal and some horn resonance is suggested in *M. giganteus* (Fig. 4.13B,C) but was not apparent in *M. eugenii* (Fig. 4.4).

Since there is amplification of sound pressure by the external ear in *M. eugenii* and *M. giganteus*, it may be expected to influence the hearing threshold curve. Unfortunately no data on absolute thresholds or frequency sensitivity exists for any Macropod. In other marsupials such as *Trichosurus vulpecula* (Gates and Aitkin 1982) and *Didelphis virginianus* (Ravizza *et al.* 1969) neural and behavioural thresholds are most sensitive between 2-32kHz. Similar auditory sensitivity may also exist for *M. eugenii* since the head and pinnae are comparable in size to *T. vulpecula* (Table 4.1). The amplified sound pressure in the external ear is likely to have a significant effect on the frequency response but remains to be tested. On the other hand, the species-specific vocalizations of *M. giganteus* (Fig. 4.19) clearly have significant sound energy in the frequency range which would result in high pressure amplification (Fig. 4.13) and appreciable directionality (Fig. 4.15) in the ear canal. In the cat there is evidence that pinnaless auditory thresholds can be up to 20dB poorer than normal, particularly for frequencies above about 1kHz (Flynn and Elliott 1965). Such a result supports the present findings that the pinna acts as an acoustic transformer and would play a significant role in improving absolute sensitivity to sound.

Directionality

The directional responses of the left and right pinnae in both Macropods are in essentially mirror-image relationship, and the direction of the acoustic axis of each response pattern simply shifts, to a first approximation, as the pinna is moved. Normal directivity patterns are abolished subsequent to pinna removal as seen in both species. The present findings are supported by similar observations in the cat (Middlebrooks and Pettigrew 1981; Phillips et al. 1982; Calford

and Pettigrew 1984).

The physical basis for the directionality of the pinna can be explained by the diffraction properties of its horn-like opening (Figs. 4.1, 4.12) which was useful in describing its action as an acoustic transformer (see above). From the present study directionality increases with frequency, as is to be expected from standard wave theory. However the pinnae of *M. eugenii* and *M. giganteus* are not ideal receivers due to their lack of complete symmetry and attachment to the head at one end. Nevertheless these pinnae can be considered, to a first approximation, in terms of the diffraction properties of a circular aperture (Beranek 1954). In both species, comparison between the directionality of the pinna and that expected for an equivalent circular aperture in an infinite baffle (-3dB down) has a close correspondence for most of the frequency range tested. At low frequencies (<3kHz) the pinna of *M. eugenii* behave like a larger aperture (Fig. 4.8) corresponding more closely with the long axis of pinna face (taken as a diameter). Likewise at high frequencies above 15kHz, in *M. eugenii* directionality is closer to that predicted from the short axis or width of the pinna (Table 4.1). A similar situation exists for the pinna of *M. giganteus* below 2.5kHz (Fig. 4.16) however at higher frequencies (up to 40kHz) ear canal directionality remains close to that predicted by the average radius of the pinna mouth (Table 4.1). Clearly diffraction by a circular aperture is a useful first approximation for understanding the directional properties of the Macropod pinna and similar results have been obtained for the cat's pinna by measuring the solid angle derived from the directional sensitivity of the cochlear microphonic potential (Phillips et al. 1982; Calford and Pettigrew 1984).

The occurrence of nulls in the directivity patterns of the external ears of *M. eugenii* and *M. giganteus* compare favourably with the expected semi-angle of the main lobe in the directivity pattern of a circular opening of equivalent radius (Figs. 4.9, 4.17). In the case of a baffled opening with the same effective radius as the pinna face, the formation of diffraction nulls in frontal space theoretically would be limited to frequencies above 8.2 kHz in *M. eugenii* (Fig. 4.9) and 5.2kHz in *M. giganteus* (Fig. 4.17). This is the limit for nulls occurring along the plane of the opening (see APPENDIX 2) and the appearance of nulls about 90° off-axis in the directivity patterns of *M. eugenii* and *M. giganteus* are close to this limit. The nulls in the observed directivity patterns do not completely encircle the main lobe as would be expected for an ideal aperture (Figs. 4.5, 4.14). This may be due to the asymmetry of the pinnae, particularly in the vertical plane since the openings are formed from an oblique truncation of the pinna's cone-like structure (Figs. 4.1, 4.12). The situation is also complicated by the presence of rearward nulls below about 8kHz in *M. eugenii* (Fig. 4.9) and 5kHz in *M. giganteus* which cannot occur for an opening in a plane wall. These nulls, which occur behind the plane of opening of the pinna are probably comparable to the diffraction patterns which would result from an aperture at the end of a long pipe (Beranek 1954) or possibly an oblique termination, considering the morphology of the pinnae (see Figs. 4.1, 4.12).

The directivity patterns for both *M. eugenii* and *M. giganteus* are essentially non-directional below about 2 kHz and similarly for the cat (Wiener *et al.* 1966; Middlebrooks and Pettigrew 1981; Phillips et al. 1982; Calford and Pettigrew 1984). A criterion for the onset of directionality is arbitrary, but the present data show a very sharp

increase in directionality near 1.6kHz in *M. giganteus* (Fig. 4.15) and 4.0kHz in *M. eugenii* (Fig. 4.7). These are close to the wavelengths which would begin to produce significant directionality for a circular aperture (*ka* = 1.25; Fletcher and Thwaites 1979) given the difference in size between the open faces of the two pinnae (Table 4.1)

In both Macropod external ears there is amplified sound pressure reaching the eardrum at frequencies where significant directionality starts to occur. A high degree of amplification is produced by the pinna acting as an acoustic transformer and by meatus resonance. A pressure gain is maintained for frequencies above the resonance peak of the meatus by the increasing efficiency of the horn-like pinna. Above 4kHz in *M. giganteus* and 5kHz in *M. eugenii* highly directional responses for the external ear are produced by a combination of sound pressure being amplified on-axis and severe attenuation from null points both behind and in front of the plane of opening of the pinna. From these findings, the design of the external ear, in particular a mobile pinna, can be seen to have a strategic value in the detection and localization of sound. Each pinna can rotate independently through angles of up to 100° in both Macropods and under normal circumstances the faces are held at 40° to the horizontal plane (Figs. 4.1 and 4.12). This results in the acoustic axis being close to the horizon for frequencies which produce high gain and directionality (Figs. 4.11, 4.18). In azimuth, there is some dependency on frequency for the acoustic axis position in *M. eugenii* probably due to the slight asymmetry of cross-section (see Fig. 4.1B) but this was not apparent for the pinna of *M. giganteus* which is very similar in shape. For the most part the azimuthal orientation of the acoustic axis depends on the position of the pinna on the head in these Macropods. In the cat it has been suggested that the spatial

location of the acoustic axis may be frequency dependent (Phillips et al. 1982; Calford and Pettigrew 1984) but these results could be an artifact produced by distortion of the pinna following surgical procedures and unnatural positioning of the pinnae.

TABLE 4.1: DIMENSIONS AND PARAMETERS FOR VARIOUS EXTERNAL EARS IN VERTEBRATES

SPECIES	PINNA/OUTER EAR CAVITY (MOUTH)				DIRECTIONALITY		PINNA/OUTER EAR CAVITY (THROAT)		HORN LENGTH			MEATUS	TYMPANIC MEMBRANE	HORN PARAMETERS		
	circum-ference $2\pi a$ (cm)	av. radius a (cm)	height (cm)	width (cm)	onset ka=1.25 (kHz)	high ka = 3 (kHz)	circum-ference $2\pi a$ (cm)	av. radius a (cm)	Long (cm)	Short (cm)	Average (ℓ) (cm)	length (cm)	av. radius (cm)	G_∞ (dB)	cone angle	$\frac{2a}{\ell}$ (mouth)
Macroderma gigas[a]	10.7	1.7	5.6	2.2	4.0	9.6	4.0	0.4	4.3	0.6	2.4	1.1	0.14	13	29°	1.4
Nyctophilus gouldi[a]	5.3	0.85	2.8	1.2	8.1	18	1.1	0.2	2.2	0.4	1.3	0.25	0.14	13	27°	1.3
Macropus eugenii[a]	16	2.5	7.0	3.5	2.7	6.4	2.5	0.4	7.5	1.5	4.5	1.6	0.25	16	25°	1.1
Macropus giganteus[a]	24.5	3.9	8.2	3.0	1.76	4.2	6.9	1.1	9	2	5.5	3.2	0.27	11	27°	1.4
Tyto alba[a]	19	3.0	7.0	4.5	2.3	5.4	2.2	0.4	7.0	1.8	4.4	0.8	0.46	18	30°	1.4
Myotis l. lucifugus[b]	3.8	0.6	1.4	0.7	11.0	27										
Plecotus townsendii[b]	8.4	1.3	3.7	1.2	5.0	12										
Felis catus[c]	14.5	2.3	5.5	3.0	2.9	7.1	2.5	0.4	6.0	2.5	4.3	2				
Trichosurus vulpecula[c]	14.2	2.3	5.8	3.3	3.0	7.3			5.5	1.1	3.3					

a = present study, b = Grinnell & Grinnell 1965, c = personal observations

Fig. 4.1. The general morphology of the pinna of *Macropus eugenii* .

A. Pinna face viewed frontally (on-axis) indicating the leading edge (Fr), tragal notch (TN) and tympanic membrane (TM).

B. Horizontal cross-section midway through pinna showing slight asymmetry of the pinna flange.

C. Side view of pinna showing inclination to the vertical plane and location of acoustic axis. S: surface of skull, M: meatus, V: vertical plane. The drawings are based on photographs and endocasts of the external ear using silicon moulding rubber. The pinna was removed close to the surface of the skull(S), at the junction between the meatus and the pinna (see Table 4.1).

Macropus eugenii

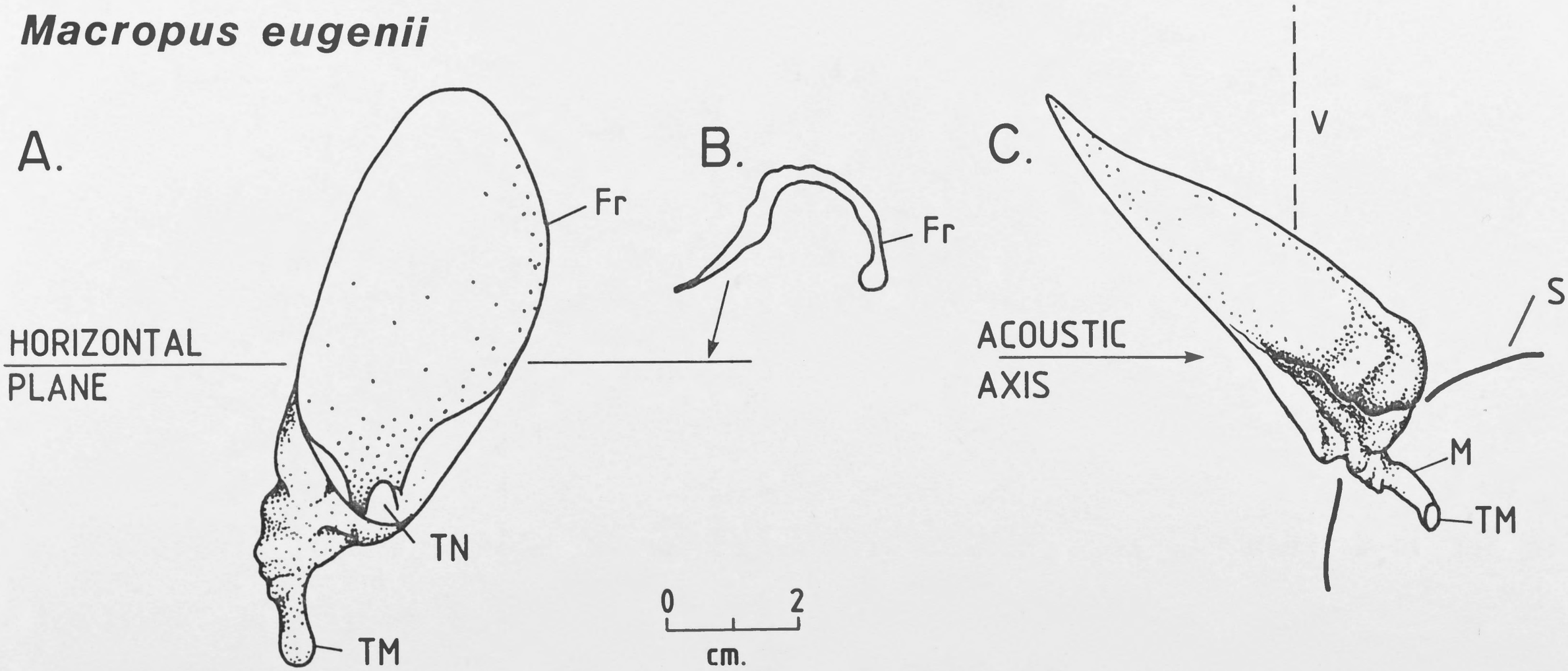

Fig. 4.2. Polar response patterns in *Macropus eugenii* based on the pressure response in the ear canal in azimuth (A) or elevation (B) at 6 and 10kHz. 0dB = 100 dB re. 20 μPa; free field sound pressure level indicated by filled circle on polar plot. Decreasing sound pressure re. 0dB is towards the centre of polar diagram. Schematic head of *M. eugenii* in A indicates approximate position of elevated planes shown in B. The position of the acoustic axis is indicated in A as the peak in the polar response pattern. In this example the pinnae are in the resting position.

A.

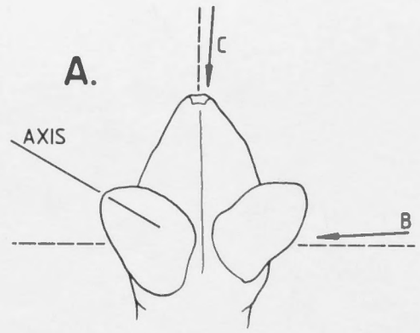

B.

Macropus eugenii

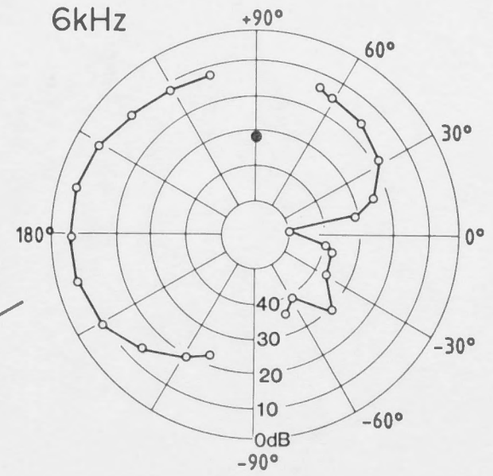

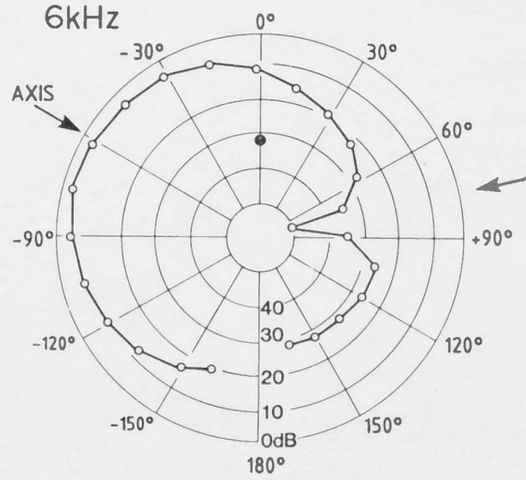

C.

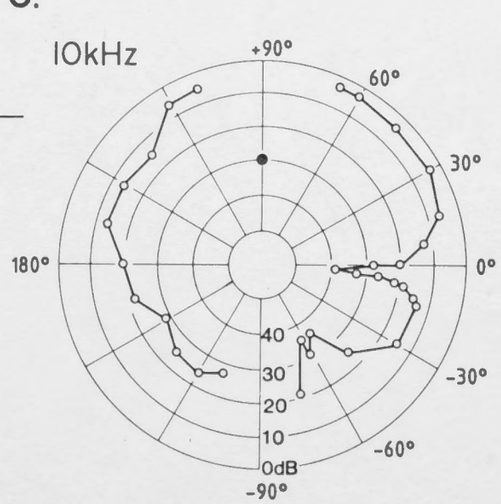

ELEVATION

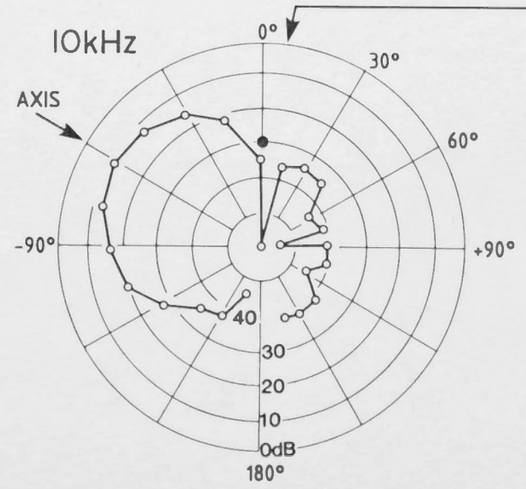

AZIMUTH

Fig. 4.3. Measurement of the acoustic pressure gain (in dB) for four separate ears of *Macropus eugenii* as a function of stimulus frequency. Inset shows "on-axis" view of the left ear.

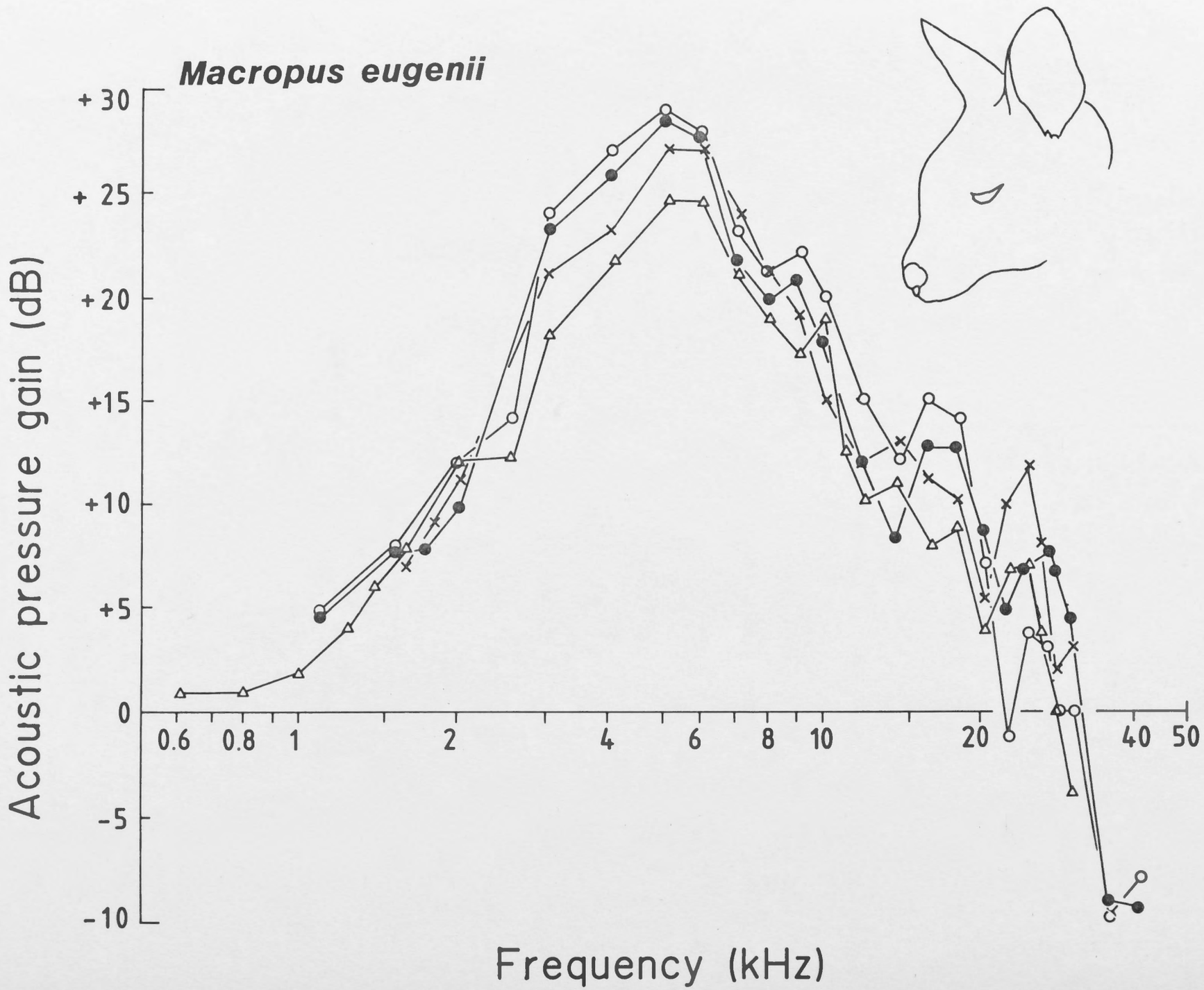
Macropus eugenii
+30
+25
+20
+15
+10
+5
0
-5
-10
Acoustic pressure gain (dB)
0.6
0.8
1
2
4
6
8
10
20
40
50
Frequency (kHz)

Fig. 4.4. A: Pressure gain curve of a single ear of *Macropus eugenii* for three conditions: normal curve (solid line, filled circles), artifically enlarged pinna (dotted line), pinna removed (open circles, solid line).

B. Pinna gain for three ears estimated by the difference between pinna intact and pinna removed curves (as in A). Dotted curve represents the expected gain curve for a finite conical horn based on the dimensions of the pinna of *M. eugenii* (Table 4.1). For calculation of the gain curve of a finite conical horn see text and APPENDIX 1. The *ka* values are also indicated on the abscissa and based on the ratio of the circumference of the pinna face to the wavelength (Table 4.1 and text).

C. Average gain curve of the pinna based on the curves in B. (solid curve). Dotted curves are the expected gain curves for a finite paraboloidal, conical and exponential horn based on the dimensions of the pinna of *M. eugenii* (see Table 4.1). For details of calculation see APPENDIX 1 and text.

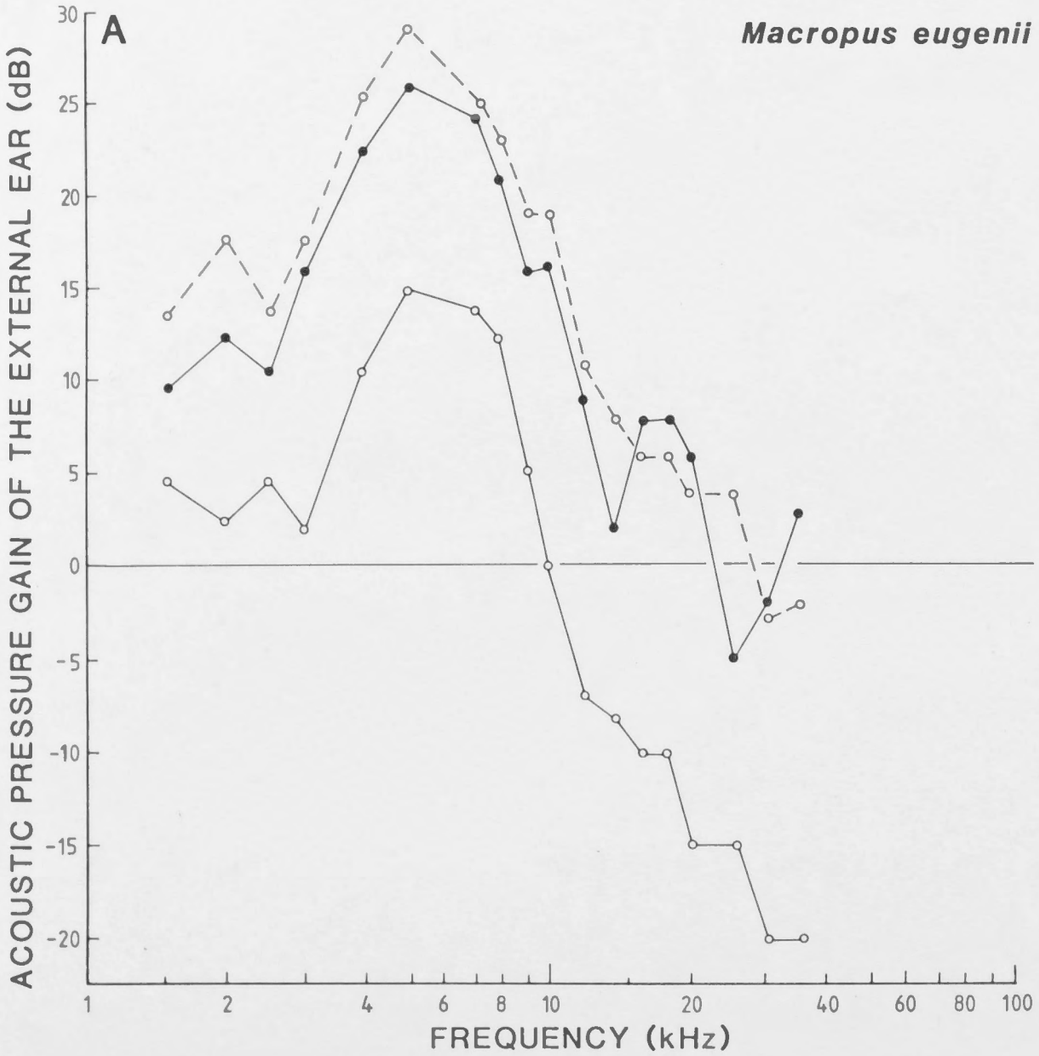
A
Macropus eugenii
ACOUSTIC PRESSURE GAIN OF THE EXTERNAL EAR (dB)
30
25
20
15
10
5
0
-5
-10
-15
-20
1
2
4
6
8
10
20
40
60
80
100
FREQUENCY (kHz)

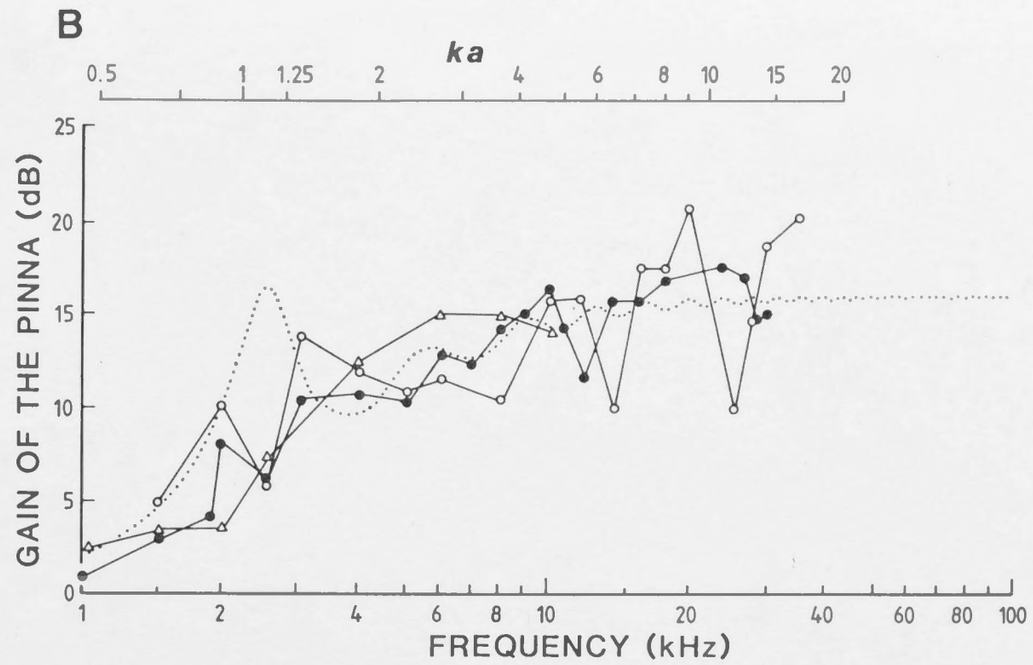
B
ka
0.5
1
1.25
2
4
6
8
10
15
20
GAIN OF THE PINNA (dB)
25
20
15
10
5
0
1
2
4
6
8
10
20
40
60
80
100
FREQUENCY (kHz)

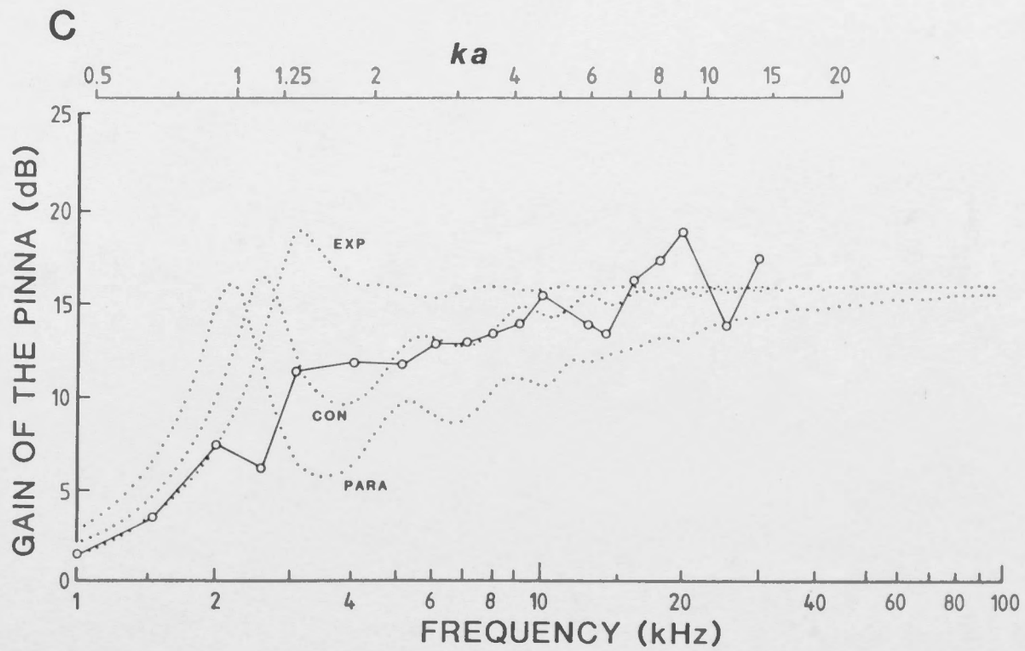
C
ka
0.5
1
1.25
2
4
6
8
10
15
20
GAIN OF THE PINNA (dB)
25
20
15
10
5
0
EXP
CON
PARA
1
2
4
6
8
10
20
40
60
80
100
FREQUENCY (kHz)

Fig. 4.5. A series of iso-intensity contour plots showing development of directionality for the left ear of *Macropus eugenii* (in resting position) at 6 test frequencies. The acoustic axis is located within the 1dB contour (open circles). 5dB contours are plotted relative to the on-axis pressure. The closeness of the contours indicate steep angular gradients, which are usually associated with low pressure regions such as nulls (indicated as a short thick line or dot). The data plotting co-ordinate system is a zenithal projection of a hemisphere (see MATERIALS AND METHODS).

Macropus eugenii

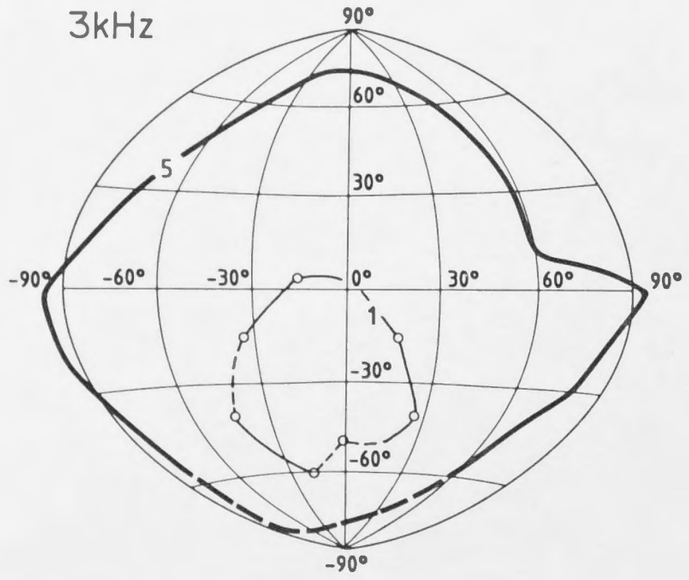

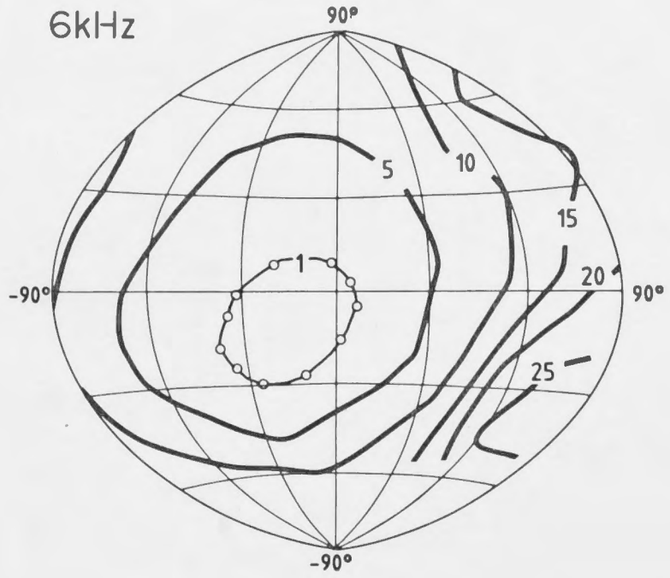

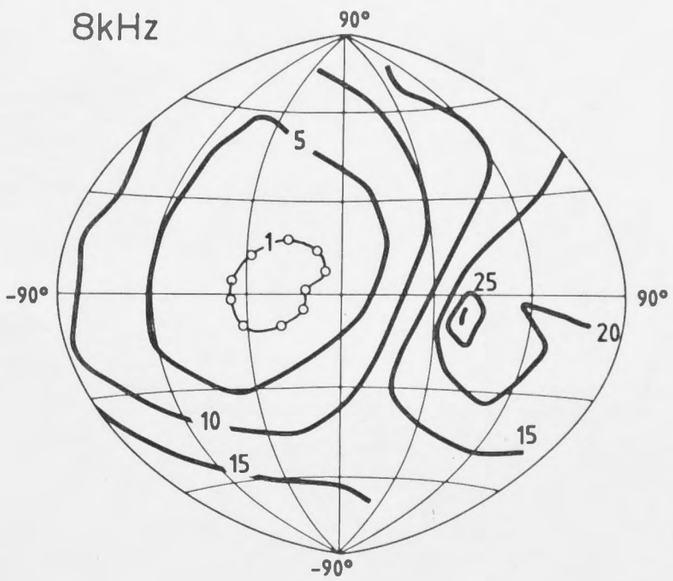

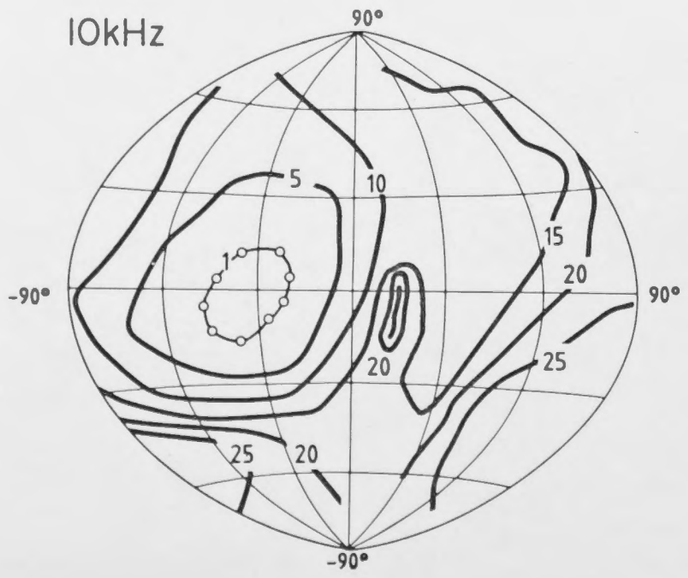

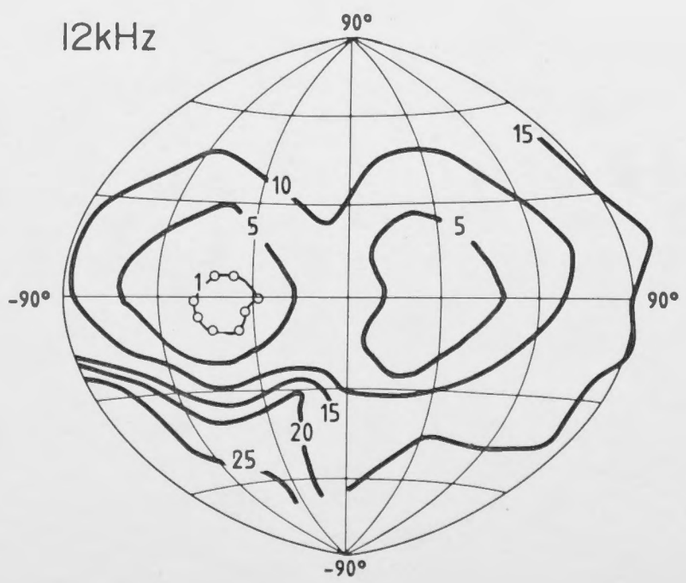

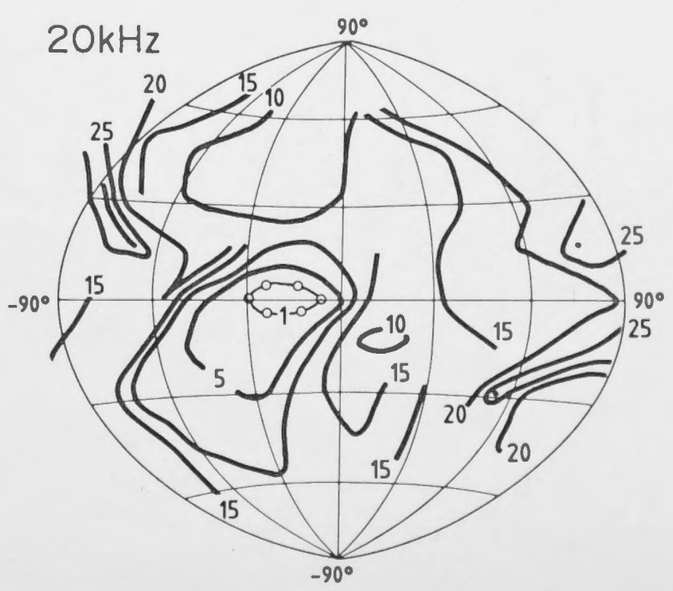

Fig. 4.6. Polar response curves showing directionality for a right ear of *Macropus eugenii*, taken on the horizontal plane. Decreasing sound pressure occurs towards the centre of polar diagram as defined in Fig. 4.2. 0°/180° is the midline with 0° forward, + 90° = ipsilateral and -90° = contralateral. The development of the acoustic axis and nulls can be compared to Fig. 4.5. Note that the correct alignment of the pinna in the vertical plane (see Fig. 4.1C) results in both the acoustic axis and the frontal null being on the horizon, for example at 10kHz.

Macropus eugenii

3kHz

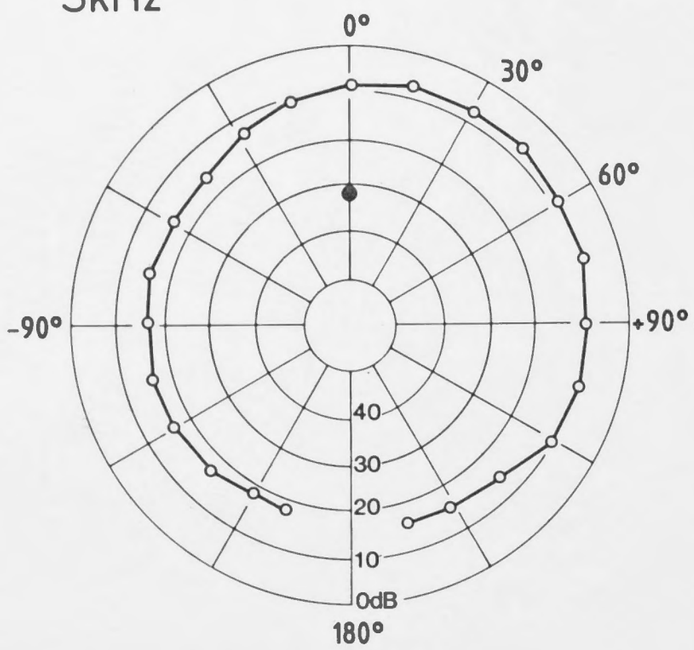

5kHz

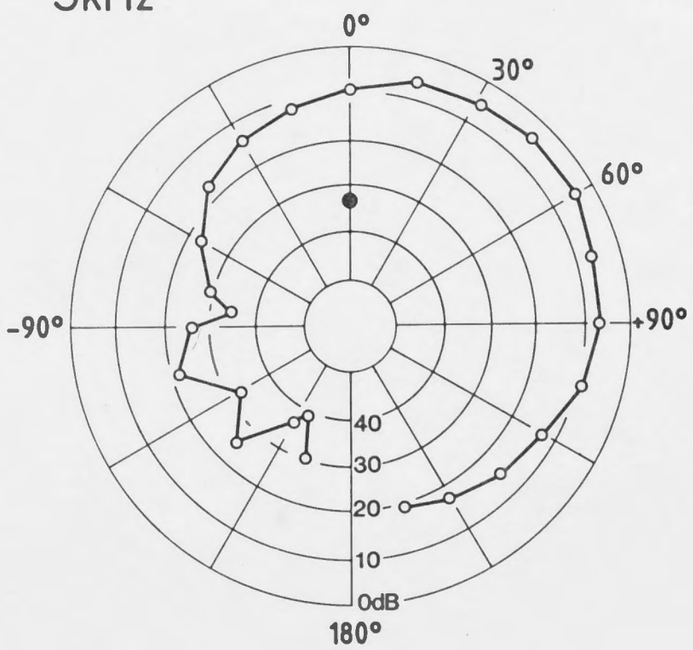

6kHz

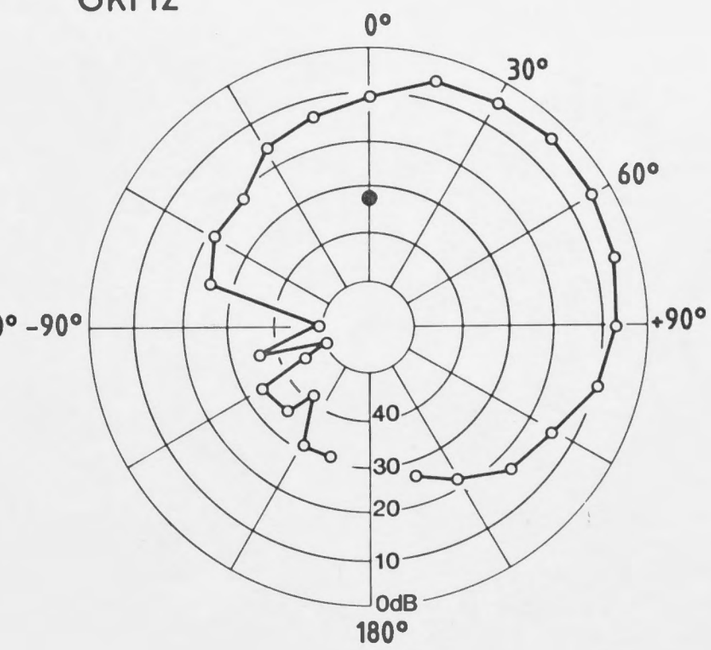

8kHz

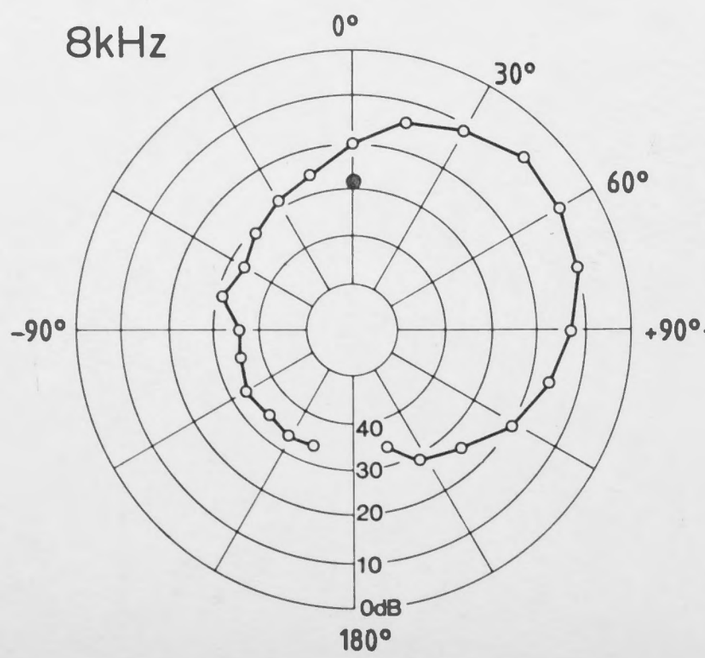

10kHz

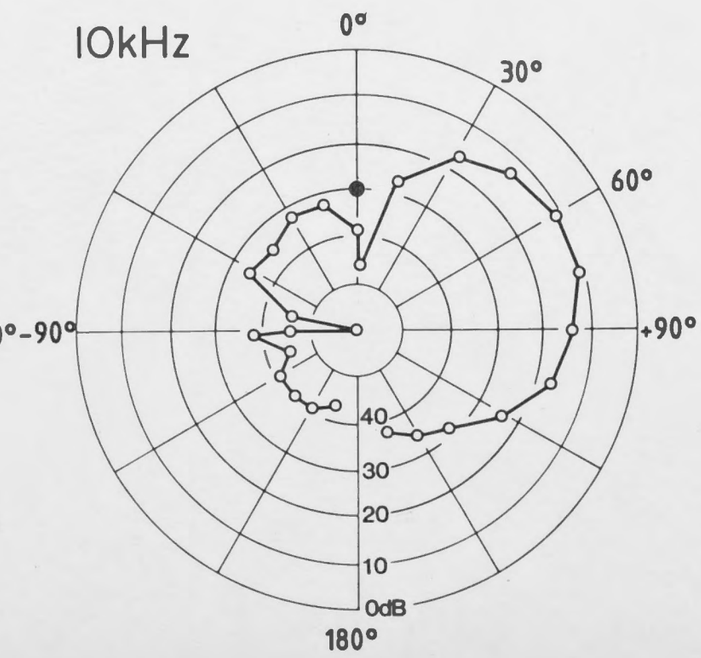

12kHz

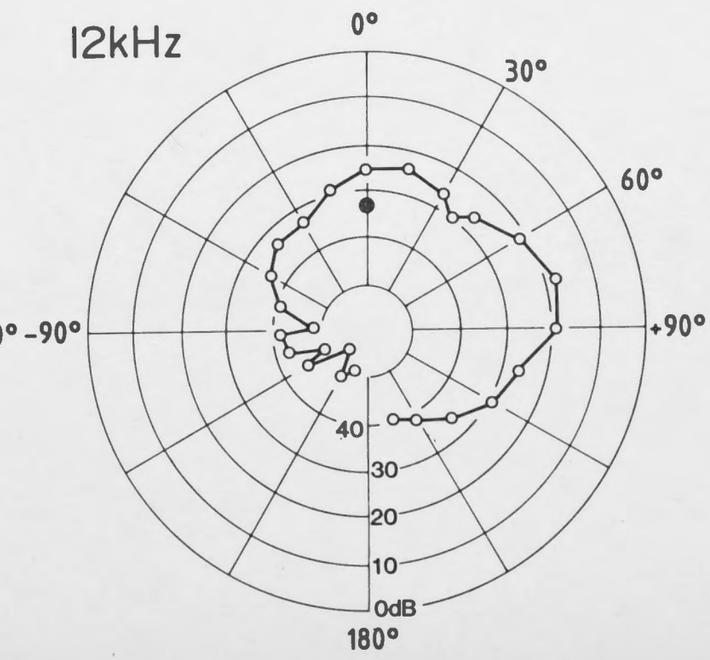

Fig. 4.7. The maximum difference in sound pressure (dB_{max}) for the ear canal directivity patterns of *Macropus eugenii* as a function of stimulus frequency for 4 ears. The ratio between the circumference of the pinna face and the wavelength (*ka*) is represented along the abscissa (see text for details).

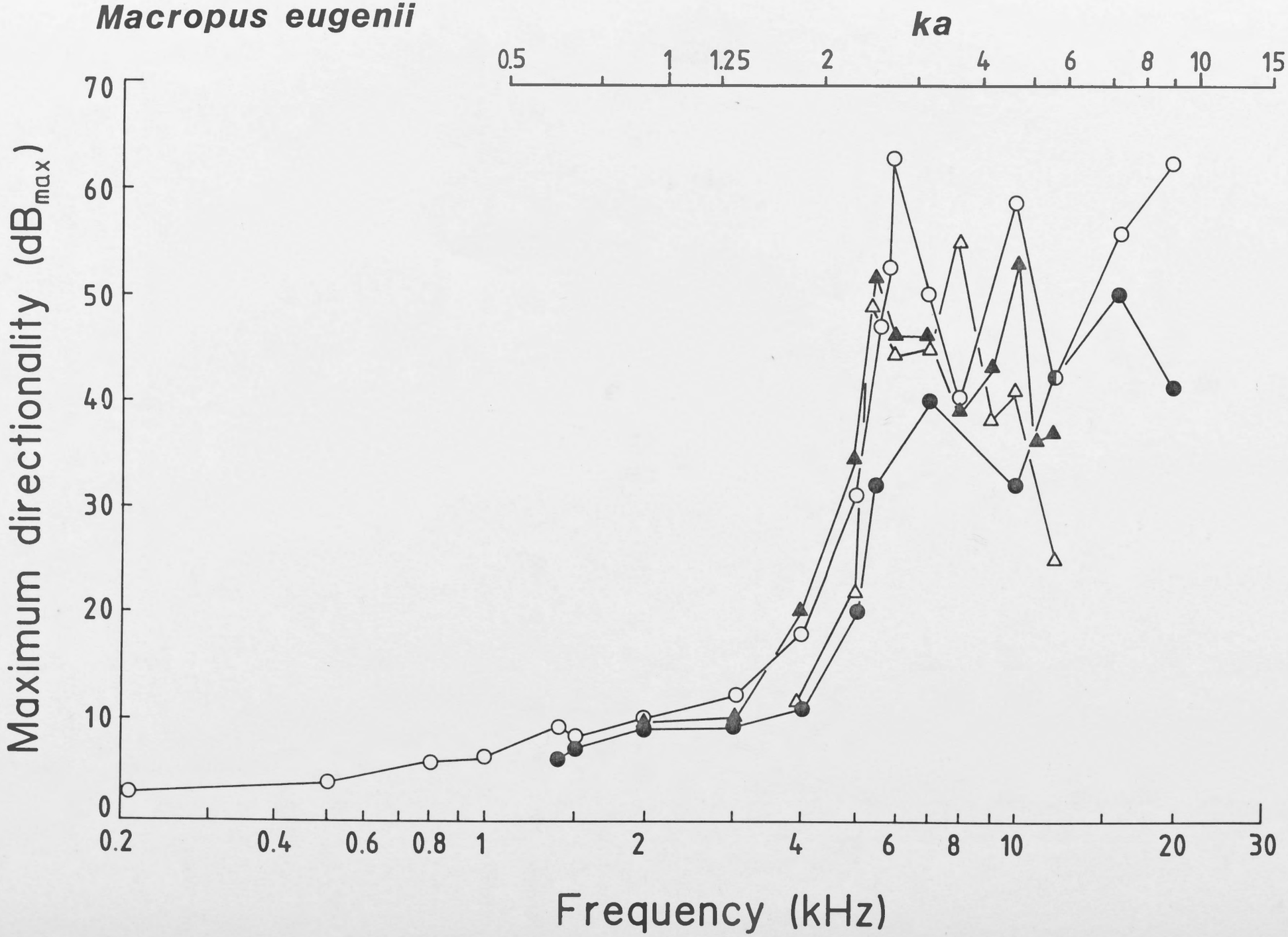
Macropus eugenii
ka
0.5
1
1.25
2
4
6
8
10
15
Maximum directionality (dB$_{max}$)
70
60
50
40
30
20
10
0
0.2
0.4
0.6
0.8
1
2
4
6
8
10
20
30
Frequency (kHz)

Fig. 4.8. Measurement of the angular width or acceptance angle (degrees) of the main lobe of the directivity patterns of *Macropus eugenii* for 4 ears. Values determined -3dB below the on-axis pressure peak and expressed as the full angular width (2θ°). Due to the asymmetry of the directivity patterns (see Fig. 4.5) azimuth (A) and elevation (B) components are plotted separately. Expected acceptance angles are shown for sound diffraction by a circular aperture (dashed curves), corresponding to the average radius of the pinna opening (a = 2.5cm; see Table 4.1). For calculations of acceptance angle as a function of frequency for a circular aperture in a plane wall see APPENDIX 2.

A.

B.

AZIMUTH

ELEVATION

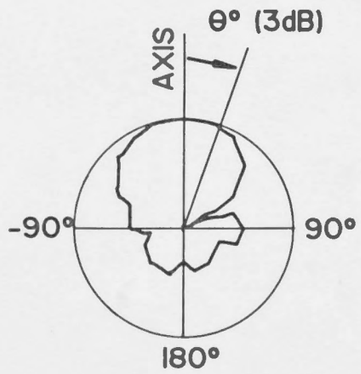

3dB acceptance angle (degrees)= 2θ°

2.5 = a(cm)

180°
160°
140°
120°
100°
80°
60°
40°
20°
0°

Macropus eugenii

1 2 4 6 8 10 20 30 40 50

Frequency (kHz)

2.5 = a(cm)

180°
160°
140°
120°
100°
80°
60°
40°
20°
0°

1 2 4 6 8 10 20 30 40 50

Frequency (kHz)

Fig. 4.9. Angular separation between nulls in directivity patterns and the acoustic axis, as a function of frequency in *Macropus eugenii*. Dashed line is the expected curve for diffraction nulls generated by a circular aperture of radius a = 2.5cm in an infinite baffle (which equals the average radius of the wallaby pinna face). For details of calculations see APPENDIX 2 and text. The theoretical curve can only apply in front of the plane of the aperture as indicated on the graph at 90° (the frequency limit at ka = 3.83 is indicated also). If the aperture or pinna were considered to be at the end or side of a long pipe then rearward nulls are possible and a calculated null position is indicated by arrow, taken from Beranek (1954).

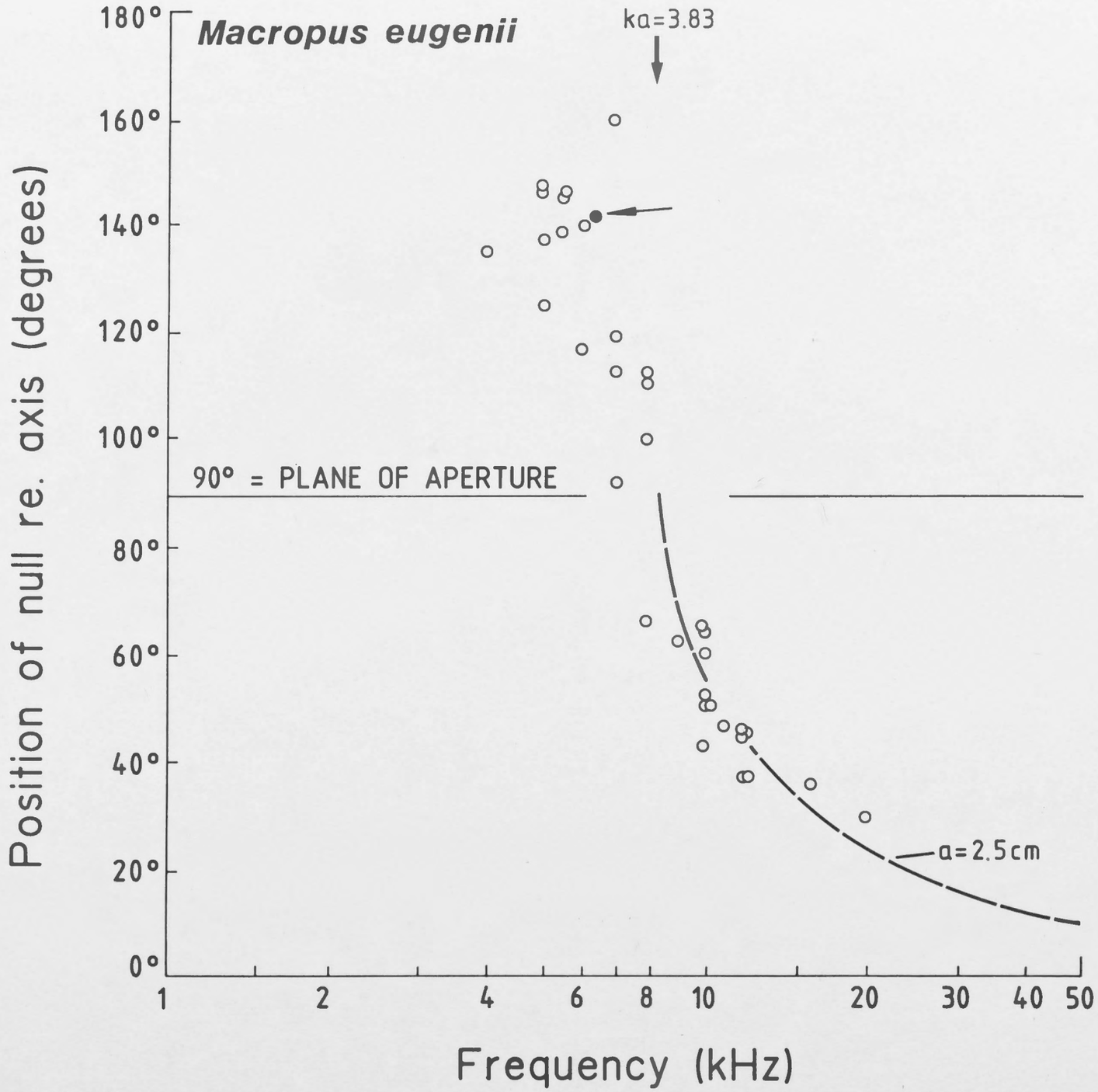
Macropus eugenii
ka=3.83
180°
160°
140°
120°
100°
80°
60°
40°
20°
0°
90° = PLANE OF APERTURE
a=2.5cm
Position of null re. axis (degrees)
1
2
4
6
8
10
20
30
40
50
Frequency (kHz)

Fig. 4.10. Effect of pinna removal on directionality in *Macropus eugenii*.

A. At 6kHz, the acoustic axis and associated iso-intensity contour pattern is severely disrupted following pinna removal, with an upward shift in the new position of maximum pressure and the 5dB contour almost fills the hemisphere.

B. Polar plot shows loss of gain (near axis) and loss of rearward null following pinna removal.

Free field sound pressure is indicated by the filled circle. 0dB level = 100 dB re 20 μPa, with decreasing pressure towards centre of polar diagram as for Figs. 4.2 and 4.6.

A.

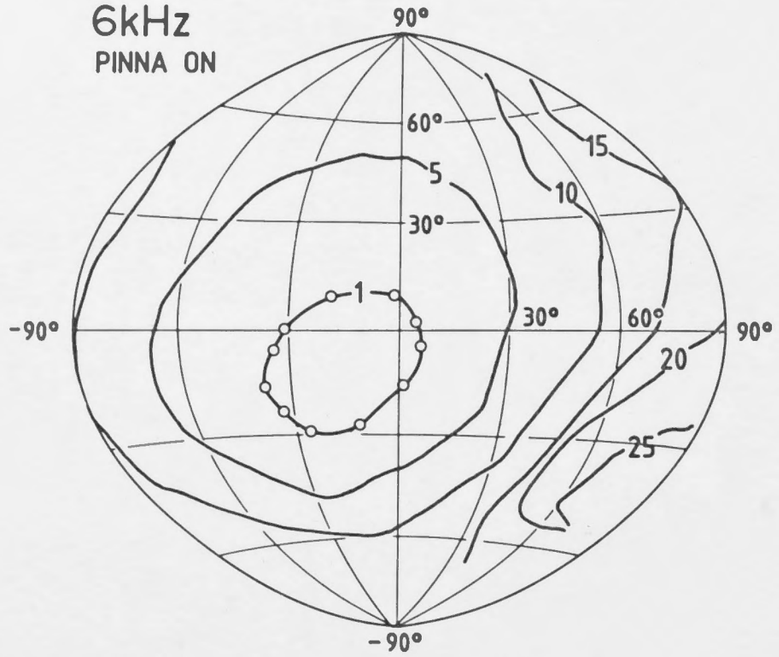

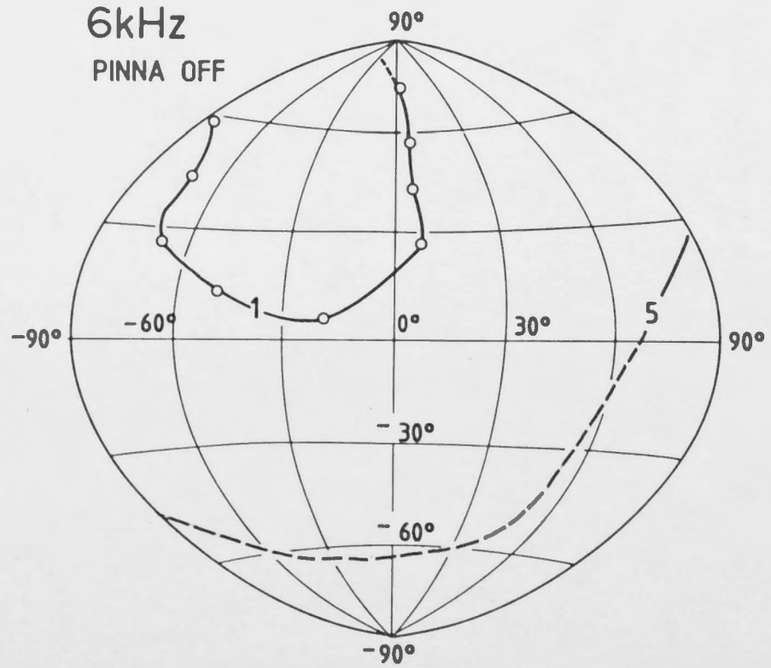

B.

Macropus eugenii

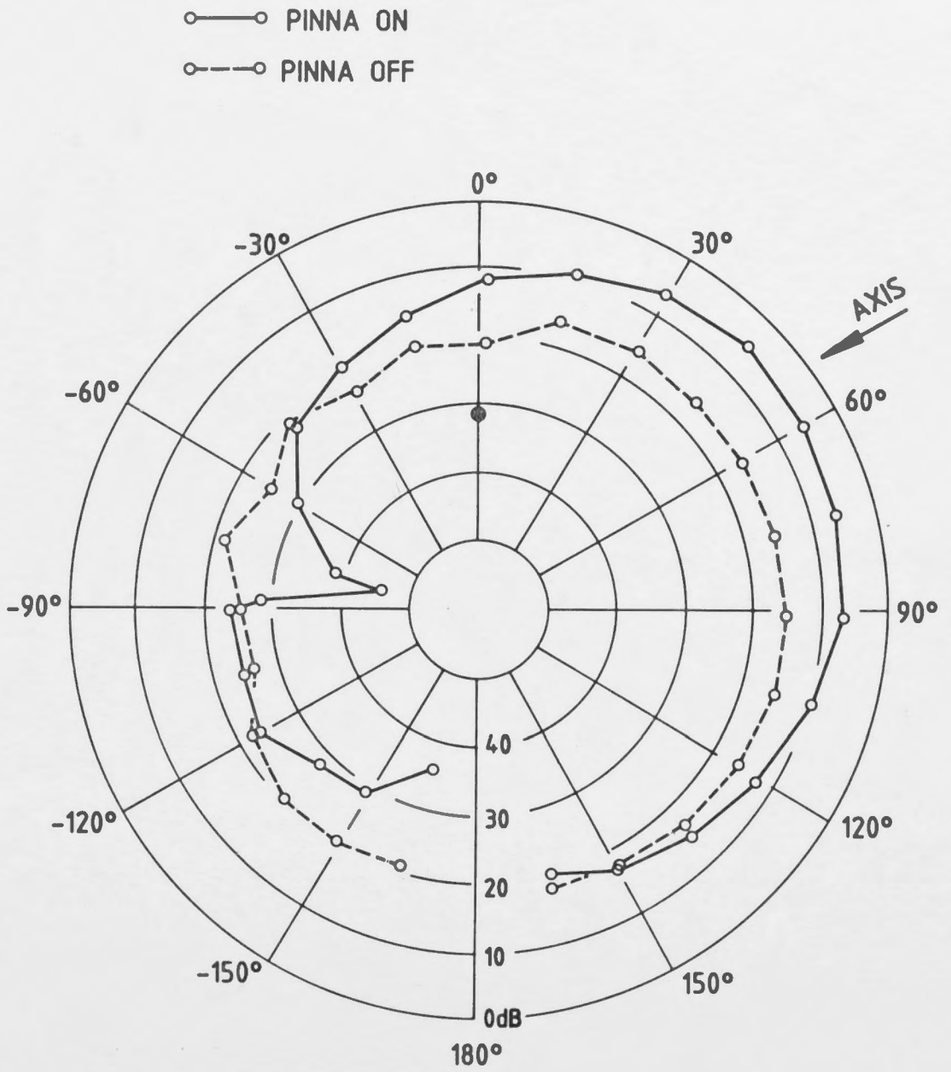

Fig. 4.11. The effect of frequency on the spatial location of the acoustic axis in both azimuth (A) and elevation (B) for *Macropus eugenii*. Data from two ears, both maintained in the natural resting position (see Fig. 4.1C and 4.2).

Macropus eugenii

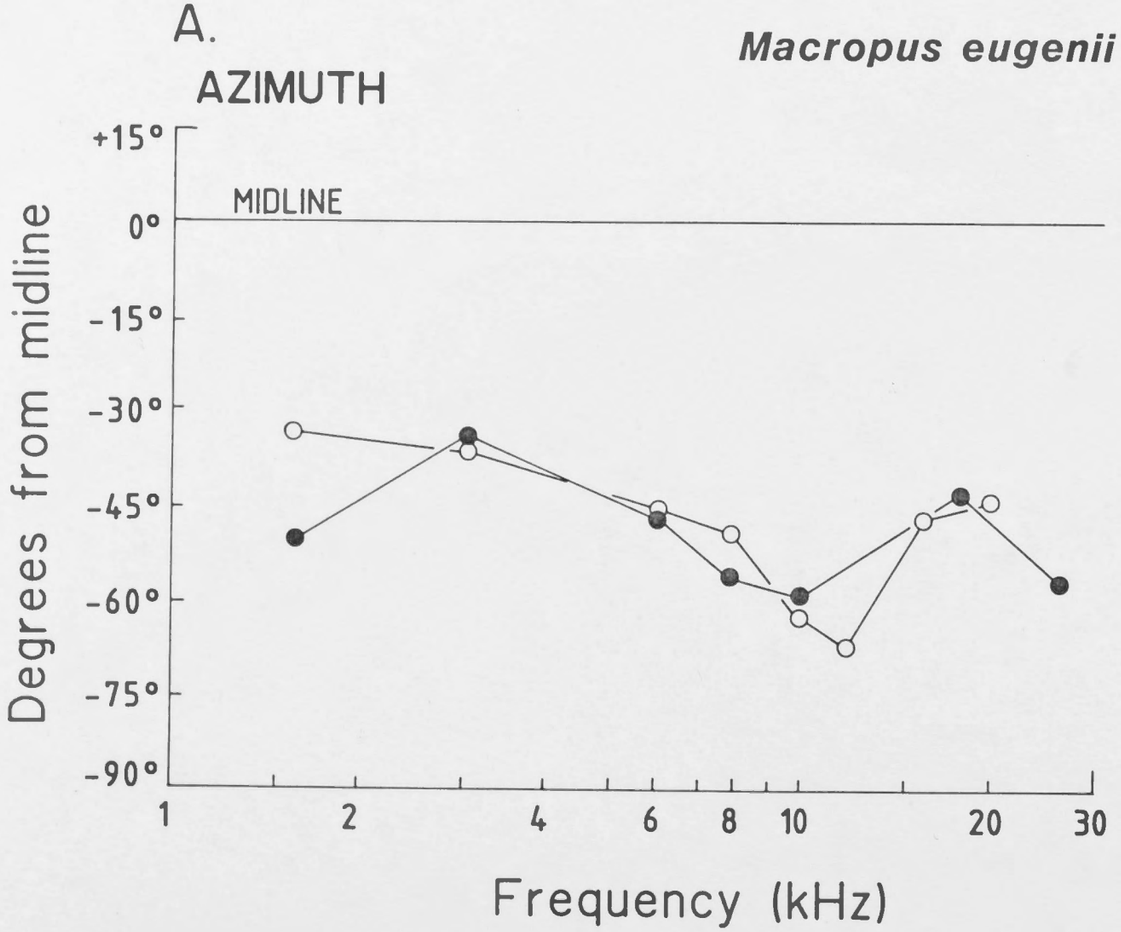

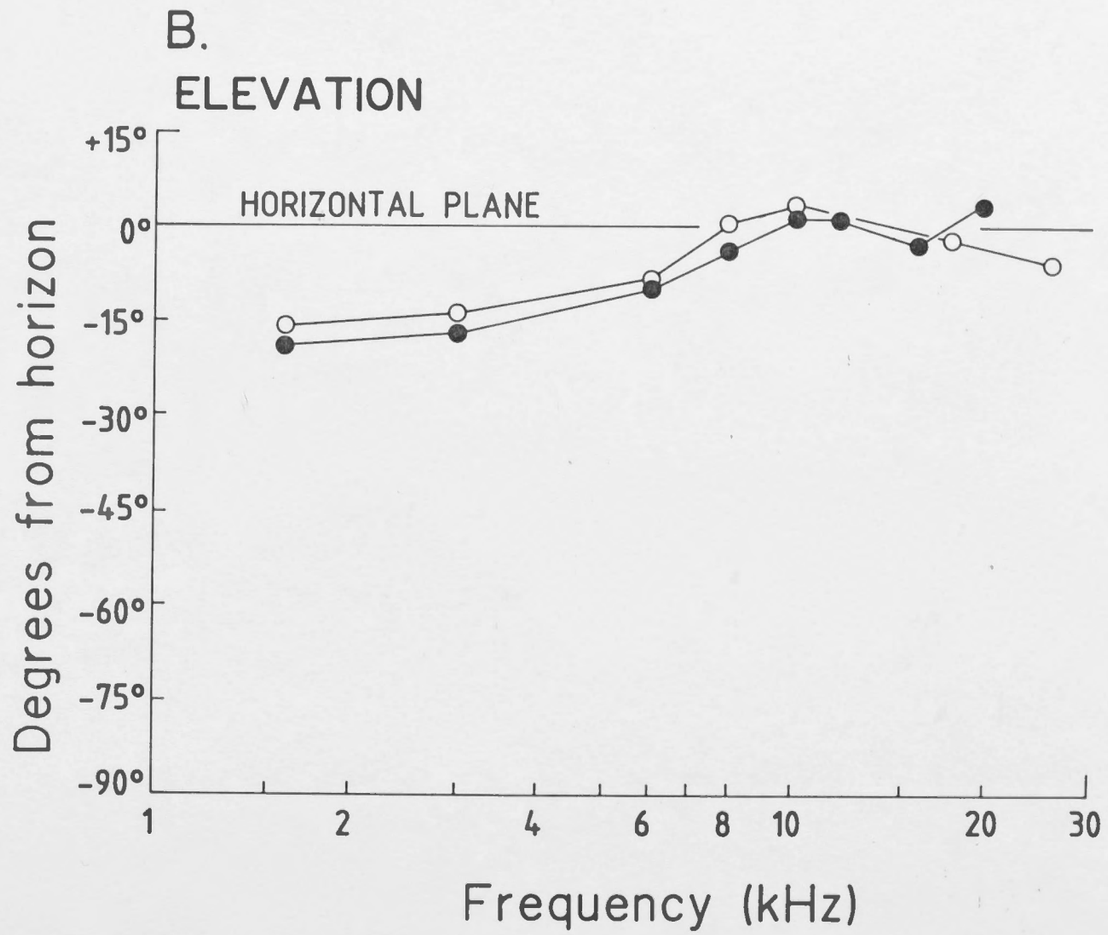

Fig. 4.12. General appearance of head and pinna of the grey kangaroo, *Macropus giganteus*.

A. Frontal view of head with pinnae approximately in the resting position.

B. Sagittal view of head with pinnae in forward, alert position.

C. Sagittal view of head with pinnae in rearward alert position.

From a single frame analysis of pinna movement between the positions shown in B and C, angular velocities of the pinna approach 500°/sec (total rotation 100°).

A

B

C

Macropus giganteus

Fig. 4.13: Acoustic pressure gain measured by a microphone implanted into the base of the ear canal near the tympanic membrane in *Macropus giganteus*.

A. Normal gain curve for three intact external ear (solid curves). Dashed line is a typical pressure gain curve measured in the ear canal for a single ear after pinna removal.

B. Effective gain curves for the pinna in three *M. giganteus* based on the difference curves computed from normal and pinna removed gain (as shown in A). Dotted line is expected gain curve for a finite conical horn based on the dimensions of the pinna of *M. giganteus* (see Table 4.1 and Fig. 4.12). For details of conical horn gain calculation see APPENDIX 1 and text. The ratio between the circumference of the open face of the pinna (mouth) and the stimulus wavelength (*ka*) is indicated by a scale at the top of the graph (see Beranek 1954).

C. Average gain curve of the pinna for *M. giganteus* based on data in B (solid line). Dotted lines indicate the expected gain for a finite paraboloidal, conical and exponential horn based on the dimensions of the pinna as shown in Table 4.1. For details of theoretical calculations for horn gain see APPENDIX 1 and text.

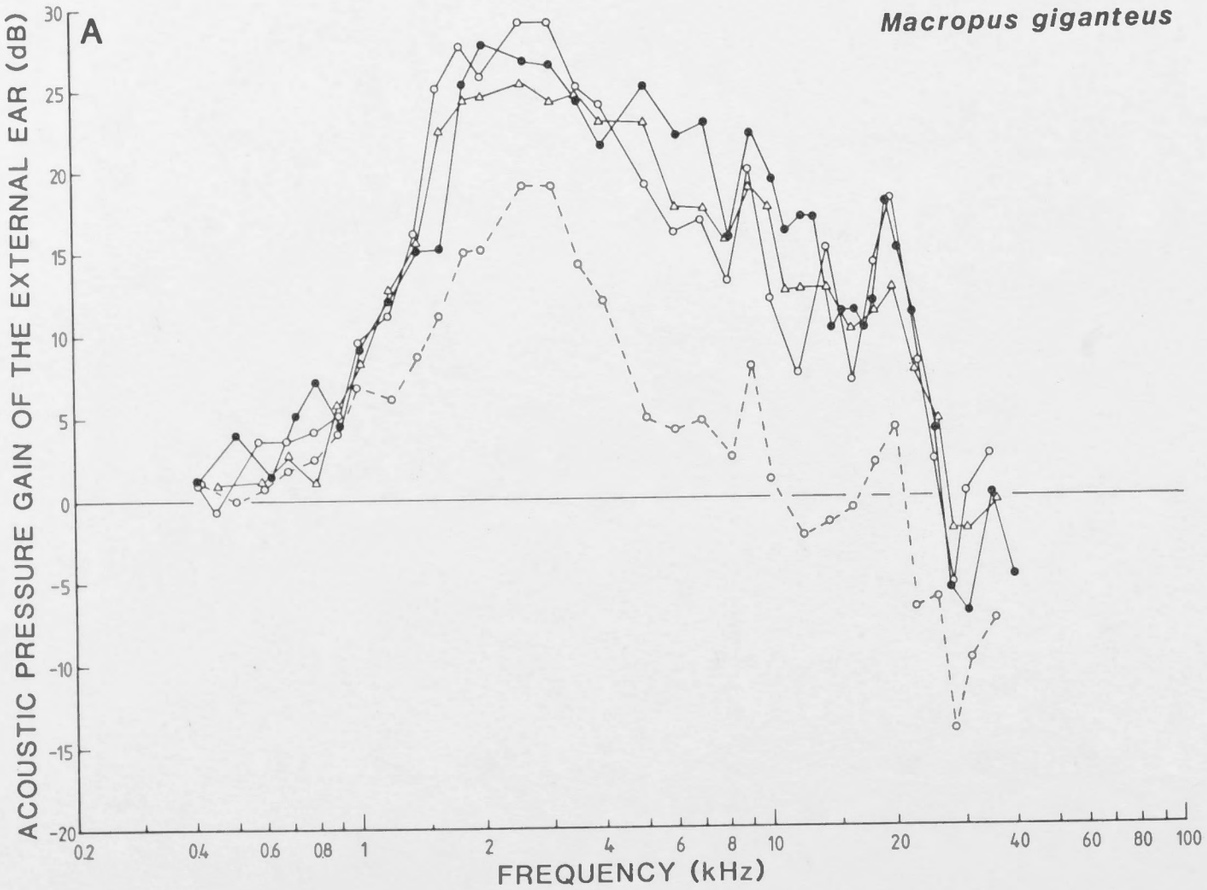
A
Macropus giganteus
ACOUSTIC PRESSURE GAIN OF THE EXTERNAL EAR (dB)
30
25
20
15
10
5
0
-5
-10
-15
-20
0.2
0.4
0.6
0.8
1
2
4
6
8
10
20
40
60
80
100
FREQUENCY (kHz)

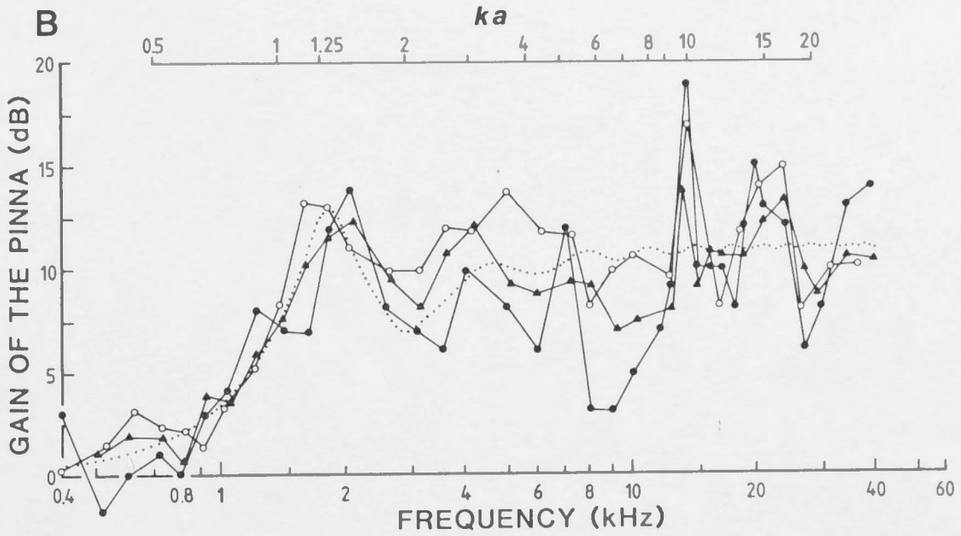
B
ka
0.5
1
1.25
2
4
6
8
10
15
20
GAIN OF THE PINNA (dB)
20
15
10
5
0
0.4
0.8
1
2
4
6
8
10
20
40
60
FREQUENCY (kHz)

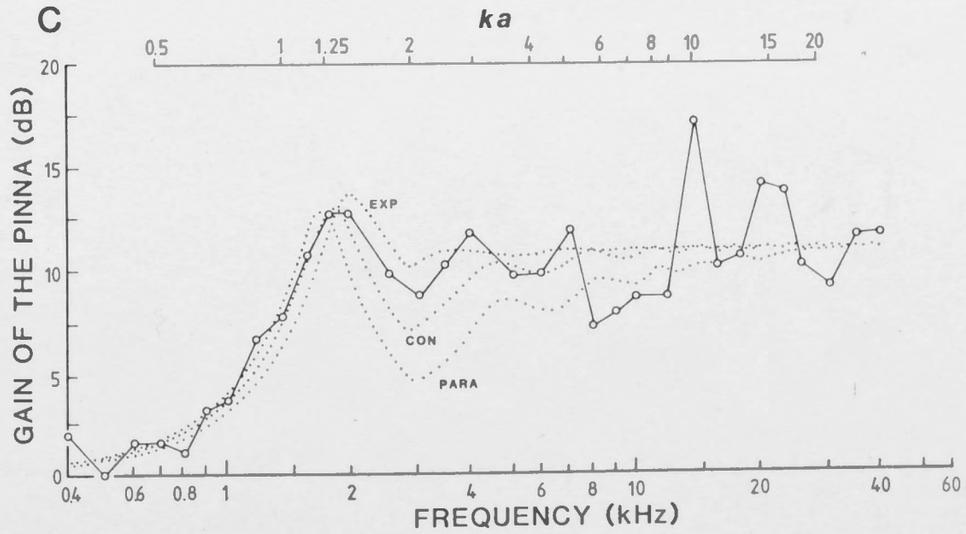
C
ka
0.5
1
1.25
2
4
6
8
10
15
20
GAIN OF THE PINNA (dB)
20
15
10
5
0
EXP
CON
PARA
0.4
0.6
0.8
1
2
4
6
8
10
20
40
60
FREQUENCY (kHz)

Fig. 4.14: A series of iso-intensity contour plots at various test frequencies for the left ear of *Macropus giganteus*. Pinna position is close to the resting position as shown in Fig. 4.12A (see also pinna and head positions for of *Macropus eugenii*, Figs. 4.4 and 4.6). The position of the acoustic axis is surrounded by a 1dB contour (open circles) and the other contour lines represent decreasing sound pressure at 5dB intervals relative to the on-axis pressure. The data is plotted on a zenithal projection of the frontal hemisphere (for details see MATERIALS AND METHODS).

Macropus giganteus

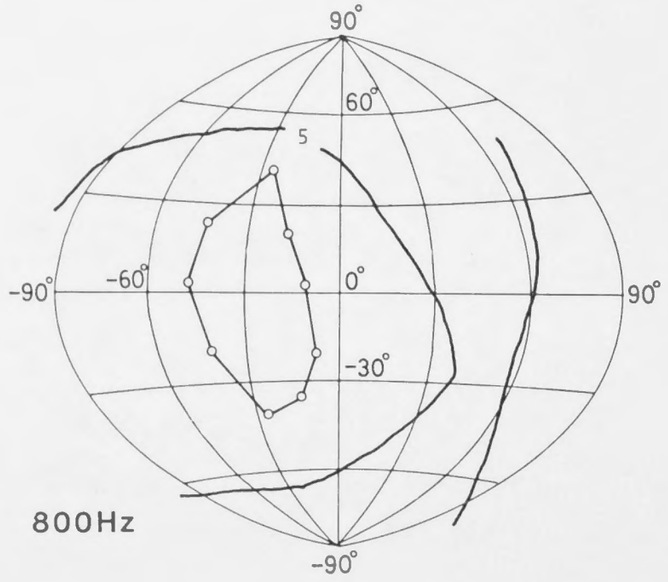

800Hz

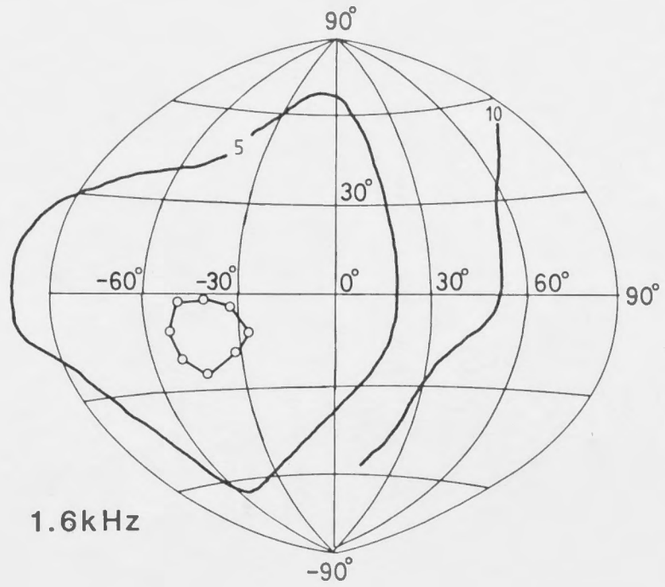

1.6kHz

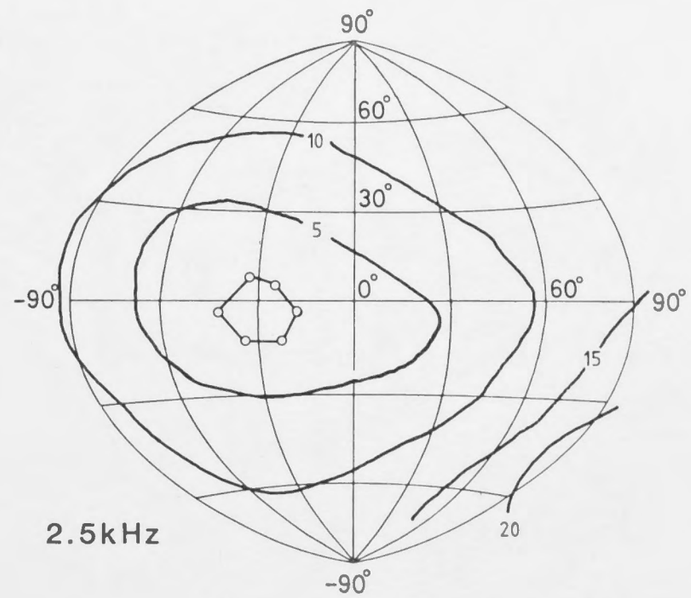

2.5kHz

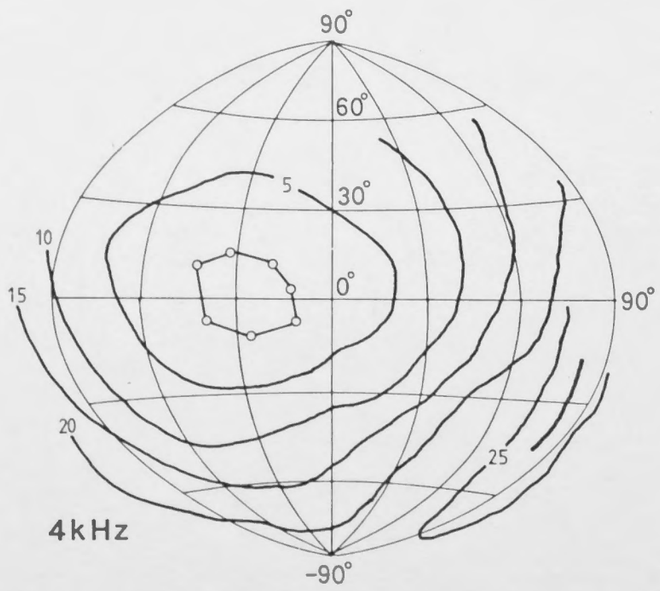

4kHz

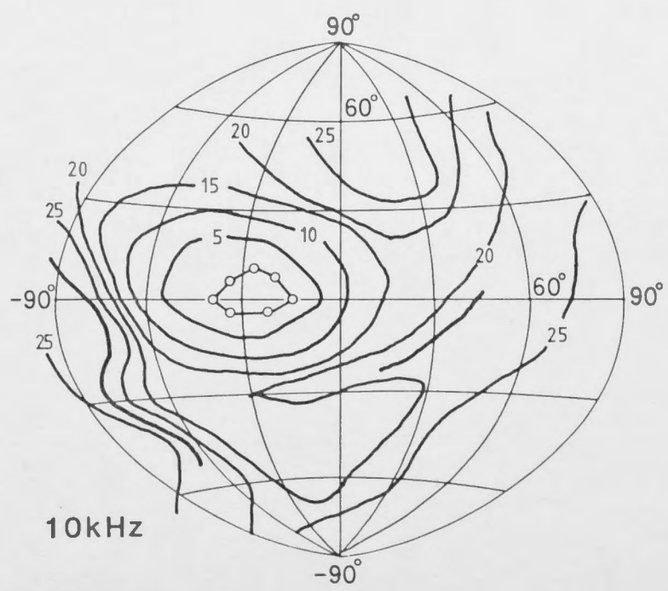

10kHz

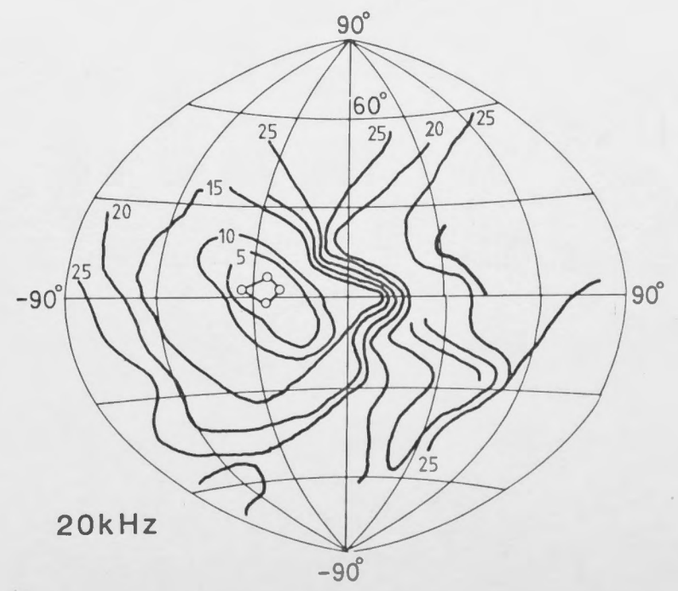

20kHz

Fig. 4.15: The maximum directionality (dB_{max}) as defined by the greatest difference in sound pressure between two points on a directivity pattern, as a function of frequency for three ears of *Macropus giganteus*. The ratio between the circumference of the open face of the pinna and the wavelength (*ka*) in *M. giganteus* is represented as a scale at the top of the graph (a = 3.9cm; Table 4.1).

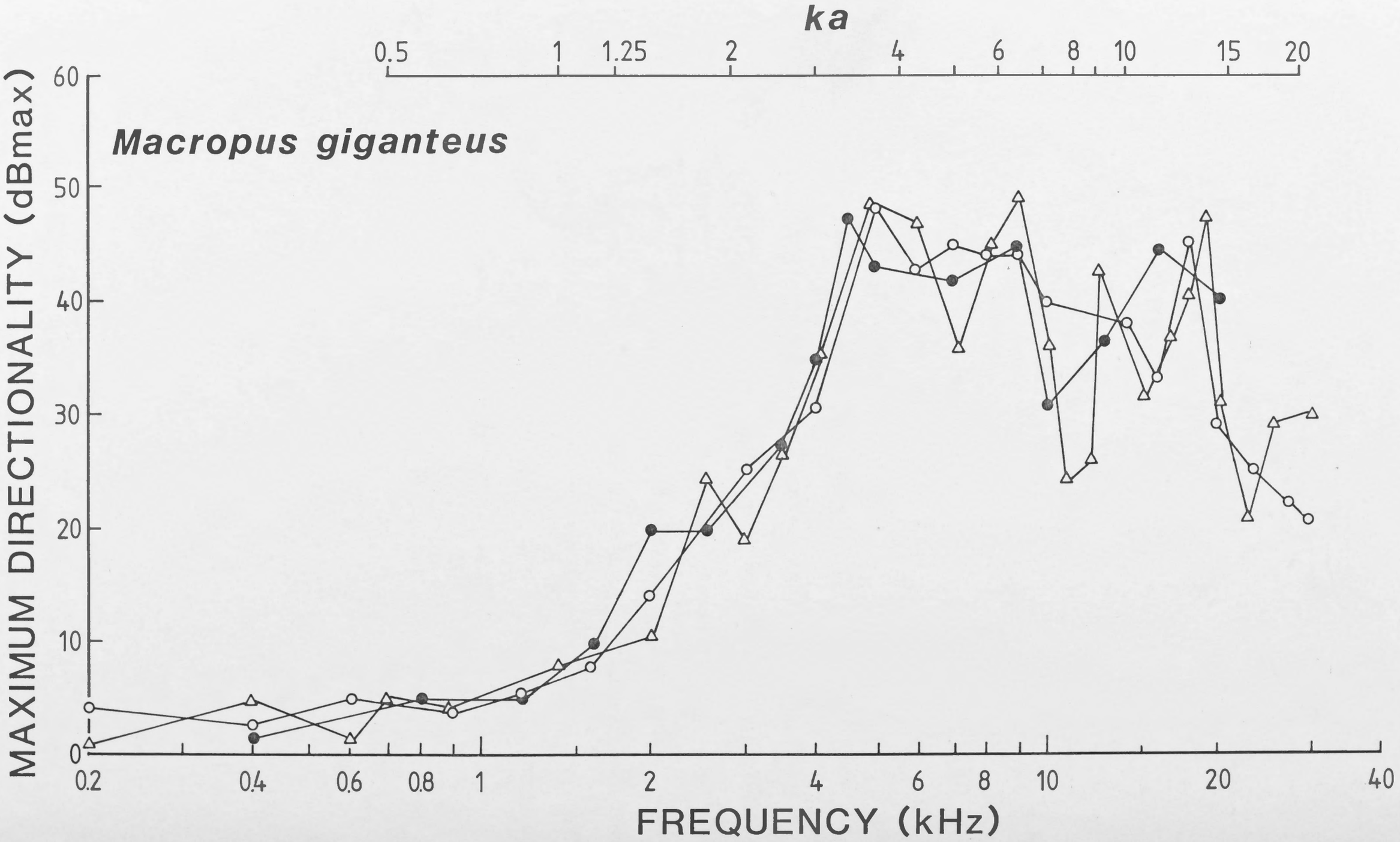
ka
0.5
1
1.25
2
4
6
8
10
15
20
Macropus giganteus
MAXIMUM DIRECTIONALITY (dBmax)
60
50
40
30
20
10
0
0.2
0.4
0.6
0.8
1
2
4
6
8
10
20
40
FREQUENCY (kHz)

Fig. 4.17: Angular separation between nulls and the acoustic axis as a function of frequency for directivity patterns recorded in the ear canal of *Macropus giganteus* (N = 3). Solid curve represents the expected semi-angle which would result from sound diffraction by a circular aperture in a plane wall with a radius equal to the average radius of the open face of the pinna in *M. giganteus* (a = 3.9cm; Table 4.1). The maximum semi-angle for diffraction by a circular aperture in a plane wall occurs at 90° as indicated. Therefore the lower frequency limit for nulls occuring in frontal space is indicated at ka = 3.83 (see Beranek 1954).

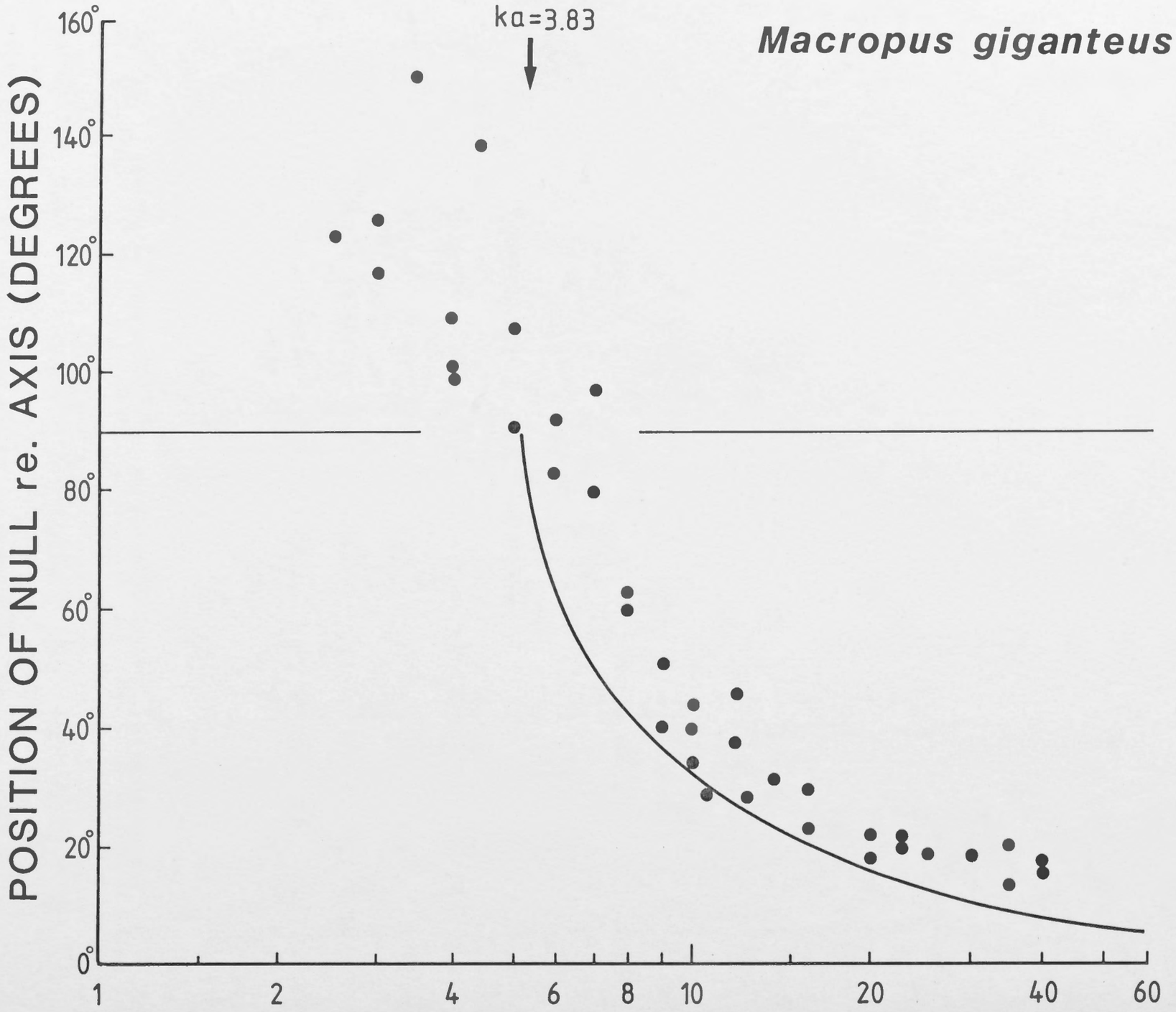
ka=3.83
Macropus giganteus
POSITION OF NULL re. AXIS (DEGREES)
160°
140°
120°
100°
80°
60°
40°
20°
0°
1
2
4
6
8
10
20
40
60

Fig. 4.18: The effect of frequency on the average position of the acoustic axis (three ears) in azimuth (A) and elevation (B) in *Macropus giganteus*. Vertical bars = standard errors. Data were collected for pinnae approximately in the resting position as shown in Fig. 4.12A.

A. AZIMUTH

Macropus giganteus

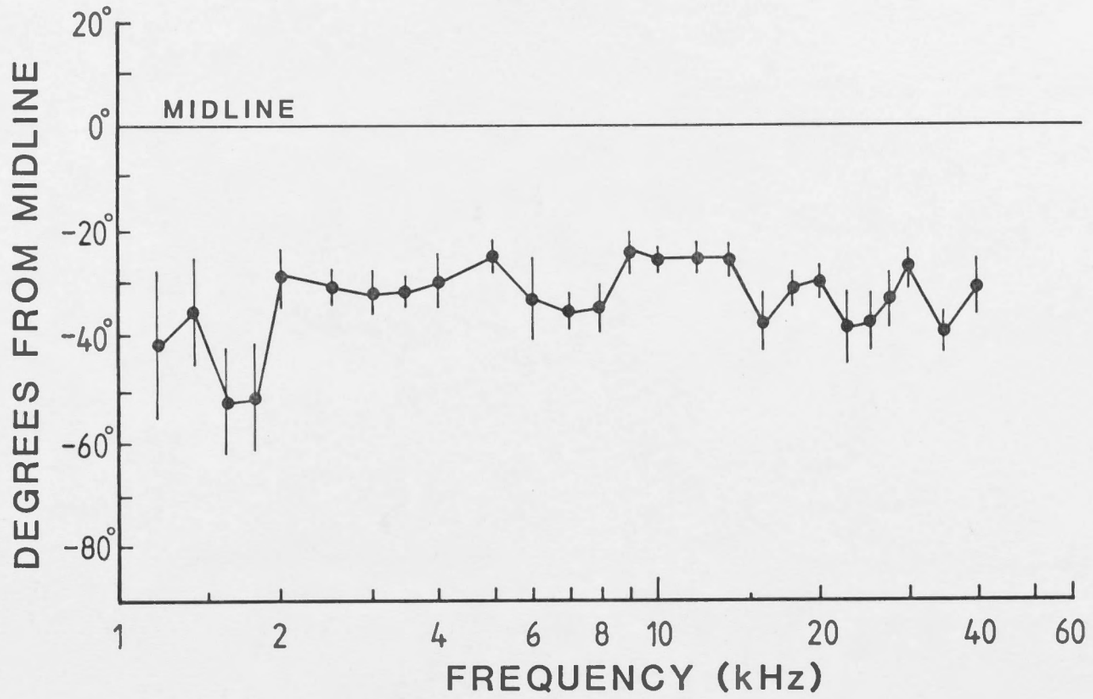

B. ELEVATION

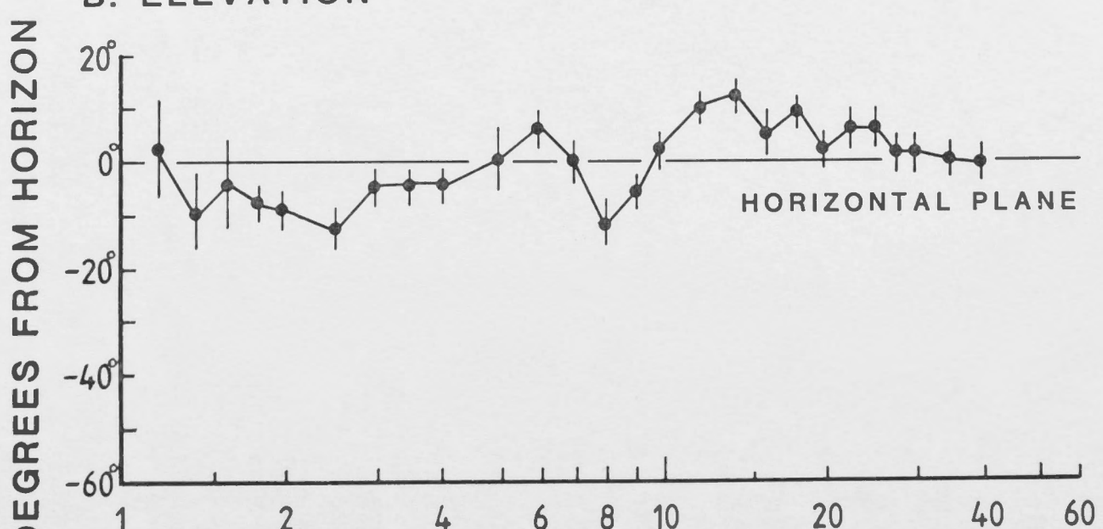

Fig. 4.19: Sonograms of species-specific vocalizations of *Macropus giganteus*.

A. "Clucking" call of adult female.

B. "Hur" call of adult male (fighting).

C. "Distress" call of isolated juvenile (pouch young).

D. "Aggressive" call of juvenile (pouch young).

Macropus giganteus

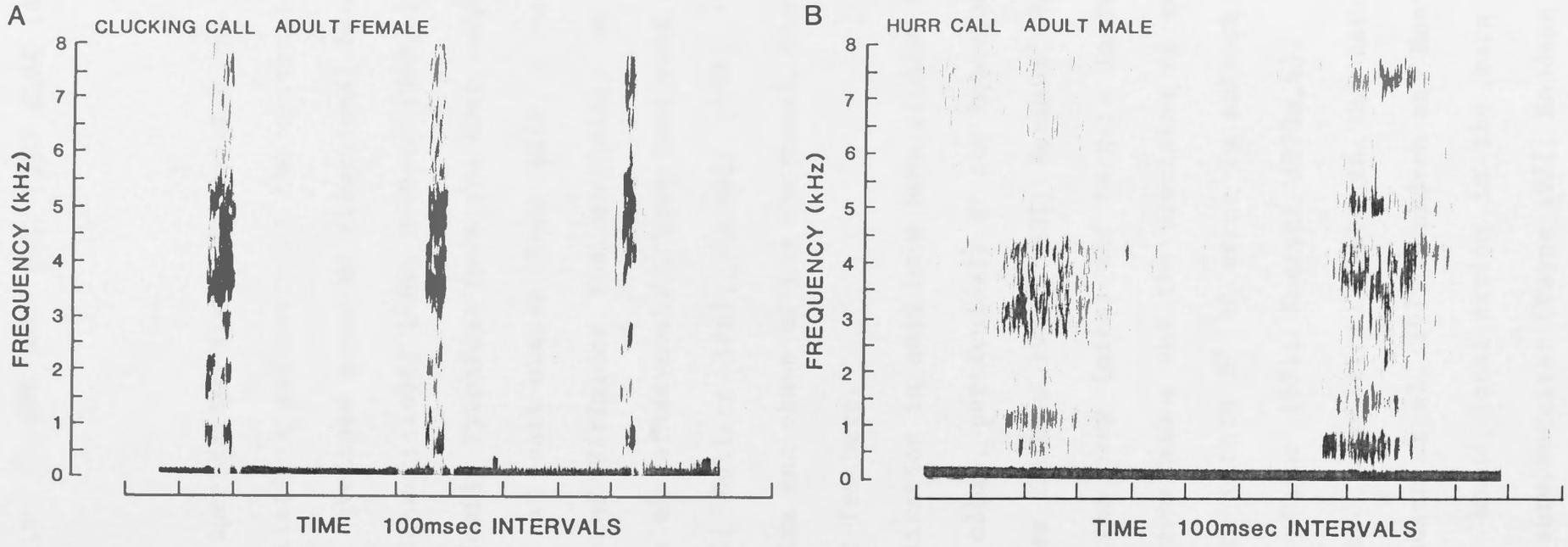

CHAPTER 5: ACOUSTICAL PROPERTIES OF THE EXTERNAL EAR AND DIRECTIONAL HEARING IN THE BARN OWL, *TYTO ALBA* [AVES: TYTONIDAE]

INTRODUCTION

Nocturnal owls are the most specialized birds for hearing and many species are remarkable for the bilateral asymmetry of the external ear which has been linked to a highly developed sense of directional hearing (Stresemann 1934; Pumphrey 1948; Schwartzkopff 1962; Norberg 1968, 1977, 1978; Payne 1971). Owls of the family Tytonidae have the most complete facial ruff and disk producing a heart-shaped face with a masked appearance. In both Tytonidae and Strigidae the morphology of the external ear and the various forms of ear asymmetry, have been used as a taxonomical character (Kaup 1862; Collett 1881; Pycraft 1898, 1903; Norberg, 1977) and includes the size and shape of the ear canal, the pre and post-aural skin folds and ruff feathers.

The mechanisms of sound localization in owls have been studied most extensively in the barn owl (*Tyto alba*), particularly at the behavioural and neural levels (for reviews see Knudsen 1980, 1981; Konishi 1983). The barn owl will accurately strike prey (mice) and targets in total darkness by the use of acoustic cues alone and the precision of sound localization for such tasks occurs within 5° of error in azimuth and elevation (Payne and Drury 1958; Payne 1971; Konishi 1973a,b). The accuracy of head orientation towards acoustic targets in the dark is within 2° in both dimensions (Knudsen *et al.* 1979; Knudsen and Konishi 1979). The current theories of sound localization in the barn owl assume that the ear acts as a pressure receiver (Payne 1971; Knudsen and Konishi 1979; Knudsen 1980). On this basis sound localization is thought to involve interaural intensity and time (phase) cues which are

analyzed entirely by the central auditory pathway. This view is consistent with existing theories for mammals whose ears are pressure receivers (Erulkar 1972; Gourevitch 1980; see also CHAPTER 2 and 4). In the barn owl, it has been concluded that the perception of sound elevation is determined by binaural intensity cues and that sound azimuth is determined by binaural time cues (Knudsen 1980; Konishi 1983). The facial ruff is seen as contributing to interaural intensity differences and this cue is reduced following ruff removal. Consequently ruff removal decreases the ability to localize sound in elevation, whilst azimuthal localization is largely unaffected (Konishi 1973a; Knudsen and Konishi 1979). In contrast, the barn owl will re-orient it's head in azimuth by manipulation of interaural time delays through earphones (Moiseff and Konishi 1981b). At the neural level, the receptive fields of auditory neurones in the space-mapped region of the midbrain (Knudsen and Konishi 1978a,b) are sensitive to interaural time and intensity differences (Moiseff and Konishi 1981a). The neural mechanisms responsible for this sensitivity are believed to be generated in the auditory nuclei of the brainstem (Moiseff and Konishi 1983; Sullivan and Konishi 1984; Takahashi *et al.* 1984).

The problems of understanding the mechanisms of directional hearing in owls as well as birds in general, have been recognized for a long time and arise because of the traditional view that the avian ear is a pressure receiver (Schwartzkopff 1950, 1952, 1962). Hearing in birds is restricted to frequencies usually well below 10kHz and such wavelengths are poorly diffracted by the head, yielding small interaural intensity differences. The relatively small size of a bird head also reduces interaural time disparities to values well below 100 μsec. Nevertheless, the barn owl for example, can make an accurate judgement

of sound location based on binaural time disparities as small as 4 μsec (Knudsen 1980). The degree of phase-locking by neurones of the nucleus magnocellularis in the barn owl (Sullivan and Konishi 1984) shows an extended high frequency range compared with previous reports in birds and mammals (Johnson 1974; Woolf and Sachs 1977; Sachs *et al.* 1980) and reinforce the idea that the barn owl's auditory system can process interaural time cues by a neural temporal code.

Despite the current views on sound localization in the barn owl, an alternative directional mechanism is possible because directionally sensitive hearing can be produced by the pressure gradient principle. Such a mechanism was first proposed for insect ears (Pumphrey 1940, Autrum 1942) for which experimental evidence is available in several species (for reviews see Michelsen and Nocke 1974; Michelsen 1979, 1983). The operation of pressure gradients for directional hearing is known to occur in non-mammalian terrestrial vertebrates such as frogs (Chung *et al.* 1978; Pettigrew *et al.* 1978) and birds (Coles *et al.* 1980; Hill *et al* 1980; Lewis and Coles 1980). The pressure gradient (or pressure difference) depends on the simultaneous action of sound waves incident to both sides of a membrane and this principle has been used for many years in the design of directional microphones (Olson 1947). When the sound pressures are closely matched on either side of a membrane the net driving force or pressure will depend on the relative phase of the waves. Since the phase difference depends on the relative length of the sound paths to each side of the membrane, the acoustical interaction can be highly sensitive to direction. In biological systems an asymmetrical pressure gradient receiver often occurs when two tympana are acoustically coupled by an air-filled cavity or tube so that there is a directionally dependent phase shift between the external and

internal pressures at each tympanum (Fletcher and Thwaites 1979; Michelsen 1979). In birds pneumatization of the skull forms an interaural canal which directly connects the two middle ear cavities (Wada 1923) and of crucial interest to directional hearing in owls is the fact that their interaural canals are the largest and most patent of all birds (Tiedemann 1810; Stellbogen 1930; Stresemann 1934; Payne 1971; Norberg 1978). Therefore it is reasonable to expect the owl ear to behave as a pressure gradient receiver despite negative findings so far (Schwartzkopff 1962; Payne 1971; Moiseff and Konishi 1981b).

This chapter examines the acoustical and directional properties of the external ear of the barn owl (*Tyto alba*) by measuring sound pressure in the ear canal. This approach provides a valuable comparison between the acoustical properties of the highly specialized external ear of *T. alba* with the pinna systems of bats (CHAPTER 2) and Macropods (CHAPTER 4). In addition the directional sensitivity of the ear is studied by recording cochlear microphonic CM potentials in order to determine the role of pressure and/or pressure gradients in the directional hearing of the barn owl.

MATERIALS AND METHODS

Subjects and preparation

A total of 6 adult barn owls (*Tyto alba*) were used for recordings of the cochlear microphonic (CM) potentials and biophysical measurements of sound pressure using probe microphones. The owls (average body weight = 375g) were initially anaesthetized with a combination of Ketamine (20mg/kg) and Rompun (2.5 mg/kg) and maintained under anaesthesia by supplementary injections of the same drugs. The head was held in position by a small metal foot attached to the dorsal skull by

dental acrylic cement and connected to an adjustable, locking ball joint. Fine insulated silver wires were implanted bilaterally onto the surface of the round window membrane. An indifferent electrode was attached to the dorsal neck musculature. Access to the round window of the cochlea was gained by boring a small hole in the ventro-medial skull, medial to the tympanic ring. After visually positioning the silver wire electrode by inserting it through the hole in the skull, the hole was then resealed with dental cement. Physiological recordings were terminated by sacrificing the animal by a drug overdose. Subsequently, without altering the head position, small probe microphones (1/4" Bruel and Kjaer Type 4138) were implanted into the side of each ear canal close to the outside surface of the tympanic membrane.

Stimuli and recordings

Each owl was placed in the centre of an anechoic room (as described in CHAPTERS 2, 3 and 4) and supported by a platform. For the biophysical measurements of sound pressure, pure tone stimuli were generated by an oscillator (Hewlett-Packard Model 3300A) and connected to an amplifier (Pioneer BP-320) via an attenuator (Hatfield Type 2125). The amplified signal was connected to a loudspeaker (Motorola piezohorn KSN 1025A for frequencies 1.5 - 16kHz or a Clarion electrodynamic speaker for frequencies 0.5-2.0kHz). One of these transducers was mounted on a trolley attached to a vertical semi-circular aluminium arc (diameter 94cm). This arc was pivoted at the floor and ceiling of the anechoic room and was rotated by a remotely controlled motor attached to the base. The trolley carrying the loudspeaker was pulled along the arc by a second motor. Using this system the sound source was able to be positioned with an accuracy of ± 0.5° in azimuth and elevation.

Electrical recordings of CM potentials from the implanted round window electrodes were amplified (Tektronix FM 122 pre-amplifier) and displayed on an oscilloscope screen. The root-mean-square (RMS) voltages of undistorted CM waveforms were determined by a narrowband (6Hz) wave analyzer (Marconi Model XT). The wave analyzer also provided a signal source for pure tone stimuli in the same frequency range as for the biophysical measurements. CM amplitude was converted to changes in sensitivity to sound pressure (dB). This calibration procedure was performed at the sound direction of maximum CM amplitude (for each test frequency) and then measuring the changes in CM amplitude as a function of the sound pressure level (SPL). The output voltage from the probe microphones in each ear canal was measured directly as absolute sound pressure (RMS) re. 20 μPa by a measuring amplifier (Bruel and Kjaer Type 2510; linear 2Hz-200kHz) via a Krohn-Hite filter (Model 3220; high pass 100Hz).

To study directionality CM and probe microphone pressure measurements were plotted on a zenithal projection of the frontal hemisphere (see Fig. 5.5). This projection is the same as used in CHAPTERS 2 and 4 and is approximately equal area (distortion of solid angle less than 5%) for spatial locations greater than about 30° from the poles. Data were collected in the form of "iso-intensity" contours by connecting points of equal sound pressure or CM amplitude (dB) relative to the maximum value for a given frequency. Measurements of acoustic pressure gain in the ear canal were obtained by the difference between probe microphone sound pressures and the free field. The free field sound pressure was established without the animal by placing a reference microphone (¼" Bruel and Kjaer Type 4138) at the position normally occupied by the centre of the owl's head and facing the

loudspeaker (0° azimuth; 0° elevation).

RESULTS

Structure of the external ear and skull

The structure of the external ear in the barn owl has been described in detail by several authors (Kaup 1862; Pycraft 1898; Freye 1953; Payne 1971; Konishi 1973a; Knudsen 1980). Superficially the barn owl head appears as two flat facial discs which meet over the beak at an angle of about 50° to the midline (Figs. 5.1, 5.3). When the feathers of the facial disk are removed several rows of special densely packed feathers which form the facial ruff are revealed (Fig. 5.1C and see Payne 1971). The outer tips of these feathers form the heart shape of the owl's head and the open face of the ruff has a maximum height and width of about 7 cm and 4.5 cm respectively (Table 5.1). Inside the open face of the ruff a cavity is formed by the side of the head and the curvature of the ruff feathers. Within this outer ear cavity (as defined by Norberg 1977) are two asymmetrically placed opercula or pre-aural ear flaps at the temporal side of each eye. When viewed along the visual axis, the ear flaps obscure the ear openings which are on the side of the head between the ear flaps and the base of the ruff feathers (Figs. 5.1C, 5.2, 5.3; Payne 1971; Konishi 1973a; Knudsen 1980). The left and right ear flaps and the ear openings are the same size and shape (Payne 1971; Norberg 1977) however these structures are bilaterally asymmetrical because they are equally offset from the horizontal plane (Fig. 5.1C. 5.2). The left ear opening is about 0.7cm higher than the right and both openings lie on an interaural plane inclined about 12° to the horizontal (Fig. 5.2B). In the sagittal plane the ruff has a curved appearance (Fig. 5.1A) and the ear flaps are

mutually inclined by about 27° (Fig. 5.2A). A detailed pterylological and photographic examination of the owl head reveals that both facial ruffs are symmetrical, as far as can be determined, and therefore ear asymmetry in this species is due to the positioning of the ear openings and flaps only. The ear canals have a slightly different orientation due to the position of the openings, but they both have a length of about 0.8cm. The tympanic membranes are not normal terminations at the end of each ear canal but have complete bilateral symmetry as in all owl species with ear asymmetry (Norberg 1977).

The skull of the barn owl is symmetrical (Payne 1971; Norberg 1977) and the left and right middle ear cavities are connected by an open passageway in the ventral skull. This interaural cavity or canal is formed by a bilateral connection between a bony canal and a third air chamber called the sphenoid sinus, located in the basisphenoid bone (see Payne 1971; Fig. 5.3). The shortest sound path between the tympanic membranes through this internal connection is about 2.2cm in length (Fig. 5.3).

Pressure gain in the ear canal

Intact System

The maximum sound pressure measured in each ear canal was compared to the free sound field in order to estimate the acoustic gain of the external ear. Above 2.5kHz the spatial location of the peak sound pressure in each ear canal was defined as the *acoustic axis* (see CHAPTER 2 and 4 and below) and the speaker was maintained on-axis at each test frequency. The results in Fig. 5.4B show that in the intact external ear there is no pressure amplification below about 1kHz i.e. the sound pressure in the ear canal equals that of the free field. Above 1kHz there is a progressive increase in pressure amplification which reaches

about 20dB at 3kHz. Above 3kHz the level of amplification plateaus at about 20dB up to 9kHz whereupon the gain decreases sharply to about 6dB at frequencies of 12-15kHz. As the high frequency hearing limit for the barn owl is close to 12kHz (Konishi 1973a) data collection was limited to 16kHz.

Effect of facial ruff removal

The design of the facial ruff in the barn owl suggests that it should have significant sound diffraction properties. The ruff encircles the ear opening, analogous to the concha and flange of the mammalian pinna (Konishi 1973a; Norberg 1977; Knudsen 1980), and ruff removal has been shown to decrease the accuracy of sound localization and sensitivity to sound (Konishi 1973a; Knudsen and Konishi 1979).

After collecting the normal gain curves as seen in Fig. 5.4B, the entire facial ruff and lore feathers were cut off, reducing the owls head to a hawk-like appearance (Fig. 5.2B). A typical example of the acoustical effect of ruff removal is shown in Fig. 5.4B. There is an overall decrease in sound pressure compared to normal for frequencies below 10kHz. With the ruff removed the resulting pressure gain curve in the ear canal shows two peaks with the lower peak of 8dB around 3kHz and the higher peak of 12dB near 10kHz and a central bandwidth from 4-8kHz has residual gain of less than 7dB. The two peaks in gain at 3 and 10kHz seen in Fig. 5.4B are unlikely to be harmonics of a meatus resonance (compare Figs. 2.2, 4.4, 4.13) since the ear canal itself is about 0.8cm in length and the fundamental mode of closed-tube resonance is too high (11kHz) to account for the result. If the pressure peaks are in fact harmonics, then the path length for quarter wave resonance will be about 2.7cm, which would involve the interaural cavity.

Effect of the pre-aural ear flap

The effect of ear flap removal altered the sound pressure in the ear canal by a maximum of only 4dB in the frequency range 2-14kHz and the effects were not systematic (Fig. 5.4A). Since the pre-aural skin folds in owls are under muscular control (Stellbogen 1930; Schwartzkopff 1962; Payne 1971; Norberg 1978), the earflaps of the barn owl were moved manually to see if there was any effect on the sound pressure in the ear canal. Pushing the flap as far forward as possible or back towards the ruff changed the sound pressure in the ear canal by only 3dB for frequencies up to 10kHz.

Acoustic gain of the outer ear cavity and ruff

The presence of the facial ruff was shown to have a major influence on the sound pressure in the ear canal and the effective gain of the ruff can be estimated by the difference curve between the intact and ruff-removed gain as shown in Fig. 5.4B. The results of such calculations are shown in Fig. 5.4C as an average gain curve from four ears and the amplifying effect of the ruff gradually increases from 4dB to 13dB as frequency increases from 1.5-8kHz. Above 8kHz the pressure gain contributed by the ruff decreases rapidly to 0dB near 12kHz.

The gain curve shown in Fig. 5.4C can be modelled acoustically by treating the outer ear cavity of the barn owl as a simple horn. Although the outer ear cavity is essentially formed by the ruff, the inside surface of the cavity clearly involves most of the side of the face and some of the lore feathers (Figs. 5.1 and 5.3). In Fig. 5.4C the expected excess pressure at the throat of a finite paraboloidal, conical and exponential horn have been plotted in comparison to the experimental data. These expected curves are based on the physical dimensions of the outer ear cavity (see Table 5.1; Figs. 5.1,5.3). The

exact equations for each finite horn and the methods for calculating the throat pressure are given in APPENDIX 1. The mouth of the horn is formed by the open face of the ruff and has an average radius of 3cm. The throat of the horn is taken as the entrance to the ear canal (ear opening) which has an average radius of 0.4cm. The outer ear cavity is not symmetrical, particularly in horizontal cross-section and the longest sound path to the ear opening (7cm) begins slightly below the beak at the anterior edge of the ruff (Fig 5.1C). The shortest path (1.8cm) occurs at a position close to the ear opening at the tips of the ruff feathers immediately lateral to the ear flaps (Figs. 5.1C, 5.3A,B). Therefore the length of the horn has been estimated as the average distance from the throat to the longest and shortest sides of the cavity (4.4cm).

In Fig. 5.4C the average gain curve of the outer ear cavity is probably closest to that predicted by an equivalent conical horn up to 8kHz, given that the expected curve contains resonance peaks which are not evident experimentally. The exponential horn curve significantly over estimates the gain, whereas the paraboloidal horn under estimates the gain above about 2.5kHz. Horn resonance is predicted because the dimensions of the outer ear cavity are comparable to or less than the relevant sound wavelengths and therefore the cavity must be considered finite in length. Nevertheless, the experimental curve is remarkably close to the expected curve for a conical horn if the expected pressure gain is interpolated without the resonance. The lack of resonance peaks in the experimental data is probably due to the extreme oblique truncation of the outer ear cavity (Fig. 5.3) which considerably reduces the reflection co-efficient of the open mouth (Fletcher pers. comm.). At very high frequencies it is to be expected that the excess pressure

at the ear opening or throat of the outer ear cavity should reach a maximum value (G_∞) of 18dB (APPENDIX 1; Table 5.1). However it is clear from Fig 5.4C that such a plateau is never reached experimentally, particularly if compared to the conical horn curve, and a maximum pressure gain of only 13dB is seen between 5-8kHz. This value probably results from the horn-like properties of the outer ear cavity but for higher frequencies the conical model does not explain the data. Here the rapid loss in amplification may result from sound reflection away from the ear canal opening due to the concave walls of the ruff (Fig. 5.3 and see DISCUSSION this chapter). In order to test this possibility, measurements of sound pressure were also obtained in one specimen by placing an 1/8" Bruel and Kjaer (Type 4148) microphone within the outer ear cavity between the rear of the ear flap and the inside surface of the ruff (Fig. 5.3). The results in Fig. 5.4D show that the amplification of sound pressure follows a similar trend to the ear canal measurements for the intact cavity (compare with Fig. 5.4B) but gain in the cavity remains above 15dB up to 16kHz, unlike the large losses experienced in the ear canal above 9kHz. This result suggests that sound is reflected away from the ear canal opening. Sound pressure amplification measured near the ear opening after the ruff removal rises gradual to about 16dB at 16kHz (Fig. 5.4D) but without the peaks seen for the ear canal under the same conditions (Fig. 5.4B). For the most part, the pressure difference curve between the intact and ruff removed condition measured outside the ear opening (Fig. 5.4D) confirms the pressure gain of the outer ear cavity measured in the ear canal (Fig. 5.4C). However, above 10kHz a slightly higher pressure gain is detected in this part of the cavity compared with the ear canal.

Ear canal directionality

Directivity patterns

The directional sensitivity of sound pressure in the ear canal becomes significant above 2.5kHz whereupon the directivity patterns are characterised by a main lobe of high pressure located in the frontal hemisphere. The region of peak pressure is defined as the acoustic axis, consistent with the definition in CHAPTERS 2 and 4 and other studies in mammals (Middlebrooks and Pettigrew 1981; Phillips *et al.* 1982). A typical series of directivity patterns for the left and right ear canals are shown in Fig. 5.5 for frequencies between 3-9kHz and were obtained by plotting speaker locations of equal pressure. The data points are represented as "iso-intensity" contours on a two dimensional projection of the owl's frontal hemisphere (see MATERIALS AND METHODS). The contour lines represent the progressive decrease in sound pressure (dB) relative to the maximum on-axis pressure. The directivity patterns closely resemble those illustrated by Payne (1971) for the barn owl at similar frequencies. The axis of the main lobe which defines the direction of the acoustic axis, is surrounded by a series of concentric ellipses or ovals of decreasing sound pressure. An increase in frequency produces a more directional main lobe as judged by the closeness of the contour lines indicating an increased spatial gradient (dB/degree). The iso-intensity contour lines also become elongated in the horizontal plane at high frequencies, particularly on the leading edge of the pattern i.e. towards the midline. In addition, above 5kHz the main lobe is bordered by troughs of low pressure which cause secondary lobes in the directivity patterns. The regions of low pressure contain extreme minima or approximate nulls which form crescent shapes around the main lobe. The development of directionality can be

quantified by measuring the maximum difference in sound pressure for directivity patterns as a function of frequency as shown in Fig. 5.6A. The results show that directionality in the ear canal becomes appreciable above 3kHz and highly directional above 6kHz due to high pressure amplification and nulls in the directivity patterns.

Vertical asymmetry

With the midline of the head aligned in the vertical plane, there is a vertical disparity between the directivity patterns for the left and right ear canals (Fig. 5.5). The average separation between the acoustic axes is 27° in elevation and relatively independent of frequency (Fig. 5.9C; for azimuth effects see below). The right ear acoustic axis is higher than the left and the *acoustic horizon* can be defined as the plane where the acoustic axes are equally offset from the horizontal plane i.e. ± 13.5° for the right and left ear respectively. In fact, the directivity patterns for pressure in each ear canal are inverted forms and can be super-imposed on one another by 180° rotation.

Directivity of the main lobe

Both the increase in directionality as a function frequency (Figs. 5.5, 5.6A) and the generation of nulls seen in ear canal measurements (Fig.5.5) strongly suggest that the outer ear cavities are diffracting the incident sound waves. Fig. 5.7 shows the change in the full angular width or acceptance angle (2θ°) of the main lobe of ear canal directivity patterns measured -3dB from the on-axis pressure as a function of frequency. Acceptance angles were measured separately for azimuth (Fig. 5.7A) and elevation (Fig. 5.7B), and as frequency increases from 2-14kHz average values decrease from 130°-30° and 90°-28° respectively. The experimental data in Fig. 5.7 can be compared with diffraction theory by treating the open face of the outer ear cavity as,

for simplicity, a single circular aperture (see APPENDIX 2). The perimeter of the outer ear cavity of the barn owl is 19cm and for the most part it is delineated by the tips of the ruff feathers (see Fig. 5.1, 5.3, Table 5.1) and some of the lore feathers. The expected curve in Fig. 5.7 is based therefore on a circular aperture with an average radius of 3cm and is a good fit to the experimental data, particularly in azimuth for frequencies between 5-10kHz (Fig. 5.7A). At lower frequencies the pressure response in the ear canal is somewhat less directional than would be predicted, whereas above 10kHz it becomes slightly more directional. In elevation (Fig. 5.7B) the observed directionality is somewhat closer to that produced by a circular aperture of radius 3.5cm which corresponds to the height of the ruff considered as a diameter (see Fig. 5.1 and Table 5.1). Taken together the azimuthal and elevational components of the ear canal directionality combine to produce an elliptical main lobe (Fig. 5.5) which may result from the somewhat elliptical shape of the open face of the outer ear cavity (Fig. 5.1).

Nulls

Above 5kHz the regions of low pressure forming deep troughs or nulls were important features of well-defined ear canal directionality. The degree of directionality or sharpness of the main lobe was clearly influenced by the angle separating the acoustic axis and the null regions or "lows" as noted by Payne (1971). This relationship was quantified as a function of wavelength as shown in Fig. 5.8A,B. Since nulls do not completely encircle the main lobe (Fig. 5.5) the angular separation was estimated from the plane which included both the maximum and minimum sound pressure. The most extensive nulls were in the lateral quadrants relative to the acoustic

axis, whereas medially located nulls close to the horizontal plane were difficult to determine due to the progressive elongation of the main lobe in azimuth (Fig. 5.5). Nevertheless, the laterally placed nulls moved closer to the acoustic axis from about 90° to 32° as frequency was increased from 5-12kHz (Fig. 5.8A). The large angles between medial nulls and the acoustic axis are plotted in Fig. 5.8B and emphasize the relatively poor directionality which exists towards the front of the owl as a result of the asymmetry of the main lobe in azimuth.

Sound diffraction theory predicts that nulls will occur in the directivity patterns of a circular aperture as derived in APPENDIX 2. The expected curve for diffraction nulls is plotted in Fig. 5.8 for a circular aperture of radius 3.0cm which is the average radius of the open face of the outer ear cavity (as above Table 5.1). The observed semi-angles for laterally placed nulls (rearward, Fig. 5.8A) are close to expected values, given that the effective aperture may range between 3.0-3.5cm depending of the orientation of the null. The angles between the acoustic axis and the medial (frontal) null regions (Fig 5.8B) which exceed 70° for all frequencies are not explained by a simple diffraction model and may be due to the asymmetrical shape of the outer ear cavity.

Movement of the acoustic axis with frequency

Fig. 5.5 suggests that as frequency was increased there was a tendency for the acoustic axes to move towards the midline and away from the horizontal plane. These effects are summarized in Fig. 5.9A,B,C. In elevation, the acoustic axes for both ears are within ± 6° of the horizontal plane below 4kHz. As the directivity patterns become more directional the vertical disparity between the acoustic axes increases to 27° and remains relatively independent of frequency (Fig. 5.9C). This vertical disparity appears to result from the anatomical asymmetry

of the ear openings. The ear flaps are symmetrically placed over the entrance to each ear canal and the angle of inclination between the surfaces of the ear flaps is 27° (Fig.5.2A) which equals the vertical disparity between the acoustic axes. Therefore the acoustic horizon bisects the two planes which are perpendicular to the surface of each ear flap (Fig. 5.2A). Based on this anatomical asymmetry, it follows that the acoustic axis will be below the horizontal plane for the left ear and above this plane for the right ear, despite the fact that the left ear opening appears higher than the right (Fig. 5.1C, 5.2B). In azimuth, the acoustic axes for both ears move symmetrically towards the midline starting from about 50° ipsilateral at 2kHz (Fig. 5.9B). The rate of movement is about 20°/octave up to 10kHz but for higher frequencies the axis remains within 5° ipsilateral to the midline.

In treating the outer ear cavity as a conical horn it is assumed for simplicity that the geometrical and acoustical axes are co-incident. However, it is clear from the structure of the outer ear cavity that it is highly asymmetrical in horizontal cross-section due to the unequal length of the lateral side wall formed by the ruff and the side of the face (Fig. 5.3). It seems likely that movement of the acoustic axis in azimuth results from the asymmetry of the outer ear cavity and in fact the outer ear cavity resembles an obliquely truncated cone. A simple acoustical model can be developed to understand the frequency dependence of the acoustic axis. This model is based on the geometry of the outer ear cavity (Fig. 5.3C) and treated in a similar fashion to the pinnae of *M. gigas* and *N. gouldi* (CHAPTER 2; APPENDIX 3). The expected values for acoustic axis positions are plotted in Fig. 5.9B and by comparison with the experimental values for axis position the two curves are in good agreement. The predicted rate of movement

for the acoustic axis in azimuth is 20°/octave as observed, but the position is overestimated by 5°. Such an error is not surprising since the calculations are based on the largest useful mouth (see APPENDIX 3). In reality the axis may be closer to the true cone axis which is difficult to estimate from the irregular structure of the outer ear cavity. Theoretically the most lateral acoustic axis would occur at 40° from the midline at 3.4kHz, which indicates that the acoustic axis at this frequency is approximately normal to the plane of opening of the facial ruff (see Fig. 5.3). Furthermore, the acoustic axis would cross the midline at 22kHz but this frequency is inaudible to the barn owl (Konishi 1973a). Clearly movement of the acoustic axis suggests that the radius of the mouth of the outer ear cavity, at least in azimuth, varies as a function of frequency. Consequently, the estimate of mouth radius as used for predicting acoustic gain and directionality is for simplicity, an average value, but it is nevertheless useful in describing the acoustical properties of the outer ear cavity (and the pinnae of *M. gigas* and *N. gouldi*, CHAPTER 2).

Effect of facial ruff and ear flap removal

Removal of the facial ruff was found to substantially reduce ear canal directionality and also reduce the vertical asymmetry between the two ears. Fig 5.10 shows that normal directivity patterns (compare Fig. 5.5) are severely disrupted following ruff removal and an acoustic axis was difficult to define. There was considerable expansion and irregularity of the iso-intensity contours resulting in only a 10dB change in sound pressure over the entire frontal hemisphere even at high frequencies. In addition, the normal diffraction nulls disappeared

following ruff removal and were replaced by a very low spatial gradient.

Removal of an ear flap, or moving it forwards or backwards produced no gross changes in directionality. In Fig. 5.11 it can be seen that ear flap removal does not significantly alter the position of the acoustic axis or diffraction nulls. There is a marginal loss in directionality for the main lobe (slight expansion of contours) but this is probably within the error of measurement. It is possible that the ear flap may play an acoustic role in influencing directionality for high frequencies such as 13kHz as reported by Payne (1971) but such frequencies are not audible to the barn owl (Konishi 1973a).

CM directionality

Directivity patterns

CM amplitudes were expressed as sensitivity changes (dB) relative to the maximum amplitude and were plotted as a function of sound direction in a similar fashion to the measurement of sound pressure in the ear canal (Fig. 5.5). It was found that CM directionality became appreciable above 3kHz (Fig. 5.6B) and for higher frequencies a region of maximum amplitude was evident. This region is defined as the CM axis and as for the acoustic axis, forms a main lobe which can be depicted as a series of iso-intensity (amplitude) contours (Fig. 5.12). Below 5kHz the CM directivity patterns are very similar to pressure measurements in the ear canal appearing as concentric elliptical-type contours (Fig. 5.12). The frequency development of CM directionality is summarized in Fig. 5.6B and is similar to the ear canal except that maximum directionality (dB_{max}) is limited by the dynamic range of the CM which does not exceed 35dB. Unlike the ear canal, CM directionality was

abruptly lost above 9kHz (Fig. 5.6B).

Above 5.5kHz CM directivity patterns are distinct from ear canal directionality (Fig. 5.5, 5.12) and typically the CM main lobe elongates into a plane of very low directionality (CM axial plane). Individual CM directivity patterns appear as diagonal or tilted bands of relatively high amplitude extending up to 90° from the axis (Fig. 5.12). In the frequency range 6-10Hz the CM axial planes are orientated about 45° to the vertical for the left ear and 75° to the vertical for the right ear and approximately symmetrical about the interaural midline (Fig. 5.13). The bands of high CM amplitude were bordered on either side by extensive null regions running parallel to the axis and followed by secondary lobes at greater angles from the central maxima. Such a "polarization" of the main lobe produces a plane with very low directivity (CM axial plane) and a CM directional plane with very high directivity which are approximately perpendicular to each other (Fig. 5.12).

Directivity of the main lobe

The acceptance angle ($2\hat{\theta}$) of the CM main lobe was measured at -3dB below the amplitude at the CM axis for both the axial and directional planes. The results for the CM axial plane are shown in Fig. 5.7C and the acceptance angle tends to decrease from over 180° to about 50° as frequency increases from 2 to 6kHz. This trend is similar to that seen for the ear canal measurements (Fig. 5.7A,B). However above 6kHz the CM acceptance angles start to increase rapidly as the CM loses directionality in this plane. In the directional plane (Fig. 5.7D) acceptance angles above 5kHz suggest that the CM is up to 20° more directional than the ear canal (Fig. 5.7A,B), and CM acceptance angles as low as 18° occur up to 9kHz.

Nulls

The regions of extremely low CM amplitude which occurred close to the CM axis contributed substantially to the directional plane and their angular separation from the CM axis is summarized in Fig. 5.8C. Deep troughs or approximate nulls occurred between 6-9kHz only and were generally within 15-30° of the CM axis. CM nulls were therefore about 25° closer to the CM axis compared to the acoustic axis, except below 6kHz (Fig 5.8A,C). These results indicate a much sharper main lobe for CM directionality compared with the ear canal over a more restricted band width.

Movement of the acoustic axis with frequency

In Fig. 5.12 it can be seen that the CM directivity patterns for both ears tended to move towards the midline and upwards as a function of increasing frequency. These effects are summarized in Fig. 5.9D,E,F. In elevation both CM axes are located below the horizontal plane between 2-5kHz. The left ear CM axis is higher than the right by an average of 13° in this frequency range, with the left ear being about 7° below the horizon compared with 20° for the right ear (Fig.5.9F). Above 5kHz the left ear CM axis moves upwards crossing the horizon at 6-7kHz and is about 15° above it at 9-10kHz. The right ear CM axis also moves upwards but remains 5° below the horizon from 7-10kHz.

In azimuth both CM axes approach the midline symmetrically starting from about 60° ipsilateral at 2kHz (Fig. 5.9D,E). As frequency increases the CM axes migrate towards the midline at 37°/octave and this trend continues up to 10kHz, whereupon the CM abruptly loses directionality. Both CM axes cross the midline close to 7kHz and eventually reach 25-30° contralateral at 10kHz.

Pressure gradient effects

Within a restricted bandwidth from 5-10kHz the characteristics of CM directionality do not correspond to the diffraction model for the pressure response of the ear canal as would be expected for a pressure receiver (e.g. Fig. 5.5; Middlebrooks and Pettigrew 1981; Phillips *et al* 1982). Since the barn owl head is endowed with a well-developed interaural cavity (Fig. 5.3; Payne 1971), the efficient transmission of sound through this cavity should result in a pressure gradient at each tympanic membrane. Under such circumstances the effective pressure causing the tympanic membrane to vibrate is produced by the instantaneous difference between the interacting pressures. Thus the amplitude of the net pressure (P_{net}) at each tympanic membrane will be given by

$$P_{net} \sin (wt + \phi_1) = P_i \sin wt - P_e \sin (wt + \phi) \qquad (16)$$

where P_i and P_e represent the internal and external pressures respectively, w is the angular frequency, t is time, ϕ is the phase difference between the two pressures, and ϕ_1 is the resultant phase shift (see also Michelsen and Nocke 1974; Nocke 1975). The net sound pressure will be a maximum when the phase angle between the external and internal pressures at the tympanic membrane approaches 180°. Conversely the net sound pressure will be a minimum when the phase angle approaches zero. The phase angle results from the difference between the sound path length to each side of the tympanic membrane. In the barn owl this distance is a function of the angle of incidence and the length of the interaural pathway (Fig. 5.3). In the barn owl interaural time differences (disparities) for the external sound path to the tympanic

membranes have been measured as a function of azimuth (Moiseff and Konishi 1981a) and the internal sound path is about 2.2cm giving an interaural transmission time of 73 μsec (Fig. 5.3). If it is assumed that there are no amplitude losses or additional delays in transmission through the interaural cavity then, for sound travelling at a constant velocity, the maximum amplitude of vibration of the tympanic membrane will be determined by the sound direction which produces a phase shift of $n\pi$ between the interacting sound pressures. Clearly the interaural time disparity required to produce such a phase shift at each membrane will be a function of the stimulus wavelength in order to maintain a half wavelength path length difference. Since interaural time disparities in the ear canal are also a function of sound direction, the relationship described by Moiseff and Konishi (1981a) can be used to predict the azimuth position of the maximum amplitude of P_{net} as defined in Eqn (16). The results of such a calculation are plotted in Fig. 5.9EF and show that the expected azimuthal position of the maximum net pressure as a result of a pressure gradient moves from 80° ipsilateral to 8° contralateral as frequency increases from 2 to 10kHz. The average rate of movement of the expected maximum response is about 40°/octave and crosses the midline near 7kHz because the internal separation of the tympanic membranes is about a half wavelength at this frequency. The results compare favourably with the observed movement of the CM axes for both ears and contrast with the movement of the acoustic axis (Fig. 5.9B).

In a pressure gradient receiver, the angular separation between the maximum and minimum amplitudes of vibration of the tympanic membrane will occur for a relative change in the phase angle of $n\pi$. When equal amplitude pressures occur on both sides of the tympanic membrane the

minimum amplitude will be zero i.e. a null will result. Fig. 5.8C shows the expected angular separation between nulls and the maximum response amplitude as a function of frequency. The semi-angle decreases from 76° to 15° between 3-15kHz. In the frequency range 6-9kHz the observed position of nulls in the directional plane of the CM (Fig. 5.9C) are very similar to the expected null positions suggesting that they are generated by a pressure gradient at the tympanic membrane.

When two opposing sound waves interact at a membrane a 3dB decrease in the amplitude of the net sound pressure relative to the maximum pressure will occur when the phase difference across the membrane is $\frac{n\pi}{2}$ (i.e. a path length difference of n x one quarter of the wavelength) and thus the angle of incidence will vary as a function of wavelength. This expected -3dB acceptance angle (2θ°) for the pressure gradient response is plotted in Fig. 5.7D from 2-15kHz for the directional plane of the CM. The observed values are in good agreement with the expected acceptance angles, although they are slightly more directional by about 10° in the higher frequency range (7-10kHz). These results further support the idea that the directional plane of the main lobe of the CM can be explained in terms of the pressure gradient.

Ear blocking

In an attempt to disrupt the transmission of sound through the owl's interaural cavity, one ear canal was blocked with wet cotton wool, blue-tak or silicone rubber. Ipsilaterally, the effect of blocking decreased the maximum amplitude of the CM by 4-15 dB between 5-8 kHz, consistent with previous observations in the barn owl (Knudsen and Konishi 1980; Knudsen *et al.* 1984). A significant effect on CM directionality from the blocking of the contralateral ear was demonstrated only when silicone rubber was used to fill the entire ear

canal. The results of such a procedure are shown in Fig. 5.14 for CM directivity patterns at 6 and 8kHz. The main effect of blocking the contralateral ear canal was to alter some of the CM nulls into localized regions of high amplitude or to create new regions of low amplitude. Overall, the central high amplitude CM axial plane was relatively undisturbed but some broadening of the main lobe and a slight repositioning of the CM axis was noted.

DISCUSSION

The data presented in this chapter suggest that the directional properties of the barn owl ear result from the interaction of two independent physical mechanisms, namely sound diffraction and pressure gradients. Monaural directionality of the barn owl ear was measured by changes in the amplitude of the CM which is proportional to the net driving pressure on the tympanic membrane. Up to 5kHz CM directional sensitivity is similar to the pressure response in the ear canal which is determined by sound diffraction. However, between 5-9kHz, CM directivity patterns can be explained by pressure gradients at the tympanic membrane, implying that sound is effectively transmitted along the interaural cavity. If the interaural canal functions as an internal waveguide coupling the two tympanic membranes, then the acoustic behaviour of this system may approximate a doublet tube ear (Fletcher and Thwaites 1979).

The pressure gradient will control the directional response of the barn owl ear as long as there is a phase shift across the tympanic membrane, providing the pressures are closely matched. In a doublet tube ear the response will be directional in the interaural plane intersecting the openings, which would normally be the horizontal plane for symmetrical ears. In the barn owl however this plane is tilted by 12° to the horizon because the ear openings are asymmetrical (Figs. 5.1, 5.2). Consequently planes of equal interaural phase (or time) difference (parallel to the interaural midline) will be inclined to the midline of the head by a similar angle as in *Aegolius funereus* (Norberg 1968, 1978). In the present study as frequency increases, the axial planes of the main lobes of both left and right ear CM directivity patterns tend to rotate away from the interaural midline (Fig. 5.13) and the orientation of the axial planes remains approximately symmetrical about the interaural midline.

In addition to the dominant effect of the pressure gradient between 5-9kHz, ear directionality is also influenced by diffraction. Sound pressure is transformed by the horn-like external waveguide which couples the tympanic membrane to the sound field (see below). The type of outer ear cavity found in the barn owl is principally formed by the facial ruff and is unique to nocturnal owls, not being found in other avian families. Acoustically, the directionality and gain of the outer ear cavity is remarkably similar to the mammalian pinna (see CHAPTER 2 and 4 and GENERAL DISCUSSION AND CONCLUSIONS). Unlike many mammalian pinnae the outer ear cavities of the barn owl are fixed in relation to the head but there is considerable overlap between the major lobes of their directivity patterns in frontal space. Such a situation facilitates a pressure gradient at each tympanic membrane because the sound pressures at the two ports are closely matched (Fig. 5.5). A frontal zone of low interaural pressure difference is maintained by movement of the main lobes towards the midline as frequency increases (Fig. 5.9A,B) despite a highly directional pressure response in the ear canal above 5kHz (Fig. 5.6A). Part of the process to create a pressure gradient at the tympanic membrane also involves the relative loss of directionality in azimuth between the converging acoustic axes as indicated by the asymmetry of the main lobes (Fig. 5.5).

It is important to understand that the diffraction limited pressure response in the ear canal places a spatial limitation on the occurrence of a pressure gradient at the tympanic membranes. Instead of bands of equal CM amplitude completely encircling the head, which may be expected from a pure pressure gradient receiver, the CM iso-intensity contours are restricted in the axial plane (Fig. 5.12). Presumably this is because the pressures differ by more than 6dB or so on either side of the tympanic membrane due to diffraction effects, which effectively eliminate a pressure gradient irrespective of the phase shift (Michelsen

and Nocke 1974).

Diffraction of sound by the outer ear cavity is also likely to affect the orientation of the main lobes of the CM directivity patterns. This is because the equal pressure (intensity) difference contours in the ear canal rotate counter-clockwise with increasing frequency as a result of the bilateral asymmetry of the main lobes and their frequency dependent azimuthal position (Figs. 5.5, 5.9A,B,C; see also Knudsen and Konishi 1979; Knudsen 1980, 1981). Assuming that sound propagates efficently through the interaural canal it seems likely that the spatial distribution of interaural intensity differences up to about 6dB would significantly affect the pressure gradient and cause the CM axial planes to diverge from the orientation of the equal phase difference contours as seen in Fig. 5.13. However, direct acoustical measurements near each side of the tympanic membrane are needed to confirm this suggestion.

Sound Diffraction

Ear canal directionality was found to be closely related to sound diffraction by a single circular aperture and is determined by the average radius of the open face of the ruff. In comparison to physical systems (Beranek 1954), the outer ear cavity generates a directional response above 2kHz because the wavelength becomes less than the circumference of the opening ($ka > 1$) and the pressure response in the ear canal becomes highly directional above 5kHz ($ka > 3$; see Fig. 5.6A and GENERAL DISCUSSION AND CONCLUSIONS). It is misleading to regard the ruff as a parabolic reflector (Konishi 1973a; Knudsen and Konishi 1979; Knudsen 1980) since the acoustical properties of the outer ear cavity are principally determined by diffraction at the open face and the (conical) horn-like coupling to the tympanic membrane, at least for the

audible bandwidth (Konishi 1973a).

The movement of the acoustic axis in azimuth is probably related to the geometry of the outer ear cavity by virtue of the oblique truncation of the opening (see APPENDIX 3 and GENERAL DISCUSSION AND CONCLUSION). The elevated location of the acoustic axes in the barn owl are relatively independent of frequency but there is a vertical asymmetry as previously reported for *Tyto alba* (Payne 1971; Knudsen and Konishi 1978b), also in *Asio otus* (Schwartzkopff 1962) and *Aegolius funereus* (Norberg 1968, 1978). As determined in the present study the vertical disparity between the left and right acoustic axes is 27° and the azimuthal plane bisecting this angle conveniently defines the acoustic horizon. This plane probably corresponds to the visual horizon which was estimated from photographs of natural head orientation, but not confirmed opthalmoscopically by retinal landmarks (Pettigrew and Konishi 1976; Knudsen *et al.* 1977; Pettigrew 1979). Acoustic axis asymmetry is due to the physical displacement of the ear openings in the otherwise mirror-image symmetry of the facial ruffs. In contrast to the grossly asymmetrical cross-section in azimuth, the left and right facial ruffs are fairly symmetrical in the vertical plane and the ear openings are equally offset from the horizon (Fig. 5.1A, 5.2A). Both of the ear canals yield similar directivity patterns but in an inverted form, with the left ear axis being directed below the horizon despite the entrance to the left ear canal being anatomically higher than the right, and *vice versa* (Fig. 5.5).

Role of the pre-aural ear flaps

An acoustical role for the pre-aural ear flaps in the hearing of the barn owl is doubtful based on the present observations. Although the flaps are placed directly in front of the ear openings and their

surfaces are orientated normal to each acoustic axis in the vertical plane, movement of the flaps or even complete removal had a negligible effect on pressure gain or directionality as measured in the ear canal. It is possible that the ear could be sensitive to small changes in the pressure difference at the tympanic membrane caused by movement of the ear flap (only pressure effects were examined) but it is difficult to imagine any systematic effect on directionality which could be produced by voluntary control of position. Payne (1971) reported that movement of the ear flap had a significant effect on ear canal directionality but he only reported a test at 13kHz, a frequency which is not localized and probably inaudible to the barn owl (Konishi 1973a,b; Knudsen and Konishi 1979). Payne (1971) also observed that pushing forward the feather conches (ruff) at 5kHz altered the directivity pattern but this would be expected from distortion of the mouth of a horn. Amongst owls there is considerable variation in the design of pre-aural flaps. In *Phodilus badius* which is closely related to the barn owl, there is no pre-aural skin fold despite a prominent ruff (Pycraft 1903; Norberg 1977). Perhaps the ear flaps have a protective role, for example during flight near obstacles, combat with prey or reducing wind turbulence near the ear opening. Under natural conditions most of the movement of the ear flaps and the ruff occur between sleep and the alert or hunting postures (Payne 1971) but observations in *A. funereus* suggest that these structures are stationary during sound localization (Norberg 1970, 1978).

Previous studies of ear directionality in owls

Payne (1971) found that in the barn owl both CM and ear canal measurements produced the same directivity patterns implying that the ear acted as a pressure receiver. Likewise in *Asio otus* Schwartzkopff

(1962) concluded that both CM and auditory nerve (N_1) directionality were a result of sound diffraction by the head. In contrast, the data of Knudsen and Konishi (1978b) indicate that N_1 directionality has sharper peaks and nulls at 6kHz compared to the pressure measurements in the ear canal. Their data support the idea of a middle ear mechanism which enhances directionality since both CM (this chapter) and N_1 measurements are equivalent measures of 'monaural' directionality. It is important to note however that the asymmetrical patterns of ear canal and CM directivity for each ear in the barn owl make it essential to examine directionality in two dimensional space, rather than a single polar plot through the midline or horizontal plane alone as used by Knudsen and Konishi (1978b).

It is difficult to explain why previous studies on ear directionality in owls have not detected the effect of pressure gradients. Payne's (1971) CM directionality may have been adversely affected by cochlear non-linearities due to the use of intense sound stimuli. He reported that acoustical activation of the middle ear reflex caused serious problems in collecting CM data and may have reduced interaural sound transmission at critical sound directions thereby disrupting the pressure gradient. In birds, an acoustic middle ear reflex has been reported only in owls e.g. *Asio otus* (Golubeva 1972) and *Strix aluco* (Oekinghaus and Schwartzkopff 1983) but sensitivity to sound is modulated by only a few decibels. In the present study the effects of the middle ear reflex were detected as a slight decrease or increase in CM amplitude at high or low sound pressures respectively. In the present study the use of sound pressures below 70dB SPL and continuous tones (c.f. Payne 1971) allowed these effects to decay after several seconds and did not significantly alter the CM directivity

patterns. In Asio otus the averaging of individual directivity patterns between birds had the effect of reducing directional sensitivity particularly by smoothing out nulls (Schwartzkopff 1962; Payne 1971).

In the barn owl, dichotic stimulation has shown that above 3kHz sound pressure appears to be highly attenuated by the interaural cavity and prevents a pressure gradient at the membrane (Moiseff and Konishi 1981a). Such an observation conflicts with the present data as CM directionality between 5-9kHz appears to be dominated by the effect of pressure gradients at the tympanic membrane, resulting from the transmission of sound through the interaural cavity. These opposing views cannot be resolved until further measurements are made of the acoustical properties of the interaural canal. There may be a substantial difference in the acoustical transmission properties of the avian interaural cavity between unilateral closed field stimulation of the ear canal (Hill et al. 1980; Rosowski and Saunders 1980; Moiseff and Konishi 1981a) compared to the free field situation (Hill et al. 1980). In the quail, for example, sound pressures in the interaural canal are much higher using free field stimulation compared to unilateral sound stimulation (Hill et. al. 1980). In the case of the barn owl, the closed field technique of measuring interaural transmission (Moiseff and Konishi 1981a) could produce a pressure minimum at the contralateral tympanic membrane as a result of resonance by the internal head cavities. Under these circumstances the interaural canal may appear to attenuate sound pressure particularly at 7-8kHz (Moiseff and Konishi 1981a; Figs. 3 and 4) if a pressure node occurs at the open end of the tube-like cavity (approximately 22mm in length), due to half wavelength resonance (Beranek, 1954). However this suggestion remains speculative at present and further experiments are needed to test for the possibility of resonance in the interaural cavity, both under closed field and free field conditions.

Pressure gain by the external ear

Since the maximum amplification of pressure in the ear canal reached 20-25dB between 4-9kHz the acoustic gain may influence the absolute sensitivity of the owl's auditory system. This restricted bandwidth for high pressure gain of the signal closely matches the most sensitive region of hearing in the barn owl where behavioural and neural thresholds are as low as -20dB (Konishi 1973a) and -11dB SPL (Knudsen 1984) respectively. It is impossible to isolate the tympanic membrane and expose it directly to the incident sound field but the removal of a part of the external ear such as the facial ruff is known to reduce the barn owl's sensitivity to sound by at least 10-15dB (Konishi 1973a; Knudsen and Konishi 1979). Such an effect of ruff removal is consistent with the present data which show the gain of the ruff to be about 13dB in the range 6-8kHz (Fig. 5.4C). The feathers of the facial ruff are crucial to the formation of the outer ear cavity which acts as an acoustic transformer and the gain curve for the ruff is, to a first approximation, close to that of a simple conical horn up to about 8kHz. The outer ear cavity becomes a reasonably efficient sound collector above 6kHz as the gain is within 6dB of the expected high frequency of maximum 18dB (see Fig. 5.4C and Table 5.1) but rapidly loses efficiency above 8kHz. The high frequency loss of pressure in the ear canal most likely results from a significant reflection of sound waves away from the entrance to the ear canal opening. The ruff and outer ear cavity do not form a paraboloidal horn (see Fig. 5.4C) or reflector (c.f. Konishi 1973a; Knudsen 1980), at least not in the acoustical sense, but there may be sufficient reflection of sound away

from the throat at high frequencies in order to reduce throat pressure, due to its concave internal surfaces (see Figs. 5.1, 5.3). The sharp loss in pressure gain reaching the tympanic membrane above 9kHz may help to explain the steep high frequency roll-off in the audiogram (Konishi 1973a) but the actual upper limit of hearing is probably determined at the level of the auditory nerve.

The outer ear cavity did not show any clear resonance (Fig. 5.4C) which is expected for an ideal finite horn (see APPENDIX 1; GENERAL DISCUSSION AND CONCLUSION; Beranek, 1954). The lack of horn resonance may be due to the asymmetrical structure of outer ear cavity since the opening of the ruff is an oblique truncation in horizontal cross-section which will reduce the reflection co-efficient of the mouth (Fletcher, pers. comm.). Instead, a resonance involving the interaural cavity and ear canal is apparent (Fig.5.4B) and not the meatus *per se* as in mammals (see CHAPTERS 2 and 4; Wiener *et al.* 1966; Shaw 1974).

Further evidence which suggests an amplifying role for the outer ear cavity and ruff, comes from a comparison of the audiograms of nocturnal owls with those of other avian species (Van Dijk 1973; Dooling 1980; Knudsen 1980). Owls with specialized external ears have, on average, behavioural thresholds to sound which are 10dB more sensitive in the range 3-8kHz compared to owls with unspecialized external ears. The "average" diurnal bird audiogram has a maximum sensitivity of 10dB SPL compared with an average of -18dB SPL for nocturnal owls (Konishi 1973a; Van Dijk 1973).

Neural coding of auditory space and sound localization

The data presented in this chapter concern the peripheral mechanisms of directional hearing in the barn owl and the results can be used to speculate on the directional properties of the central auditory system where considerable data exist (for reviews see Knudsen 1980, 1981, 1983b; Konishi 1983).

The neural substrates for sound localization in the barn owl are spatial receptive fields which exist for certain populations of auditory neurons as found in the forebrain (Knudsen et al. 1977) and midbrain (Knudsen and Konishi 1978a,b,c; Moiseff and Konishi 1981b; Knudsen 1982; Takahashi et al. 1984; Knudsen 1984). The response properties of space-specific or space-mapped auditory neurons (limited field type) in the midbrain bear a close relationship to the frequency range and regions of frontal space which are accurately localized by the barn owl (Konishi 1973a,b; Knudsen et al. 1979; Knudsen and Konishi 1979). The current view of the mechanisms by which auditory space is encoded in the barn owl brain assumes a neural comparison of the directional cues with the ear considered as a pressure receiver i.e. interaural pressure (intensity) and time or phase. The results presented in this chapter suggest that some revision of this view is necessary. In the critical bandwidth between 5-9kHz, the ear of the barn owl appears to be directionally sensitive due to the pressure gradient and not simply due to the directional information via sound diffraction which would

be available to the tympanic membrane as a pressure receiver. If pressure gradients exist at the tympanic membrane in the free field, then the neural (and behavioural) data from dichotic sound stimulation experiments may need to be re-interpreted (Moiseff and Konishi 1981b, 1983; Takahashi et al. 1984; Sullivan and Konishi 1984). This is because the response properties of auditory neurons which are correlated with experimental variation of interaural intensity or time, as a result of sound stimuli generated in an artificial closed field, may also involve changes in the pressure gradient at the tympanic membrane. Clearly the acoustical properties of the interaural canal during closed field stimulation need to be carefully compared to its properties in the free field as suggested above (see also Hill et al. 1980). Indeed the narrow range of pressure and phase difference which are needed to establish a pressure gradient at a membrane (Michelsen and Nocke 1974) are closely matched to the "binaural" sensitivity of auditory neurons which respond to experimentally produced interaural intensity and time differences (Moiseff and Konishi 1981b, 1983; Takahashi et al. 1984). If sound waves are efficiently transmitted through the interaural cavity between 5-9kHz, then relatively small interaural differences in pressure (less than 10dB) and time (less than 40μsec) could acoustically alter the net pressure acting on each tympanic membrane and perhaps account for the observed neural sensitivity to these parameters. Possibly the need to process interaural time by phase-locked neural responses as a neural code for sound direction may be less important than has been suggested (Sullivan and Konishi

1979) since a comparable phase shift across the tympanic membrane of a pressure gradient ear produces considerable directional sensitivity.

It is known that the phase-locked discharges of neurones from the nucleus laminaris in the barn owl (Sullivan and Konishi 1984) extend to higher frequencies in comparison with other birds and mammals (Sachs et al. 1980). Even so, it is difficult to understand how such responses can provide an accurate temporal code for sound direction in the barn owl by the analysis of interaural time disparities. This is because the degree of phase-locking (or vector strength) is very low in the frequency band 4-9kHz (Sullivan and Konishi 1984) which is most accurately localized by the barn owl (Konishi 1973b; Knudsen and Konishi 1979). In addition, vector strength is intensity dependent (Sachs et al. 1980) and above 4kHz high sound pressures (80dB above threshold) are needed to generate a significant phase-locked response in the nucleus laminaris (Sullivan and Konishi 1984). Moreover the barn owl can easily locate "faint" sounds (Knudsen et al. 1979; Knudsen and Konishi 1979) and space-mapped neurons have well defined receptive fields at low intensities (Knudsen and Konishi 1978a,b,c; Knudsen 1982, 1984). Therefore the phase-locked component of a neural response is likely to be negligible at these levels, except for low frequencies (below 3kHz) which are not localized by the barn owl. In contrast, pigeons can localize frequencies as low as 125Hz (Jenkins and Masterton 1979) and phase-locked neural responses would be highly significant at this frequency (Coles and Aitkin 1979).

Ear blocking

A significant effect on CM directionality was produced by blocking the contralateral ear canal suggesting that sound is transmitted via the interaural canal. The blocking effects were not as dramatic as demonstrated in the quail where CM directionality can be eliminated by blocking the contralateral ear canal (Coles *et al.* 1980). In the barn owl, contralateral ear blocking did not produce CM directionality equivalent to a pressure response based on sound diffraction, as would be expected by eliminating the pressure gradient. No explanation can be given at present though perhaps the quality of the ear canal blocking may be an important factor in disrupting pressure gradients since alternative sound paths may exist (Michelsen and Nocke 1974). Previously in the barn owl, ear canal blocking experiments have been performed and the effect on neuronal spatial receptive fields depends on frequency, goodness of fit and type of material (Knudsen and Konishi 1980; Knudsen, Esterly & Knudsen 1984; Knudsen, Knudsen & Esterly 1984). In the study by Knudsen and Konishi (1980) spatial receptive fields tended to enlarge and were relocated in space compared to normal, but spatial coding was not completely disrupted. Similarly, the behavioural effect of ear occlusion tends to produce only moderate errors in localization particularly in elevation (Knudsen and Konishi 1979). Further blocking experiments are needed to clearly demonstrate the effect of interaural transmission on ear directionality in the barn owl.

Auditory space and frequency

Previously in the barn owl, the role of frequency has not been recognized as an important factor in the directional mechanism (Knudsen and Konishi 1978a,b) although both the neural coding of auditory space and accurate localization depend on a narrow band of frequencies (Konishi 1973b; Knudsen and Konishi 1979). As shown in the present study, ear directionality is clearly a function of frequency since it can be demonstrated that the spatial location of the major lobe of the CM directivity pattern is controlled by the wavelength. Movement of the CM axis, which represents the maximum net pressure at the membrane as generated by the pressure gradient (Fig. 5.9E), clearly contrasts with the movement of the acoustic axis (Fig. 5.9B). In azimuth, the region of space mapped by the CM axis corresponds closely to that seen neurally in the midbrain (Knudsen and Konishi 1978a,b). Taking into consideration crossed pathways from the ear to the midbrain, the azimuth limits for the best areas of space-mapped neurons range from 60° contralateral to 15° ipsilateral (Knudsen and Konishi 1978a,b) and exactly the same range is covered by the CM axis as frequency increases from 2-8.5kHz (Fig. 5.9DE). In both cases there is an equivalent, 'binaural' overlap of ±15° about the midline, which is seen at the forebrain level as well (Knudsen *et al.* 1977). Interestingly, the length of the interaural canal produces a CM axis for each ear which is very close to the midline and acoustic horizon near 7kHz which is the frequency best localized by the barn owl (Konishi 1973b; Knudsen and Konishi 1979).

page 129 follows

TABLE 5.1: DIMENSIONS AND PARAMETERS FOR VARIOUS EXTERNAL EARS IN VERTEBRATES

SPECIES	PINNA/OUTER EAR CAVITY (MOUTH)				DIRECTIONALITY		PINNA/OUTER EAR CAVITY (THROAT)		HORN LENGTH			MEATUS	TYMPANIC MEMBRANE	HORN PARAMETERS		
	circum-ference $2\pi a$ (cm)	av. radius a (cm)	height (cm)	width (cm)	onset ka=1.25 (kHz)	high ka = 3 (kHz)	circum-ference $2\pi a$ (cm)	av. radius a (cm)	Long (cm)	Short (cm)	Average (ℓ) (cm)	length (cm)	av. radius (cm)	G_∞ (dB)	cone angle	$\frac{2a}{\ell}$ (mouth)
Macroderma gigas[a]	10.7	1.7	5.6	2.2	4.0	9.6	4.0	0.4	4.3	0.6	2.4	1.1	0.14	13	29°	1.4
Nyctophilus gouldi[a]	5.3	0.85	2.8	1.2	8.1	18	1.1	0.2	2.2	0.4	1.3	0.25	0.14	13	27°	1.3
Macropus eugenii[a]	16	2.5	7.0	3.5	2.7	6.4	2.5	0.4	7.5	1.5	4.5	1.6	0.25	16	25°	1.1
Macropus giganteus[a]	24.5	3.9	8.2	3.0	1.76	4.2	6.9	1.1	9	2	5.5	3.2	0.27	11	27°	1.4
Tyto alba[a]	19	3.0	7.0	4.5	2.3	5.4	2.2	0.4	7.0	1.8	4.4	0.8	0.46	18	30°	1.4
Myotis l. lucifugus[b]	3.8	0.6	1.4	0.7	11.0	27										
Plecotus townsendii[b]	8.4	1.3	3.7	1.2	5.0	12										
Felis catus[c]	14.5	2.3	5.5	3.0	2.9	7.1	2.5	0.4	6.0	2.5	4.3	2				
Trichosurus vulpecula[c]	14.2	2.3	5.8	3.3	3.0	7.3			5.5	1.1	3.3					

a = present study, b = Grinnell & Grinnell 1965, c = personal observations

Fig. 5.1. General appearance of the head of the barn owl (*Tyto alba*).

A. Sagittal view of head showing curvature of facial ruff.

B. Frontal view of intact head.

C. Frontal view of head with feathers of the facial disk removed to reveal the outer ear cavity formed by the feathers of the facial ruff. Note the asymmetrical position of the ear flaps near each eye.

A

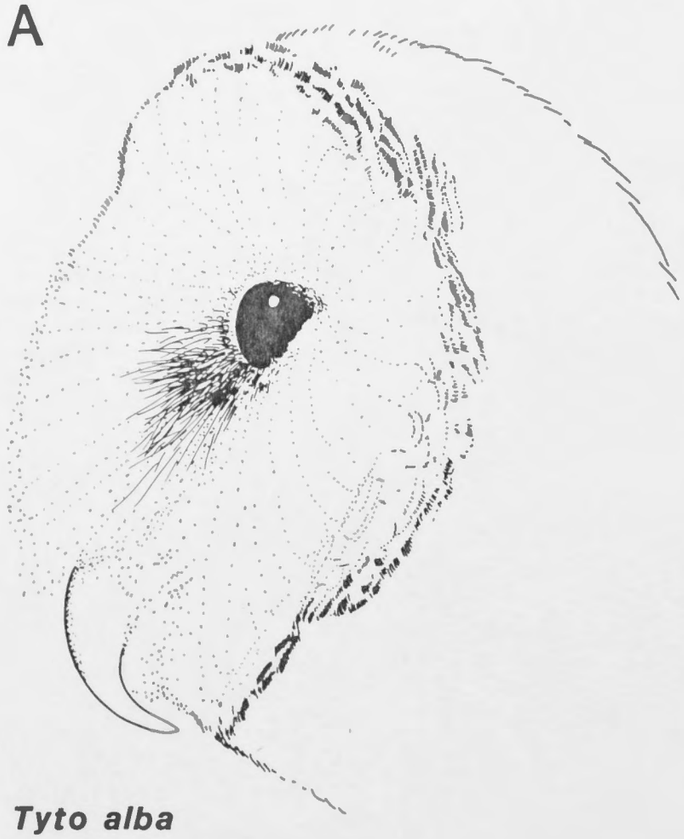

B

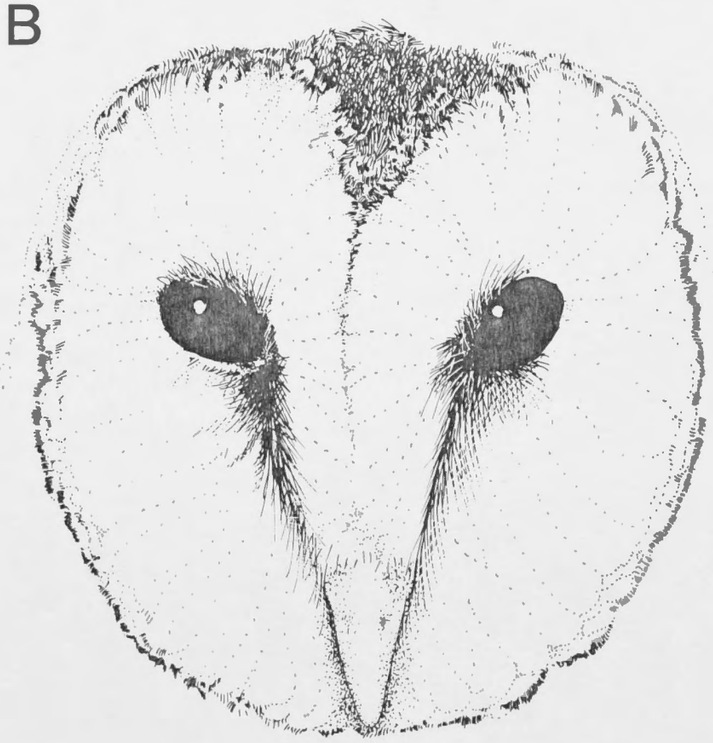

C

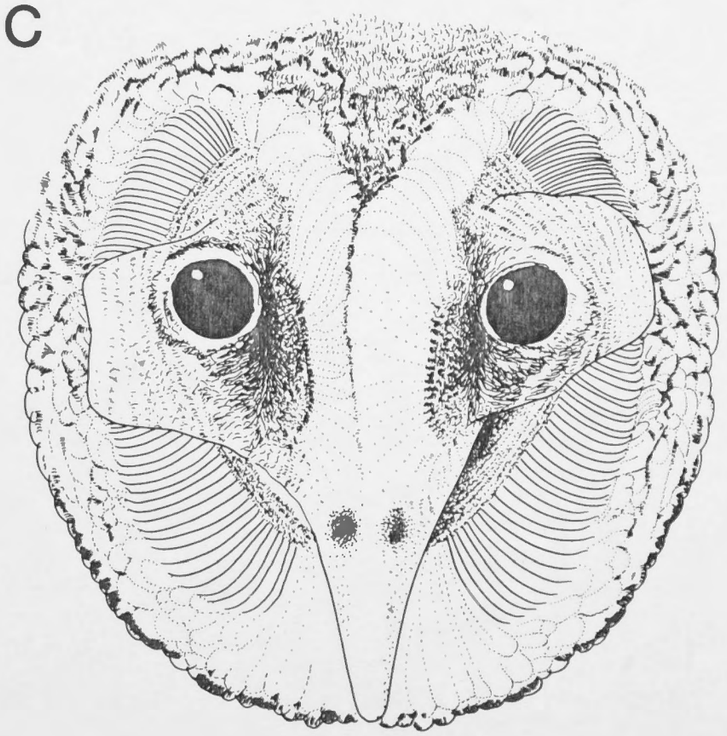

Tyto alba

Fig. 5.2. A. Schematic diagram of the left and right sides of the head of *Tyto alba* with the feathers of the head removed. The outline of the head shows the line of insertion of the facial ruff feathers (arrow). The angles of the left and right ear flaps are indicated by a straight line and are mutually inclined by 27°. The surface of each ear flap is normal to the acoustic axis of each ear. The right and left acoustic axes are + 13.5° from the acoustic horizon respectively (see text). Note that the ear canal openings are located behind each ear flap and equally offset from the horizon.

B. Frontal view of the head of *T. alba* (compare Fig. 1B,C) with all head feathers removed revealing asymmetrical ear flaps (ear openings indicated by dotted outline). The interaural axis is defined by the plane joining the two ear openings and is tilted by 12° to the horizontal plane of the head. Likewise the perpendicular plane to the interaural axis (interaural midline) is inclined by 12 to the vertical plane of the head (midline).

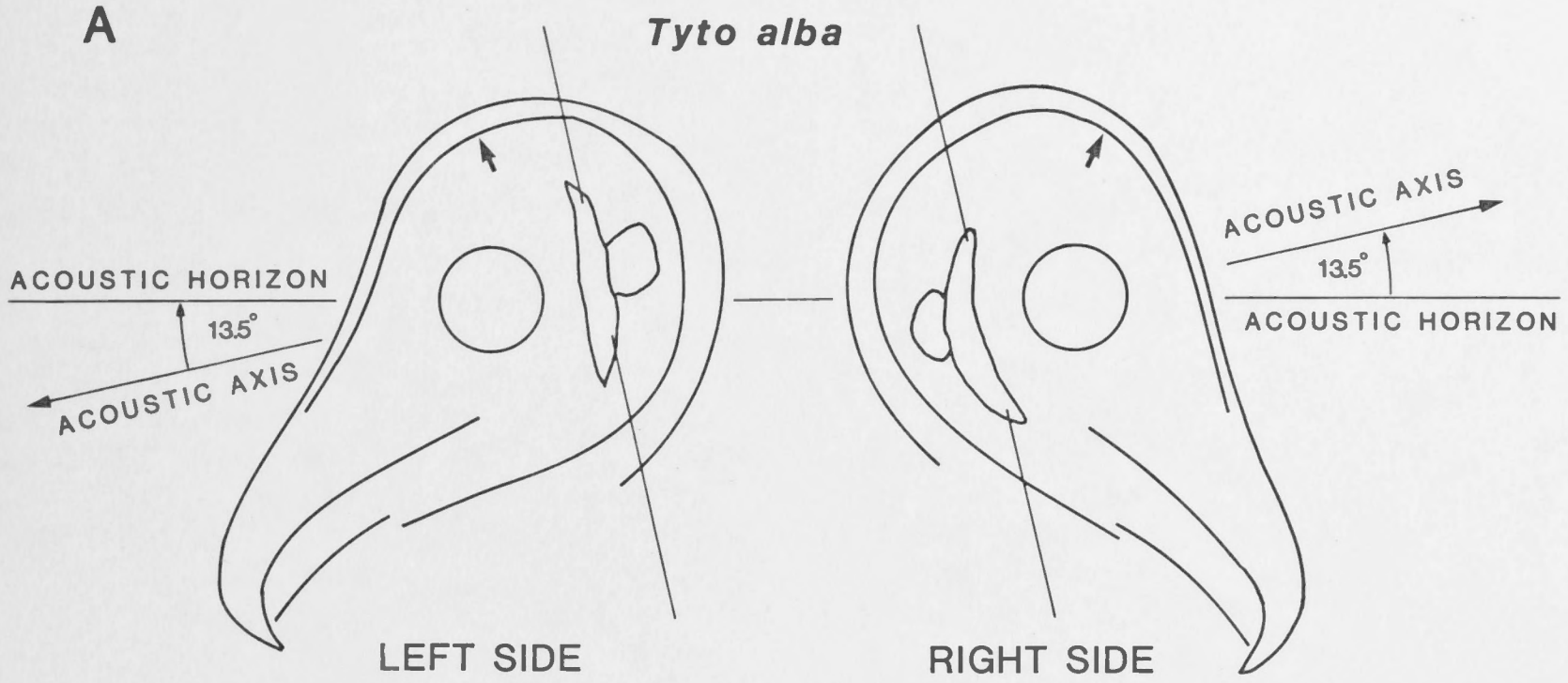
A
Tyto alba
ACOUSTIC HORIZON
13.5°
ACOUSTIC AXIS
ACOUSTIC AXIS
13.5°
ACOUSTIC HORIZON
LEFT SIDE
RIGHT SIDE

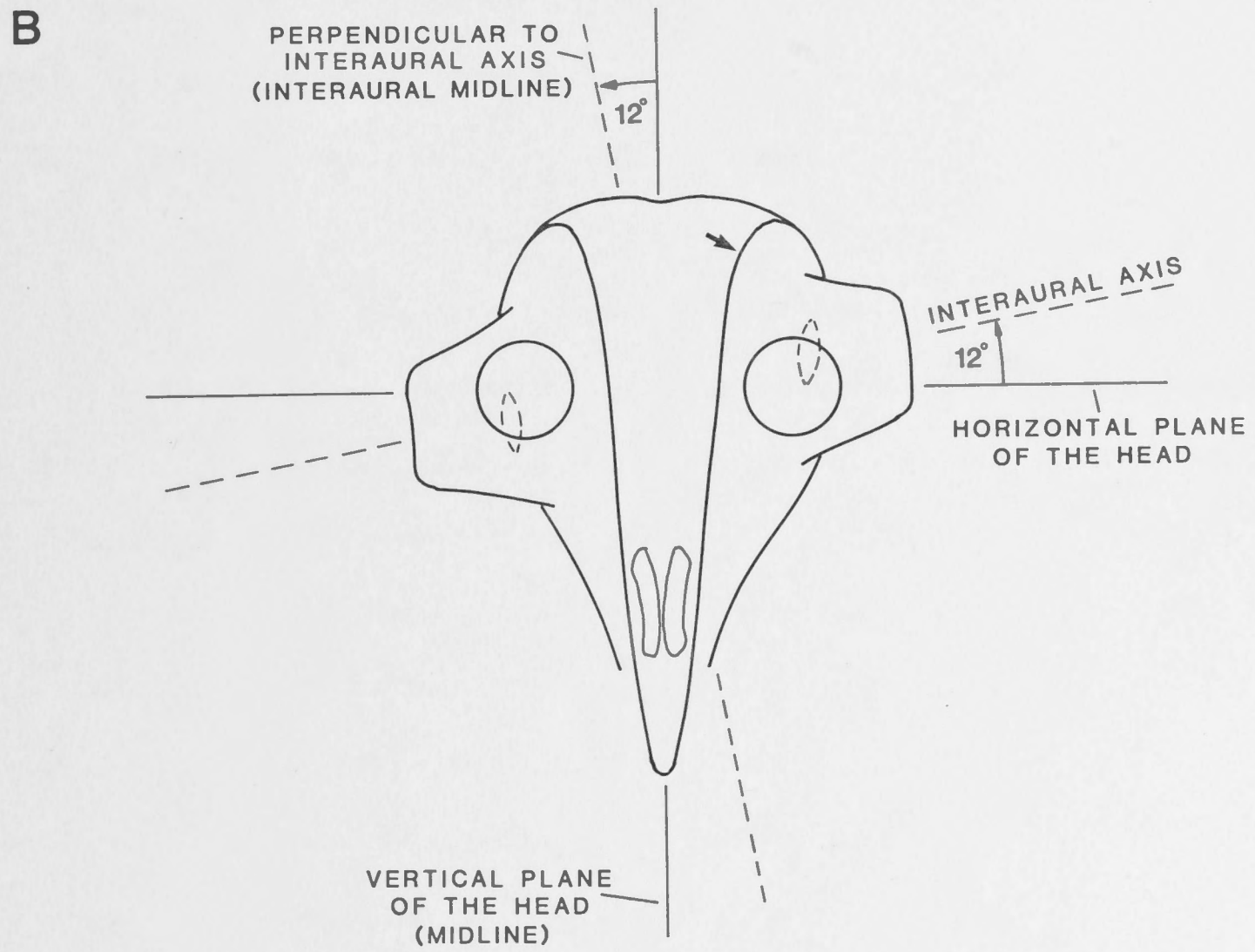
B
PERPENDICULAR TO
INTERAURAL AXIS
(INTERAURAL MIDLINE)
12°
INTERAURAL AXIS
12°
HORIZONTAL PLANE
OF THE HEAD
VERTICAL PLANE
OF THE HEAD
(MIDLINE)

Fig. 5.3. Horizontal view of the head of *Tyto alba* revealing the structure of the external and middle ears.

A. Intact head emphasising the facial disks and perimeter of the ruffs. The plane of the open face of each ruff is inclined by 50 to the midline. In A the head is tilted upwards slightly compared to the cross sections in B and C in order to emphasize the facial disks and ruffs (see also Fig. 5.1).

B. Similar view as A, but skull is outlined to show the structure of the interaural cavity, ear canals, tympanic membrane and profile of the ruff feathers. The location of the ear flap is also outlined.

C. Highly schematic diagram of the barn owl head in horizontal cross-section showing the key dimensions of the outer ear cavity, ear canal and interaural cavity. External dashed lines indicate the orientation of the plane of the open face of the facial ruff. The relevant dimensions of the outer ear cavity are in millimeters and used to predict the movement of the acoustic axis with frequency in azimuth (see APPENDIX 3 and text). a_o = mouth of the outer ear cavity at the approximate truncation point. Tympanic membranes are indicated by short dashed lines at the base of the ear canals. In addition, the interaural separation of the tympanic membranes (22mm) are indicated and used to predict pressure gradient effects at the membrane (see text). The asymmetry of the ear canal and ear canal opening is not indicated in this diagram (see B).

A

B

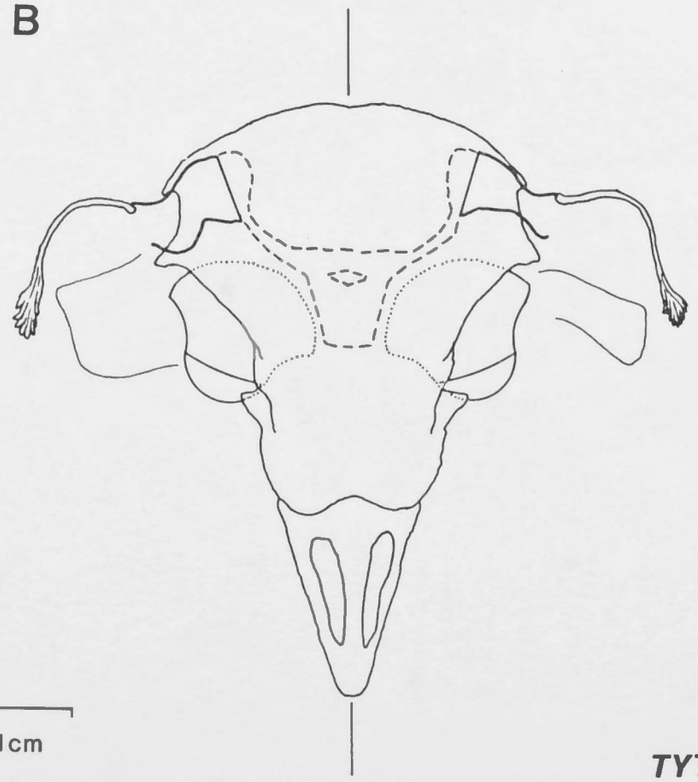

C

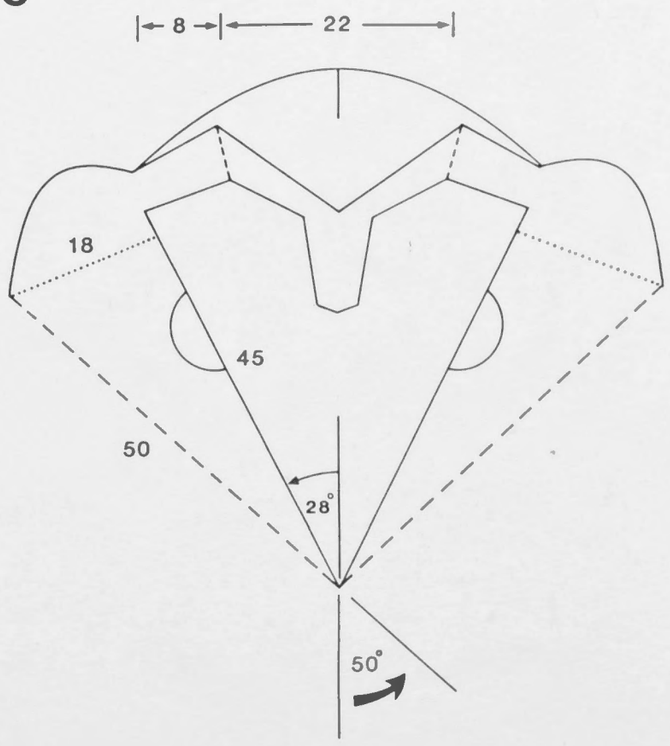

TYTO ALBA

Fig. 5.3. Horizontal view of the head of *Tyto alba* revealing the structure of the external and middle ears.

A. Intact head emphasising the facial disks and perimeter of the ruffs. The plane of the open face of each ruff is inclined by 50 to the midline. In A the head is tilted upwards slightly compared to the cross sections in B and C in order to emphasize the facial disks and ruffs (see also Fig. 5.1).

B. Similar view as A, but skull is outlined to show the structure of the interaural cavity, ear canals, tympanic membrane and profile of the ruff feathers. The location of the ear flap is also outlined.

C. Highly schematic diagram of the barn owl head in horizontal cross-section showing the key dimensions of the outer ear cavity, ear canal and interaural cavity. External dashed lines indicate the orientation of the plane of the open face of the facial ruff. The relevant dimensions of the outer ear cavity are in millimeters and used to predict the movement of the acoustic axis with frequency in azimuth (see APPENDIX 3 and text). a_o = mouth of the outer ear cavity at the approximate truncation point. Tympanic membranes are indicated by short dashed lines at the base of the ear canals. In addition, the interaural separation of the tympanic membranes (22mm) are indicated and used to predict pressure gradient effects at the membrane (see text). The asymmetry of the ear canal and ear canal opening is not indicated in this diagram (see B).

A

B

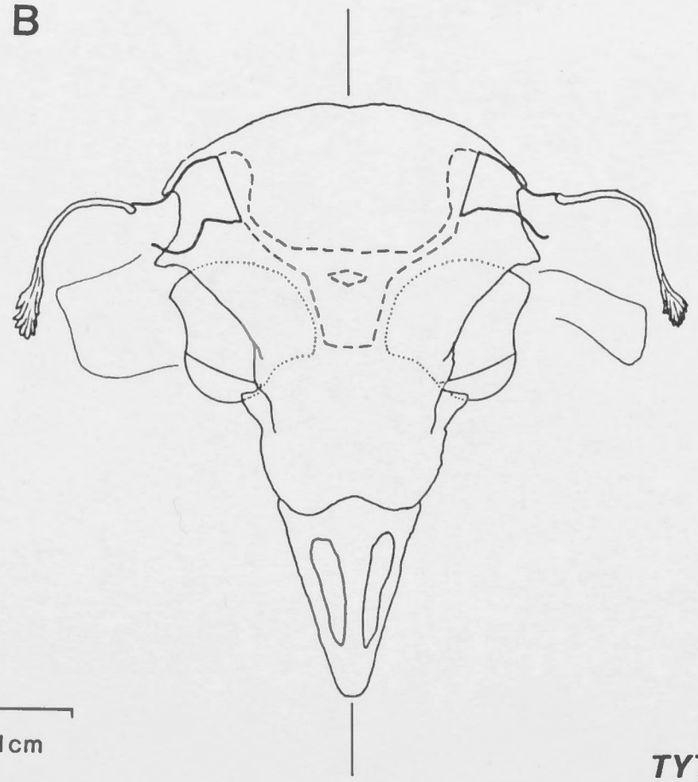

C

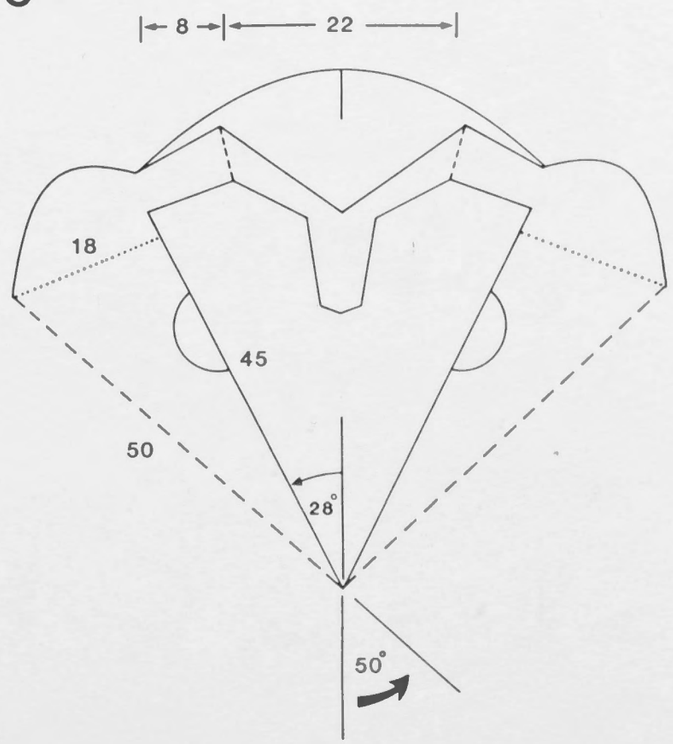

TYTO ALBA

Fig. 5.4. Measurements of acoustic pressure gain in the ear canal and facial ruff of *Tyto alba*.

A. The effect of ear flap removal on the pressure gain in the ear canal.

B. Normal acoustic pressure gain measured in the ear canal for four ears. Dashed curve is a typical example of the gain curve after ruff removal (see Fig. 5.1 and 5.2).

C. Average gain curve (N = 4) for the outer ear cavity calculated from the difference between normal and ruff removed gain curves (as in B). Vertical bar = standard error; remaining bars have been omitted for clarity. Expected gain curves for finite paraboloidal, conical and exponential horn are indicated (dotted curves) and based on the dimensions of the outer ear cavity (see Table 5.1 and APPENDIX 1)

D. Measurements of acoustic gain obtained from a ($\frac{1}{8}$" Bruel and Kjaer Type 4148) microphone placed in the outer ear cavity in front of the ear canal opening (see text). Solid curve (filled circles) is gain for the intact head, dashed curve (filled circles) is gain with the ruff removed. The difference curve (solid curve open circles) is an equivalent measure for the gain of the facial ruff as in C. Note that above 10kHz higher pressure gains are experienced in the actual outer ear cavity compared to inside the ear canal (C, and see text).

In both C and D, the ratio between the circumference of the open face of the ruff and the wavelength (ka) is indicated as a scale on the abscissa (a = 3cm; Table 5.1).

Tyto alba

A. EFFECT OF EAR FLAP REMOVAL

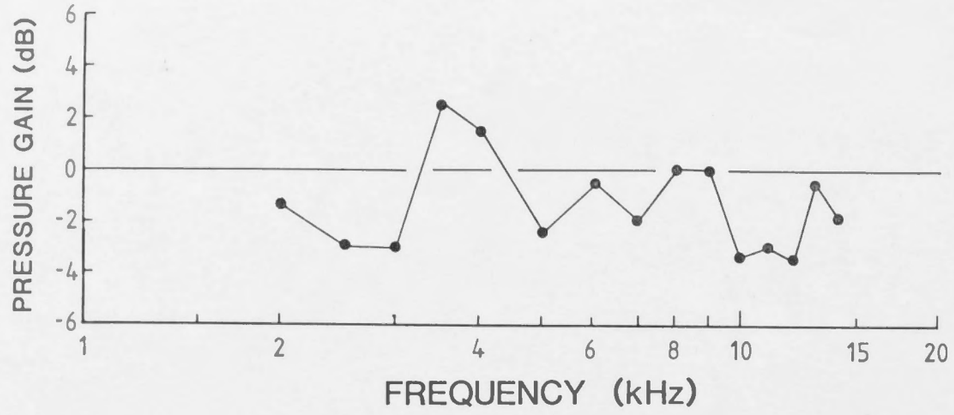

B. EAR CANAL

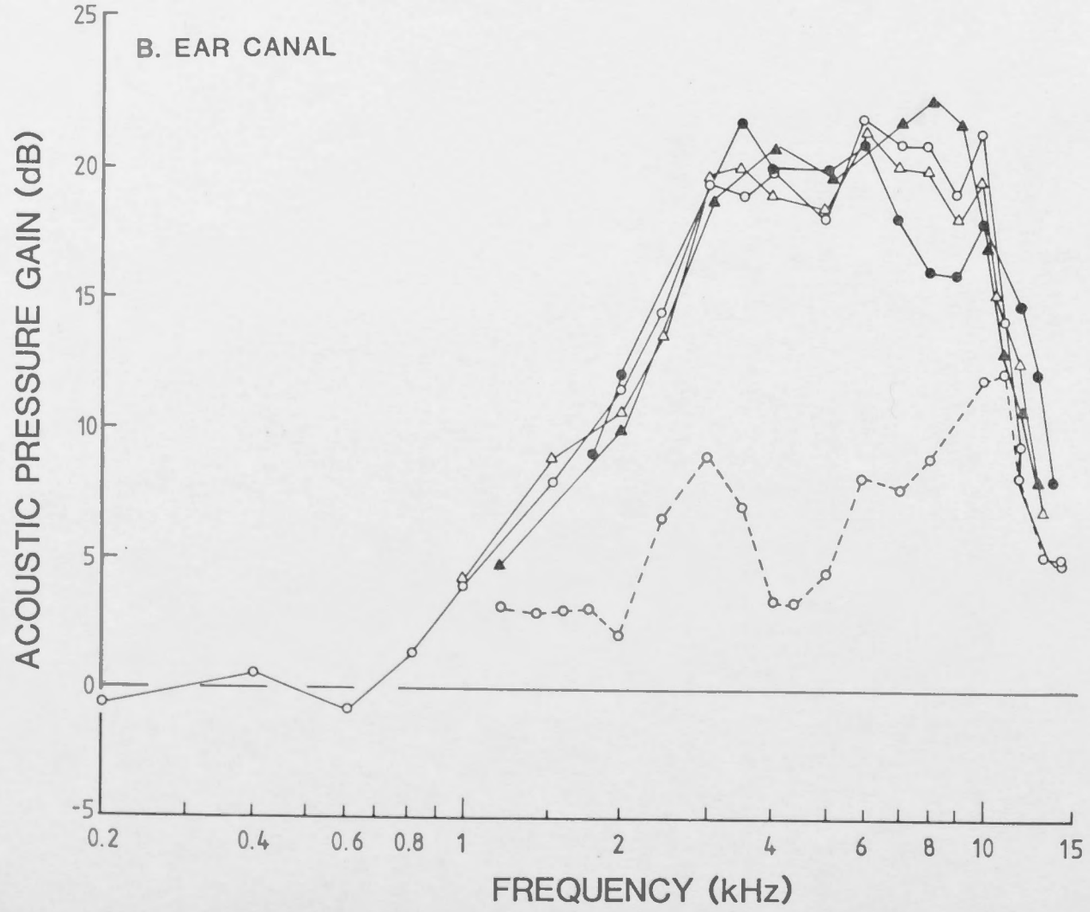

ka

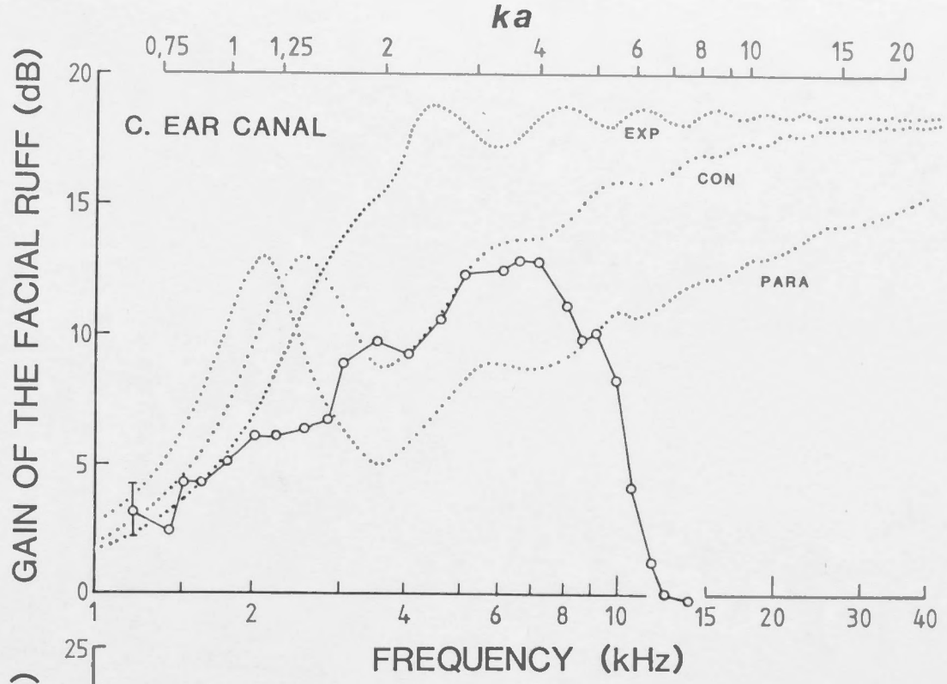

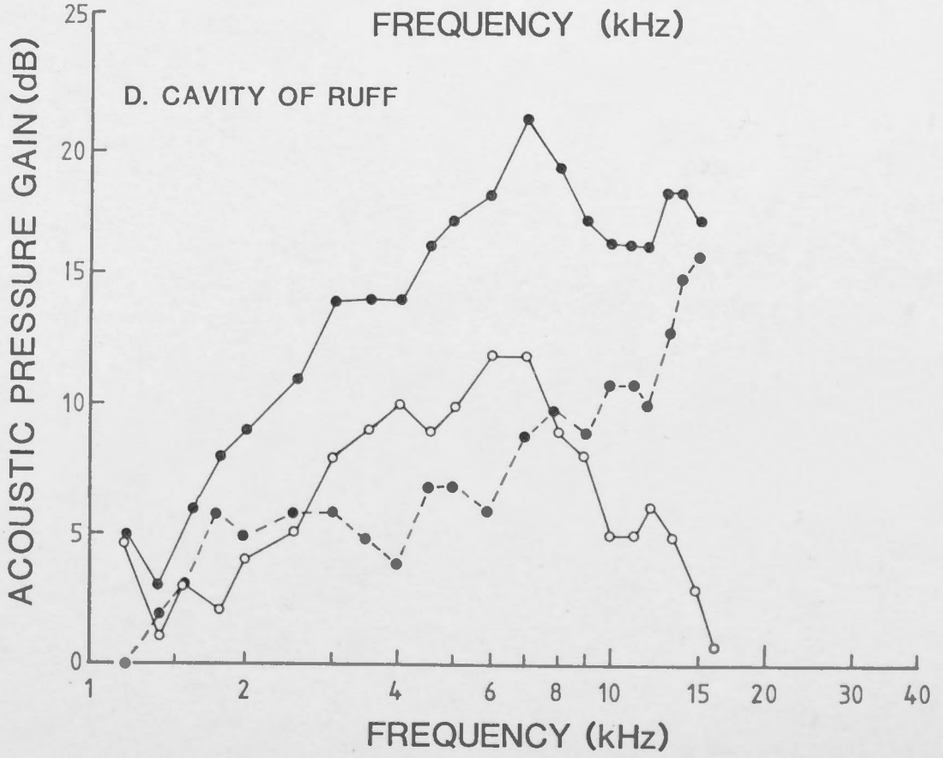

Fig. 5.5. A series of iso-intensity contours for the left and right ear canals of *Tyto alba* plotted on a two dimensional zenithal projection of frontal hemisphere (for definitions see METHODS AND METHODS). Stimulus frequency as indicated. The contours represent decreasing pressure in dB relative to the maximum value at the acoustic axis.

Tyto alba

EAR CANAL

LE

3kHz

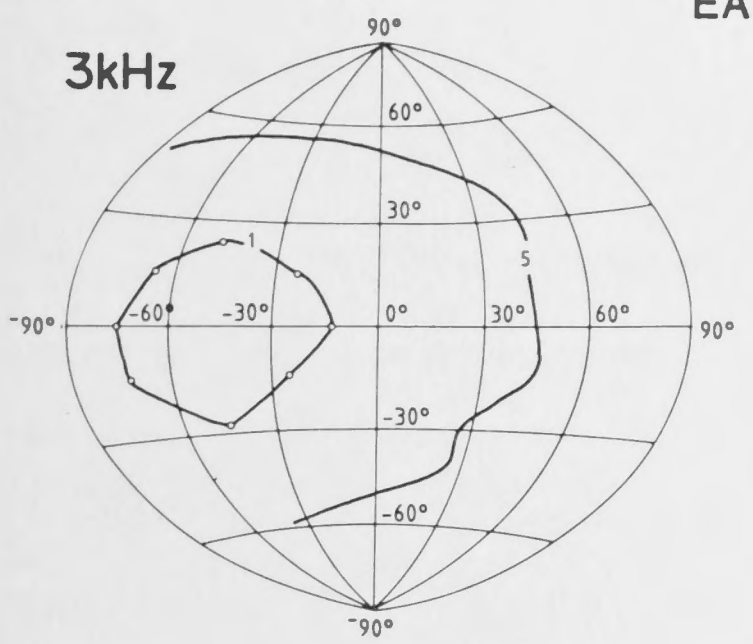

5kHz

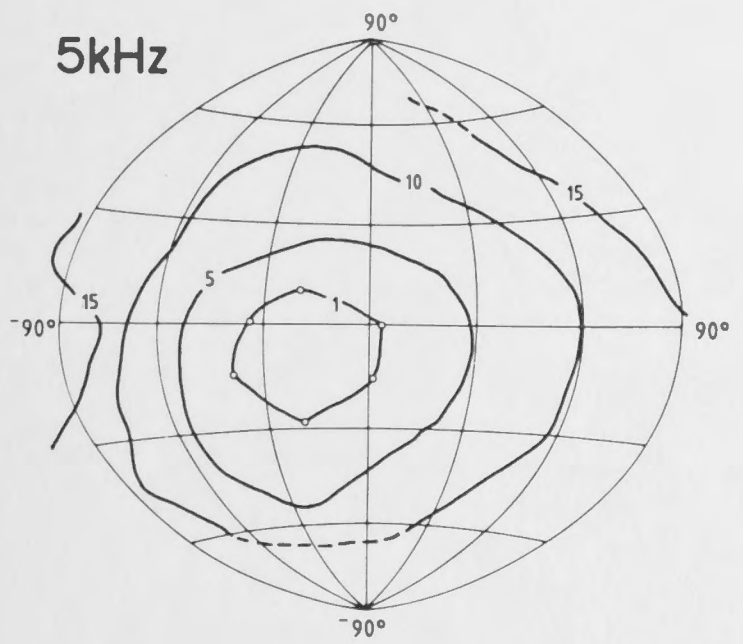

7kHz

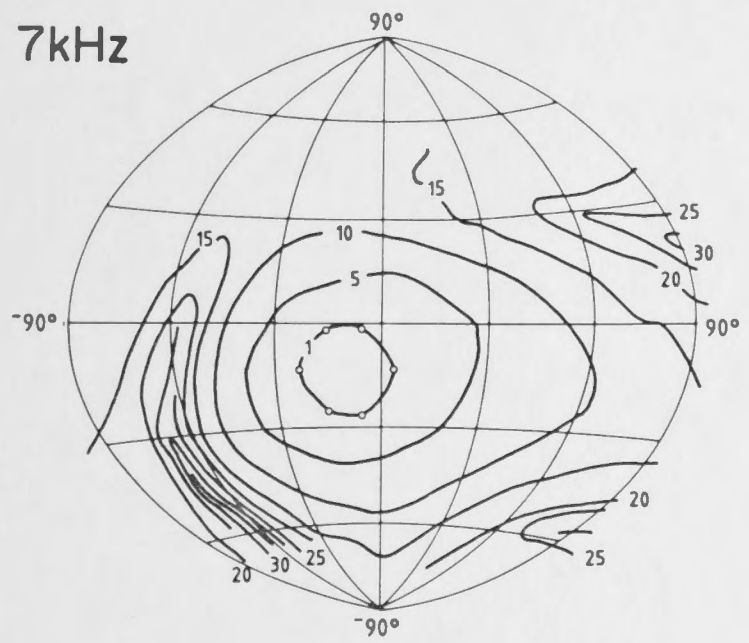

9kHz

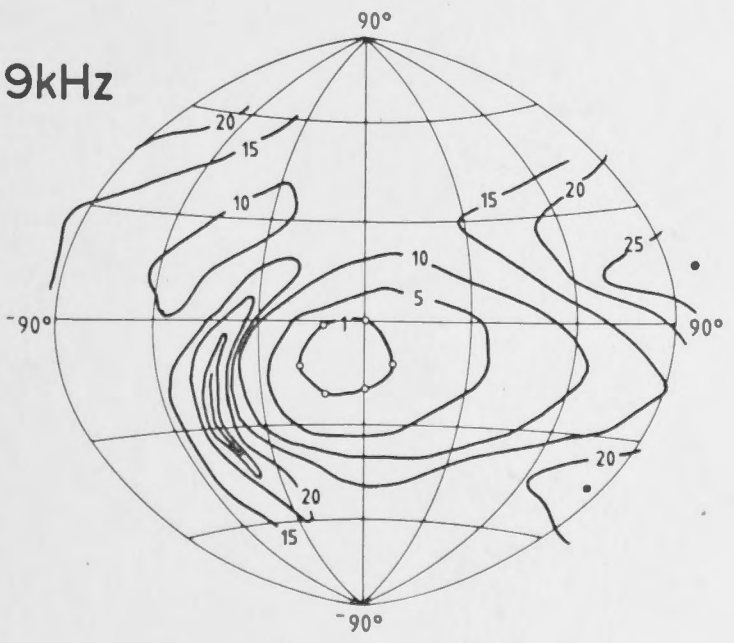

RE

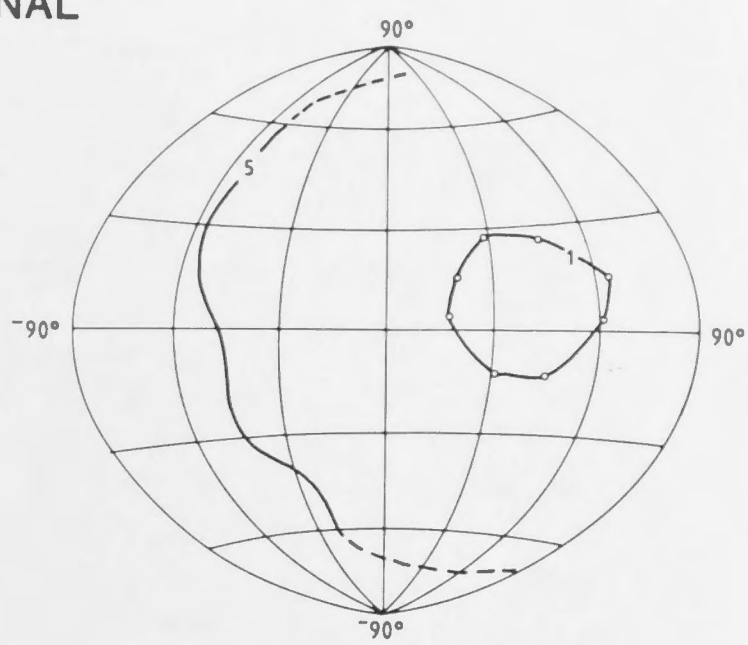

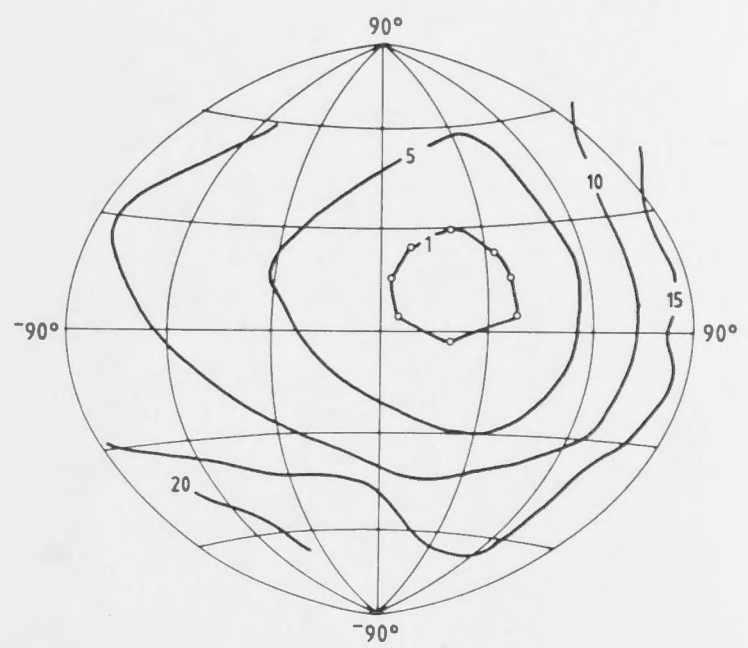

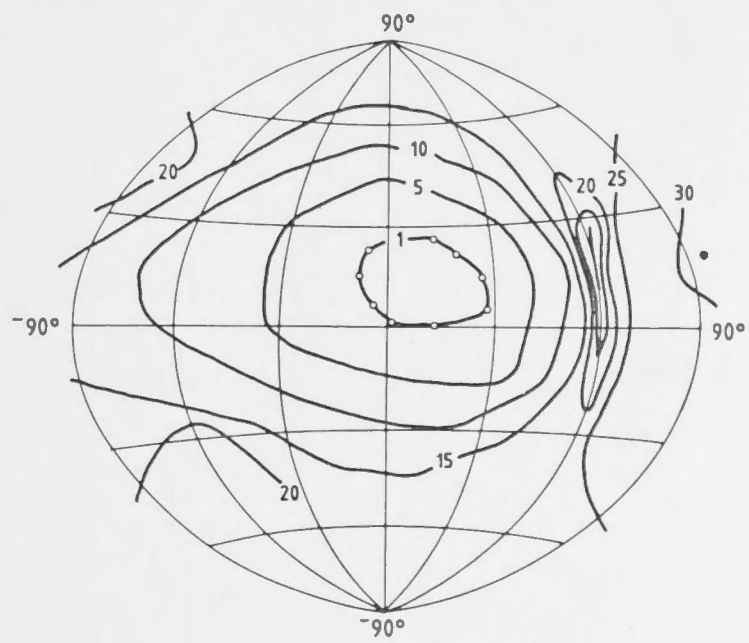

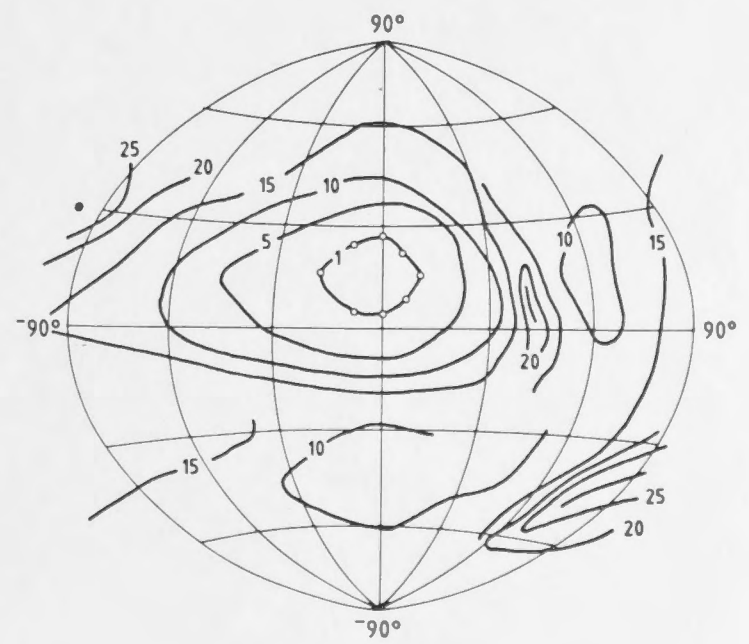

Fig. 5.6. A. Maximum directionality in *Tyto alba* defined as the greatest difference in sound pressure (dB_{max}) between any two points on a directivity pattern, as a function of stimulus frequency for five ears. The rapid increase in maximum directionality above 3kHz results from the presence of approximate nulls in the directivity patterns (see Fig. 5.5). The ratio of the circumference of the open face of the ruff to the wavelength (ka parameter) is comparable to the development of directionality for a circular aperture (see Beranek 1954; Fletcher and Thwaites 1979).

B. Maximum directionality for the cochlear microphonic (CM) potentials based on the maximum difference in CM amplitude for directivity patterns from five ears. (see also Fig. 5.12). Note the abrupt loss of CM directionality above 9-10kHz compared to the pressure response in the ear canal (A).

Tyto alba

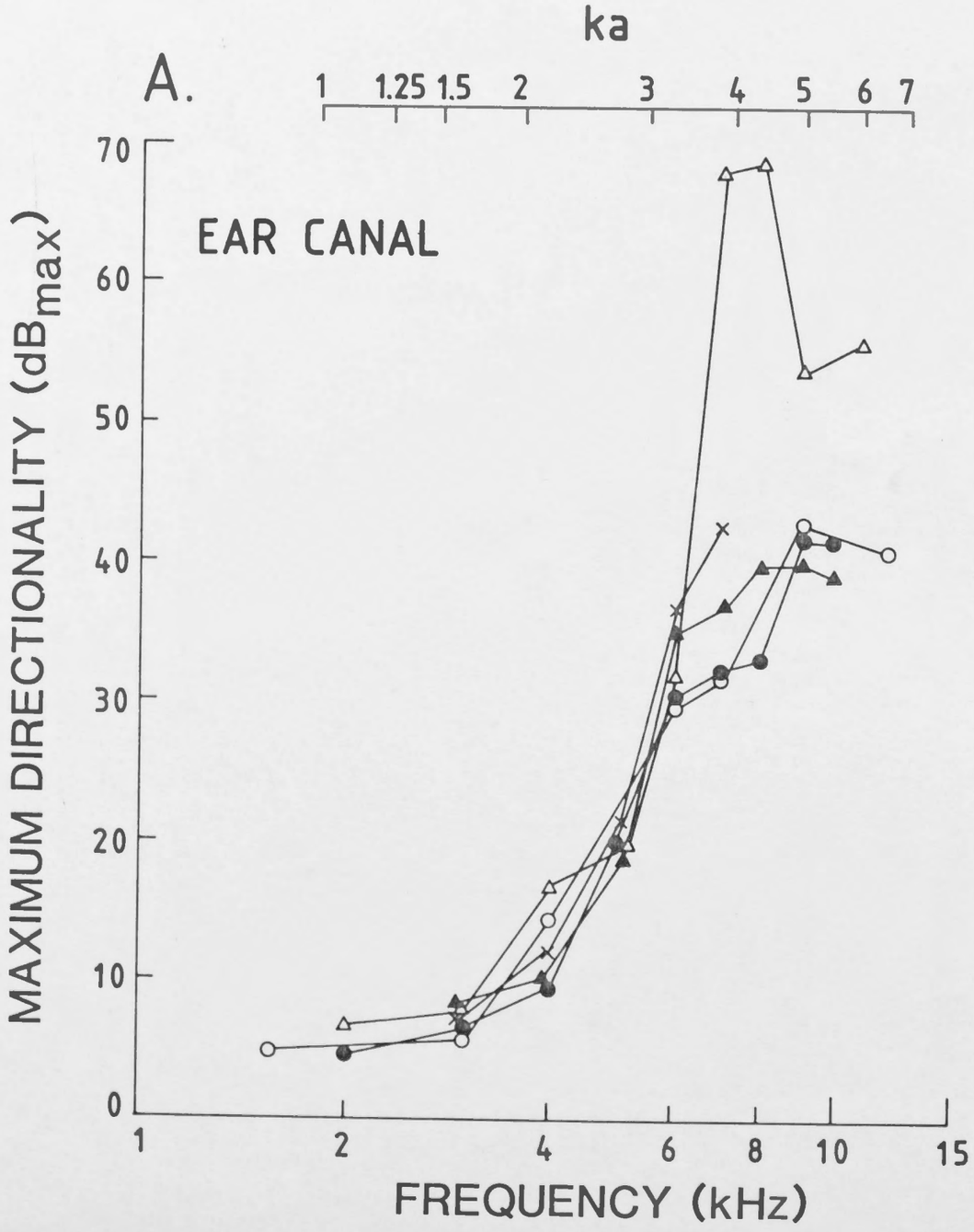
ka
A.
1 1.25 1.5 2 3 4 5 6 7
EAR CANAL
MAXIMUM DIRECTIONALITY (dB$_{max}$)
70
60
50
40
30
20
10
0
1 2 4 6 8 10 15
FREQUENCY (kHz)

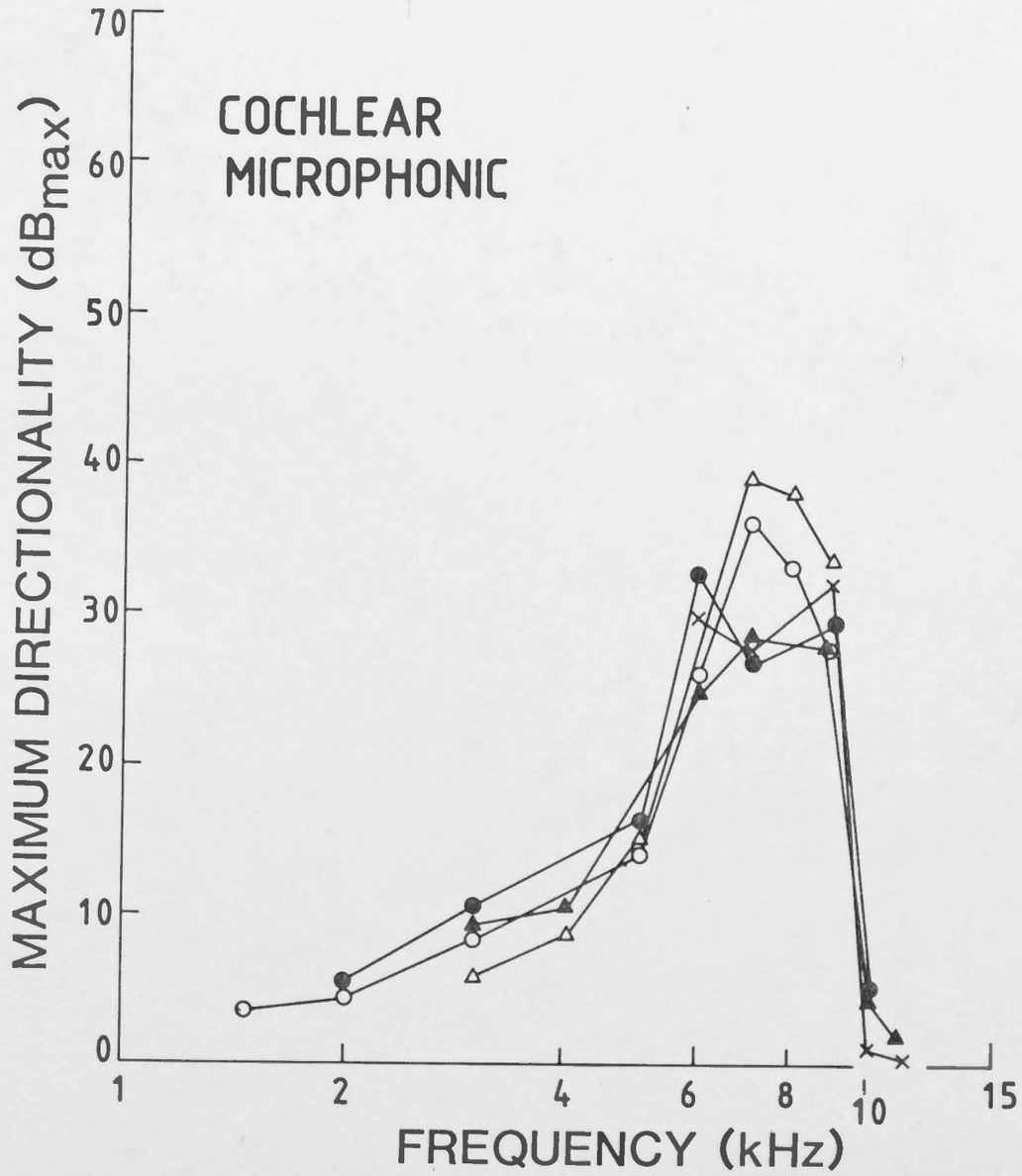
B.
COCHLEAR MICROPHONIC
MAXIMUM DIRECTIONALITY (dB$_{max}$)
70
60
50
40
30
20
10
0
1 2 4 6 8 10 15
FREQUENCY (kHz)

Fig. 5.7. Measurement of acceptance angle (-3dB relative to on-axis sound pressure) for directivity patterns in the ear canal and CM.

A and B. Filled circles are -3dB acceptance angles ($2\theta°$) in the azimuth and elevation for the directivity patterns by the ear canal. Solid curve estimates the -3dB acceptance angle which would be expected to result from sound diffraction of a circular aperture of radius 3cm which is equivalent to the average radius of the open face of the facial ruff (see Fig. 5.1 and Table 5.1). For calculation of expected curve see APPENDIX 2 and text.

C and D. Distribution of -3dB acceptance angles for CM directivity patterns as a function of frequency. In C acceptance angles are measured along the plane of minimum directionality (CM axial plane). In D as in C, but acceptance angles measured along the (maximum) directional plane of the CM. In C and D solid curves are expected acceptance angles based on sound diffraction as in A and B. In D dashed curve is the expected -3dB acceptance angle (relative to the maximum net pressure) which would result from a pressure gradient at the tympanic membrane (see text and Eqn (16)).

Tyto alba

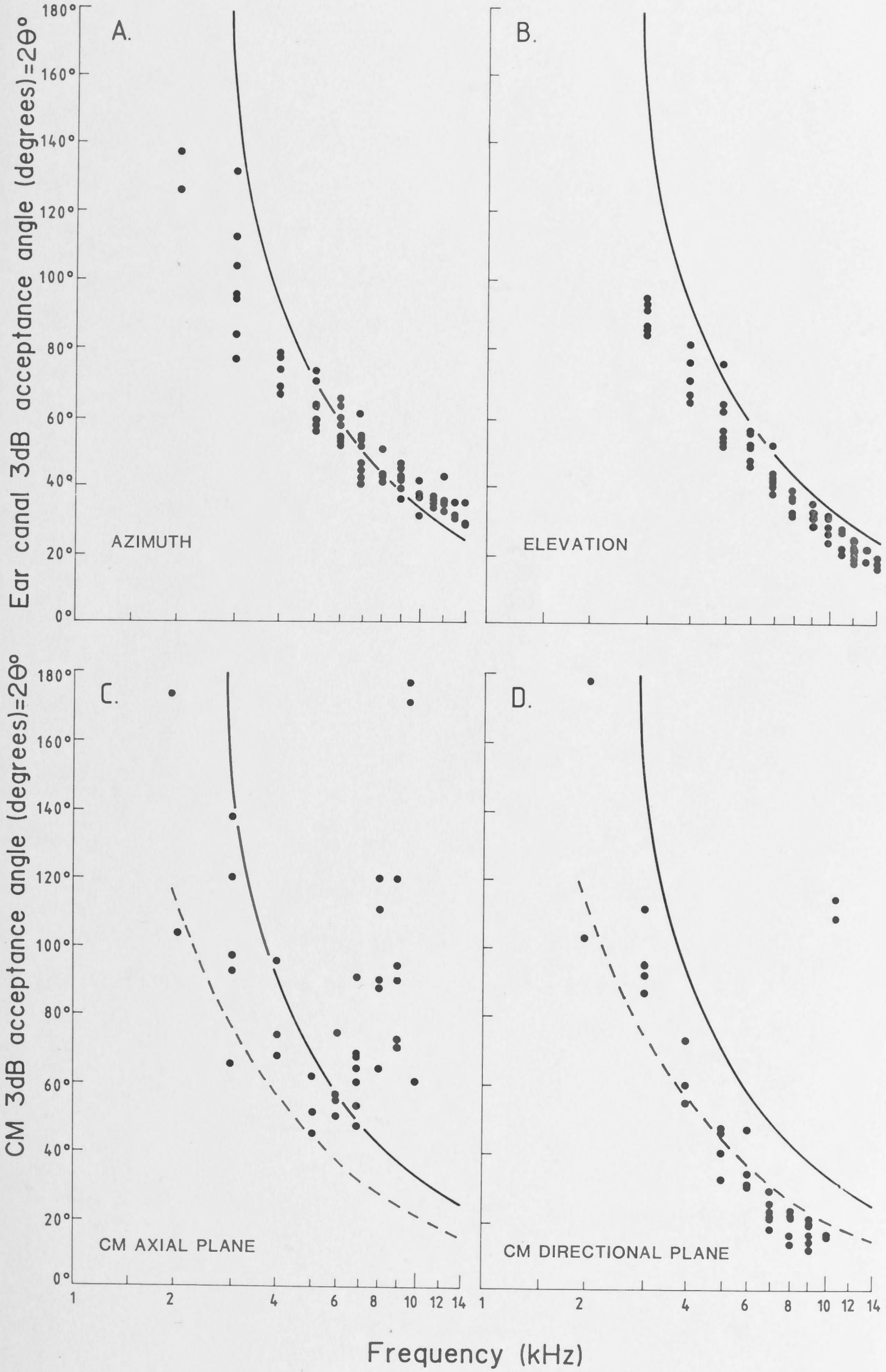
A.
B.
C.
D.
Ear canal 3dB acceptance angle (degrees)=2Θ°
CM 3dB acceptance angle (degrees)=2Θ°
180°
160°
140°
120°
100°
80°
60°
40°
20°
0°
AZIMUTH
ELEVATION
CM AXIAL PLANE
CM DIRECTIONAL PLANE
1
2
4
6
8
10
12
14
Frequency (kHz)

Fig. 5.8. A and B. Angular separation between nulls and on-axis sound pressure (semi-angle) measured from directivity patterns in the ear canal (as in Fig. 5.5). Solid curve in A,B and C is expected semi-angle which would result from sound diffraction by a circular aperture of the same average radius as the open face of the facial ruff (a = 3cm, see Table 5.1). Arrow in A indicates low frequency limit of maximum semi-angle (90° off-axis) for an aperture in a plane wall expressed as ka = 3.83 (see Beranek 1954). In A. data points are derived from lateral (or rearward) nulls relative to the acoustic axis (see Fig. 5.5). In B. null positions are derived from medial (or frontally) placed nulls relative to the acoustic axis (see Fig. 5.5).

C. Angular separation between CM nulls and maximum CM amplitude (CM axis) measured along the CM directional plane (see Fig. 5.12 and text). In C dotted curve is the expected semi-angle which would result from a pressure gradient produced by acoustical interference at the tympanic membrane (see Eqn. (16) and text).

Tyto alba

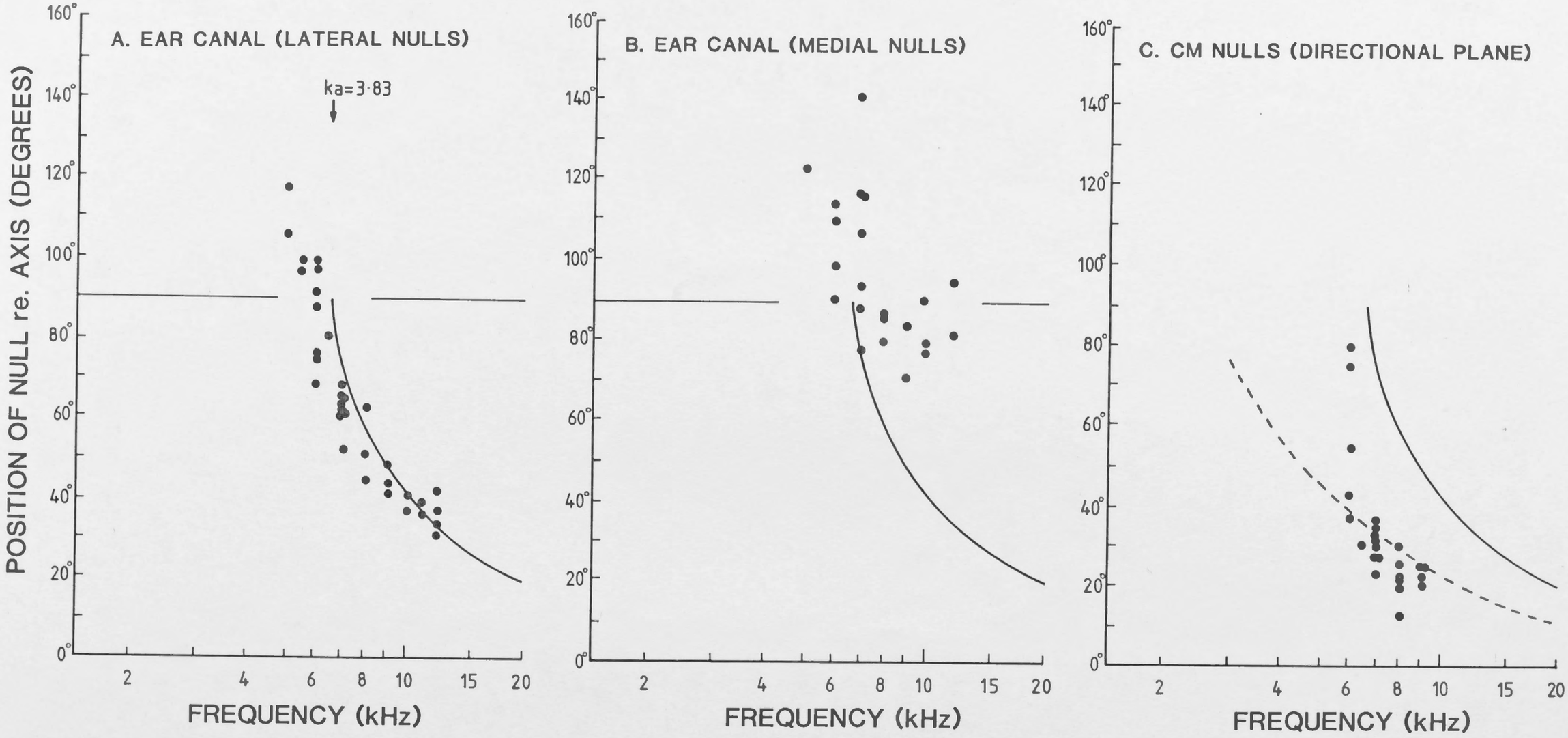
A. EAR CANAL (LATERAL NULLS)
ka=3·83
B. EAR CANAL (MEDIAL NULLS)
C. CM NULLS (DIRECTIONAL PLANE)
POSITION OF NULL re. AXIS (DEGREES)
160°
140°
120°
100°
80°
60°
40°
20°
0°
2
4
6
8
10
15
20
FREQUENCY (kHz)

Fig. 5.9. Movement of the acoustic and CM axes in space as a function of frequency.

A. Two-dimensional plot of the left ear acoustic axis (number = kHz and position) and -1dB contour relative to the on-axis pressure.

B and C. Average movement of the acoustic axes for four left (open circles) and four right (closed circles) ears in azimuth (B) and elevation (C). Vertical bars in B and C are the standard error, others have been omitted for clarity (also for E and F). In B. the average rate of movement of the acoustic axis (four ears) towards the midline is 20°/octave and is comparable to the expected movement of the acoustic axis (dashed curves) predicted from the geometry of the asymmetrical cross-section of the outer ear cavity in azimuth (see Fig. 5.3). For details of calculation see APPENDIX 3 and text. In C. both acoustic axes are maintained approximately 13.5° above or below the acoustic horizon (see Fig. 5.2A) for frequencies above 5kHz.

D. Two-dimensional plot of the left ear CM axis with details as in A.

Tyto alba

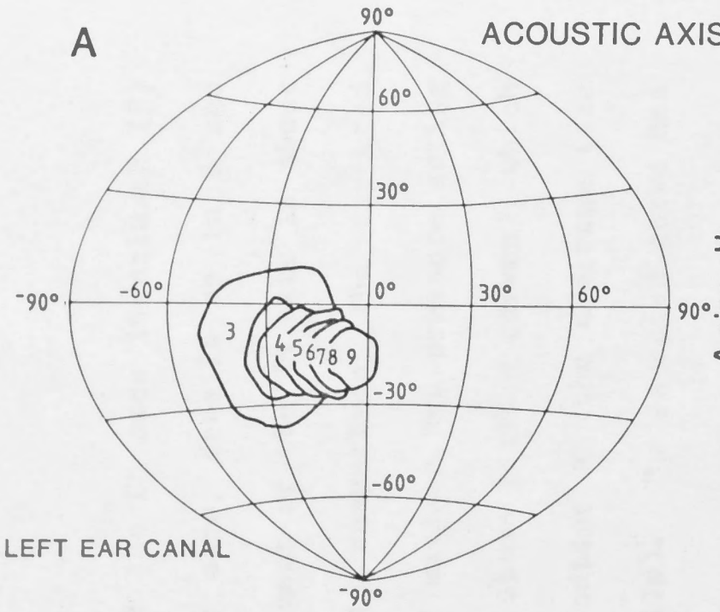

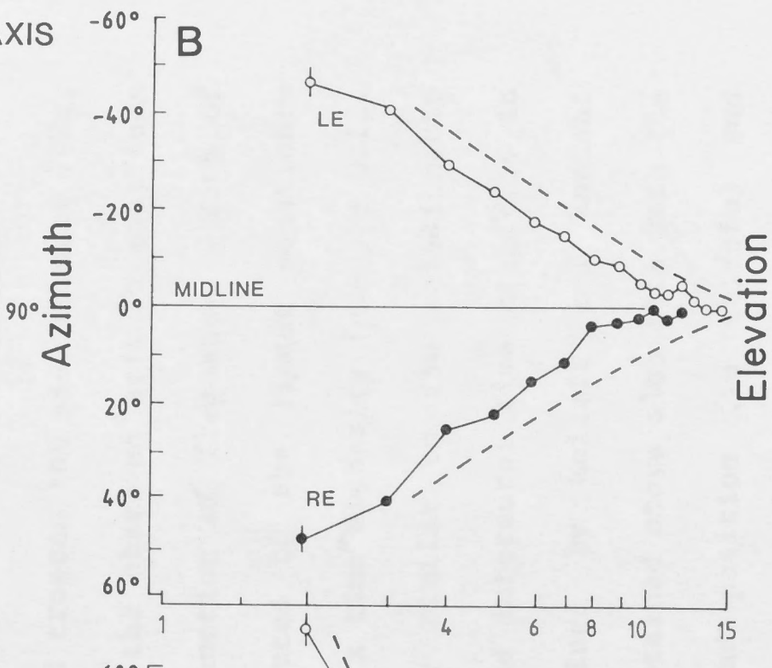

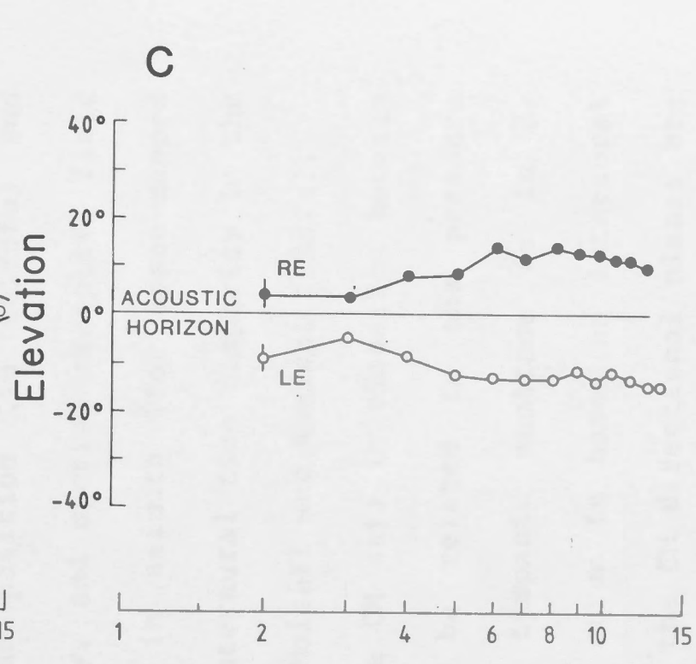

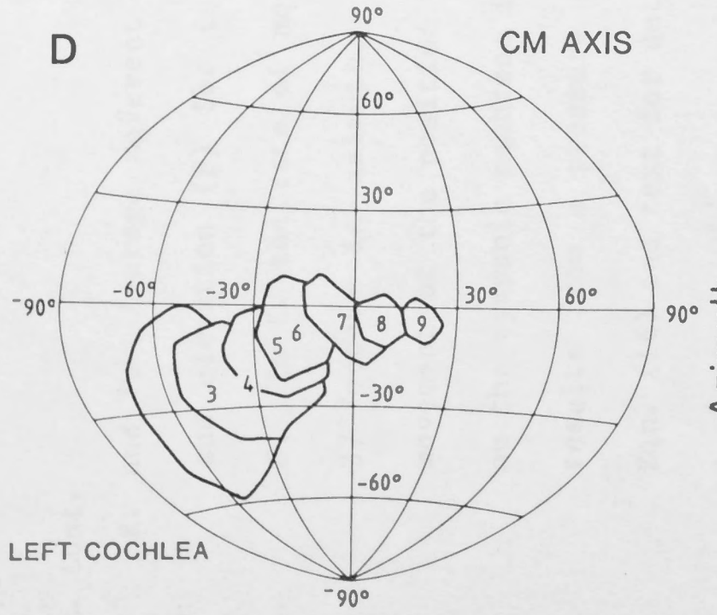

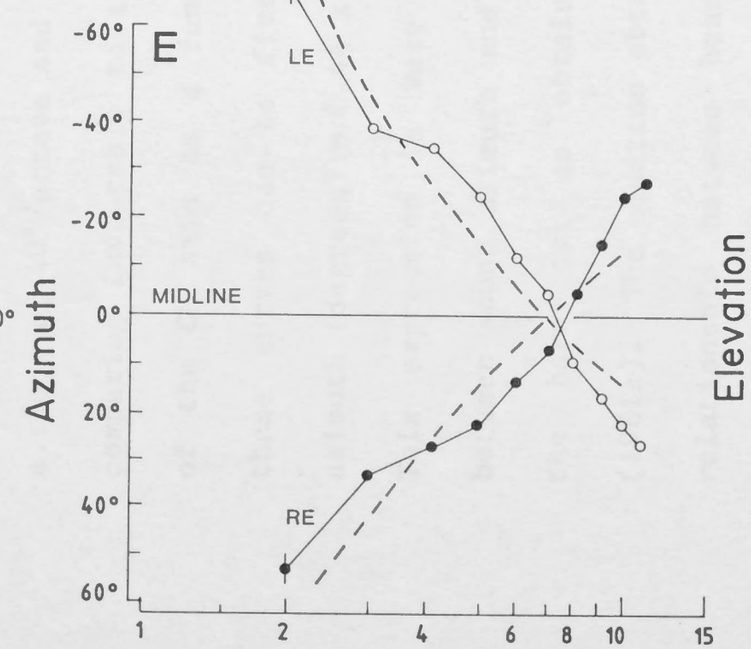

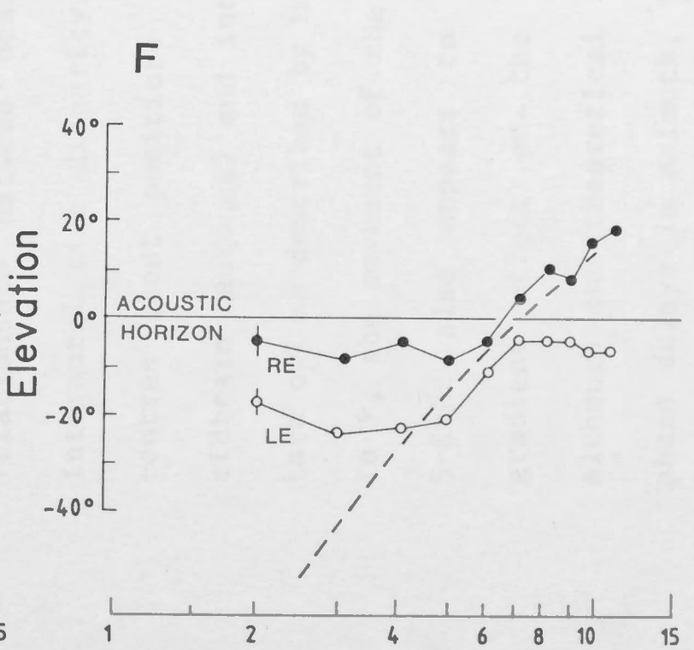

Frequency (kHz)

Fig. 5.9. Cont.

E. and F. Average movement of the CM axes in azimuth (E) and elevation (F) for four ears, details as in B and C. In E. the rate of movement of the CM axis is about 37°/octave in azimuth. In comparison, the expected movement of the position of maximum net pressure acting on the tympanic membrane is shown (dashed curves), which results from a pressure gradient at the membrane (see Eqn. (16) and text for details). The expected curve has a slope of 40°/octave and crosses the midline near 7kHz, comparing favourably to the observed azimuth positions of the CM axis as a function of frequency. Both of these curves can be fitted to the linear equation:-

azimuth (degrees) = 0.44 x time disparity (μsec) + 0.12.

This expression is very similar to the relationship between sound azimuth and interaural time disparity in the barn owl as obtained by Moiseff and Konishi (1981a). The equation obtained above also fits both the relationship between head position (in azimuth) and interaural time disparity, and spatial receptive field centres (best position) in azimuth (for space-mapped midbrain neurones) and interaural time disparity in the barn owl as described by Moiseff and Konishi (1981a).

In F, the movement of the CM axis in elevation between 5-8kHz also appears to be related to the pressure gradient effect on the tympanic membrane as in E. Although the theoretical curve is based on interaural phase delays in azimuth, the CM directional planes are tilted (see Figs. 5.12, 5.13) and therefore have an azimuth and elevation component.

Fig. 5.10. Directivity patterns for pressure measurements in the left and right ear canals after removal of the facial ruff at 6kHz and 9kHz. Compare with normal ear canal directionality as shown in Fig. 5.5. Details as for Fig. 5.5.

Tyto alba

EAR CANAL
RUFF REMOVED

LE

6kHz

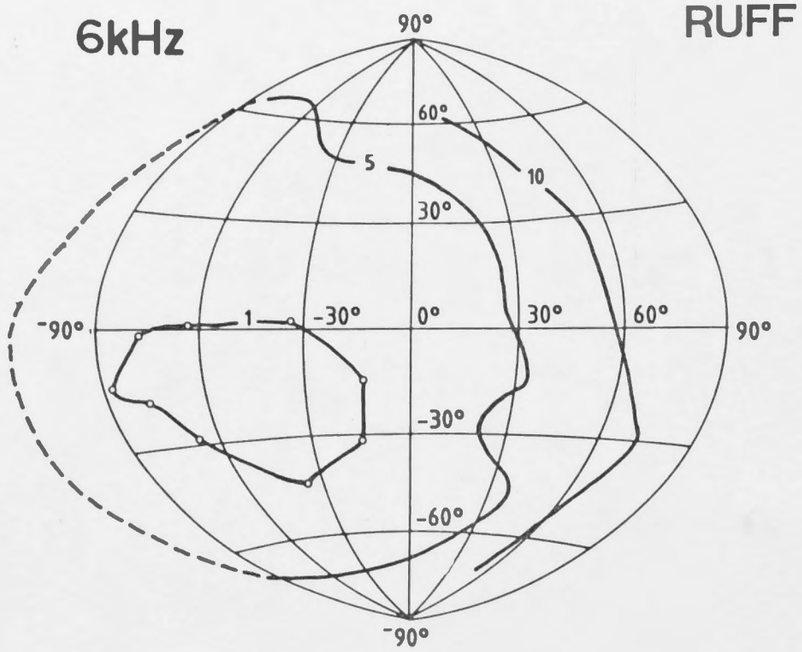

RE

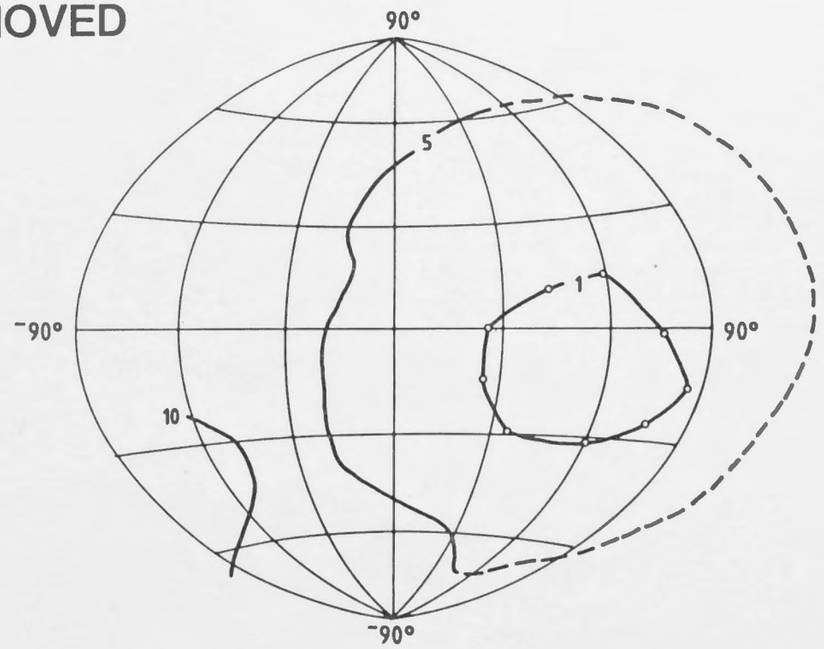

9kHz

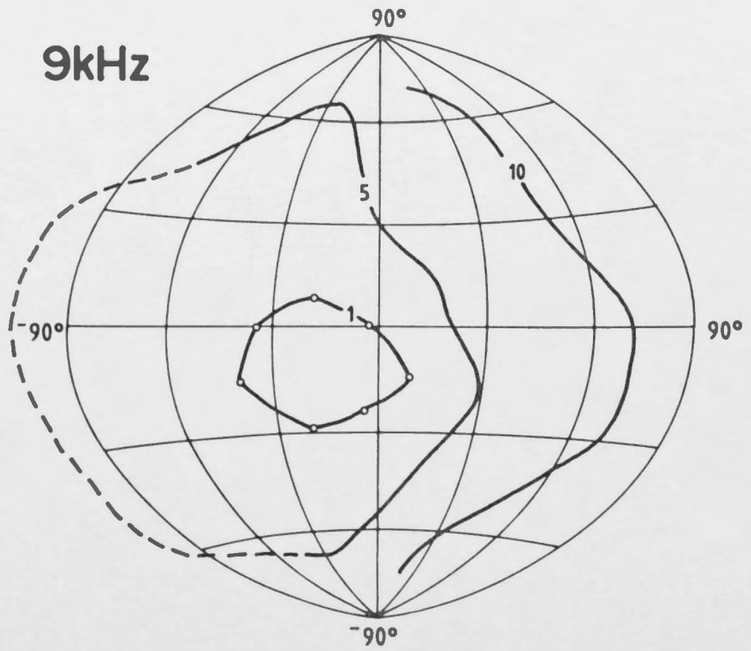

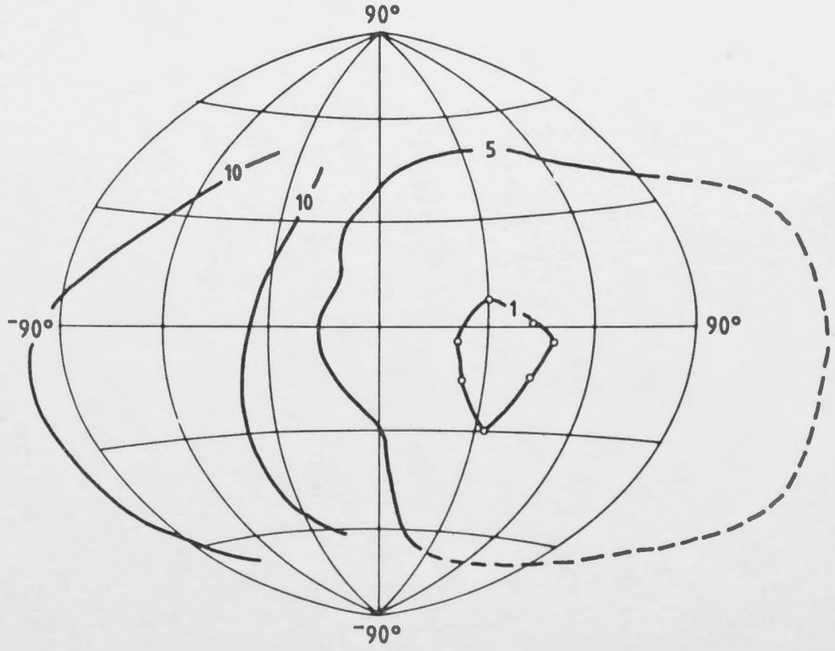

Fig. 5.11. Comparison between directivity patterns at 7kHz measured in the left ear canal before and after ear flap removal. Details as for Fig. 5.5

EAR CANAL

7kHz
LE

NORMAL

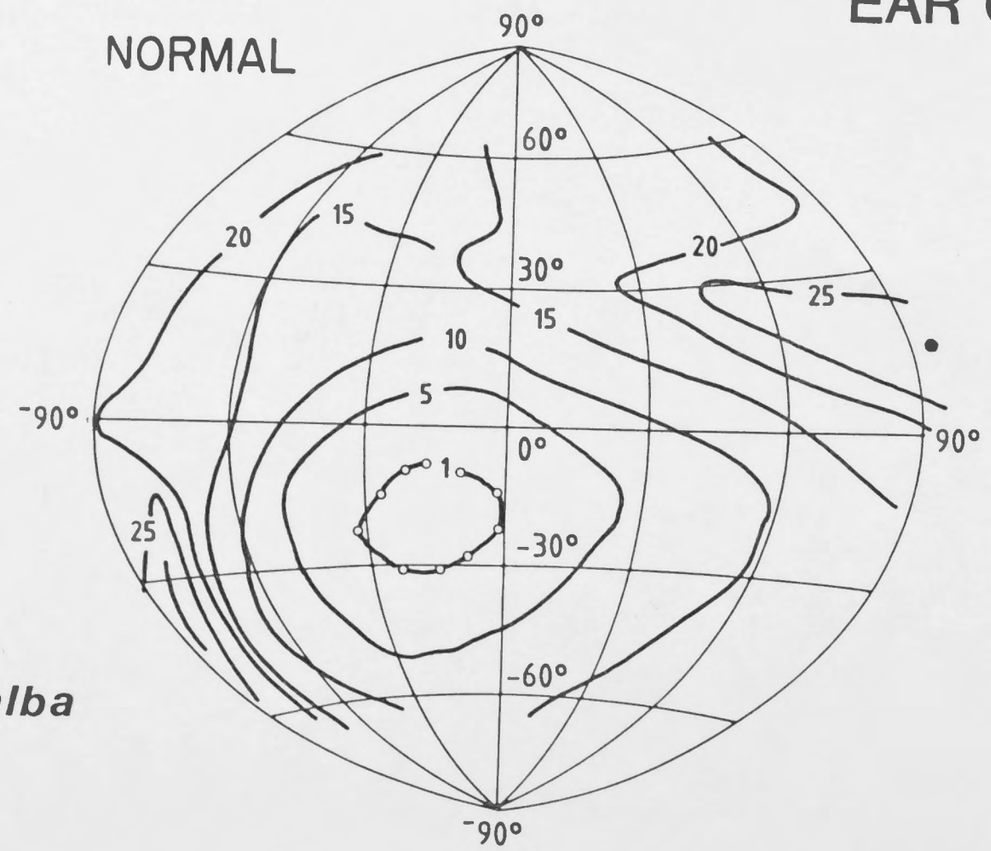

EAR FLAP
REMOVED

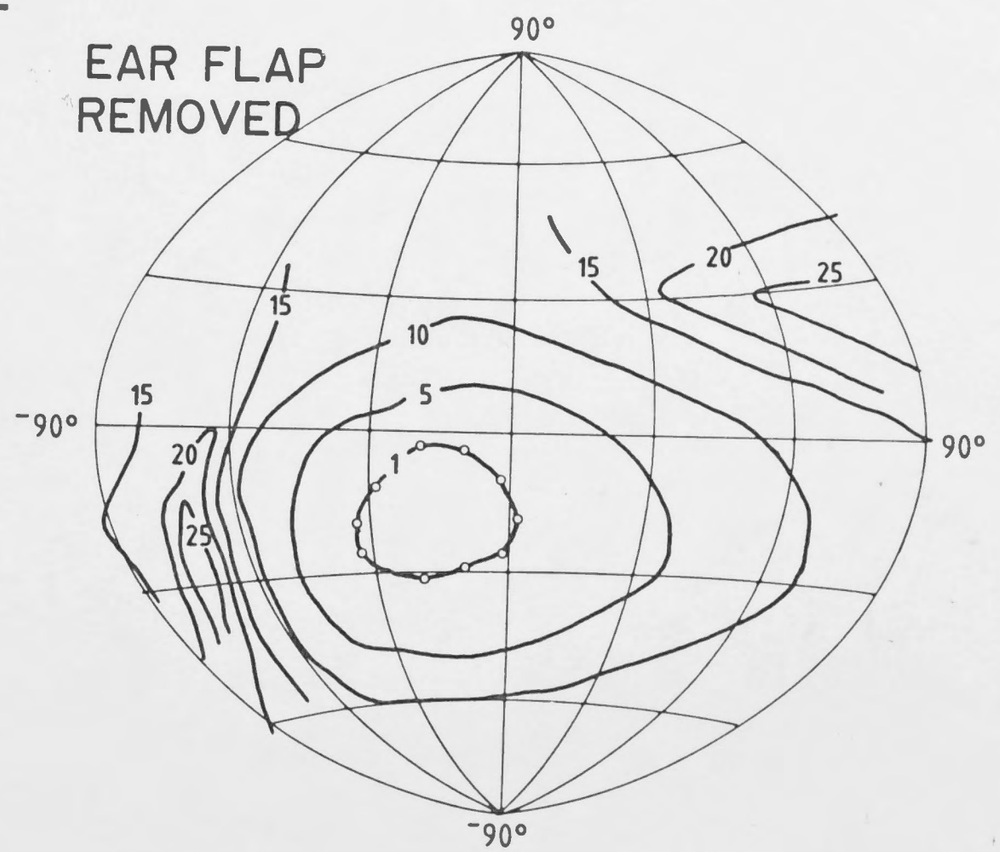

Tyto alba

Fig. 5.12. A series of two-dimensional directivity plots for CM recordings from the left and right ear. Contours represent regions of equal CM amplitude expressed as decreasing sensitivity to sound in dB relative to the maximum on-axis CM amplitude.

Tyto alba

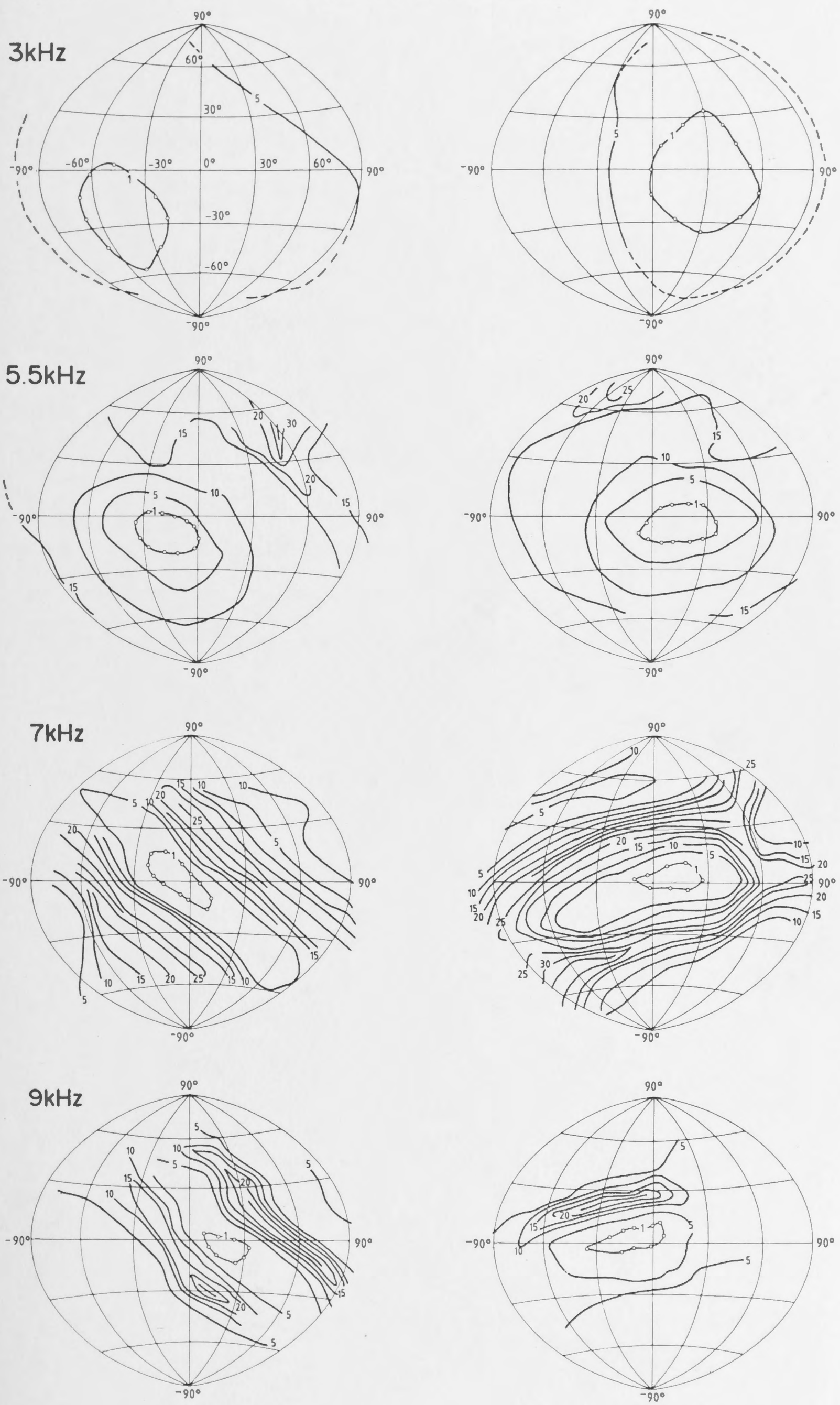
LE
COCHLEAR MICROPHONIC
RE
3kHz
5.5kHz
7kHz
9kHz
90°
-90°
60°
30°
0°
-30°
-60°

Fig. 5.13. A. Summary of the orientation of CM axial planes as indicated in Fig. 5.12, relative to the vertical plane of the barn owl head (see Fig 5.2B). Filled circles = left ear CM; open circles = right ear CM. The average inclination of the plane bisecting the CM axial planes of each ear is shown by a solid line with filled circles. Between 6-10kHz the left and right ear CM axial planes are symmetrical about a plane inclined by 15° to the vertical which is close to the interaural midline as shown in B (see Fig 5.2B). The interaural axis is tilted by 12° relative to the reference planes of the head due to the asymmetrical positions of the ear openings (see Fig. 5.2 also text).

B. The average inclination of the CM axial planes (above 6kHz) taken from A and superimposed (not projected) on the zenithal projection of frontal space to show the relationship to the interaural and head reference planes of the barn owl (see also Fig 5.2C). L, average orientation of left CM axial plane; R, average orientation of right CM axial plane; M, average orientation of plane of symmetry.

A

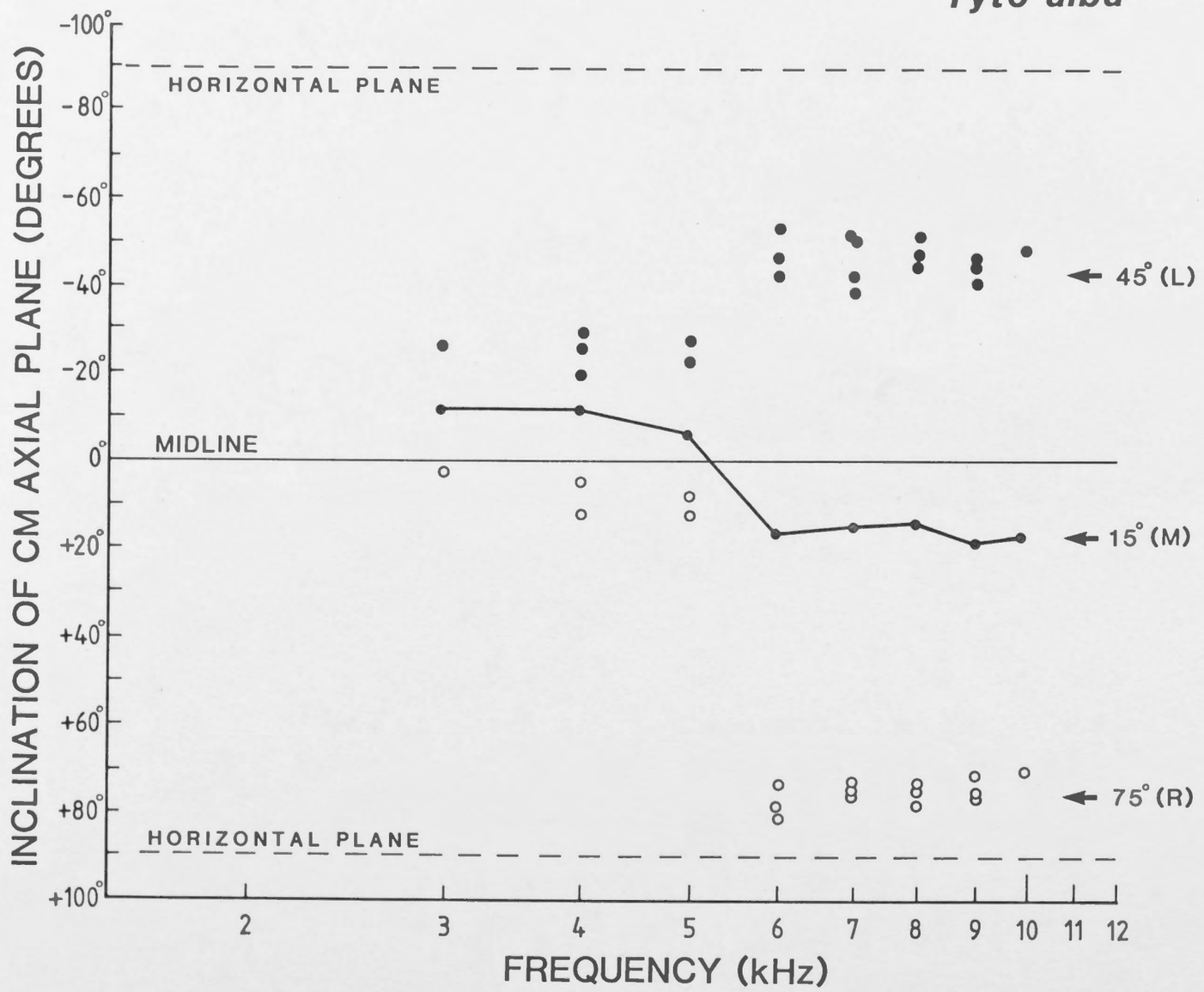
Tyto alba
INCLINATION OF CM AXIAL PLANE (DEGREES)
-100°
-80°
-60°
-40°
-20°
0°
+20°
+40°
+60°
+80°
+100°
HORIZONTAL PLANE
MIDLINE
HORIZONTAL PLANE
45° (L)
15° (M)
75° (R)
2
3
4
5
6
7
8
9
10
11
12
FREQUENCY (kHz)

B

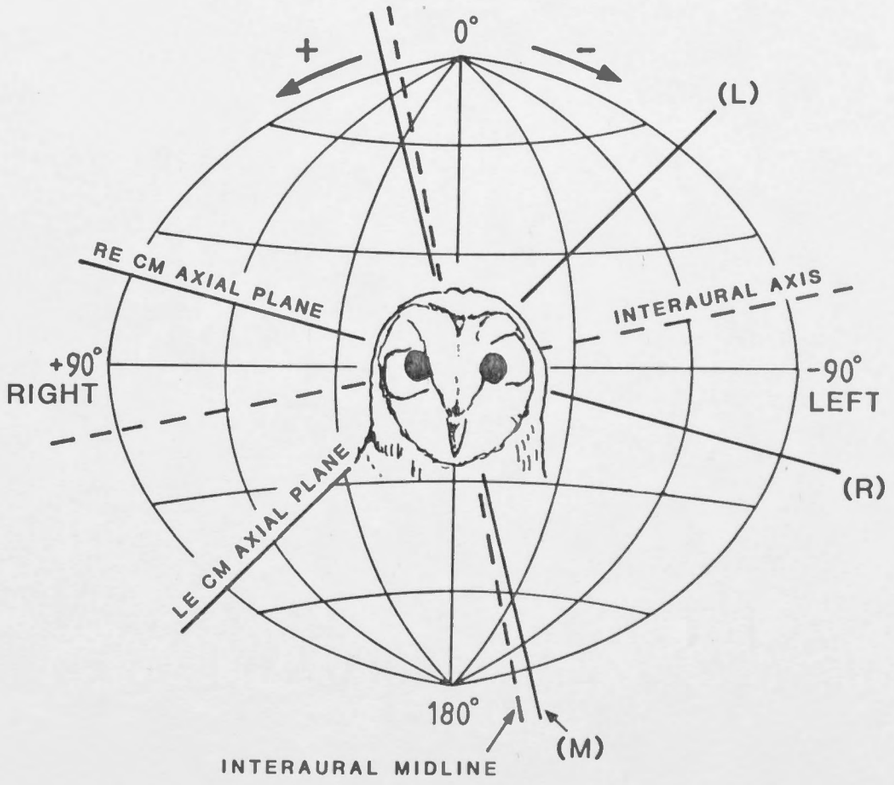
0°
+
-
(L)
RE CM AXIAL PLANE
INTERAURAL AXIS
+90°
RIGHT
-90°
LEFT
(R)
LE CM AXIAL PLANE
180°
(M)
INTERAURAL MIDLINE

Fig. 5.14. A comparison between CM directivity patterns for the left ear at 6kHz and 8kHz under normal conditions and with the contralateral ear canal blocked with silicon rubber. Details as for Figs 5.5, 5.12.

Tyto alba

NORMAL

CONTRA BLOCKED

COCHLEAR MICROPHONIC

6kHz
LE

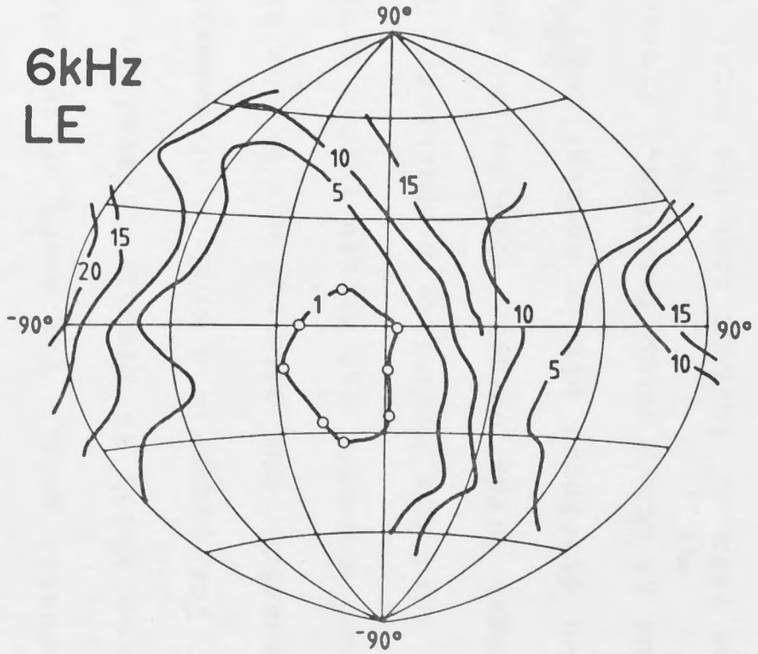

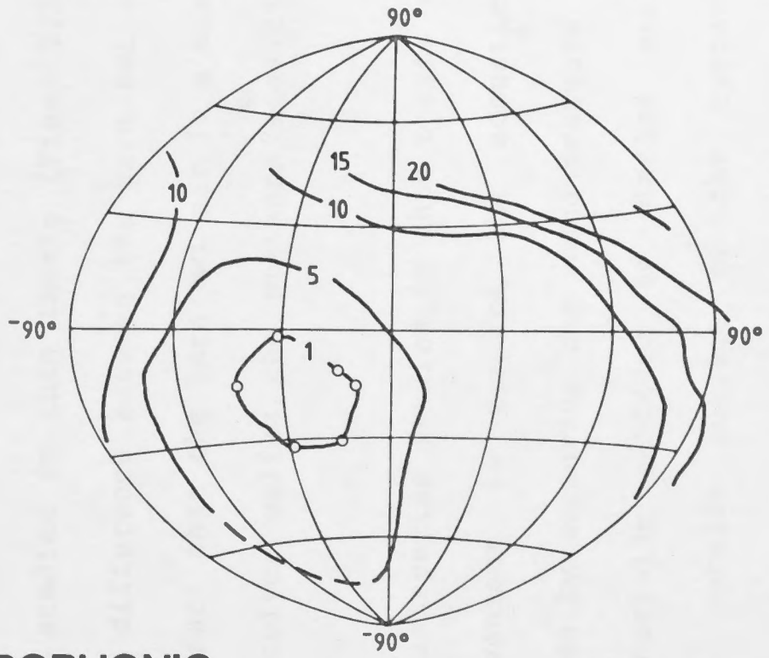

8kHz
LE

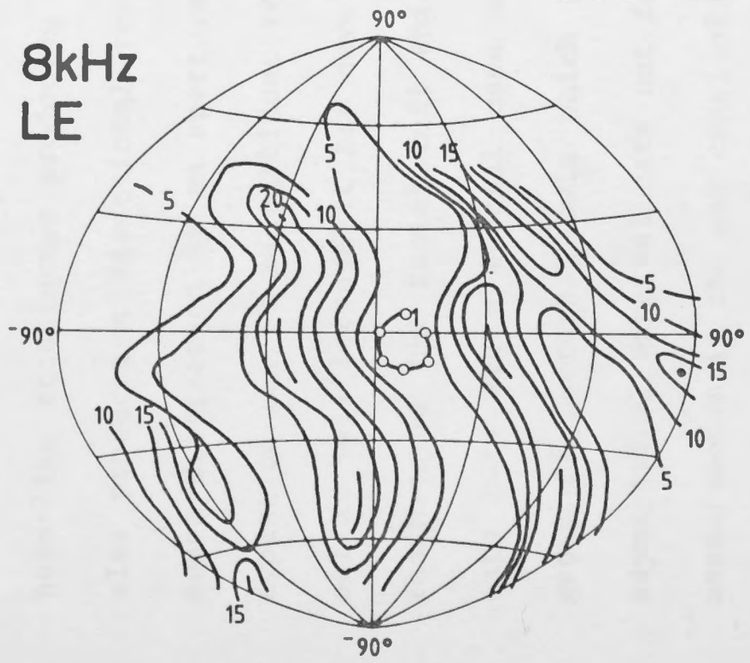

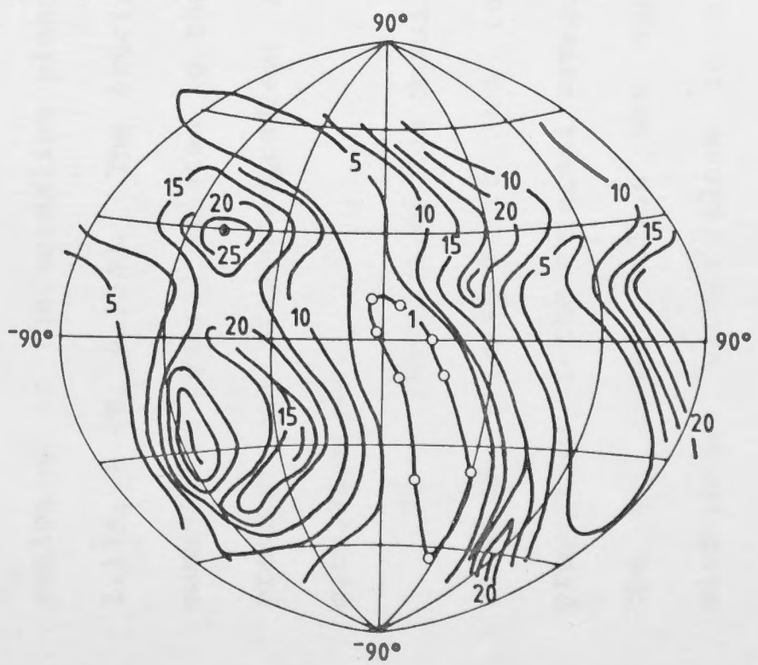

CHAPTER 6: GENERAL DISCUSSION AND CONCLUSIONS

In each of the mammalian species studied in this thesis an important feature of the external ear is the pinna because it acts as a horn-like transformer producing acoustic gain. The mouth of the pinna also produces a directional response which is closely related to the sound diffraction by an aperture. The pinna is a product of mammalian evolution but it is pertinent to consider the external ear of the barn owl as well because it has developed an outer ear cavity formed by the feathers of the facial ruff which also has horn-like properties. The barn owls are a special case amongst birds because they belong to a group of nocturnal owls which have developed highly specialized, and asymmetrical external ears not found in other avian families. Pressure measurements in the ear canal of the barn owl suggest that the outer ear cavity has acoustical properties similar to a finite conical horn in the important sound localization bandwidth (Fig. 5.4D) and is therefore analogous to the mammalian pinnae studied in this thesis (Figs. 2.2A, 2.11A, 4.4B, 4.13A). The crucial difference between the barn owl and mammals in general relates to the fact that the barn owl ear is a mixed pressure and pressure-gradient receiver unlike the pressure sensitive mammalian ear.

Since the ears of the mammalian species studied in this thesis are pressure receivers it was convenient to compare the acoustical properties of the external waveguide by measuring the sound pressure in the ear canal. This was successfully achieved by placing probe microphones either close to the outside surface of the tympanic membrane, as in the Macropods, or by replacement at the tympanic membrane as in the Microchiropterans. In the barn owl the acoustical measurements in the ear canal allowed a direct comparison with the

pressure response of the mammalian external ear.

In the case of the Macropods and the barn owl, the probe microphone was inserted into the ear canal as close as possible to the tympanic membrane. This insertion technique was chosen principally for anatomical considerations, since in these animals the tympanic membrane is an oblique termination of the ear canal and replacement of the tympanic membrane by the microphone is difficult. In the cat, Khanna and Stinson (1985) have indicated that there may be no precise "sound pressure at the eardrum", since the eardrum also forms an oblique termination of the ear canal. In addition, at high frequencies (above 10kHz in the cat) the presence of standing waves in the canal may produce pressure minima close to the eardrum, which can effect the pressure measurements depending on the position of the probe tip (Khanna & Stinson 1985). In the barn owl the microphone was positioned adjacent to the tympanic membrane and would not be expected to experience pressure minima due to standing waves in the ear canal since the ear canal is short (8mm) and measurements were generally limited to 10kHz. However resonance of the head cavities, including the interaural cavity, may to contribute to the ear canal pressure as discussed in chapter 5. For the Macropods, pressure measurements in the ear canal were obtained for frequencies up to 40kHz and thus several pressure minima and maxima can occur along the ear canal during higher modes of resonance. Given the limitations of placing a microphone (1/4" Bruel and Kjaer) close to the eardrum, it is assumed that as a pressure receiver, the eardrum would also experience similar pressure

variations. In the Microchiroptera, the tympanic membranes were approximately perpendicular terminations of the ear canal and microphone replacement of the tympanic membrane was relatively straightforward. In these cases the limitations of pressure measurement in the ear canal depend on the assumption that the tympanic membrane is a relatively rigid termination (Moller 1983).

The measurements of acoustic gain for the external ears of each vertebrate species have shown that sound pressure can be amplified by up to about 25dB in each system (Figs. 2.2B, 2.11B, 4.3, 4.13B, 5.4B). The present results suggest that one role of the external ear may be to improve sensitivity to sound and therefore enhance hearing thresholds and although the response of the tympanic membrane may be proportional to pressure in mammals, there are many components of the auditory system which are also likely to influence hearing thresholds. Nevertheless, the presence of the pinna in *Macroderma gigas* and *Nyctophilus gouldi* was seen to enhance neural thresholds to sound (Figs. 2.19, 2.23) reflecting to a large extent the acoustic gain of the pinna as measured in the ear canal (Figs. 2.2B, 2.11B). Likewise behavioural thresholds to sound are higher following pinna removal in cats and suggest that the pinna may contribute to the frequency dependent amplification of pressure (Flynn and Elliott, 1965). The maximum acoustic gain of the pinnae studied in this thesis range up to about 15dB and compare favourably with a variety of other mammalian species (Shaw 1974).

There have been several attempts to compare the acoustic tracheae in several species of insects with acoustic horns in terms of the possible amplification of pressure at the tympana (Lewis 1974; Seymour *et al.* 1978; Larsen 1981; Hill and Oldfield 1981). In *Ruspolia differens* for example, the potential pressure gain by the trachea can be estimated theoretically to be 17dB by reference to the anatomy (Lewis

1974). Experimentally, a maximum pressure gain of 10dB can be measured by laser interferometry at the tympanum in *R. differens* and *Tettigonia viridissima* (Seymour *et al.* 1978). In these species about 14dB of acoustic gain can be estimated by the impulse response of the tympanum (Larsen 1981). In other insect species, direct acoustical measurements have been made using probe microphones attached to the distal end of the acoustic trachea (Hill and Oldfield 1981) and show amplification of pressure up to 15dB which is consistent with the increase in neural thresholds produced by abbreviation of the leg trachea.

Although the technique of pinna removal to estimate acoustic gain is only approximate since the pinna and meatus are acoustically coupled, the results presented here can be modelled reasonably closely by the gain of a simple finite conical horn. This approach is also valid for the barn owl except that the facial ruff is removed as an integral part of the outer ear cavity. Obviously there are severe limitations placed on designing a horn-like cavity from feathers since the outer ear cavity in the barn owl behaves like a finite conical horn up to 8kHz only (Fig. 5.4A). The pinna can operate as a fairly efficient, albeit non-ideal horn, at higher frequencies as in the case of bats (Figs. 2.2A, 2.11A) but the efficiency of a horn-like outer ear cavity in the barn owl need only be limited to frequencies below 10kHz because of low frequency hearing in birds. In general, the efficiency of the horn-like pinnae or outer ear cavity as sound collectors increases rapidly above a "cut-off" frequency region where the circumference of the mouth approaches and starts to exceed the wavelength ($ka > 1$, see Fig. 6.1A and Beranek 1954). The term cut-off frequency is used loosely because it strictly applies to sound propagation in infinite exponential and catenoidal horns (Olson 1947). As the horns in question here are approximately

conical they will also show a rapid deterioration in their propagation characteristics below certain frequencies which will depend on the cone angle (Fletcher and Thwaites 1979). A further consideration for these biological horns is that their "finite" length will produce resonance in the frequency range of increasing horn efficiency, which will tend to improve the pressure response at the tympanic membrane (see below and APPENDIX 1; Olson 1947; Fletcher and Thwaites 1979).

An obvious feature of the design of the mammalian pinna or outer ear cavity in the barn owl, which detracts from the idealness of a horn is the structural asymmetry. In the Macropods, the pinna is largely asymmetrical in the vertical plane (Figs. 4.1, 4.12) whereas in the Microchiropteran bats a severe asymmetry of the pinna exists in both dimensions (Figs. 2.1, 2.10). In the barn owl, the outer ear cavity is largely asymmetrical in the horizontal plane only (Figs. 5.1; 5.3). The obliquely truncated appearance of these horn-like soundguides made it necessary to assume "average" dimensions such as the radius of the mouth, and length of the horn which are obviously complicated by a frequency dependence for the position of the acoustic axis in *M. gigas*, *N. gouldi* and *T. alba* (Figs. 2.8, 2.16, 4.11, 4.18, 5.9 and see below). In terms of the finite length of the horns studied here, resonance can be expected to varying degree based on their idealized dimensions. Indeed, experimental observations suggest resonance for the pinnae of *M. gigas*, *N. gouldi* and *M. giganteus* (Figs. 2.2, 2.11, 4.13) which is generally consistent with the expected resonance of an equivalent finite (conical) horn. It seems likely that the variability in the resonance peaks or even the absence of resonance for any of the pinnae or the outer ear cavity of the owl is due to the obliquely truncated openings of these structures. A mathematical solution to the

problem of obliquely truncated horns is almost intractable but an oblique truncation will tend to reduce the reflection co-efficient at the mouth and, depending on the exact nature of the asymmetry, could easily reduce resonance (Fletcher pers. comm.). Horn resonance if apparent ranges between a half and quarter-wave length series depending on the flare of the horn as calculated from APPENDIX 1 (see also Olson 1947). If the pinnae or outer ear cavity are considered as finite conical horns then they each have a similar cone angle (25° - 30°; Table 6.1). However in each case the average diameter of the mouth is close to or exceeds the effective acoustic length of the horn which will tend to diminish resonance (Beranek 1954). In addition horn resonance should begin to disappear when the ratio of the circumference to the mouth compared to the wavelength (ka) exceeds about 1.25 (Fletcher and Thwaites, 1979), as indicated in Figs. 2.2, 2.11, 4.4, 4.13, 5.4). Certainly these biological horns cannot be considered "infinite" in the sense of no resonance (Beranek 1954) in view of the relevent wavelengths used for hearing and acoustic communication in these species (see below).

A second source of resonance in the external ear comes from the meatus which behaves acoustically like a closed tube. Therefore the fundamental frequency of quarter-wavelength resonance produces a pressure peak at or near the position of the tympanic membrane since the membrane normally represents a fairly rigid termination (Wiener *et al.* 1966; Shaw 1974; Moller 1983). Comparisons of the length of the meati of the species used in this thesis are made in Table 6.1. In *M. gigas*, *M. eugenii* and *M. giganteus* closed-tube resonance is strongly suggested by the gain curve of the external ear without the pinna (Figs. 2.2, 4.4, 4.13). In *N. gouldi* meatus resonance can also be identified from the

acoustical measurements (Fig. 2.11) but it is very weak, possibly due to the extremely short length of the meatus in this species (Table 2.1). The situation is more complicated in the barn owl because although there is a short meatus, the interaural cavity probably resonates in conjunction with the ear canal (Fig. 5.4) and may have an important role in the formation of a pressure gradient at the tympanic membrane (see DISCUSSION, CHAPTER 5).

To be useful in improving sensitivity to sound by the auditory system, biologically significant sounds should contain energy at frequencies where appreciable acoustic gain occurs in the external ear and also where the horn-like pinna or outer ear cavity is efficient. In the absence of neural or behavioural data for hearing in the Macropod species, the species-specific vocalizations described for *M. giganteus* fulfil this requirement since significant energy in the calls occurs above 1.5kHz (compare Figs. 4.13; 4.19). In the case of *Macroderma gigas* the energy in low frequency social communication calls in particular (Figs. 3.4, 3.6) are optimized with respect to the acoustical properties of the external ear and neural sensitivity to sound (Fig. 2.18). This is also true for the more limited observations in *Nyctophilus gouldi* for which the isolation call of the neonate has considerable energy below 25kHz (Figs. 2.22, 2.26). In both of these species of bats the frequency range which is used for sonar processing (Figs. 2.26, 3.1) is matched by a local peak in acoustic gain at the external ear (Figs. 2.2, 2.11) as well as the high frequency (ultrasonic) peak in the neural audiogram which may result from further specialization in the auditory system (Figs. 2.18, 2.22). Finally, the most sensitive hearing range in the barn owl is well known and occurs between 4-8kHz (Konishi 1973a,b; Knudsen and Konishi 1979; Knudsen

1984). Clearly the bandwidth of maximum pressure gain in the ear canal of the barn owl (Fig. 5.4) corresponds very closely to the most sensitive hearing range and is likely to have a major influence on auditory sensitivity to sound (see DISCUSSION, CHAPTER 5), notwithstanding the effect of a pressure gradient on the sensitivity of the ear.

DIRECTIONALITY

The existence of a horn-like external waveguide in the mammals and the barn owl as described in this thesis, has an important influence on ear directionality. Each external ear experiences a pressure response where the directionality is closely linked to sound diffraction by the open mouth of the pinna or, in the case of the barn owl, the open face of the ruff. With the exception of the barn owl, these ears are typical of mammalian auditory systems where directionality is produced by the aperture of a horn-like soundguide connected to a tympanic membrane which would otherwise have little inherent directionality. The directional response in the ear canal is due to the horn mouth which is exposed to the sound field rather than a result of diffraction by the surface of a hard sphere (head) as originally proposed for all vertebrate systems. Of course there are many mammals such as the primates where head shadow may have a dominant influence on directionality, in conjunction with a horn-like pinna (see Erulkar 1972; Shaw 1974). In this thesis the external ears are relatively large in comparison with the dimensions of the head and in each mammal the sound collecting surface, i.e. the pinna face, is placed on top of the head. In the barn owl, the facial ruff enlarges the entire head to form the outer ear cavity and consequently the influence of the head is involved in so far as the side of the face forms part of the outer ear cavity

(Figs. 5.1, 5.2; see also *M. gigas* and *N. gouldi* Figs. 2.1, 2.10).

In each external ear examined in this thesis, the directionality of the pressure response in the ear canal for the intact system is explained to a first approximation by the sound diffraction of a circular aperture. Ideal horn receivers are considered non-directional when the circumference of the aperture exceeds twice the wavelength ($ka < 0.5$; Beranek 1954) and all the external ears examined in this thesis are essentially non-directional using this criterion (see Table 6.1; Fig. 6.1B). Furthermore these external ears generate a directional response when the radius of the opening starts to exceed one fifth of a wavelength i.e. $ka > 1.25$ and become highly directional for $ka > 3$ (Fig. 6.1B; Beranek 1954; Fletcher and Thwaites 1979). So generally speaking, the average radius of a pinna opening can be used to determine the onset of directionality ($ka = 1.25$), and not the long axis or height of the pinna, as previously suggested by Phillips *et al.* (1982). For an elliptical-type of opening, sound wavelengths equal to the long axis of the pinna face produce a highly directional response ($ka =$ or 3.14; see Fig. 6.1B). The directional characteristics of the main lobe can be compared to diffraction theory (see APPENDIX 2) and for each external ear directionality depends on the relationship between the size of the opening and the wavelength which is summarized in Figs. 6.1 and 6.2. Consequently larger pinnae are more directional at lower frequencies with the pinna of *Macropus giganteus* and *Nyctophilus gouldi* being the two extreme cases considered in this thesis (see Table 6.1).

Although the acoustical measurements of directionality can be related to a circular aperture, the elliptical shape of the openings could account for some asymmetry in the directivity patterns (Figs. 2.4, 2.12, 4.5, 4.6, 4.14, 5.10). The circular aperture model is

satisfactory for the present data but it is useful to note that some gain in directionality particularly in elevation can result from a vertically orientated (major axis) elliptical opening. But given the experimental errors in measuring the directional responses in the ear canal, a pinna opening for example would need to be extremely asymmetrical or slit-like before losing substantial directionality in the plane of the minor axis.

A diffraction-limited neural response can be recognized in the inferior colliculus of *M. gigas* and *N. gouldi* by axial-type spatial receptive fields (Fig. 6.2C) as observed in other mammals (Semple *et al.* 1983; Moore *et al.* 1984a,b). In the cat both ear canal and CM directionality are similar (Middlebrooks and Pettigrew 1981; Phillips *et al.* 1982; Calford and Pettigrew 1984) as would be expected in a pressure receiver and closely linked to axial-type receptive fields which have been recorded from midbrain (Semple *et al.* 1983; Moore *et al.* 1984a,b) and cortical auditory neurons (Middlebrooks and Pettigrew 1981). Axial fields seem to be a general feature of neurons in the inferior colliculus of both echolocating (Fuzessary and Pollak 1984; Jen and Sun 1984) and non-echolocating mammal species (Semple *et al.* 1983; Moore *et al.* 1984a,b). If directionality in the central auditory pathway is limited by the directionality of the pinna then spatial acuity may well depend on the absolute size of the pinna. There are binaural neural mechanisms which may sharpen directionality by crossed inhibition in the afferent pathways (e.g. Grinnell 1963b; Grinnell and Grinnell 1965; Neuweiler 1970) and EI/IE neurones have been described in detail from dichotic experiments (see Erulkar 1972). However the relationship between binaural cell types and free field directionality in the inferior colliculus remains to be examined in detail. There is

evidence that auditory neurons of the superior colliculus in the guinea pig, which belong to the neural space map, rely totally on the binaural integrity of the auditory pathway (Palmer and King 1983, 1985) for their directionality. However, it has not been clearly resolved whether the formation of spatial receptive fields and a space map in the superior colliculus depend on monaural or binaural inputs, stimulus levels above threshold or even the influence of pinna position (Palmer and King 1982, 1983, 1985; King and Palmer 1983; Wise and Irvine 1983; Middlebrooks and Knudsen 1985; King 1985).

It is curious that the barn owl should develop a specialized external ear analogous to the mammalian pinna, particularly in view of the fact that birds already have an ear which is inherently directional due to pressure gradients at the tympanic membrane (Coles *et al.* 1980; Hill *et al.* 1980; Lewis and Coles 1980). The outer ear cavities are designed to generate main lobes of highly amplified sound pressure (due to horn characteristics) which are strategically directed towards the front of the barn owl's head. In order to facilitate a pressure gradient at the tympanic membrane it is imperative that the two fixed receiving horns create a spatial zone with a low interaural pressure difference (see DISCUSSION CHAPTER 5). The resultant ear (CM) directionality combines the advantages of pressure gradients and sound diffraction to produce superior spatial acuity for the barn owl (Knudsen 1980), compared to an equivalent mammalian system based on sound diffraction alone. It follows that sound localization may be equally precise in mammals but either a very large pinna may be needed depending on the wavelength, or alternatively small pinnae may be used in combination with ultrasound as seen in echolocating bats (Simmons *et al.* 1983; Masters *et al.* 1985).

The foregoing discussion suggests that there may be an important relationship between the directional properties of horn-coupled pressure receivers and biologically significant sounds. For example, the dominant energy band in a sonar signal will produce a highly directional response, if the wavelengths are approximately the height of the pinna as noted in several echolocating species by Simmons (1982). These wavelengths may also be highly amplified by the external ear. In this context the relatively large pinnae of *Macroderma gigas* (Table 6.1) provide directionality at lower frequencies than would otherwise be needed, simply on the basis of sonar signal processing. Whilst it has been possible to identify a low frequency social communication channel (Fig. 2.18 and see CHAPTER 3) in *M. gigas* for which sound localization would probably be important, the issue of passive localization for prey capture is highly relevant in this species of Megadermatid bat, as suggested in *Megaderma lyra* (Fiedler 1979; Neuweiler 1983, 1984; Neuweiler *et al.* 1984; Schmidt *et al.* 1984). The extremely high sensitivity to sound in the upper audio bandwidth in *Macroderma gigas* (Fig. 2.18) is analogous to the highly sensitive hearing in the barn owl (Konishi 1973a). The size of the pinna in *M. gigas* is important for producing directionality in this lower frequency hearing range. Further experiments are needed to determine the role of passive hearing in *M. gigas* particularly for prey capture, including the frequency band required and accuracy of localization for this task.

AUDITORY SPACE AND FREQUENCY

An interesting property of the pinnae of *Macroderma gigas* and *Nyctophilus gouldi* and also the outer ear cavity of the barn owl was a frequency dependence for the location of the main lobe of the directivity patterns measured in the ear canals (Figs. 2.7, 2.8, 2.16,

5.9). Both Macropod pinnae are asymmetrical in vertical cross-section, but they did not exhibit any significant movement of the acoustic axis with frequency, except perhaps for a slight shift in elevation in *M. eugenii* (Figs. 4.11, 4.18 and see DISCUSSION CHAPTER 4). Obviously a biological horn such as the pinna or outer ear cavity needs to be "extremely" asymmetrical before the acoustic axis will deviate from the geometric axis, given the irregular shapes involved. The physics of obliquely truncated horns is extremely difficult to predict mathematically, and an exact solution is beyond the scope of this thesis. Nevertheless, a simple acoustical model was developed based on the geometry of the pinna or outer ear cavity treated as a conical horn, which accounts for the movement of the acoustic axis, at least for limited but important bandwidths (see APPENDIX 3). Without more detailed acoustical considerations, it would appear that in each case the acoustic axis approaches the cone axis as frequency increases (Figs. 2.8, 2.16, 5.3, 5.9). It can be assumed that there is a tendency for the maximum sound energy (acoustic axis) to be intercepted by a plane normal to the pinna face (as in a right cone) and that there is likely to be a maximum half-wavelength limit imposed on the position of this mouth in the asymmetrical cavity by the interference of sound waves travelling the longer path down the extended edge of the oblique truncation (APPENDIX 3). The significance of this finding for hearing and sound localization is not clear at present but relates to the anatomical design of the pinna or outer ear cavity. The frequency dependent position of the acoustic axis and spatial receptive fields in the midbrain of *Macroderma gigas* (Fig. 2.21) are similar to the relationship between ear directionality and neuronal spatial receptive fields in *Pteronotus parnellii* (Fuzessery and Pollak 1984). Both

Macroderma gigas and *Pteronotus parnellii* are bats with restricted ear movements and under such circumstances auditory space may be mapped neurally by the tonotopic organization. The stability of such maps would need to be tested because any significant ear movement will cause the same problems for the mapping of space at the neuronal level as is seen in mammals with mobile ears (see below). In head referenced auditory systems such as in humans, there is evidence that spectral cues by the pinna form the basis for vertical localization (e.g. Butler 1974; Oldfield and Parker 1984a,b). For the barn owl, frequency dependent movement of the main lobes in azimuth for the pressure response in the ear canal (Fig. 5.9) is important for maintaining the pressure balance at the two input ports, for a restricted region of frontal space (see DISCUSSION CHAPTER 5). Whilst this frequency dependent movement of the acoustic axis is important for maintaining a pressure gradient at the tympanic membrane, it is clear that the spatial location of the CM axis (Fig. 5.9) is determined by a different mechanism. It has been shown that the CM axis position, particularly in azimuth, is closely related to the stimulus directions which would be expected to produce the maximum net pressure at the tympanic membrane by the acoustical interference of opposing sound waves (Fig. 5.9). The pressure gradient also accounts for the directivity of the main lobe in the CM directional plane (Figs. 5.7, 5.8). Thus the amplitude of vibration of the tympanic membrane in the barn owl depends intimately on the wavelength and the phase or time delays introduced by the internal and external waveguides to the tympanic membrane.

AUDITORY SPACE

Ear directionality is a two dimensional phenomenon since a spatial gradient exists in both azimuth and elevation unless a pinna opening for

example, becomes a very narrow slit. In many mammals the pinnae rotate independently, largely in the horizontal plane and thus the orientation of the pinna face to the sound source determines the pressure response. Consequently directional cues based on the interaural pressure (intensity) difference must depend on the relative position of the two pinnae to each other and the head. Under these circumstances it is reasonable to expect a continuously variable set of binaural disparities which could be analysed by the nervous system. The problem which arises in mammals with mobile pinnae relates to the synthesis of a neural map of auditory space. For mammals, such as the Macropod species studied in this thesis, the axial-type receptive fields of auditory neurones which would exist in the auditory system are likely to be relocated in space if the pinna is repositioned on the head. Such an effect has been reported for cortical neurons in the cat (Middlebrooks and Pettigrew 1981), inferior colliculus neurons in the cat (Aitkin *et al.* 1984) and the echolocating bat *Eptesicus fuscus* (Jen and Sun 1984). It is therefore possible for a single auditory neuron to map different regions of space depending on the natural range of pinna movements. Under such circumstances it is difficult to imagine how a neural map of auditory space comparable with that found in the barn owl midbrain (Knudsen and Konishi 1978a,b) could exist in the auditory system of mammals with significant pinna mobility. Some attempts to find neural space maps in the mammalian auditory system have reported a topographical representation of auditory space from deeper layers of the superior colliculus in the guinea pig (Palmer and King 1982; King and Palmer 1983; Palmer and King 1983, 1985) and in the cat (Middlebrooks and Knudsen 1984) but unsuccessfully in the bat *Eptesicus fuscus* (Poussin and Schlegel 1984; Jen *et al.* 1984; Shimozawa *et al.* 1984). It

is not known if these space maps are independent of pinna position but it has been reported that eye position can influence auditory receptive fields in the superior colliculus (Jay and Sparks 1982, 1984). The role of binaural processing needs to be firmly established since there is an indication that the space map in the superior colliculus of the guinea pig can be based on monaural or binaural hearing (Palmer and King 1983, 1985). Interestingly, the monaural space map in the guinea pig depends on the presence of the (immobile) contralateral pinna, but it is not known if the position of the acoustic axis of the pinna is frequency dependent, as in *M. gigas* and *N. gouldi*. Also, in the cat an auditory space map has been reported in the deeper layers of the superior colliculus (Middlebrooks and Knudsen 1984) but the acoustic axis of the pinna is not frequency dependent for natural "alert" pinna positions (Phillips *et al.* 1982; Calford and Pettigrew 1984).

A serious complication for the understanding of the neural mechanisms of auditory space mapping in the barn owl results from the data presented in this thesis. A frequency dependence is established for auditory space at the level of the cochlea which is largely due to the pressure-gradient at the tympanic membrane. This implies that auditory space can be mapped neurally by virtue of the tonotopic organization of the afferent auditory pathway. Studies on the neural mapping of auditory space in the barn owl midbrain have not recognized the role of frequency, apart from the fact that sounds are localized within a narrow bandwidth (Konishi 1973a; Knudsen and Konishi 1979). However, the azimuth position of the best area for limited field auditory neurons in the optic tectum of the barn owl show a significant movement towards the midline with increasing best frequency (Knudsen 1984). It has been previously reported that the neural mapping of

auditory space in the frog midbrain is based on tonotopicity (Pettigrew *et al.* 1978) and ear directionality in the frog is based on pressure gradients (Chung *et al.* 1978) as described here in CHAPTER 5 for the barn owl.

The possibility of using frequency to code for auditory space is very attractive because it provides a physical reference which cannot be generated by the nervous system. Such a scheme is feasible for a pressure gradient ear but requires the appropriate acoustical pathways at the periphery. Clearly a frequency dependent space map is not available to mammals such as the cat, or the Macropods studied here because no significant frequency dependent shift in the acoustic axis is evident. It is therefore pertinent to consider the external ears of bats like *Macroderma gigas*, *Nyctophilus gouldi* and *Pteronotus parnellii* for which the position of the acoustic axis does vary with frequency for certain frequency ranges. Characteristically these bats are unable to make gross pinna movements which is strikingly apparent in *Macroderma gigas* because of the complete fusion of the pinnae at the midline. It is possible to speculate that head-referenced directionality at the periphery may necessitate the frequency dependent movement of the main lobe of the ear directivity patterns. The neural consequences would then be a neural space map involving the tonotopic organization which has hitherto not been implicated in space mapping in mammals *per se*, except in the study of the bat *Pteronotus parnellii* (Fuzessery and Pollak 1984). At the other extreme it is possible to imagine that a neural space map may become head referenced in mammals with mobile pinnae if an efference copy of ear position was integrated with auditory sensory neurones.

TABLE 6.1: DIMENSIONS AND PARAMETERS FOR VARIOUS EXTERNAL EARS IN VERTEBRATES

SPECIES	PINNA/OUTER EAR CAVITY (MOUTH)				DIRECTIONALITY		PINNA/OUTER EAR CAVITY (THROAT)		HORN LENGTH			MEATUS	TYMPANIC MEMBRANE	HORN PARAMETERS		
	circum-ference $2\pi a$ (cm)	av. radius a (cm)	height (cm)	width (cm)	onset ka=1.25 (kHz)	high ka = 3 (kHz)	circum-ference $2\pi a$ (cm)	av. radius a (cm)	Long (cm)	Short (cm)	Average (ℓ) (cm)	length (cm)	av. radius (cm)	G_∞ (dB)	cone angle	$\frac{2a}{\ell}$ (mouth)
Macroderma gigas[a]	10.7	1.7	5.6	2.2	4.0	9.6	4.0	0.4	4.3	0.6	2.4	1.1	0.14	13	29°	1.4
Nyctophilus gouldi[a]	5.3	0.85	2.8	1.2	8.1	18	1.1	0.2	2.2	0.4	1.3	0.25	0.14	13	27°	1.3
Macropus eugenii[a]	16	2.5	7.0	3.5	2.7	6.4	2.5	0.4	7.5	1.5	4.5	1.6	0.25	16	25°	1.1
Macropus giganteus[a]	24.5	3.9	8.2	3.0	1.76	4.2	6.9	1.1	9	2	5.5	3.2	0.27	11	27°	1.4
Tyto alba[a]	19	3.0	7.0	4.5	2.3	5.4	2.2	0.4	7.0	1.8	4.4	0.8	0.46	18	30°	1.4
Myotis l. lucifugus[b]	3.8	0.6	1.4	0.7	11.0	27										
Plecotus townsendii[b]	8.4	1.3	3.7	1.2	5.0	12										
Felis catus[c]	14.5	2.3	5.5	3.0	2.9	7.1	2.5	0.4	6.0	2.5	4.3	2				
Trichosurus vulpecula[c]	14.2	2.3	5.8	3.3	3.0	7.3			5.5	1.1	3.3					

a = present study, b = Grinnell & Grinnell 1965, c = personal observations

Fig. 6.1. A. Comparison of the average acoustic pressure gain of the various pinnae and outer ear cavity of *Tyto alba* as a function of the ratio between the circumference of the open mouth to the wavelength (*ka*).

B. Comparison of the average maximum directionality (dBmax) for ear canal measurements for the species studied in this thesis as a function of *ka* value.

A

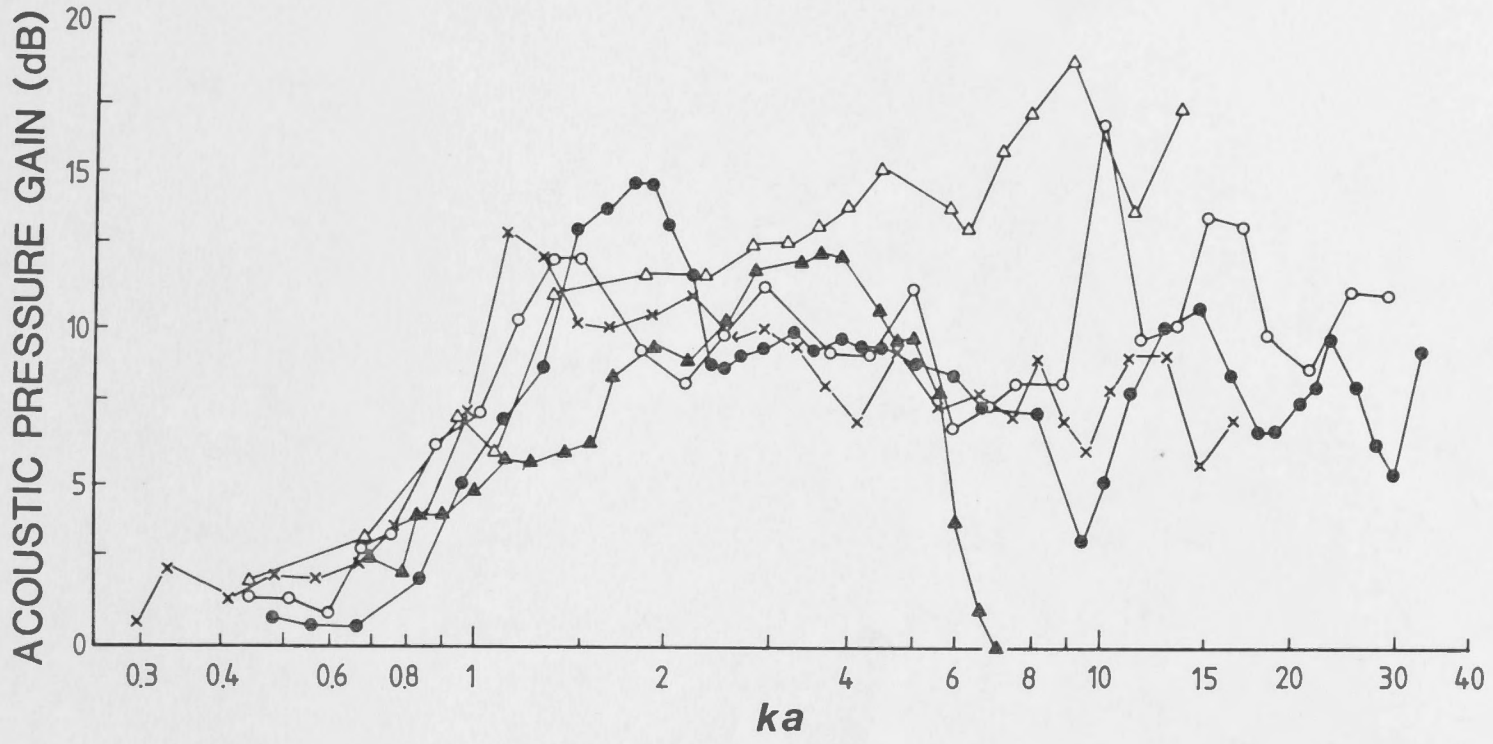
ACOUSTIC PRESSURE GAIN (dB)
0
5
10
15
20
0.3
0.4
0.6
0.8
1
2
4
6
8
10
15
20
30
40
ka

B

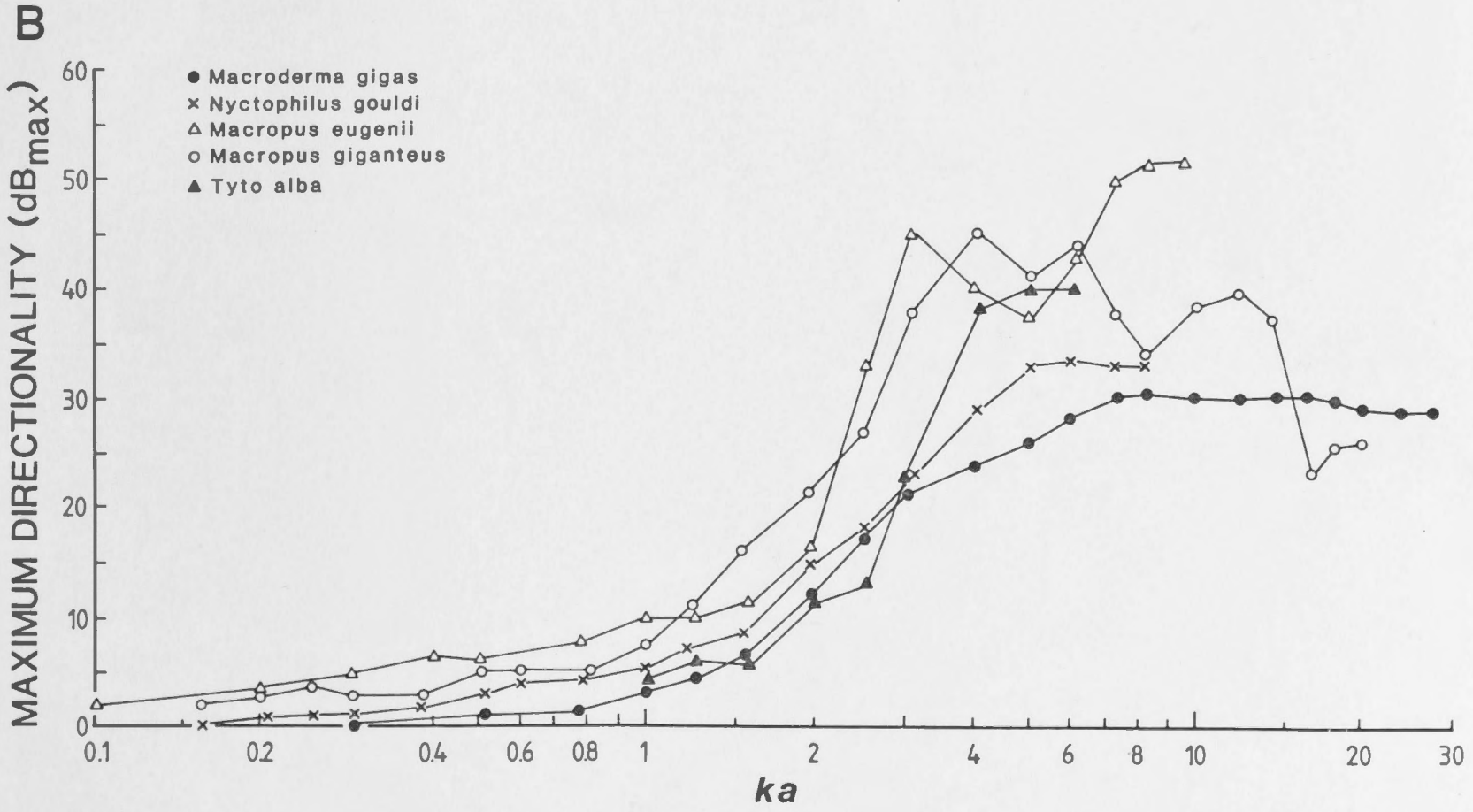
MAXIMUM DIRECTIONALITY (dB$_{max}$)
● Macroderma gigas
× Nyctophilus gouldi
△ Macropus eugenii
○ Macropus giganteus
▲ Tyto alba
0
10
20
30
40
50
60
0.1
0.2
0.4
0.6
0.8
1
2
4
6
8
10
20
30
ka

Fig. 6.2. A. and B. Comparison of -3dB acceptance angles (A) and null positions (B) as a function of *ka* values and based on the pressure measurements of directionality in the ear canals of the species studied in this thesis. Values are combined averages for azimuth and elevation measurements.

C. Comparison of average receptive field size (axial-type) for inferior colliculus neurones in *Macroderma gigas* and *Nyctophilus gouldi* as a function of the *ka* value for the pinna mouth.

In A,B and C, the dashed lines are the expected sound diffraction curves for a circular aperture expressed in terms of *ka* (see APPENDIX 2).

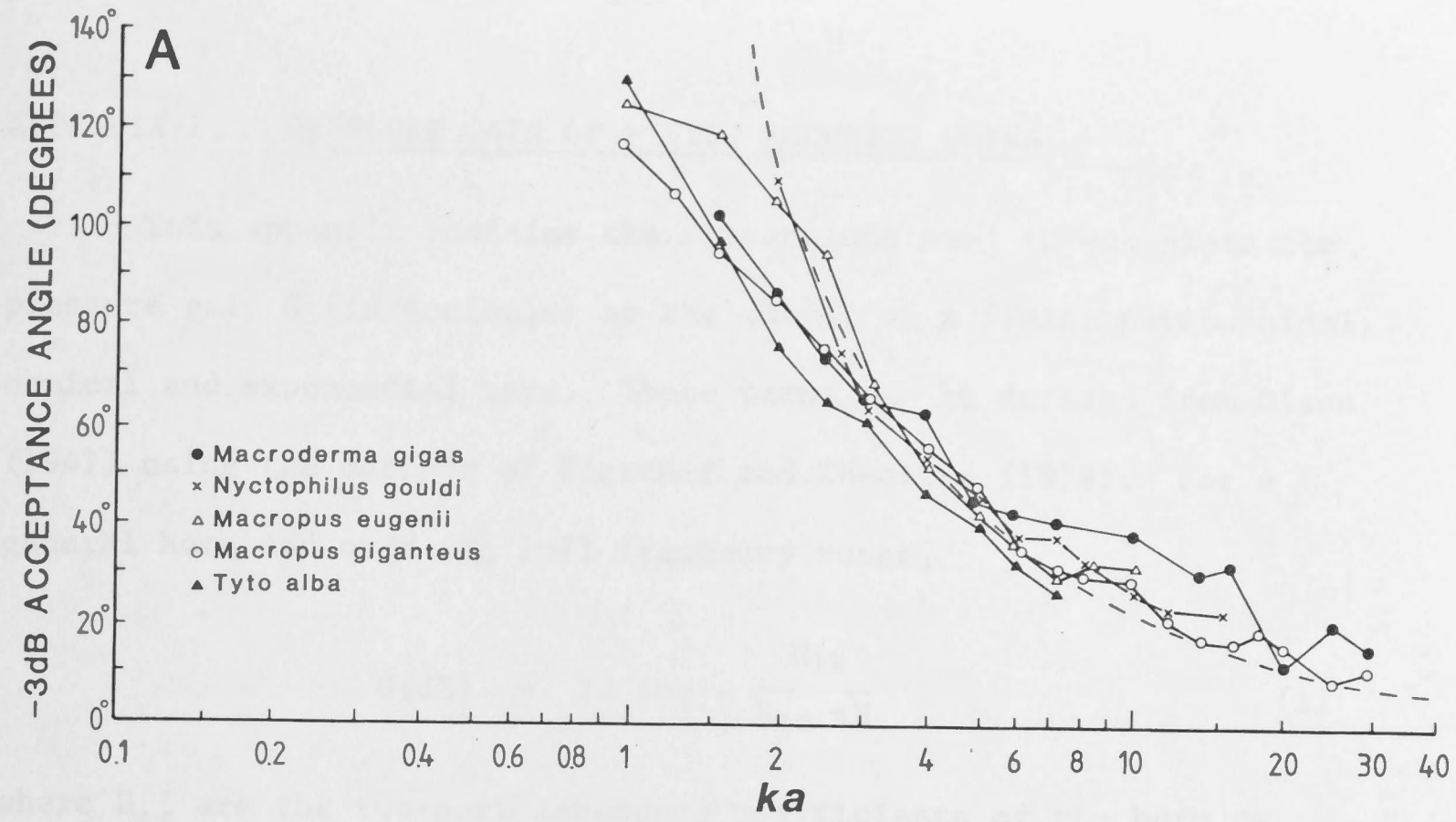
A
-3dB ACCEPTANCE ANGLE (DEGREES)
140°
120°
100°
80°
60°
40°
20°
0°
● Macroderma gigas
× Nyctophilus gouldi
△ Macropus eugenii
○ Macropus giganteus
▲ Tyto alba
0.1
0.2
0.4
0.6
0.8
1
2
4
6
8
10
20
30
40
ka

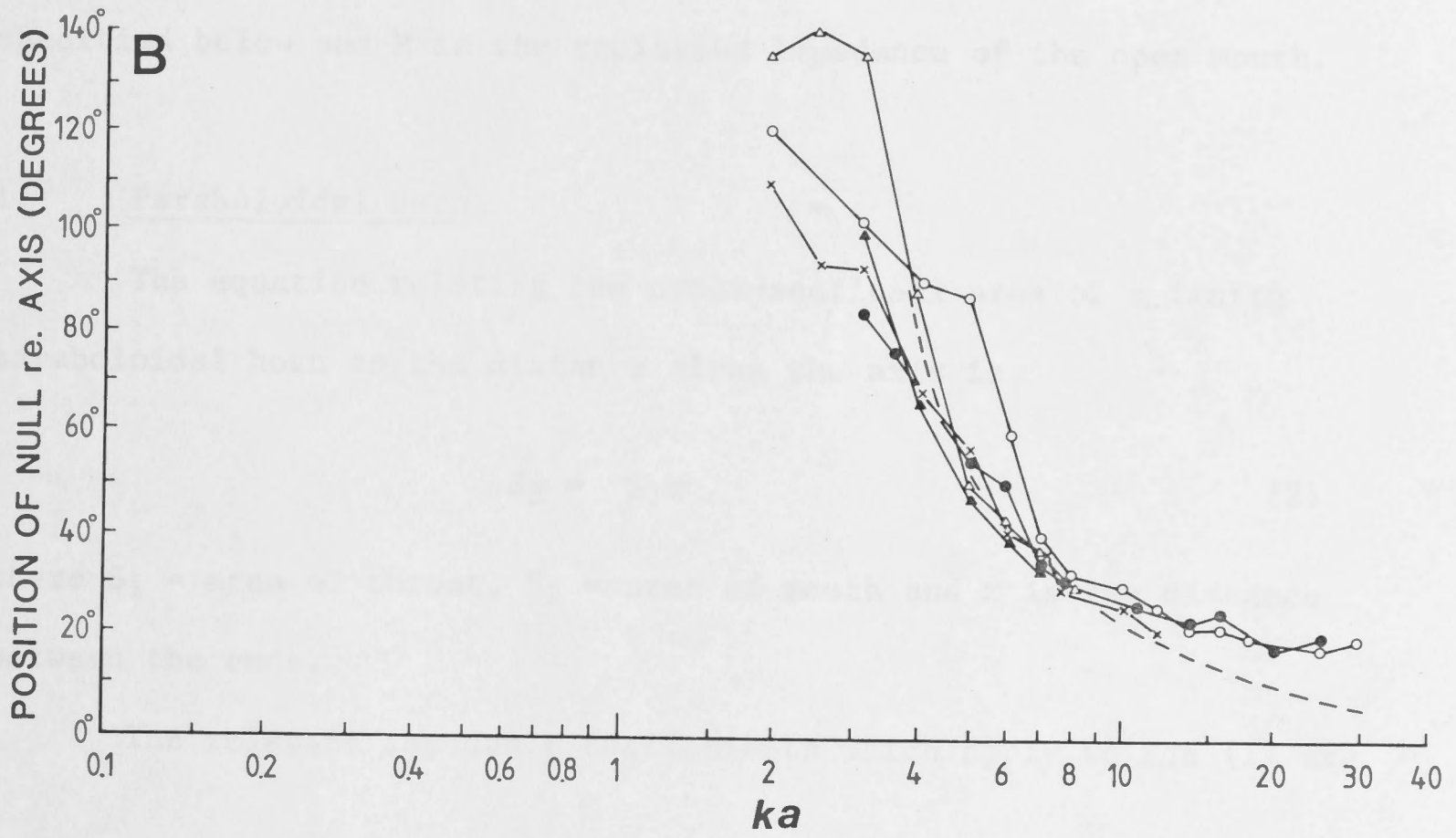
B
POSITION OF NULL re. AXIS (DEGREES)
140°
120°
100°
80°
60°
40°
20°
0°
0.1
0.2
0.4
0.6
0.8
1
2
4
6
8
10
20
30
40
ka

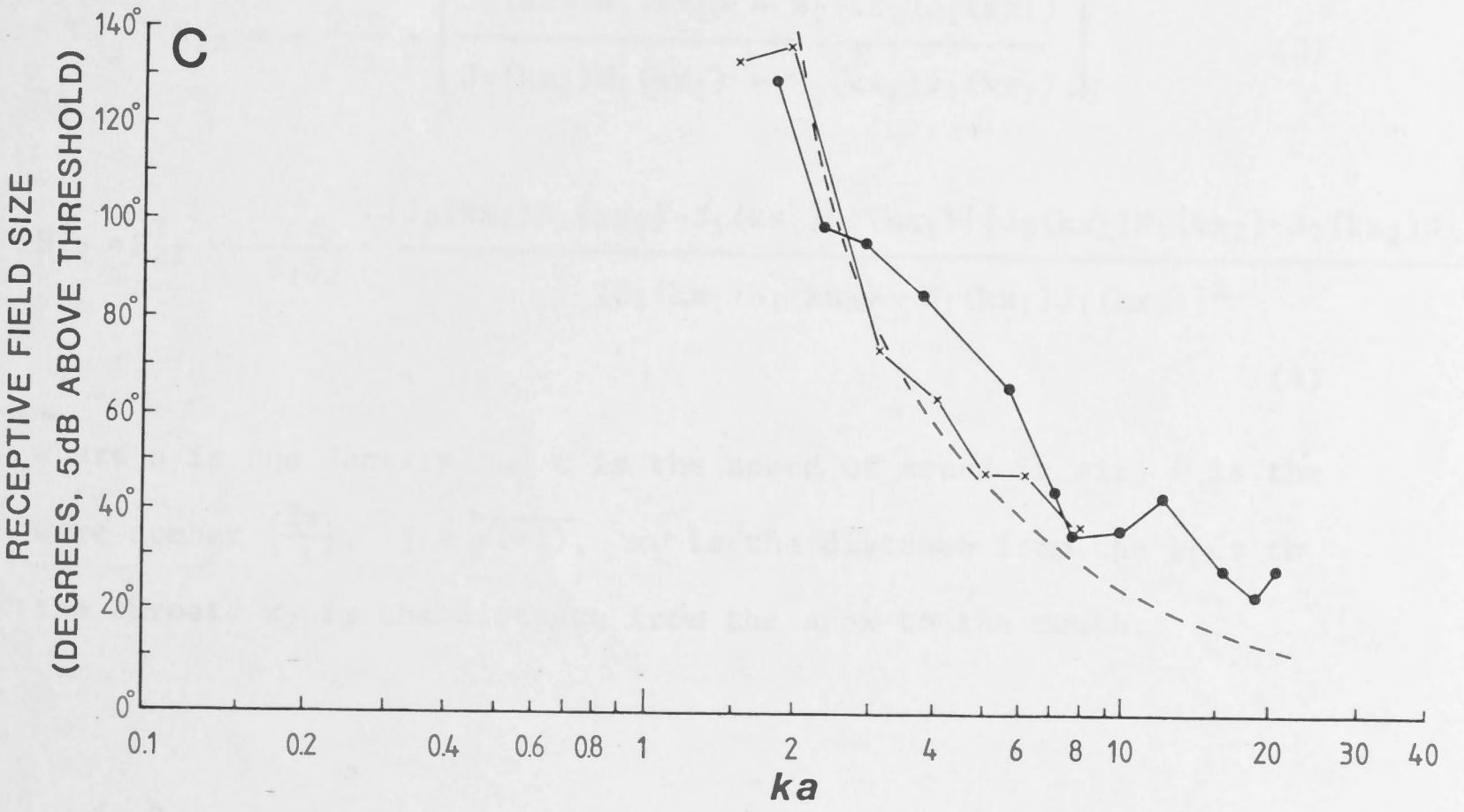
C
RECEPTIVE FIELD SIZE
(DEGREES, 5dB ABOVE THRESHOLD)
140°
120°
100°
80°
60°
40°
20°
0°
0.1
0.2
0.4
0.6
0.8
1
2
4
6
8
10
20
30
40
ka

APPENDIX 1. PRESSURE GAIN OF FINITE ACOUSTIC HORNS

This appendix contains the expressions used to calculate the pressure gain G (in decibels) at the throat of a finite paraboloidal, conical and exponential horn. These terms can be derived from Olson (1947) using the methods of Fletcher and Thwaites (1979). For a general horn and over the full frequency range,

$$G(dB) = 20 \log_{10} \frac{H_{12}}{H_{22} + R} \qquad (1)$$

where H_{ij} are the two-port impedance coefficients of the horn as specified below and R is the radiation impedance of the open mouth.

1. Paraboloidal horn

The equation relating the cross-sectional area of a finite paraboloidal horn to the distance along the axis is,

$$S_2 = S_1 x \qquad (2)$$

where S_1 = area of throat, S_2 = area of mouth and x is the distance between the ends.

The relevant impedance coefficients which apply to Eqn (1) are

$$H_{22} = - \frac{j\rho c}{S_2} \cdot \left[\frac{J_0(kx_2)N_1(kx_1) - N_0(kx_2)J_1(kx_1)}{J_1(kx_2)N_1(kx_1) - N_1(kx_2)J_1(kx_1)} \right] \qquad (3)$$

$$H_{12}^2 = H_{21}^2 = - \frac{\rho c}{S_1 S_2} \cdot \frac{[J_0(kx_1)N_1(kx_1) - J_1(kx_1)N_0(kx_1)][J_0(kx_2)N_1(kx_2) - J_1(kx_2)N_0(kx_2)]}{[J_1(kx_1)N_1(kx_2) - N_1(kx_1)J_1(kx_2)]^2} \qquad (4)$$

where ρ is the density and c is the speed of sound in air, k is the wave number $\left(\frac{2\pi}{\lambda}\right)$, $j = \sqrt{(-1)}$, x_1 is the distance from the apex to the throat, x_2 is the distance from the apex to the mouth.

J_0 and J_1 are cylindrical Bessel functions of order zero and one respectively and N_0 and N_1 are Neumann functions of order zero and one respectively. Tables of these Bessel functions and modified Bessel functions can be found in standard acoustic texts, e.g. Morse (1948).

2. Conical Horn

The equation relating the cross-sectional area of a finite conical horn to the distance along the axis is,

$$S_2 = S_1 x^2 \tag{5}$$

where S_1 = area of throat, S_2 = area of mouth and x is the distance between the ends. The relevant impedance coefficients are

$$H_{22} = \frac{-j\rho c}{S_2} \cdot \frac{\sin k(\ell+\theta_1)\sin k\theta_2}{\sin k(\ell+\theta_1-\theta_2)} \tag{6}$$

$$H_{12} = H_{21} = \frac{j\rho c}{(S_1 S_2)^{\frac{1}{2}}} \cdot \frac{\sin k\theta_1 \sin k\theta_2}{\sin k(\ell+\theta_1-\theta_2)} \tag{7}$$

where ρ is the density and c is the speed of sound in air, k is the wave number $(2\pi/\lambda)$, ℓ is length of the horn, $j = \sqrt{-1}$. The quantities θ_1 and θ_2 are given by $k\theta_1 = \tan^{-1} kx_1$ and $k\theta_2 = \tan^{-1} kx_2$ where x_1 is the distance from the apex to the throat and x_2 the distance from the apex to the mouth.

3. Exponential Horn

The equation relating the cross-sectional area of a finite exponential horn to the distance along the axis is

$$S_2 = S_1 e^{mx} \tag{8}$$

where S_1 = area of throat; S_2 = area of mouth, x is the distance between the ends and m is the flare constant. The relevant impedance coefficients which apply to Eqn (1) are

$$H_{22} = - \frac{j\rho c}{S_2} \cdot \frac{\cos(b\ell-\theta)}{\sin b\ell} \qquad (9)$$

$$H_{12} = H_{21} = - \frac{j\rho c}{(S_1 S_2)^{\frac{1}{2}}} \cdot \frac{\cos\theta}{\sin b\ell} \qquad (10)$$

where $\theta = \tan^{-1}(a/b)$ given that $a = m/2$, and $b = \frac{1}{2}\sqrt{(4k^2 - m^2)}$. As above ρ is density and c is the speed of sound in air, k is the wave-number, ℓ is the length of the horn, $j = \sqrt{-1}$.

The radiation impedance of the mouth R for the above horns can be calculated from expressions given in standard texts on acoustical theory (Olson 1947). For convenience, values of R can be estimated from the graphical solution given by Olson (1947) Fig. 5.2.

The above expressions for each horn were evaluated using a computer program, for the full range of test frequencies used in each species. The results of these expected gain curves are plotted in comparison with the experimental gain curve data as shown in Figs. 2.2B,C, 2.11B,C, 4.4B,C, 4.13B,C, 5.4C.

For each of the horns mentioned above, the maximum pressure gain at the throat G_∞ at very high frequencies (neglecting resonance) will tend to

$$G_\infty(dB) = 10 \log_{10} \frac{S_2}{S_1} \qquad (11)$$

Thus the theoretical pressure gain maximum G_∞ for an efficient horn can be computed from the physical dimensions of each pinna and the outer ear cavity of the barn own (Tables 2.1, 4.1, 5.1 and 6.1) and compared with the observed pressure gains (Figs. 2.2, 2.11, 4.4, 4.13, 5.4).

APPENDIX 2. SOUND DIFFRACTION BY A CIRCULAR APERTURE

By the reciprocity theorem the directionality of a system as a sound transmitter is the same as that when it acts as a receiver. Therefore the directivity pattern for sound diffraction by a circular aperture will be equivalent to the directivity function for a rigid circular piston in an infinite baffle or plane wall (Rayleigh 1877 and Olson 1947).

The off-axis sound pressure amplitude (p_θ) relative to the axial pressure (p) is given by

$$\frac{p_\theta}{p} = \frac{2\,J_1(x)}{x} \quad \text{or} \quad \frac{2\,J_1(k a \sin\theta)}{k a \sin\theta} \tag{12}$$

where $J_1(x)$ is the cylindrical Bessel function of the first kind of order one, k is the wave number ($2\pi/\lambda$), a is the radius of the aperture, θ is the angle of the sound source from the acoustic axis and λ is the sound wavelength. The directivity function $2J_1(x)/x$ is unity for x=0 but for larger values of x it has an oscillatory behaviour with amplitude decreasing asymptotically as $x^{-\frac{3}{2}}$. Tables are given by Morse (1948). The acceptable angle for the directional response of the various ears was taken at the -3dB level for acoustical and CM measurements for which the pressure ratio, $p_\theta/p = 0.71$. By using this criterion to determine the amplitude of the directivity function $2J_1(x)/x$, the value of the angle parameter $x = 1.6$. Therefore the relationship

$$k a \sin\theta \quad \text{or} \quad \frac{2\pi a}{\lambda} \cdot \sin\theta = 1.6 \tag{13}$$

can be used to plot the variation between the -3dB acceptance angle (given at the full angular width, $2\theta°$) and the wavelength for a circular aperture of given radius, as shown in Figs. 2.5, 2.14, 4.8,

4.16, 5.7, 6.2A. Likewise a criterion of 5dB above the most sensitive threshold for neuronal (axial-type) receptive field boundaries can be compared to diffraction by a circular aperture (see Figs. 2.21, 2.25, 6.26). A -5dB acceptance angle represents a pressure ratio $p\theta/p = 0.56$ and the angle parameter $x = 2.0$, which then can be substituted into Eqn (13) to plot expected curves for diffraction (Figs. 2.21, 2.25, 6.2C).

For the circular aperture, positions of zero pressure or nulls will occur in the directivity pattern whenever the directivity function $2J_1(x)/x$ goes to zero (Morse 1948). This will occur for $x = 3.83$, 7.02, 10.17, 13.32 etc. and thus for the first zero

$$ka\sin\theta = 3.83 \text{ or } \sin\theta = \frac{1.22\lambda}{2a} \qquad (14)$$

which will define the semi-angle of the major lobe of the directivity pattern. The relationship in Eqn. (14) is plotted in Figs. 2.6, 2.15, 4.9, 4.17, 5.8, 6.2B for circular apertures with radii based on the average radii of the open faces of the pinnae and the facial ruff (see Tables 2.1, 4.1, 5.1, 6.1).

APPENDIX 3. MOVEMENT OF THE ACOUSTIC AXIS WITH FREQUENCY

The pinna of each mammal species and the outer ear cavity of the barn owl are all asymmetrical structures (Figs. 2.1, 2.10, 4.1, 4.12, 5.1, 5.3). However in treating these outer ear cavities as simple acoustical horns (APPENDIX 1) it is assumed that they are symmetrical in shape. For sound diffraction by the mouth of an ideal horn the acoustic axis will coincide with the geometric axis for all frequencies. In the case of an obliquely truncated right cone for example, it may be expected that the acoustic axis will diverge from the geometric axis of the conical horn. A simple acoustical model can be developed to understand the frequency dependence of the acoustic axis in several asymmetrical horn-like cavities and is based on the geometry of the pinna in *Macroderma gigas* and *Nyctophilus gouldi* and the outer ear cavity in *Tyto alba* as shown in Figs. 2.1, 2.10, 5.3.

In principle, most of the wave energy will be guided into the cavity of a horn receiver from a direction normal to the plane of the mouth. However, in the case of an oblique truncation, the wave fronts travelling towards the throat from the longer sides will be delayed relative to the shorter sides. In acoustical terms this delay will become important if the phase shift exceeds 180° because the path difference will start to subtract energy from the signal. This suggests that the largest useful mouth for a given wavelength is likely to occur when the path length from the normal (right-angled) truncation point to the tip of the extension is $\frac{\lambda}{2}$ (see APPENDIX 3 Fig. 1). Since the pinnae of *M. gigas* and *N. gouldi* and the outer ear cavity of *T. alba* are irregular structures and not ideal obliquely truncated horns, the plane of the normal truncation point was difficult to estimate precisely (see Figs. 2.1, 2.10 and 5.3). Nevertheless, to a first approximation the expected position of the acoustic axis (θ)

based simply on the geometry of the asymmetry of the outer ear cavity or pinna (Fig. 2.1, 2.10, 5.3) is given by

$$\cot(\theta+\phi) = \frac{2a_0 \sin\alpha}{\frac{\lambda}{2} - 2a_0\cos\alpha} \quad \text{or} \quad \frac{4a_0\sin\alpha}{\lambda - 4a_0\cos\alpha} \qquad (15)$$

where α is the angle between the approximate truncation plane and the extended edge of the horn, ϕ is the offset angle of the pinna or outer ear cavity from the midline (for azimuth effects) or the horizontal plane (for elevation effects), a_0 is the radius of the mouth at the truncation point and λ is the wavelength. The angle α can be estimated by considering the maximum length of the cavity extension (L_{max}) and the maximum diameter of the mouth of the cavity (M_{max}) as shown in APPENDIX 3, Fig. 1. The results of calculations for the expected movement of the acoustic axis as a function of frequency, based on Eqn (15) and the dimensions given in Figs. 2.1, 2.10 and 5.3 are plotted in comparison to the observed movements of the acoustic axis in azimuth and elevation where appropriate (Figs. 2.8, 2.16, 5.9).

APPENDIX 3

Fig. 1: The geometry of an approximate obliquely truncated conical horn as used to calculate the movement of the acoustic axis as a function of the wavelength. For definition of the symbols and their trigonometric relationship see text in APPENDIX 3 and Eqn. (15).

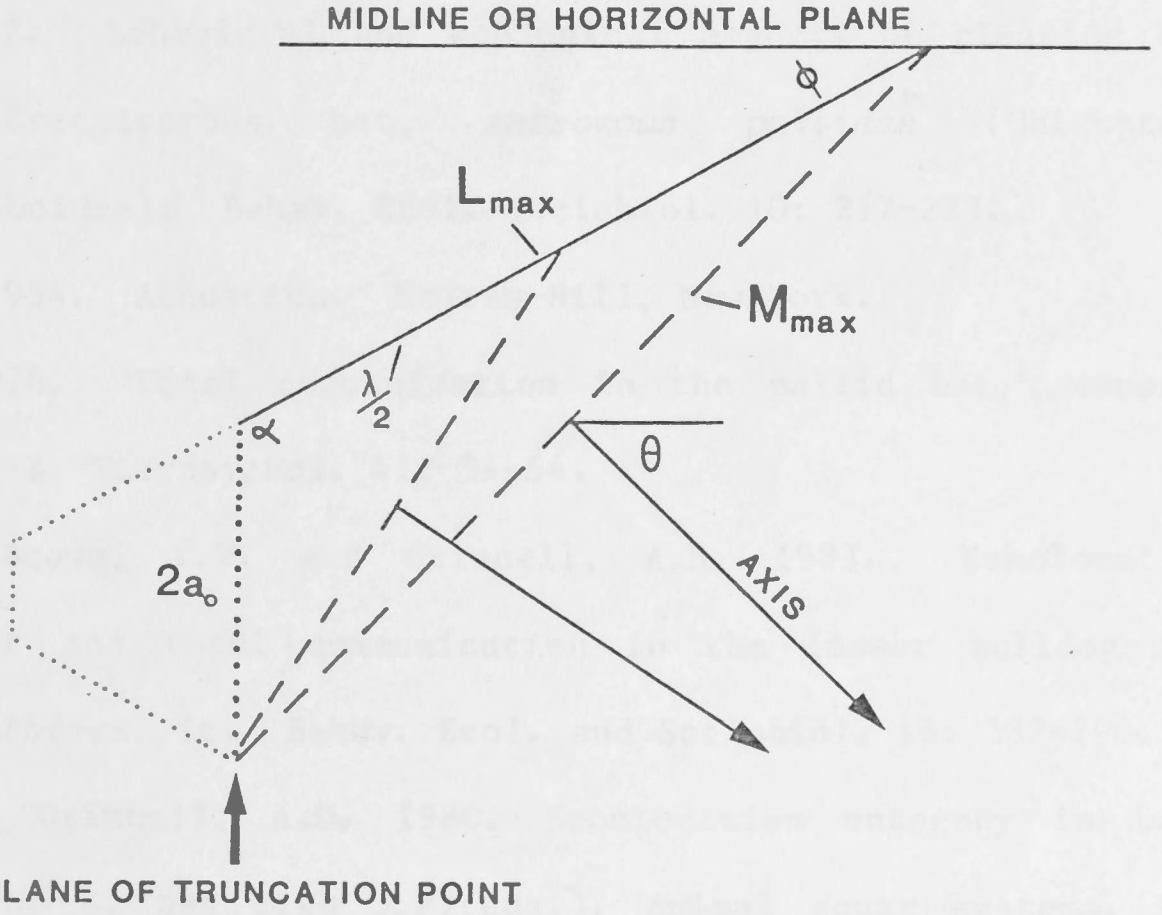

REFERENCES

Aitkin, L.M., Gates, G.R. and Phillips, S.C. 1984. Responses of neurons in inferior colliculus to variations in sound-source azimuth. J. Neurophysiol. 52: 1-17.

Autrum, H. 1942. Schallempfang bei tier und mensch Sonderdruck aus die Naturwissen. 30: 69-85.

Barclay, R.M.R. and Thomas, D.W. 1979. Copulation call of *Myotis lucifugus*: A discrete situation-specific communication signal. J. Mammal. 60: 632-634.

Batteau, D.W. 1967. The role of the pinna in human localization. Proc. Roy. Soc. London 158: 158-180.

Bell, G.P. 1982. Behavioral and ecological aspects of gleaning by a desert insectivorous bat, *Antrozous pallidus* (Chiroptera: Vespertilionidae). Behav. Ecol. Sociobiol. 10: 217-223.

Beranek, L.L. 1954. Acoustics. McGraw-Hill, New York.

Brown, P.E. 1976. Vocal communication in the pallid bat, *Antrozous pallidus*. Z. Tierpsychol. 41: 34-54.

Brown, P.E., Brown, T.W. and Grinnell, A.D. 1983. Echolocation, development and vocal communication in the lesser bulldog bat, *Noctilio albiventris*. Behav. Ecol. and Sociobiol. 13: 287-298.

Brown,P.E. and Grinnell, A.D. 1980. Echolocation ontogeny in bats. In:Busnel R.-G. and Fish J.F.(eds.). Animal sonar systems. NATO Advanced Study Institutes Ser. A., Vol. 28. Plenum Press, New.York, pp. 255-280.

Brown, P.E., Narins, P.M. and Grinnell A.D.1984. Low frequency auditory sensitivity of the pallid bat *Antrozous pallidus*. Am. Neurosci. Abst. 10:1150.

Buchler, E.R. and Childs, S.B. 1981. Orientation to distant sounds by foraging big brown bats (*Eptesicus fuscus*). Anim. Behav. 29: 428-432.

Buchler, E.R. and Mitz, A.R. 1980. Similarities in design feature of orientation sounds used by simpler nonaquatic echolocators. In: Busnel R.-G. and Fish J.F. (ed.). Animal sonar systems. NATO Advanced Study Institutes Ser. A., Vol. 28. Plenum Press, New York, pp. 871-874.

Busnel, R.-G. and Fish,J.F. 1980. Animal sonar systems. PLenum Press, New York.

Butler, R.A. 1974. Does tonotopicity subserve the perceived elevation of a sound. Fed. Proc. 33: 1920-1923.

Calford, M.B. and Pettigrew, J.D. 1984. Frequency dependence of directional amplification at the cat's pinna. Hearing Res. 14: 13-19.

Casseday, J.H. and Neff, W.D. 1973. Localization of pure tones. J. Acoust. Soc. Am. 54: 365-372.

Chalupa,L.M. and Rhoades,R.W. 1977. Response of visual, somatosensory and auditory neurones in the golden hamsters superior colliculus. J.Physiol. 270: 595-626.

Chung, S.-H., Pettigrew, A. and Anson, M. 1978. Dynamics of the amphibian middle ear. Nature 272: 142-147.

Coles, R.B. and Aitkin, L.M. 1979. The response properties of auditory neurones in the midbrain of the domestic fowl (*Gallus gallus*) to monaural and binaural stimuli. J. Comp. Physiol. 127: 241-251.

Coles, R.B., Gower, D.M., Boyd,P.J. and Lewis, D.B. 1982. Acoustic transmission through the head of the commom mole, *Talpa europaea*. J. Exp. Biol. 101: 337-341.

Coles, R.B., Konishi, M. and Pettigrew, J.D. 1982. Hearing and echolocation in the Australian grey swiftlet *Collocalia spodiopygia*. Proc. Aust. Physiol. Pharmacol. Soc. 13: 208P.

Coles, R.B., Lewis D.B., Hill, K.G., Hutchings, M.E. and Gower D.M. 1980. Directional hearing in the Japanese quail (*Coturnix coturnix japonica*). II: Cochlear physiology. J. Exp. Biol. 86: 153-170.

Collett, R. 1881. Craniets og oreaabningernes bygning hos de nordeuropaeiske arter af familien Strigidae. Forh. vidensk. Selsk. Krist., pp 1-38.

Dalland, J.I. 1965. Hearing sensitivity in bats. Science 150: 1185-1186.

Dooling, R.J. 1980. Behavior and psychophysics of hearing in birds. In: Popper, A.N. Fay, R.R. (eds) Comparative studies of hearing in vertebrates. Springer, New York, pp 261-288.

Douglas, A.M. 1967. The natural history of the ghost bat (*Macroderma gigas) (Microchiroptera: Megadermatidae*), in Western Australia. W. Aust. Nat. 10: 125-138.

Drager, U.C. and Hubel, D.H. 1975. Topography of visual and somatosensory projections to mouse superior colliculus. J. Neurophysiol.39: 91-101.

Elliott, D.N., Stein, L. and Harrison, M.J. 1959. Determination of absolute-intensity thresholds and frequency-difference thresholds in cats. J. Acoust. Soc. Am. 32: 380-384.

Erulkar, S.D. 1972. Comparative aspects of spatial localization of sound. Physiol. Rev. 52: 237-360.

Fattu, J.M. 1969. Acoustic orientation by the rabbit pinna and external auditory meatus. J. Acoust. Soc. Am. 46: 124.

Fiedler, J. 1979. Prey catching with and without echolocation in the Indian False Vampire (*Megaderma lyra*). Behav. Ecol. Sociobiol. 6: 155-160.

Fiedler, J., Kraus, H.-J. and Bruns, U. 1982. Comparative anatomy of the bat cochlea. Verh.Dtsch.Zool. Ges. 269.

Fletcher, N.H. and Thwaites, S. 1979. Physical models for the analysis of acoustical systems in biology. Quart. Rev. Biophys. 12: 25-65.

Flieger, E. and Schnitzler, H-U. 1973. Ortungsleistungen der fledermaus *Rhinolophus ferrumequinum* bei ein-und beidseitiger Ohrverstopfung. J. Comp. Physiol. 82: 93-102.

Flynn, W.E. and Elliott, D.N. 1965. Role of the pinna in hearing. J. Acoust. Soc. Amer. 38: 104-105.

Freye, H.A. 1953. Das Gehörorgan der Vögel. Wiss. Zschr. Univ. Halle. 5: 267-297.

Fullard, J.H. 1984. External auditory structures in two species of neotropical notodontid moths. J. Comp. Physiol. A. 155: in press

Fuzessery, Z.M. and Pollak, G.D. 1984. Neural mechanisms of sound localization in an echolocating bat. Science 225: 725-728.

Gatehouse, R.W. and Oesterreich, R.E. 1972. The role of the pinna and the external auditory meatus in monaural sound localization. J. Aud. Res. 12: 83-90.

Gates, G.R. and Aitkin, L.M. 1982. Auditory cortex in the marsupial possum *Trichosurus vulpecula*. Hear. Res. 7: 1-11.

Goldberg, J.M. and Brown, P.B. 1968. Functional organization of the dog superior olivary complex: an anatomical and electrophysiological study. J. Neurophysiol. 31: 639-656.

Goldberg, J.M. and Brown, P.B. 1969. Response of binaural neurons of dog superior olivary complex to dichotic tonal stimuli: some physiological mechanisms of sound localization. J. Neurophysiol. 32: 613-636.

Golubeva, T.B. 1972. The reflex activity of the tympanal muscle in the owl *Asio otus*. Zh. Evol. Biol. Fiziol. 8: 173-181.

Gordon, B. 1973. Receptive fields in the deep layers of cat superior colliculus. J. Neurophysiol. 36:157-178.

Gorlinski, I.A. 1976. Characteristics of ultrasound localization in a vertical plane by the horseshoe bat. Leningrad. Universitet. Vestnik Biologiya 13: 79-87.

Gourevitch, G. 1980. Directional hearing in terrestrial mammals. In: Popper, A.N., Fay, R.R. (eds). Comparative studies of hearing in vertebrates. Springer, New York pp 357-374.

Griffin, D.R. 1958. Listening in the dark. The acoustic orientation of bats and men. New Haven: Yale Univ. Press.

Griffin, D.R., Dunning, D.C., Cahlander, D.A. and Webster, F.A. 1962. Correlated orientation sounds and ear movements of horseshoe bats. Nature 196: 1185-1186.

Grinnell, A.D. 1963a. The neurophysiology of audition in bats: intensity and frequency parameters. J. Physiol. 167: 38-66.

Grinnell, A.D. 1963b. The neurophysiology of audition in bats: directional localization and binaural interaction. J. Physiol. 167: 97-113.

Grinnell, A.D. 1963c. The neurophysiology of audition in bats: resistance to interference. J. Physiol. 167: 114-127.

Grinnell, A.D. 1970. Comparative auditory neurophysiology of neotropical bats employing different echolocation signals. Z. Vergl. Physiologie. 68: 117-153.

Grinnell, A.D. 1973. Neural processing mechanisms in echolocating bats, correlated with differences in emitted sounds. J. Acoust. Soc. Am. 54: 147-156.

Grinnell, A.D. and Griffin, D.R. 1958. The sensitivity of echolocation in bats. Biol. Bull. 114: 10-22.

Grinnell, A.D. and Grinnell, V.S. 1965. Neural correlates of vertical localization by echolocating bats. J. Physiol. 181: 830-851.

Grinnell, A.D. and Hagiwara, S. 1972a. Adaption of the auditory nervous system for echolocation. Studies of New Guinea bats. Z. Vergl. Physiologie. 76: 41-81.

Grinnell, A.D. and Hagiwara, S. 1972b. Studies of auditory neurophysiology of non-echolocating bats and adaptions for echolocation in one-genus, *Rousettus*. Z. Vergl. Physiologie. 76: 82-96.

Grinnell, A.D. and Schnitzler, H-U. 1977. Directional sensitivity of echolocation in the horseshoe bat, *Rhinolophus ferrumequinum* II. Behavioral directionality of hearing. J. Comp. Physiol. 116: 63-76.

Guppy, A. and Coles, R.B. 1983. Feeding behaviour in the Australian ghost bat (*Macroderma gigas*) in captivity. Aust. Mammal. 6: 97-99.

Hall, L.S. and Richards, G.C. 1979. Bats of Eastern Australia. Queensland Museum Booklet No.12.

Harris, L.R., Blakemore, C. and Donaghey, M. 1980. Integration of visual and auditory space in the mammalian superior colliculus. Nature 288: 56-59.

Harrison, J.M. 1974. The auditory system of the medulla and localization. Fed. Proc. 33: 1901-1903.

Harrison,J.M., & Downey,P.1969. Intensity changes at the ear as a function of the azimuth of a tone source: a comparative study. J. Acoust. Soc. Am. 47: 1509-1518.

Hill, K.G., Lewis D.B., Hutchings, M.E. and Coles, R.B. 1980. Directional hearing in the Japanese quail (*Coturnix coturnix japonica*) I. Acoustic properties of the auditory system. J. Exp Biol 86: 135-151.

Hill, K.G. and Oldfield, B.P. 1981. Auditory function in Tettigoniidae (*Orthoptera: Ensifera*). J. Comp. Physiol. 142: 169-180.

Hind, J.E., Goldberg, J.M., Greenwood, D.D. and Rose, J.E. 1963. Some discharge characteristics of single neurons in the inferior colliculus of the cat. II. Timing of discharges and observations on binaural stimulation. J. Neurophysiol. 26: 321-341.

Jay, M.F. and Sparks, D.L. 1982. Auditory and saccade-related activity in the superior colliculus of the monkey. Neurosci. Abstr., 12: 951.

Jay, M.F. and Sparks, D.L. 1984. Auditory receptive fields in primate superior colliculus shift with changes in eye positions. Nature 309: 345-347.

Jen, P.H.-S. and Sun, X. 1984. Pinna orientation determines the maximal directional sensitivity of bat auditory neurons. Brain Res. 301: 157-161.

Jen, P.H.-S., Sun, X., Kamada, T., Zhang, S. and Shimozawa, T. 1984. Auditory response properties and spatial response areas of superior collicular neurons of the FM bat, *Eptesicus fuscus*. J. Comp. Physiol. A 154: 407-413.

Jenkins, W.M. and Masterton, R.B. 1979. Sound localization in pigeons (*Columba livia*). J. Comp. Physiol. Psychol. 93: 403-413.

Johnson, D.H. 1974. The relationship of post-stimulus time and interval histograms to the timing characteristics of spike trains. Biophys. 22: 413-430.

Kaup, J.J. 1862. Monograph of the strigidae. Trans. Zool. Soc. Lond 4: 201-260.

Khanna,S.M., & Stinson,M.R. 1985. Specification of the acoustical input to the ear at high frequencies. J. Acoust. Soc. Am. 77: 577-589.

King, A.J. 1985. Auditory and visual maps of space in the mammalian superior colliculus. Neurosci. Letts. 21: S5.

King, A.J. and Palmer, A.R. 1983. Cells responsive to free-field auditory stimuli in guinea-pig superior colliculus: distribution and response properties. J. Physiol. 342: 361-381.

Knudsen, E.I. 1980. Sound localization in birds. In: Popper, A.N., Fay, R.R. (eds). Comparative studies of hearing in vertebrates. Springer, New York, pp 289-322.

Knudsen, E.I. 1981. Hearing in the barn owl. Sci. Am. 245: 113-125.

Knudsen, E.I. 1982. Auditory and visual maps of maps of space in the optic tectum of the owl. J. Neurosci. 2: 1177-1194.

Knudsen, E.I. 1983a. Subdivisions of the inferior colliculus in the barn owl (*Tyto alba*). J. Comp. Neurol. 218: 174-186.

Knudsen, E.I. 1983b. Space coding in the vertebrate auditory system in Bioacoustics: a comparative approach (ed) Brian Lewis Pp 311-346. Academic Press, London.

Knudsen, E.I. 1983c. Early auditory experience aligns the auditory map of space in the optic tectum of the barn owl. Science 222: 939-942.

Knudsen, E.I. 1984. Auditory properties of space-tuned units in owls optic tectum. J. Neurophysiol. 52: 709-723.

Knudsen, E.I., Blasdel, G.G. and Konishi, M. 1979. Sound localization by the barn owl (*Tyto alba*) measured with the search coil technique. J. Comp. Physiol. 133: 1-11.

Knudsen, E.I., Esterly, S.D. and Knudsen, P.F. 1984 . Monaural occlusion alters sound localization during a sensitive period in the barn owl. J. Neurosci. 4: 1001-1011.

Knudsen, E.I., Knudsen, P.F. and Esterly, S.D. 1984 . A critical period for the recovery of sound localization accuracy following monaural occlusion in the barn owl. J. Neurosci. 4: 1012-1020.

Knudsen E.I. and Konishi, M. 1978a. Space and frequency are represented separately in auditory midbrain of the owl. J. Neurophysiol. 41: 870-884.

Knudsen, E.I. and Konishi, M. 1978b. A neural map of auditory space in the owl. Science 200: 795-797.

Knudsen, E.I. and Konishi, M. 1978c. Center-surround organization of auditory receptive fields in the owl. Science 202: 778-780.

Knudsen, E.I. and Konishi, M. 1979. Mechanisms of sound localization in the barn owl (*Tyto alba*). J. Comp. Physiol. 133: 13-21.

Knudsen, E.I. and Konishi, M. 1980. Monaural occlusion shifts receptive field locations of auditory midbrain units in the owl. J. Neurophysiol. 44: 687-695.

Knudsen, E.I., Konishi, M. and Pettigrew, J.D. 1977. Receptive fields of auditory neurons in the owl. Science 198: 1278-1280.

Konishi, M. 1973a. How the owl tracks its prey. Amer. Sci. 61: 414-424.

Konishi, M. 1973b. Locatable and non locatable acoustic signals for barn owls. Am. Nat. 107: 775-785.

Konishi, M. 1983. Neuroethology of acoustic prey localization in the barn owl. In: Huber, F., Markl, H. (eds). Neuroethology and behavioural physiology. Springer, Berlin, pp 303-317.

Larsen, O.N. 1981. Mechanical time resolution in some insect ears. II. Impulse sound transmission in acoustic tracheal tubes. J. Comp. Physiol. 143: 297-304.

Lawrence, B.D. and Simmons, J.A. 1982. Echolocation in bats: The external ear and perception of the vertical positions of targets. Science 218: 481-483.

Leonard, M.L. and Fenton, M.B. 1983. Habitat use by spotted bats (*Euderma maculatum*: roosting and foraging behaviour. Can. J. Zool. 16: 1487-1491.

Lewis, B. 1974. The physiology of the tettigoniid ear. I. The implications of the anatomy of the ear to its function in sound reception. J. Exp. Biol. 60: 821-837.

Lewis, B. 1983. Directional cues for auditory localization. In Bioacoustics: a comparative approach. Lewis, B. (ed). Academic Press, London. Pp 233-260.

Lewis, B. and Coles, R.B. 1980. Sound localization in birds. Trends Neurosci. 3: 102-105.

Long, G.R. and Schnitzler, H.-U. 1975. Behavioural audiograms from the bat, *Rhinolophus ferrumequinum*. J. Comp. Physiol. 100: 211-219.

Masters, W.M., Moffat, A.J.M. and Simmons, J.A. 1985. Sonar tracking of horizontally moving targets by the big brown bat *Eptesicus fuscus*. Science 228: 1331-1333.

Masterton, R.B., Thompson, G.C., Bechtold, J.K. and Robards, M.J. 1975. Neuroanatomical basis of binaural phase-difference analysis for sound localization: A comparative study. J. Comp. Physiol. Psychol. 89: 379-386.

Michelsen, A. 1979. Insect ears as mechanical systems. Amer. Sci. 67: 696-706.

Michelsen, A. 1983. Biophysical basis of sound communication. In: Lewis, B. (ed). Bioacoustics: A comparative approach. Academic Press, London. pp 3-38.

Michelsen, A. and Nocke, H. 1974. Biophysical aspects of sound communication in insects. Adv. Insect Physiol. 10: 247-296.

Middlebrooks, J.C. and Knudsen, E.I. 1984. A neural code for auditory space in the cat's superior colliculus. J. Neurosci. 4: 2621-2634.

Middlebrooks, J.C. and Pettigrew, J.D. 1981. Functional classes of neurons in the primary auditory cortex of the cat distinguished by sensitivity to sound location. J. Neurosci. 1: 107-120.

Miller, L.A. and Degn, H.J. 1981. The acoustic behaviour of four species of vespertilionid bats studied in the field. J. Comp. Physiol. 142: 67-74.

Mohres, F.P. 1967. Ultrasonic orientation in Megadermatid bats. In Busnel, R-G. (ed) Animal Sonar Systems. Vol. 1 Lab. Physiol. Acoust. C.N.R.Z., Jouy-en-Josas, France, pp. 115-127.

Mohres, F.P. and Kulzer, E. 1957. Megaderma -ein konvergenter zwischentyp der ultraschallpeilung bei fledermausen. Naturwissen. 44: 21-22.

Mohres, F.P. and Neuweiler, G. 1966. Die ultraschallorientierung der grossblatt-fledermause (Chiroptera-Megadermatidae). Z. Vergl. Physiol. 53: 195-227.

Moiseff, A. and Konishi. M. 1981a. Neuronal and behavioural sensitivity to binaural time differences in the owl. J. Neurosci. 1: 40-48.

Moiseff, A. and Konishi, M. 1981b. The owl's interaural pathway is not involved in sound localization. J. Comp. Physiol. 144: 299-304.

Moiseff, A. and Konishi, M. 1983. Binaural characteristics of units in the owl's brainstem auditory pathway: Precursors of restricted spatial receptive fields. J. Neurosci. 3: 2553-2562.

Moller, A.G. 1983. Auditory Physiology. Academic Press, New York.

Moore, D.R., Hutchings, M.E., Addison, P.D., Semple, M.N. and Aitkin, L.M. 1984a. Properties of spatial receptive fields in the central nucleus of the cat inferior colliculus. II. Stimulus intensity effects. Hearing Res. 13: 175-188.

Moore, D.R., Semple, M.N., Addison, P.D. and Aitkin, L.M. 1984b. Properties of spatial receptive fields in the central nucleus of the cat inferior colliculus. I. Responses to tones of low intensity. Hear Res. 13: 159-174.

Morse, P.M. 1948. Vibration and sound. McGraw-Hill, New York.

Neff, W.D. 1974. Sound localization. Fed. Proc. 33: 1899-1900.

Neff, W.D. and Hind, J.E. 1955. Auditory thresholds of the cat. J. Acoust. Soc. Am. 27: 480-483.

Neuweiler, G. 1970. Neurophysiologische Untersuchungen zum Echoortungssystem der GröBen Hufeisennase *Rhinolophus ferrumequinum* Schreber, 1774. Z. vergl. Physiol. 67: 273-306.

Neuweiler, G. 1983. Echolocation and adaptivity to ecological contraints. Pp 280-302. In Neuroethology and Behavioural Physiology (eds) Huber, F. and Markl, H. Springer Berlin.

Neuweiler, G. 1984. Foraging, echolocation and audition in bats. Naturwissenschaften 71: 446-455.

Neuweiler, G., Singh, S. and Sripathi, K. 1984. Audiograms of a south Indian bat community. J. Comp. Physiol. A. 154: 133-142.

Nocke, H. 1975. Physical and physiological properties of the tettigonid ("grasshopper") ear. J. Comp. Physiol. 100: 25-57.

Norberg, R.A. 1968. Physical factors in directional hearing in *Aegolius funereus* (Linne) (Strigiformes), with special reference to the significance of the asymmetry of the external ears. Ark. Zool. 20: 181-204.

Norberg, R.A. 1970. Hunting technique of Tengmalm's owl *Aegolius funereus*. Ornis. Scand. 1: 51-64.

Norberg, R.A. 1977. Occurrence and independent evolution of bilateral ear asymmetry in owls and implications on owl taxonomy. Phil. Trans. Roy. Soc. Lond. 280: 375-408.

Norberg, R.A. 1978. Skull asymmetry, ear structure and function, and auditory localization in Tengmalm's owl, *Aegolius funereus* (Linne). Phil. Trans. Roy. Soc. Lond. 282: 325-410.

Novick, A. 1958. Orientation in paleotropical bats. I. Microchiroptera. J. Exp. Zool. 138: 81-154.

Oeckinghaus, H. and Schwartzkopff, J. 1983. Electrical and acoustical activation of the middle ear muscle in a songbird. J. Comp. Physiol. 150: 61-67.

Oldfield, S.R. and Parker, S.P.A. 1984a. Acuity of sound localisation: a topography of auditory space. I. Normal hearing conditions. Perception 13: 581-600.

Oldfield, S.R. and Parker, S.P.A. 1984b. Acuity of sound localisation: a topography of auditory space. II. Pinna cues absent. Perception 13: 601-618.

Olson, H.F. 1947. Elements of acoustic engineering. Van Nostrand, New York.

Palmer, A.R. and King, A.J. 1982. The representation of auditory space in the mammalian superior colliculus. Nature 299: 248-249.

Palmer, A.R. and King, A.J. 1983. Monaural and binaural contributions to an auditory space map in the guinea-pig superior colliculus. In: Hearing-physiological basis and psychophysics (ed) Klinke and Hartman.

Palmer, A.R. and King, A.J. 1985. A monaural space map in the guinea pig superior colliculus. Hear. Res. 17: 267-280.

Payne, R.S. 1971. Acoustic location of prey by barn owls (*Tyto alba*). J. Exp. Biol. 54: 535-573.

Payne, R.S. and Drury, W.H. 1958. Marksman of the darkness. Natural History 67: 316-323.

Pettigrew, A., Chung, S.H. and Anson, M. 1978. Neurophysiological basis of directional hearing in amphibia. Nature 272: 138-142.

Pettigrew, J.D. 1979. Binocular visual processing in the owl telencephalon. Proc. Roy. Soc. Lond. B. 204: 434-454.

Pettigrew, J.D., Coles, R.B., Guppy, A., Brown, M. and Nelson, J. 1983. Sensory ability of the Australian ghost bat, *Macroderma gigas*. Neuroscience Letters Suppl. 11: S68.

Pettigrew, J.D. and Konishi, M. 1976. Neurons selective for orientation and binocular disparity in the visual wulst of the barn owl (*Tyto alba*). Science 193: 675-678.

Phillips, D.P., Calford, M.B., Pettigrew, J.D., Aitkin, L.M. and Semple, M.N. 1982. Directionality of sound pressure transformation at the cats pinna. Hear. Res. 8: 13-28.

Porter, F.L. 1979. Social behavior in the leaf-nosed bat, *Carollia perspicillata*. II. Social Communication. Z. Tierpsychol. 50: 1-8.

Poussin, C. and Schlegel, P. 1984. Directional sensitivity of auditory neurons in the superior colliculus of the bat, *Eptesicus fuscus*, using free field sound stimulation. J. Comp. Physiol. A. 154: 253-261.

Poussin, C. and Simmons, J.A. 1982. Low-frequency hearing sensitivity in the echolocating bat, *Eptesicus fuscus*. J. Acoust. Soc. Am. 72: 340-342.

Pumphrey, R.J. 1940. Hearing in insects. Biol. Rev. 15: 107-132.

Pumphrey, R.J. 1948. The sense organs of birds. Smiths Inst. Ann. Rep. No. 3954: pp 305-330.

Pycraft, W.P. 1898. A contribution towards our knowledge of the morphology of the owl. Part 1: Pterylography. Trans. Linn. Soc. Lond. 2nd Ser. Zool. 7: 223-275.

Pycraft, W.P. 1903. A contribution towards our knowledge of the morphology of the owl. Part 2: Osteology. Trans. Linn. Soc. Lond. 2nd Ser. Zool. 9: 1-46.

Pye, J.D. 1961. Echolocation by bats. Endeavour 20: 101-111.

Pye, J.D. 1980. Echolocation signals and echoes in air. In: Busnel, R.G. and Fish, J.F. (ed) Animal Sonar Systems. NATO Advanced Study Institutes Ser. A., vol. 28. Plenum Press, New York, pp. 309-354.

Pye, J.D., Flynn, M. and Pye, A. 1962. Correlated orientation sounds and ear movements of horseshoe bats. Nature 196: 1186-1188.

Pye, J.D. and Roberts, L.H. 1970. Ear movements in a Hipposiderid Bat. Nature 225: 285-286.

Rand,A.S. and Ryan, M.J. 1981. The adaptive significance of a complex vocal repertoire in a neotropical frog. Z. Tierpsychol. 57: 209-214.

Ravizza, R.J., Heffner, H.E. and Masterton, B. 1969. Hearing in primitive mammals, I: Opossum (*Didelphis virginianus*). J. Aud. Res. 9: 1-17.

Rayleigh, Lord 1876. Our perception of the direction of a source of sound. Nature 14: 32-33.

Rayleigh, Lord 1877. The theory of sound. Vols. 1 and 2. Macmillan, London.

Rayleigh, Lord 1907. On our perception of sound direction. Phil. Mag 13: 214-232.

Rose, J.E., Brugge, J.F., Anderson, D.J. and Hind, J.E. 1967. Phase-locking responses to low-frequency tones in single auditory nerve fibers of the squirrel monkey. J. Neurophysiol. 30: 769-793.

Rose, J.E., Gross, N.B., Geisler, C.D. and Hind, J.E. 1966. Some neural mechanisms in the inferior colliculus of the cat which may be relevant to localization of a sound source. J. Neurophysiol. 29: 288-314.

Rosowski, J.J. and Saunders, J.C. 1980. Sound transmission through the avian interaural pathways. J. Comp. Physiol. 136: 183-190.

Ryan, M.J. and Tuttle, M.D. 1983. The ability of the frog-eating bat to discriminate among novel and potentially poisonous frog species using acoustic cues. Anim. Behav. 31: 827-833.

Ryan, M.J., Tuttle, M.D. and Barclay, R.M.R. 1983. Behavioral responses of the frog-eating bat, *Trachops cirrhosus*, to sonic frequencies. J. Comp. Physiol. 150: 413-418.

Sachs, M.B., Wolf, N.K. and Sinnott, J.M. 1980. Response properties of neurons in the avian auditory system. In: Popper A.N. Fay R.R. (eds) Comparative studies of hearing in vertebrates. Springer, New York, pp 323-354.

Sales, G. and Pye, D. 1974. Ultrasonic communication by animals. Chapman and Hall, London.

Santibanez-H.G. 1976. The targeting reflex. Acta. Neurobiol. exp. 36: 181-203.

Schaeffer, K.-P. and Schneider, H. 1968. Reizversuche im Tectum opticum des kaninchens. Archiv. für Psychiatrie und Zeitschrift f.d. ges. Neurologie 211: 118-137.

Schlegel, P. 1977. Directional coding by binaural brainstem units of the CF-FM bat, *Rhinolophus ferrumequinum*. J. Comp. Physiol. 118: 327-352.

Schmidt, S., Türke, B. and Vogler, B. 1984. Behavioural audiogram from the bat *Megaderma lyra* (Geoffrey, 1810; Microchiroptera). Myotis 22: 62-66.

Schneider, H. and Möhres, F.P. 1960. Die ohrbewegungen der hufeisenfledermäuse (Chiroptera, Rhinolophidae) und der mechanismus des bildhörens. Zeitschrift für vergleichende Physiologie 44: 1-40.

Schnitzler, H.-U. and Grinnell, A.D. 1977. Directional sensitivity of echolocation in the horseshoe Bat, *Rhinolophus ferrumequinum*. I. Directionality of sound emission. J. Comp. Physiol. 116: 51-61.

Schnitzler, H.-U. and Henson, O. 1980. Performance of airborne animal sonar systems. In: Busnel, R.-G., Fish, J.F. (ed) Animal Sonar Systems. NATO Advanced Study Institutes, Ser. A. Vol. 28. Plenum Press, New York, pp. 109-182.

Schuller, G. 1980. Hearing characteristics and doppler shift compensation in South Indian CF-FM bats. J Comp. Physiol. 139: 349-356.

Schwartzkopff, J. 1950. Beitrag zum problem des richtungshörens bie vögeln. Z. Vergle. Physiol. 32: 319-327.

Schwartzkopff, J. 1952. Untersuchungen über die arbeitsweise des mittelohres und das richtungshören der singvögel unter verwendung von cochlea-potentialen. Z. Vergl. Physiol. 34: 46-68.

Schwartzkopff, J. 1962. Zur frage des richtungshörens von eulen (Striges). Z. Vergl. Physiol. 45: 570-580.

Searle, C.L., Braida, L.D., Cuddy, D.R. and Davis, M.F. 1975. Binaural pinna disparity: Another auditory localization cue. J. Acoust. Soc. Am., 57: 448-455.

Searle, C.L., Braida, L.D., Davis, M.F. and Colburn, H.S. 1976. Model for auditory localization. J. Acoust. Soc. Am. 60: 1164-1175.

Semple, M.N., Aitkin, L.M., Calford, M.B., Pettigrew, J.D. and Phillips, D.P. 1983. Spatial receptive fields in the cat inferior colliculus. Hear. Res. 10: 203-215.

Seymour, C., Lewis, B., Larsen, O.N. and Michelsen, A.1978. Biophysics of the ensiferan ear. II. The steady-state gain of the hearing trumpet in bush crickets. J. Comp. Physiol. 123: 205-216.

Shaw, E.A.G. 1974. The external ear. In: Autrum, H., Jung, R., Loewenstein, W.R., Mackay, D.M., Teuber, H.L. (eds) Handbook of sensory physiology Vol V/1 Springer, New York, pp 455-490.

Shimozawa, T., Suga, N., Hendler, P. and Schuetze, S. 1974. Directional sensitivity of echolocation system in bats producing frequency-modulated signals. J. Exp. Biol. 60: 53-69.

Shimozawa, T., Sun, X. and Jen, P.H. 1984. Auditory space representation in the superior colliculus of the big brown bat, *Eptesicus fuscus*. Brain Res. 311: 289-296.

Siegmund, H. and Santibanez-H.G. 1981. Effects of motor denervation of the external ear muscles on the audio-visual targeting reflex in cats. Acta Neurobiol. exp. 41: 1-13.

Simmons, J.A. 1982. The external ears as receiving antennae in echolocating bats. J. Acoust. Soc. Am. 72: S41-42.

Simmons, J.A., Kick, S.A., Lawrence, B.D., Hale, C., Bard, C. and Escudie, B. 1983. Acuity of horizontal angle discrimination by the echolocating bat, *Eptesicus fuscus*. J. Comp. Physiol. 153: 321-330.

Simmons, J.A. and Stein, R.A. 1980. Acoustic imaging in bat sonar: echolocation signals and the evolution of echolocation. J. Comp. Physiol. 135: 61-84.

Stein, B.E. and Clamann, H.P. 1981. Control of pinna movements and sensorimotor register in cat superior colliculus. Brain Behav. Evol. 19: 180-192.

Stellbogen, E. 1930. Über das äussere und mittlere ohr des waldkauzes (*Syrnium aluco* L). Z. Morph. Ökol. Tiere. 19: 687-731.

Stevens, S.S. and Newmann, E.B. 1934. The localization of pure tones. Proc. Nat. Acad. Sci. 20: 593-596.

Strahan, R. 1983. Complete book of Australian mammals. Angus and Robertson Sydney.

Stresemann, E. 1934. Handbuch der Zoologie Vol 7 Pt 2 Kükenthal, W. Krumbach, T. (ed) De Gruyter, Leipzig, pp 899.

Suga, N. 1964. Single unit activity in cochlear nucleus and inferior colliculus of echo-locating bats. J. Physiol. 172: 449-474.

Sullivan, W.M. and Konishi, M. 1984. Segregation of stimulus phase and intensity coding in the cochlear nucleus of the barn owl. J. Neurosci. 4: 1787-1799.

Suthers, R.A. and Summers, C.A. 1980. Behavioral audiogram and masked thresholds of the Megachiropteran echolocating bat, *Rousettus*. J. Comp. Physiol. 136:227-233.

Takahashi, T., Moiseff, A. and Konishi, M. 1984. Time and intensity cues are processed independently in the auditory system of the owl. J. Neurosci. 4: 1781-1786.

Tidemann, C.R., Priddel, D., Nelson, J.E. and Pettigrew, J.D. 1985. Foraging behaviour of the Australian ghost bat, *Macroderma gigas* (Microchiroptera: Megadermatidae). Aust. J. Zool. 33: 705-713.

Tiedemann, F. 1810. Zoologie II, Anatomie und Naturgeschichte der Vögel. Landshut.

Tonndorf, J. and Khanna, S.M. 1967. Some properties of sound transmission in the middle and outer ears of cats. J. Acoust. Soc. Am. 41: 513-521.

Tuttle, M.D. and Ryan, M.J. 1981. Bat predation and the evolution of frog vocalizations in the neotropics. Science 214: 677-678.

Van Dijk, T. 1973, A comparative study of hearing in owls of the Family Strigidae. Neth. J. Zool. 23: 131-167.

Vaughan, T.A. 1976. Nocturnal behaviour of the African false vampire bat (*Cardioderma cor*). J. Mammal. 57: 227-248.

Wada, Y. 1923. Beitrage zur vergleichenden physiologie des Gehörorgane. Pflüger Archiv. 202: 46-69.

Waite, E.R. 1900. Recurrence of *Megaderma gigas*. Dobson. Rec. Aust. Mus.., 3: 188-189.

Walker, E.P. 1975. Mammals of the World. Third Edition. John Hopkins University Press, London.

Webster, W.R. and Aitkin, L.M. 1975. Central auditory processing. In: Handbook of psychobiology. Gazzaniga M.S. and Blakemore C. (eds) Academic Press, London. pp. 325-364.

Wickler, W. and Uhrig, D. 1969. Verhalten und ökologische nische der gelbflügelfledermaus, *Lavia frons* (Geoffroy) (Chiroptera, Megadermatidae). Z. Tierpsychol. 26: 726-736.

Wiener, F.M., Pfeiffer, R.R. and Backus, A.S.S. 1966. On the sound pressure transformation by the head and auditory meatus of the cat. Acta Oto-laryng 61: 255-269.

Wise, L.Z. and Irvine, D.R.F. 1983. Auditory response properties of neurons in deep layers of cat superior colliculus. J. Neurophysiol. 49: 674-685.

Wise, L.Z., Irvine, D.R.F., Pettigrew, J.D. and Calford, M.B. 1982. Auditory spatial receptive field properties of neurons in intermediate and deep layers of cat superior colliculus. Neurosci. Lett. Suppl. 8: S88.

Woodsworth, G.C., Bell, G.P. and Fenton, M.B. 1981. Observations of the echolocation, feeding behaviour, and habitat use of *Euderma maculatum* (Chiroptera: Vespertilionidae) in South Central British Columbia. Can. J. Zool. 59: 1099-1102.

Woolf, N.K. and Sachs, M.B. 1977. Phase locking to tones in avian auditory- nerve fibres. J.Acoust. Soc. Am. 62: S46.